DEPARTMENT OF THE ARMY
U. S. ARMY AVIATION MATERIEL LABORATORIES
FORT EUSTIS, VIRGINIA 23604

SMFE-ADBS

JUL 9 1965

TO: Defense Documentation Center
ATTN: DDC-IR
Cameron Station
Alexandria, Virginia 22314

1. Reference TRECOM Technical Report 62-63, AD 401 149.

2. It is requested that the DDC availability notice pertaining to reproduction of this report be deleted and that microfilm copies of the report be furnished to the Department of Commerce for subsequent reproduction and sale to the public.

FOR THE COMMANDER:

RONALD P. TOWLE
Captain, AGC
Adjutant

Copy furnished:
Clearinghouse for S&T
Info, Dept of Commerce
Springfield, Va. 22151

END CHANGE PAGES

U. S. ARMY

TRANSPORTATION RESEARCH COMMAND

FORT EUSTIS, VIRGINIA

TCREC TECHNICAL REPORT 62-63

RESEARCH PROGRAM TO DETERMINE THE FEASIBILITY AND POTENTIAL OF THE GROUND EFFECT TAKE-OFF AND LANDING (GETOL) CONFIGURATION

VOLUME I

Task 9R38-11-011-01

Contract DA 44-177-TC-663

December 1962

prepared by:

VERTOL DIVISION
The Boeing Company
Morton, Pennsylvania

DISCLAIMER NOTICE

When Government drawings, specifications, or other data are used for any purposes other than in connection with a definitely related Government procurement operation, the United States Government thereby incurs no responsibility nor any obligation whatsoever; and the fact that the Government may have formulated, furnished, or in any way supplied the said drawings, specifications, or other data is not to be regarded by implication or otherwise as in any manner licensing the holder or any other person or corporation, or conveying any rights or permission, to manufacture, use, or sell any patented invention that may in any way be related thereto.

ASTIA AVAILABILITY NOTICE

Qualified requesters may obtain copies of this report from

Armed Services Technical Information Agency
Arlington Hall Station
Arlington 12, Virginia

This report has been released to the Office of Technical Services, U. S. Department of Commerce, Washington 25, D. C., for sale to the general public.

The findings and recommendations contained in this report are those of the contractor and do not necessarily reflect the views of the U. S. Army Mobility Command, the U. S. Army Materiel Command, or the Department of the Army.

HEADQUARTERS
U. S. ARMY TRANSPORTATION RESEARCH COMMAND
FORT EUSTIS, VIRGINIA

A Government review of the Boeing-Vertol Company report has been completed by the U. S. Army Transportation Research Command. The exploratory research represented by this report was undertaken to ascertain the feasibility of utilizing the ground effects principle in the design of an aircraft, thereby enabling take-off and landing over relatively unprepared terrain. The most singular achievement of this reported investigation is the advancement of knowledge in an area lacking sufficient technical information.

This report has preliminarily established that a ground effects take-off and landing vehicle (GETOL) can be designed, built, and flown. However, the test data obtained indicate that several problem areas must be resolved before such an aircraft could be competitive with existing and proposed VTOL aircraft. Therefore, on the basis of present technology, no recommendation is made to proceed with this aircraft design configuration for application to Army aviation.

FOR THE COMMANDER:

KENNETH B. ABEL
Captain, TC
Adjutant

APPROVED BY:

GARY N. SMITH
1st Lt., TC
USATRECOM Project Engineer

PROJECT 437-7820

CONTRACT DA44-177-TC-665

December 1962

TCREC 62-63

RESEARCH PROGRAM

TO DETERMINE THE FEASIBILITY AND POTENTIAL

OF THE

GROUND EFFECT TAKE-OFF AND LANDING (GETOL) CONFIGURATION

VOLUME I

REPORT NO. R276

PREPARED BY
VERTOL DIVISION
THE BOEING COMPANY
MORTON, PENNSYLVANIA

for

U. S. ARMY TRANSPORTATION RESEARCH COMMAND

FORT EUSTIS, VIRGINIA

FOREWORD

This report, as presented in Volume I and II, represents a final summary of Boeing-Vertol effort under Contract DA44-177-TC-663 to determine the feasibility and potential of the Ground Effect Take-off and Landing (GETOL) Configuration. This analytical development program was initiated in September 29, 1960 and completed on March 28, 1962 with a preliminary design of a Flight Research Vehicle (FRV).

H. Wahl, F. McHugh and R. Hooper of Boeing-Vertol guided the parametric analysis, development testing, preliminary design and report preparation under the direction of W. Stepniewski. Technical assistance and cooperation was provided by S. Spooner, J. Whitman and G. Smith of USATRECOM as well as K. Goodsen and R. Kuhn of NASA's Langley Field facility.

Major development testing was performed by NASA at Langley Field. Static room tests were performed from April 21 to June 30, 1961. Tow track testing began May 31, 1961 and was completed June 9, 1961, while wind tunnel testing of the GETOL model commenced on July 7 and ended on July 28, 1961. Planform and dynamic model testing was also conducted by Princeton and Toronto Universities.

Special mention for technical service during the life of Contract DA44-177-TC-663 go to T. Sweeney of Princeton University, B. Etkin, J. Liiva, R. Radford, and G. Kurylowich of the University of Toronto, H. Chaplin of DTMB and J. Wosser of ONR. Editorial coordinative assistance for this final report was provided by J. Gaffney.

CONTENTS

ILLUSTRATIONS

ILLUSTRATIONS (Continued)

ILLUSTRATIONS (Continued)

ILLUSTRATIONS (Continued)

ILLUSTRATIONS (Continued)

LIST OF TABLES

LIST OF SYMBOLS

Symbol	Description	Unit
A	AUGMENTATION	$\frac{L}{J} = \frac{L}{m V_J} = \frac{C_L}{C\mu}$
AR	ASPECT RATIO	
b	MODEL WING SPAN	FT
c	MODEL WING ROOT CHORD	FT
C_D	DRAG COEFFICIENT	$\frac{D}{q S_w}$
C_L	LIFT COEFFICIENT	$\frac{L}{q S_w}$
$C_{\ell'}$	ROLLING MOMENT COEFFICIENT	$\frac{R}{q S_w b}$
C_m	PITCHING MOMENT COEFFICIENT	$\frac{M}{q S_w c}$
C_μ	MOMENTUM COEFFICIENT	$\frac{J}{qS} = \frac{m V_J}{qS_w}$
C.P.	CENTER OF PRESSURE	
D	NET DRAG	LB
h	HEIGHT ABOVE GROUND BOARD	FT
HP	AIR HORSEPOWER	$\frac{\Delta PQ}{550}$ HP
j	MOMENTUM FLUX PER UNIT LENGTH	LB/FT
J	MASS FLOW RATE - $m V_J$	$\frac{\text{SLUG FT}}{\text{SEC}^2}$
L	NET LIFT	LB

LIST OF SYMBOLS

Symbol	Description	Unit
M	PITCHING MOMENT (MEASURED AT FAN CENTER LINE & WING ROOT QUARTER CHORD)	FT - LB
mac	MEAN AERODYNAMIC CHORD	FT
m	MASS FLOW RATE Q_ρ	SLUG/SEC
P_S	STATIC PRESSURE	IN ALC, LB/SQ IN
P_T	TOTAL PRESSURE	IN ALC, LBS/SQ IN
q	FREE STREAM DYNAMIC PRESSURE $\frac{1}{2}\rho V^2$	LB/SQ FT
Q	QUANTITY FLOW RATE MEASURED BEHIND THE FAN	CU FT/SEC
R	ROLLING MOMENT	FT - LB
RPM	REVOLUTION PER MINUTE	
S_J	SLOT FLOW AREA	SQ FT
S_Ω	PROJECTED WING AREA	SQ FT
t_{LE}	PROJECTED SLOT THICKNESS OF THE LEADING EDGE SLOT	INCH
t_{TE}	PROJECTED SLOT THICKNESS OF THE TRAILING EDGE SLOT	INCH
V	FREE STREAM VELOCITY	FT/SEC
V_J	AVERAGE JET EXIT VELOCITY AT SLOT $\frac{Q}{S_J}$	FT/SEC
β	INLET GUIDE VANE ANGLE	DEGREE

LIST OF SYMBOLS

Symbol	Description	Units
θ_F	ANGLE OF THE FRONT SLOT FROM THE VERTICAL (NEGATIVE IN TOWARD THE CENTER OF THE BASE)	DEGREE
θ_R	ANGLE OF THE REAR SLOT FROM THE VERTICAL (NEGATIVE IN TOWARD THE CENTER OF THE BASE)	DEGREE
ρ	MASS DENSITY OF AIR	SLUG/CU FT
ΔP	PRESSURE DROP	IN ALC, LBS/SQ IN
α	ANGLE OF ATTACK	DEGREE
ω	WING LOADING	$\frac{L}{S_W}$

SUMMARY

This final report, issued in two volumes, comprehensively presents the achievements of the Boeing-Vertol Feasibility Study of the Ground Effect Take-off and Landing (GETOL) Aircraft concept. The study was conducted under Contract DA44-177-TC-663 for USATRECOM, with joint Boeing-Vertol funding. This study results in a preliminary design of a Flight Research Vehicle (FRV) which could be used to provide the next step in GETOL development.

The GETOL aircraft concept evolved during 1959 from various efforts with Ground Effect Machines (GEM) as furthered by exploratory analytical and test work by Boeing-Vertol (Reference 1).

The object of the GETOL was to provide a relatively high speed aircraft capable of taking off and landing on a "ground cushion" from any moderately flat surface. The questions of adequate ground clearance, satisfactory propulsive capability, low internal losses, STOL capability, and proper stability and control had to be answered to truthfully assess the feasibility of the GETOL Configuration.

Consequently, the GETOL Feasibility Study consisted of the following integrated analytical and test programs:

1. Complete literature assessment
2. Internal airflow studies and tests
3. Preliminary wing planform test
4. Wind tunnel model design (5 ft. span 20 Air HP).
5. Data qualification programs:
   a) Slot flow distribution tests
   b) Static performance tests of planforms
   c) Free flight model tests
   d) Four to one (4:1) aspect ratio slotted GETOL wing wind tunnel test
   e) Investigation of the influence of the tunnel ground board boundary layer through comparative tests on a tow track.
6. The main test program was conducted in the NASA 17 x 17 ft. tunnel with the 5 ft. span model.
7. Flight Research Vehicle design

The complete GETOL program may be better visualized by the chart of the Integrated Study Program shown in the Introduction of Volume 1.

The general results of this integrated study may be summarized as follows:

1. A ground clearance of h/c = .33 can be obtained.
2. Satisfactory propulsion capabilities for take-off and forward flight can be obtained in the following manner:
   a) Nacelle doors open gradually, eventually converting to a ducted fan configuration in forward flight.

greatly reduces the mechanical complexity of the GETOL control system.

3. Internal flow losses were reduced to 20 to 30 percent by careful internal design.
4. In spite of the many design concessions forced by the GETOL system, L/D ratios indicated by tunnel tests promise a satisfactory airplane configuration.
5. STOL capability, based upon projected data, is acceptable.
6. Presently available data from this investigation indicates that the jet boundary layer on the ground has negligible effect on the wind tunnel data.
7. Inherent static stability and control in hovering appears marginal, but tests of a "T" shaped planform promise a satisfactory fix.
8. The relatively low lift per air horsepower of 3.0, obtained from the test data, are the result of poor flow distribution. It is thought that if flow distribution is improved that lift per air horsepower would also improve.
9. Compilation of broad GETOL data assembled in Volumes I and II represent basic GETOL knowledge which should be considered in itself as one of the most important results of this program.

Specific study of the flight research vehicle of the 8,000 pound gross weight class and equipped with a single Lycoming YT55-L-5 engine of 1970 shp demonstrated the following characteristics with the projected improvements:

1. Hovering altitudes of 3.6'
2. Required maximum velocity of 250 mph at sea level.
3. Take-off distance of 500' over a 50' barrier.
4. Endurance with pilot and copilot plus 400 pound payload is 1.5 hours.
5. Wind tunnel data indicated that the maximum lift/drag ratio of the model (with no attention to aerodynamic cleanliness) was 5.5; but it is estimated that for the FRV with more streamlining a maximum lift/drag ratio ≥ 7.0 can be obtained.

The conclusion reached is that the GETOL configuration, incorporating features needed for the improved Flight Research Vehicle, is feasible. The next step required in the program to confirm such feasibility is the development of the proposed Flight Research Vehicle whose details are given in Phase III of Volume I of this report.

CONCLUSIONS

correlations with data from other sources are as follows:

1. A ground clearance of h/c = .33 can be obtained (for the proposed FRV of 8,000 pound gross weight this altitude is 3.6 ft.).

2. Satisfactory propulsion capabilities can be obtained by gradually opening the nacelle doors located behind the fan.

3. Straight through fan propulsion is better than aft angled wing slots and also reduces mechanical complexity of the GETOL control system.

4. Internal flow losses were 20 to 30 percent.

5. L/D ratios indicated by wind tunnel tests of the Boeing-Vertol model are on the order of 5.5 and the L/D for the FRV, incorporating the projected streamlining, should be on the order of 7.0; on the transport aircraft (40,000 pound gross weight class) an L/D $\geq$13.0 can be expected.

6. STOL capability, as indirectly calculated from the data of this program, is acceptable (take-off distance over a 50' obstacle is $\leq$ 500' for the FRV and of the same magnitude for the 40,000 pound gross weight transports).

7. In light of the presently available information developed during this investigation, it appears that the jet boundary layer on the ground board has a negligible effect on the wind tunnel data.

8. Inherent static stability and control in hovering appear marginal but a "T" shaped planform can improve those characteristics.

9. The relatively low lift per air horsepower of 3.0, obtained from the test data, is probably the result of poor flow distribution. It is thought that if flow distribution is improved, lift per air horsepower would also improve.

10. Based upon this program, a GETOL research aircraft of the 8,000 pound gross weight class can be designed and flown; more attractive GETOL configurations can be obtained at higher gross weights. For instance, a GETOL type vehicle in the 40,000 pound category appears to be competitive with STOL and even conventional aircraft.

RECOMMENDATIONS

Vertol based upon analytical studies performed under the GETOL Feasibility Program in addition to data correlated by a survey of other non-company investigations in the GEM and GETOL configurations.

1. The relatively low lift per air horsepower is a result of poor flow distribution which requires additional testing to determine the effect of distribution on performance.

2. The inherent marginal stability and control requires testing of a cruciform "T" planform.

3. Perform mission studies in order to compare the GETOL concept with other STOL and NTOL aircraft and thus define the best area of GETOL application.

4. Initiate effort on the Flight Research Vehicle as described in Phase III, Volume I of Boeing-Vertol Report R276.

TECHNICAL PROGRAM

INTRODUCTION

The Vertol Division of The Boeing Company has been engaged in the design and test studies of the GETOL concept since 1959. These studies have been coordinated into an Integrated Study Program to determine the feasibility and potential of a GETOL type aircraft. The sequence of this program is shown on the next page and presents the various areas of investigation which can be categorized into three distinct phases:

Phase I - Determination of Preliminary Flight Research Vehicle (FRV) and Wind Tunnel Model

Phase II - GETOL Model Testing and Data Analysis

Phase III - Recommended Program for Construction of a Flight Research Vehicle (FRV)

The above phases are the same as those given in the Statement of Work, Volume II, Appendix A.

An extensive amount of engineering data made available by this testing has been analyzed in Volume I. In these analyses, pertinent design parameters have been established to facilitate the design of a GETOL aircraft. The data and analyses as well as the results are summarized in Volume I and Volume II of Boeing-Vertol Report R276.

With the results obtained from the tests and analyses and the design objectives presented in the Statement of Work Volume II, Appendix A, a Flight Research Vehicle (FRV) could then be designed with a high degree of competence. The basic features of this vehicle, recommended further test programs, and schedules are reviewed in the final portion (Phase III) of this report.

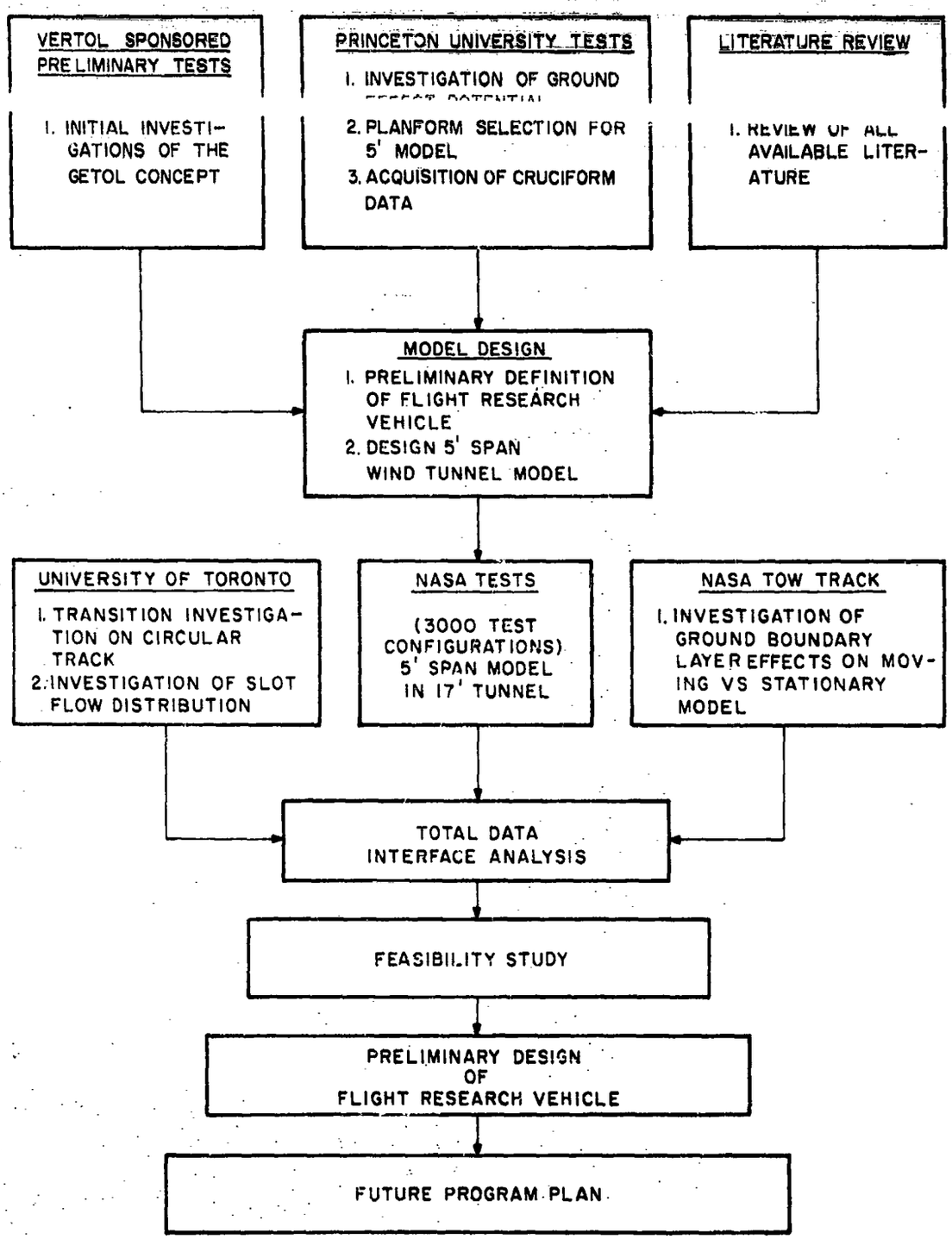
VERTOL SPONSORED PRELIMINARY TESTS
1. INITIAL INVESTIGATIONS OF THE GETOL CONCEPT
PRINCETON UNIVERSITY TESTS
1. INVESTIGATION OF GROUND
2. PLANFORM SELECTION FOR 5' MODEL
3. ACQUISITION OF CRUCIFORM DATA
LITERATURE REVIEW
1. REVIEW OF ALL AVAILABLE LITERATURE
MODEL DESIGN
1. PRELIMINARY DEFINITION OF FLIGHT RESEARCH VEHICLE
2. DESIGN 5' SPAN WIND TUNNEL MODEL
UNIVERSITY OF TORONTO
1. TRANSITION INVESTIGATION ON CIRCULAR TRACK
2. INVESTIGATION OF SLOT FLOW DISTRIBUTION
NASA TESTS
(3000 TEST CONFIGURATIONS) 5' SPAN MODEL IN 17' TUNNEL
NASA TOW TRACK
1. INVESTIGATION OF GROUND BOUNDARY LAYER EFFECTS ON MOVING VS STATIONARY MODEL
TOTAL DATA INTERFACE ANALYSIS
FEASIBILITY STUDY
PRELIMINARY DESIGN OF FLIGHT RESEARCH VEHICLE
FUTURE PROGRAM PLAN

TECHNICAL PROGRAM (PHASE I)

Phase I Determination of Preliminary Flight Research Vehicle (FRV) and Wind Tunnel Model

General

The initial qualitative studies conducted at Princeton University as company sponsored program pre-empted the Boeing-Vertol decision to further investigate the Ground Effect Take-off and Landing (GETOL) type aircraft. This led to the submittal of a proposal to USATRECOM which resulted in the award of a contract to the Vertol Division of the Boeing Company to determine the feasibility and potential of such an aircraft (see Figure 1) through comprehensive wind tunnel tests and proper design studies. Described in Phase I of this report is the initial portion of the Integrated Study Program discussed previously in the Introduction which made possible the determination of the "Second Generation Preliminary Flight Research Vehicle for GETOL". This configuration became the design basis for the GETOL wind tunnel model. The major portions of Phase I are:

1. Literature Survey
2. Analyses of GETOL Configuration
3. Analysis and Selection of the Final GETOL Configuration

Literature Review

Upon receiving the acceptance of the Plan of Performance from TRECOM, the first step taken in the Integrated Study Program was a survey of all existing literature, available to Boeing-Vertol, on Ground Effect Machines. This entailed reading through this material to digest the information, then assessing its value and relevance to a Ground Effect Take-off and Landing Aircraft. Some of the data were very applicable in the hovering mode and aided in following performance analyses. Appendix B of Volume II summarizes this effort in the following manner:

1. Date of Publication
2. Title
3. Excerpt
4. Comments

The excerpt and comments are purely the interpretations of the authors as to their immediate contribution to the subject effort.

TECHNICAL PROGRAM (PHASE I)

Analyses Of GETOL Configuration

Taking the pertinent information from the literature review, an assimilation of this information was achieved in the analyses of the GETOL configuration. The three major sections of these analyses were (1) Parametric Studies, (2) Performance Analyses, and (3) Preliminary Tests at Boeing-Vertol.

The initial step in the investigations was to list the design objectives stated in the Statement of Work (see Volume II Appendix A). Two additional objectives were established by Boeing-Vertol:

1. Have fan axis of rotation parallel to the free stream air.

2. Provide two fans outboard of fuselage.

Since the major area of the flight regime is as an airplane configuration, the fan axis of rotation must be parallel to the free stream air to provide efficient operation. This requires turning the air from the horizontal direction down into the wing and then spanwise out the wing to the slot. If one shrouded fan in the fuselage is used, the air must not only be turned through two 90 degree turns but also travel the length of half the span, thus resulting in a large internal friction loss. The use of two shrouded fans has these advantages: (1) useful fuselage (more payload capability), (2) short flow lengths (lower internal friction losses) (3) small fans and shrouds (better aerodynamics).

These objectives then formed the ground rules for the parametric studies (performance analyses and preliminary tests) discussed under Phase I. In this discussion of performance, it must be stated that the information available was for thick plenum type ground effect machines (GEM's). Very little data were available for GEM's with an internal cross section as narrow as that imposed by the airfoil section. What effects the internal thickness had on distribution and performance were not known. These effects on performance were neglected in the initial investigations conducted under Phase I.

Parametric Studies

Once the design objectives were established, an investigation of a parametric nature was initiated to study the size, gross weight and velocity attainable. Since the cross section of an airfoil is extremely low, to eliminate a drastic contraction in flow area which leads to high spanwise velocities in the wing and high friction losses, a thick airfoil was required. This is necessary from the internal flow requirements and from the external aerodynamic design in which a drag penalty resulting from thick airfoil sections must be considered. A NACA 4418 airfoil section was selected as being the best compromise of the two conditions.

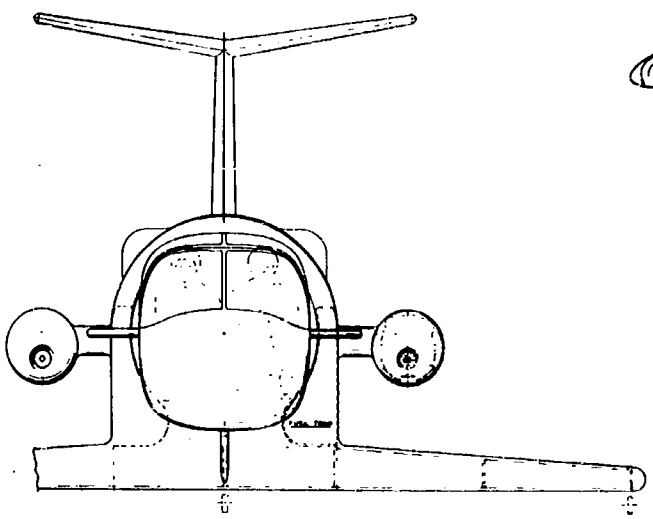

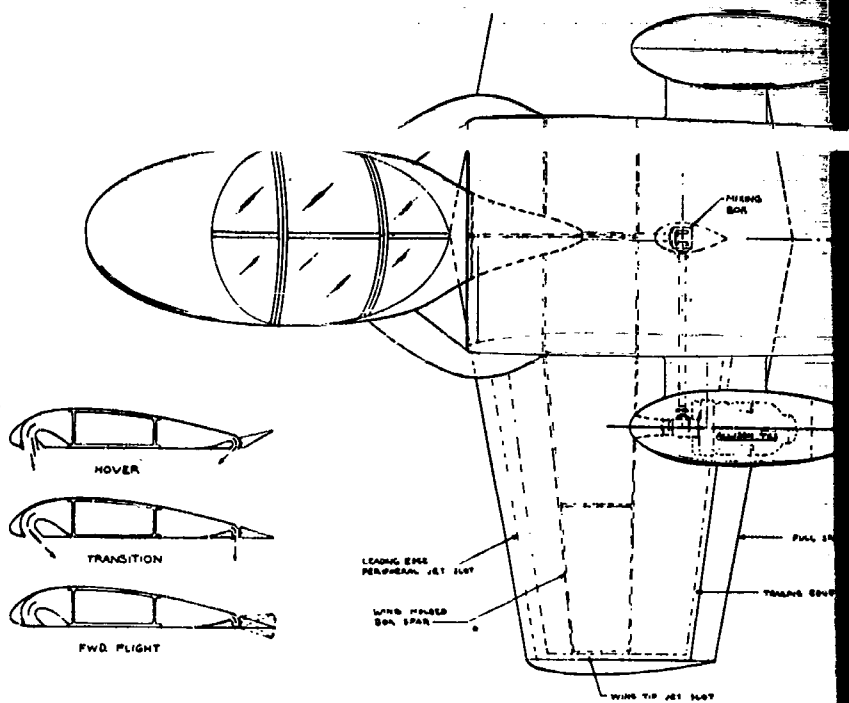

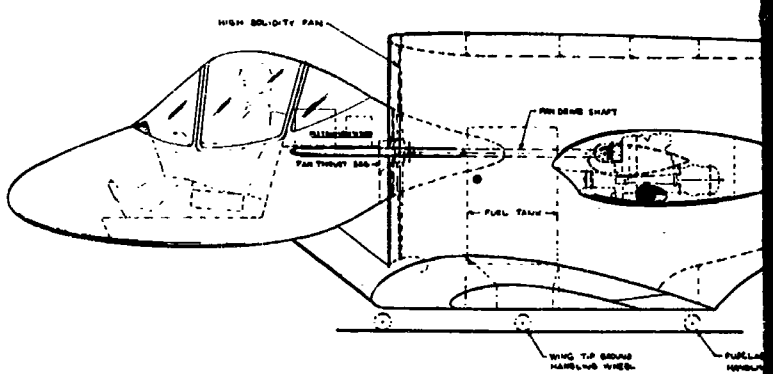

DESIGN PARAME

GW	3,000 LBS	b	
SW	130 FT²	c	
W/S	23	t	
AR	3.6	Vj	
AFAN	16 FT²	VAXIAL FA	
ASLOT	14 FT²	Q	
ANOZZLE	11 FT²	SHPTOT	
AIRFOIL	4415	Δ PFAN	

Figure 1. Propo
Configura

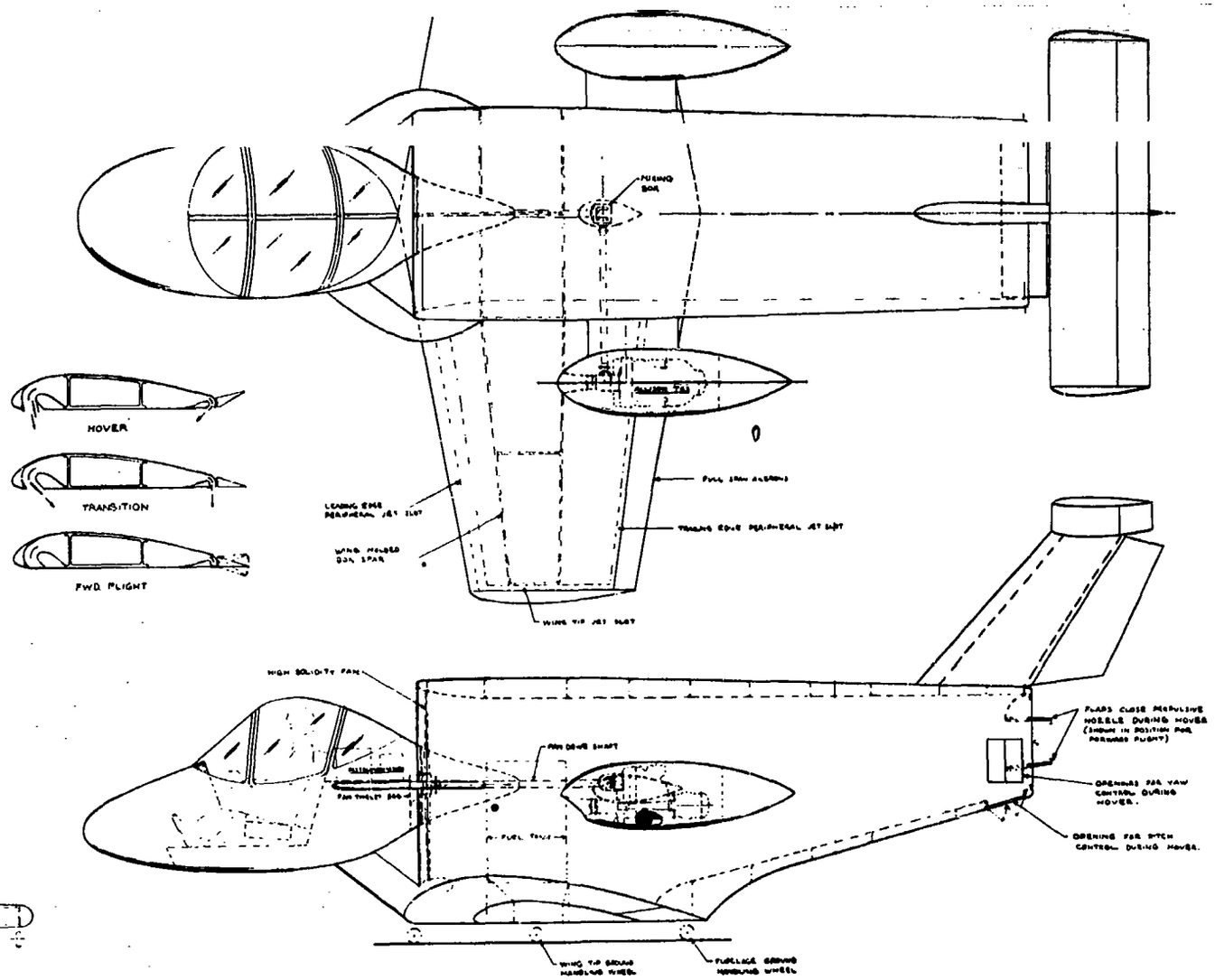

DESIGN PARAMETERS

GW	3,000 LBS	b	21.7 FT
SW	130 FT²	c	6 FT
W/S	23	t	.271 FT
AR	3.6	V_j	216 FT
AFAN	16 FT²	$V_{AXIAL\ FAN}$	
ASLOT	14 FT²	Q	3020 FT³/SEC
ANOZZLE	11 FT²	SHP_{TOT}	500 (2-T 63 ENGINES)
AIRFOIL	4415	ΔP_{FAN}	78 PSF

Figure 1. Proposed GETOL Configuration

From the Princeton data, hovering performance was obtained for Aspect Ratios of 1 to 4. For forward flight higher Aspect Ratios of 6 to 8 are best for performance requirements. A parametric study was conducted for a range of Aspect Ratio of 2 to 8 and the resulting value selected was approximately 3.35 based on its compatibility with hover and forward flight. This analysis was extended to determine the wing loading that would fulfill the hovering and the forward flight requirements and resulted in the selection of a wing loading of 20 lb/ft^2.

With the Aspect Ratio and wing loading known, a relationship was obtained between the power required per pound of gross weight and equivalent flat plate area loading. This relationship is one of major importance in determination of the power required to achieve a given maximum velocity. Since the parameters were already established and the previously discussed relationship obtained, a flat plate area loading of 900 lb/ft^2 and a power required per pound of gross weight of 0.2 hp/lb was determined as necessary for achieving a 250 MPH speed at SL. This established the basic configuration upon which the detailed analysis was performed.

Performance Analyses

With the data from the parametric analysis, a gross weight was selected and the configuration was then defined.

Layouts incorporating this information were intiated to permit more detailed analyses. To determine the required power plant, an estimation of the actual equivalent flat plate drag area was made. This permitted a performance analysis to be used in the selection of a power plant and propulsive system. Stability and control investigations were performed using the hovering data obtained from Princeton University. The configuration that resulted from these analyses is shown in Figure 2 and all discussions of performance refer to this figure.

Drag Estimation: To establish any performance characteristics, it is first necessary to develop the overall equivalent flat plate area of the configuration. This estimation, listed in Table I, was obtained by methods discussed in Reference 2. The configuration was based upon this estimation and is shown basically by Figure 2.

Power Requirements: The power requirements for a GETOL configuration were separated into two specific areas, the first, hover and the second, forward flight. At this time, these two areas were the only ones for which data had been obtained and it was further established that the power requirements for transition would not exceed that of the hovering or high speed forward flight. From the previously discussed drag analyses, power requirements were determined to obtain 250 MPH at sea level.

TECHNICAL PROGRAM (PHASE I)

TABLE I

Item	Equivalent Flat Plate Area
Fuselage	1.60
Vertical tails	.18
Tail Boom	.32
Horizontal Tail	.31
Duct	1.04
Louvres	.46
Hub & Shaft Fairings	.18
Interference	.43
TOTAL	4.52

To estimate the hover power, a flow analysis through the system had to be established. The major limiting assumption in the investigation was the flow distribution through the wing and slots. The distribution and the internal and slot velocities having been fixed, the power for hovering could be obtained. With this information, further analysis was performed and a balanced match between hovering and high forward flight (250 MPH) was achieved. This balance in power was one of the basic objectives of the GETOL design. Power requirements during transition were realized from the wind tunnel tests.

Stability and Control: By combining the peripheral jet and an airfoil section there arises a problem of the compatibility of the control system for hover and forward flight. A rectangular peripheral jet has good stability in the lateral direction and has neutral longitudinal stability at low hover heights stated in conventional aerodynamic terminology for a wing. As the height is increased the stability becomes neutral or slightly negative. The Center of Pressure for a peripheral jet is located at the 50% chord in hover. In forward flight, the Center of Pressure or lift of an airfoil is at approximately the 25% chord. This indicates that there must be a capability of handling large trim changes or obtain a method of shifting the hover Center of Pressure forward. There must also be some means of changing the stability characteristics.

From test work discussed in Reference 3, there is an increase in the above mentioned longitudinal hover stability by the addition of a lateral slot but at the

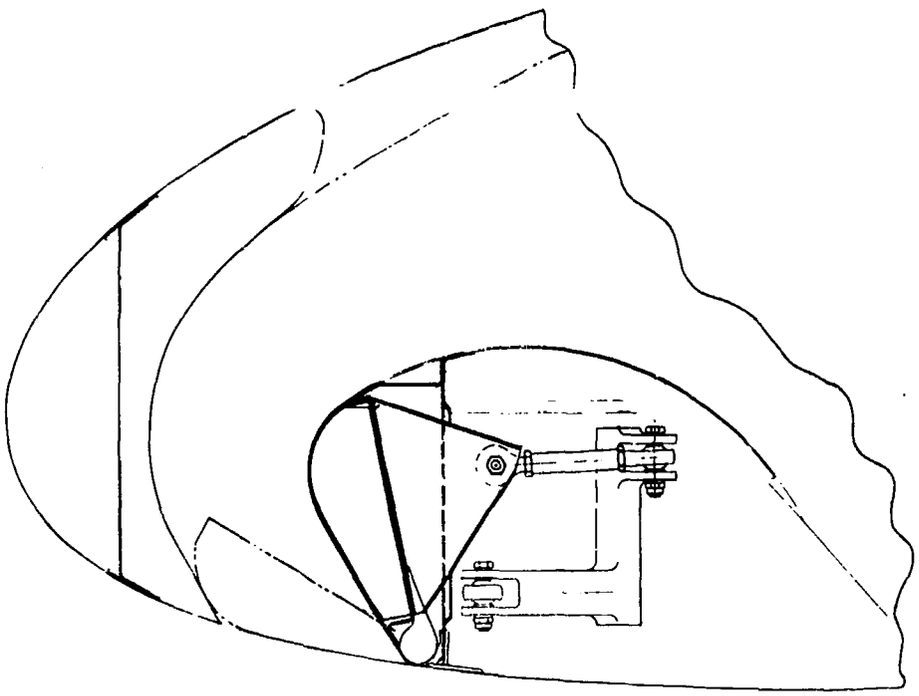

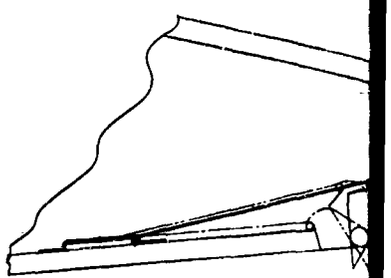

TYPICAL

TYPICAL NOSE AND TIP JET

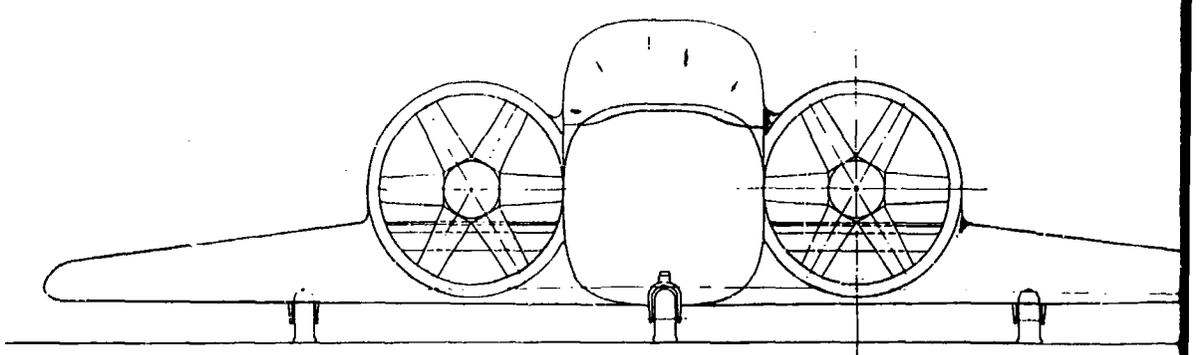

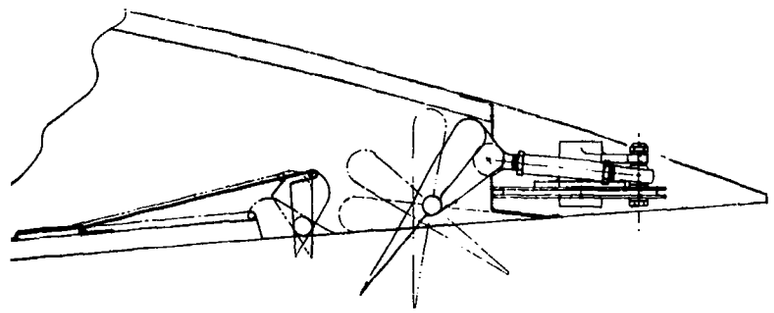

TYPICAL TRAILING EDGE JET

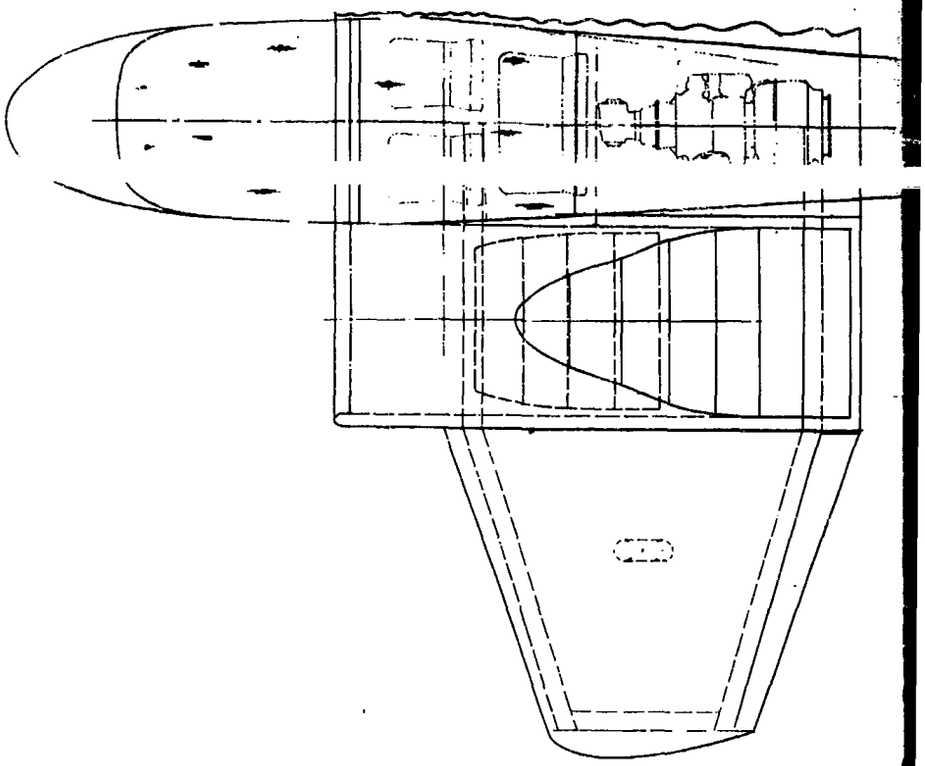

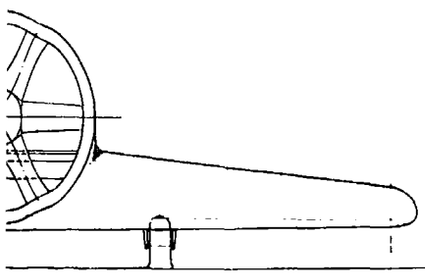

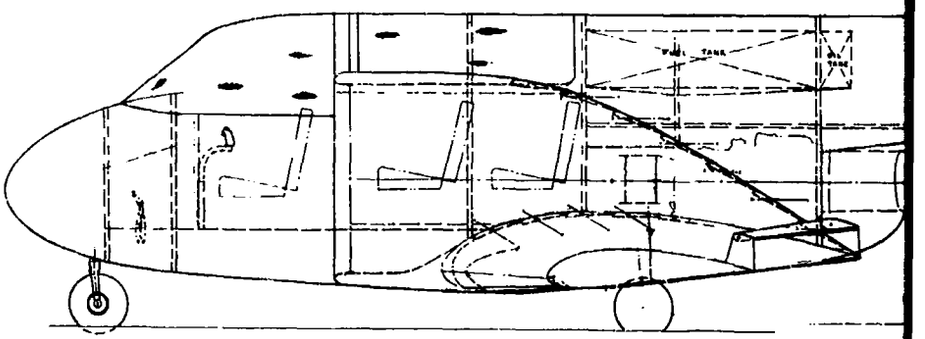

GW · · ·
SW · · ·
W/S ·
AR · ·
A FAN
A SLOT
AIRFO

2

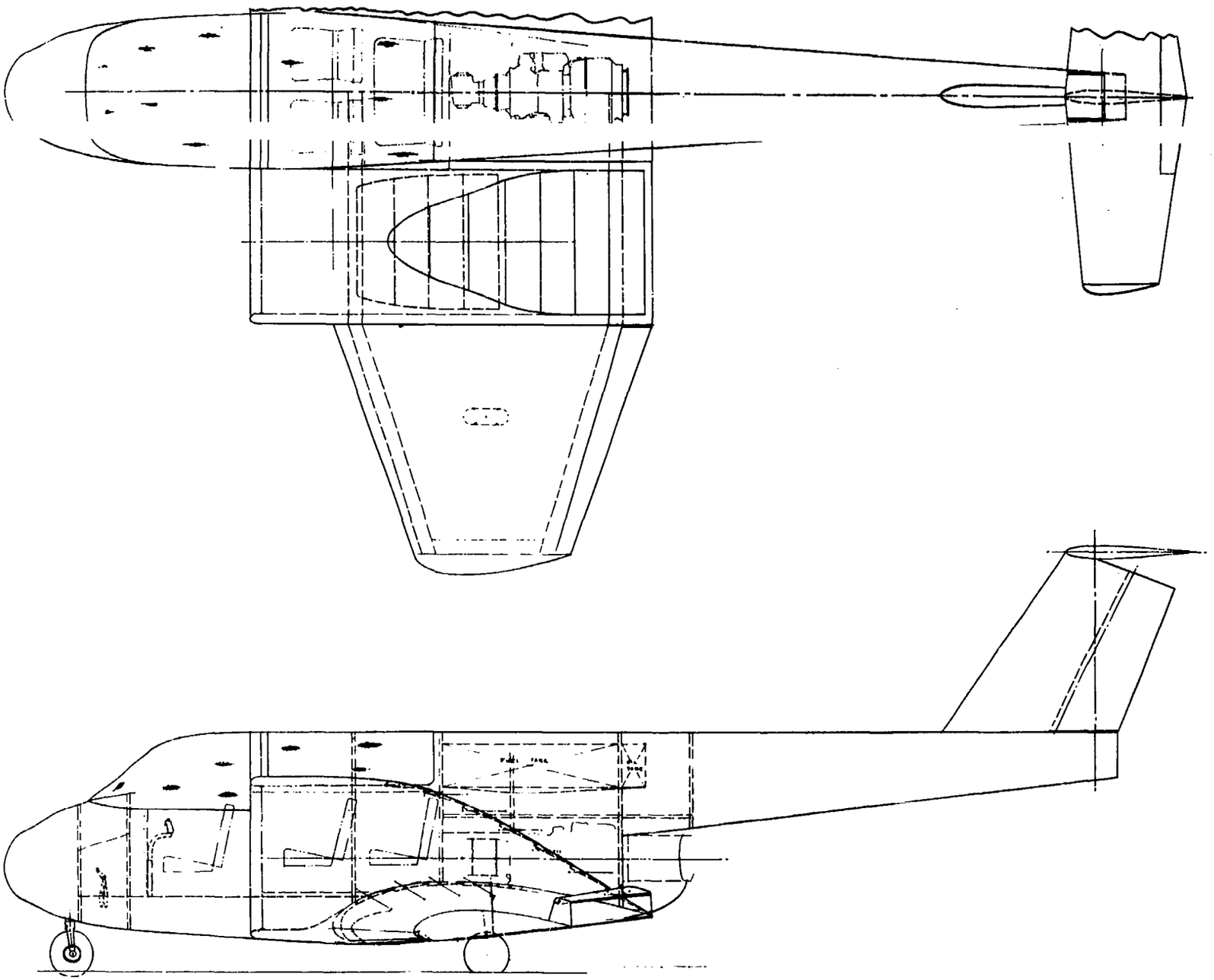

DESIGN PARAMETERS

GW	4,000 LBS	b	25.6 FT
SW	200 FT^2	C_{ROST}	9 FT
W/S	20 LB/FT^2	C_{TIP}	.4 FT
AR	3.28	V_{JAUG}	200 FT/SEC
A_{FAN}	12.1 FT^2/FAN	$V_{AXIAL\ FAN}$	200 FT/SEC
A_{SLOT}	24.2 FT^2	Q_{TOT}	4480
AIRFOIL	4418	SHP_{TOT}	1150 (1-T53 ENGINE
		ΔP_{FAN}	100 PSF

3

Figure 2. Second Generation GETOL Configuration

...aspects of performance. From the results of the Princeton tests (see Page 41) it was found that the flow distribution has a definite effect on the stability. The plenum type planforms, having an almost uniform distribution, do not have the same stability characteristics as a wing type planform because of this distribution problem. A uniform distribution could be desirable but the effect of varying distribution is not known and therefore some degree of non-uniformity may be required.

Propulsion System: The overall propulsion system is divided into the following three major areas:

1. Power Plant
2. Fan
3. Nacelle.

This system must not only provide for the hovering regimes but also for forward flight where the aircraft flies as a ducted fan configuration. The design of these items were developed from the design objectives and the results of the performance analyses.

Power Plant - To obtain the hover height of 3 feet and to have a maximum velocity of 250 MPH a power plant must have a maximum continuous rating of approximately 1200 horsepower. The engine selected for this configuration of the GETOL Flight Research Vehicle (FRV) was the T-53 (LTC1L-1) which has the following ratings:

Rating	HP	SFC	RPM
TO	1400	.605	6000
MIL	1270	.617	6000
NRP	1150	.634	6000

This engine has a constant output shaft rpm which is required to meet the design requirements of the fan.

Fan - To achieve fuselage usefulness, a two fan configuration was selected. This, in conjunction with the conditions imposed by the performance requirements, established the basic design parameters. In hovering, each fan was required to have an output of 4840 cfs with a pressure rise of 100 lb/sq. ft. As the analyses of the fan progressed, discussions were held with NASA personnel familiar with fan and compressor design. The conclusion from these discussions was to use a single stage fan with variable inlet guide vanes designed with Free Vortex Theory. This results in a uniform velocity distribution behind the fan thereby requiring minimum power and eliminating distribution problems that could arise

a 4 foot diameter fan with a hub diameter to tip diameter ratio of .4 was selected.

In forward flight a variable exit nacelle was required to operate the fan at the design point and have the required exit velocity.

Nacelle - In hovering, air from behind the fan must be directed down into the wing and in forward flight the air must be directed straight aft. To accomplish both tasks, an adjustable door is provided in the back of the nacelle. The internal contour was developed for the hover condition when this door is closed. As the air flow exits from the fan, a gradual expansion is required to decrease the velocity of the air as it enters the turning vanes in the wing. An expansion ratio of 2 was selected for the wing opening; thereby establishing the stream lines of flow in the nacelle and also the contour of the nacelle.

When the door is partially open, the major portion of the flow goes to the peripheral slot to provide lift and the remaining air issues straight back to provide propulsion. The door, having some curvature to blend with the external and internal shape, acts as an airfoil immersed in a high velocity slipstream and thus develops lift to further augment that produced by the peripheral jet.

When flying as an airplane, this door opening can be varied to achieve the desired exit velocity for maximum propulsive efficiency.

Preliminary Testing by Boeing-Vertol

Preliminary internal flow testing was conducted to determine the pertinent internal flow areas, velocity distributions, and pressure losses. These tests used varied nacelle sizes and shapes as well as a straight bellmouth entrance into the wing. The bellmouth established the conditions of no internal loss in the nacelle and perfect turning into the wing to determine the required turning radius of the air into the wing. The velocity distribution and pressure losses of this system were acceptable and it was necessary that similar results were obtained from the nacelle entrance.

Tests with different nacelle sizes were made and it was determined that the nacelle entrance was almost as efficient as the bellmouth. It was also determined that the majority of pressure losses occurred in the entrance to the wing. With proper sizing of this entrance and proper turning radius, the pressure loss could be minimized.

These tests and the results are discussed in greater detail in Phase II on Page 23.

Analysis and Selection of the Final GETOL Model Configuration

From the analyses and tests performed, a second generation GETOL Flight Research Vehicle (FRV) was designed (see Figure 3) and became the basis for the model design. Minor modifications to the fuselage and the nacelle had to be

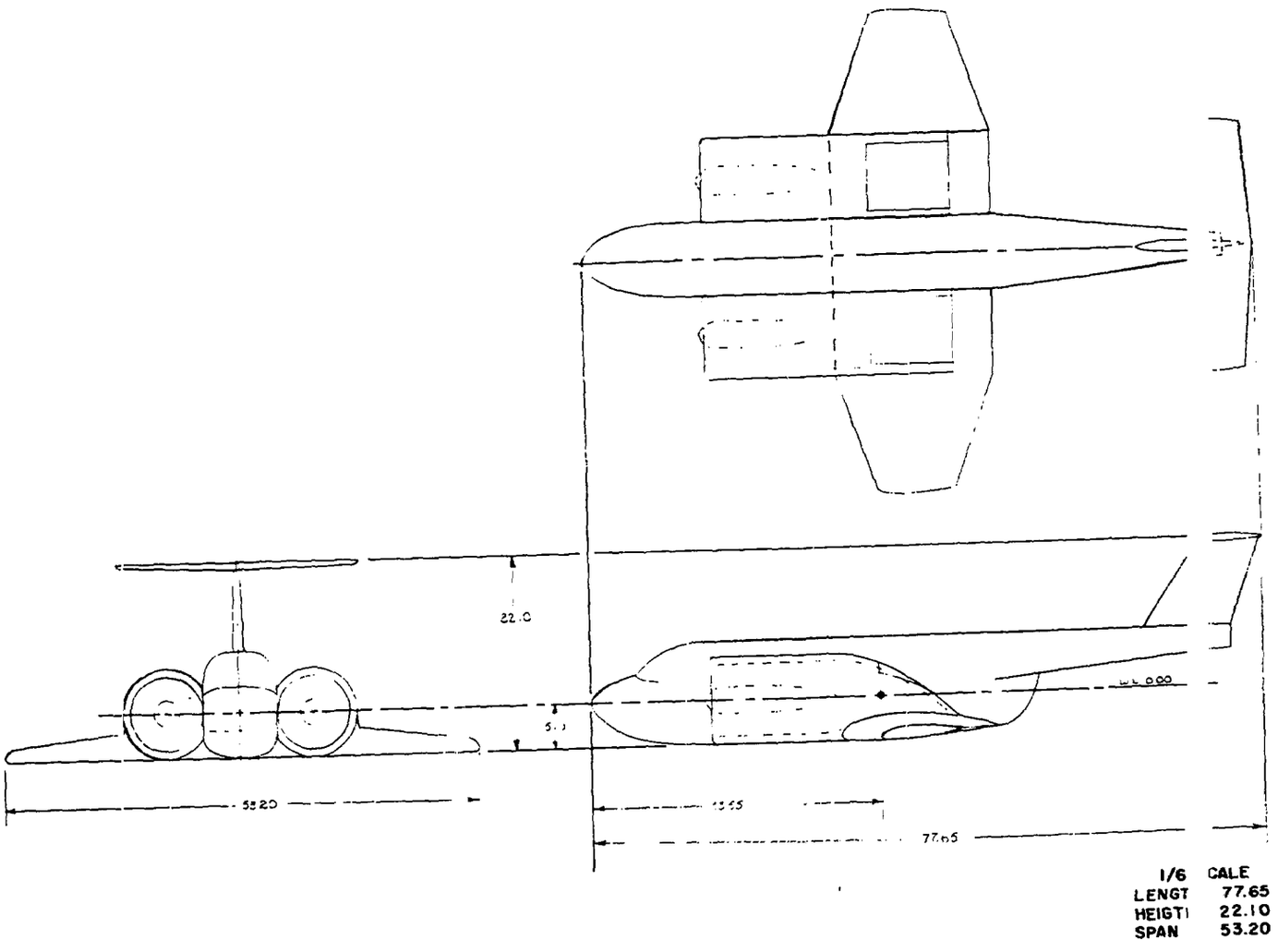

Figure 3. Configuration of the GETOL Wind Tunnel Model

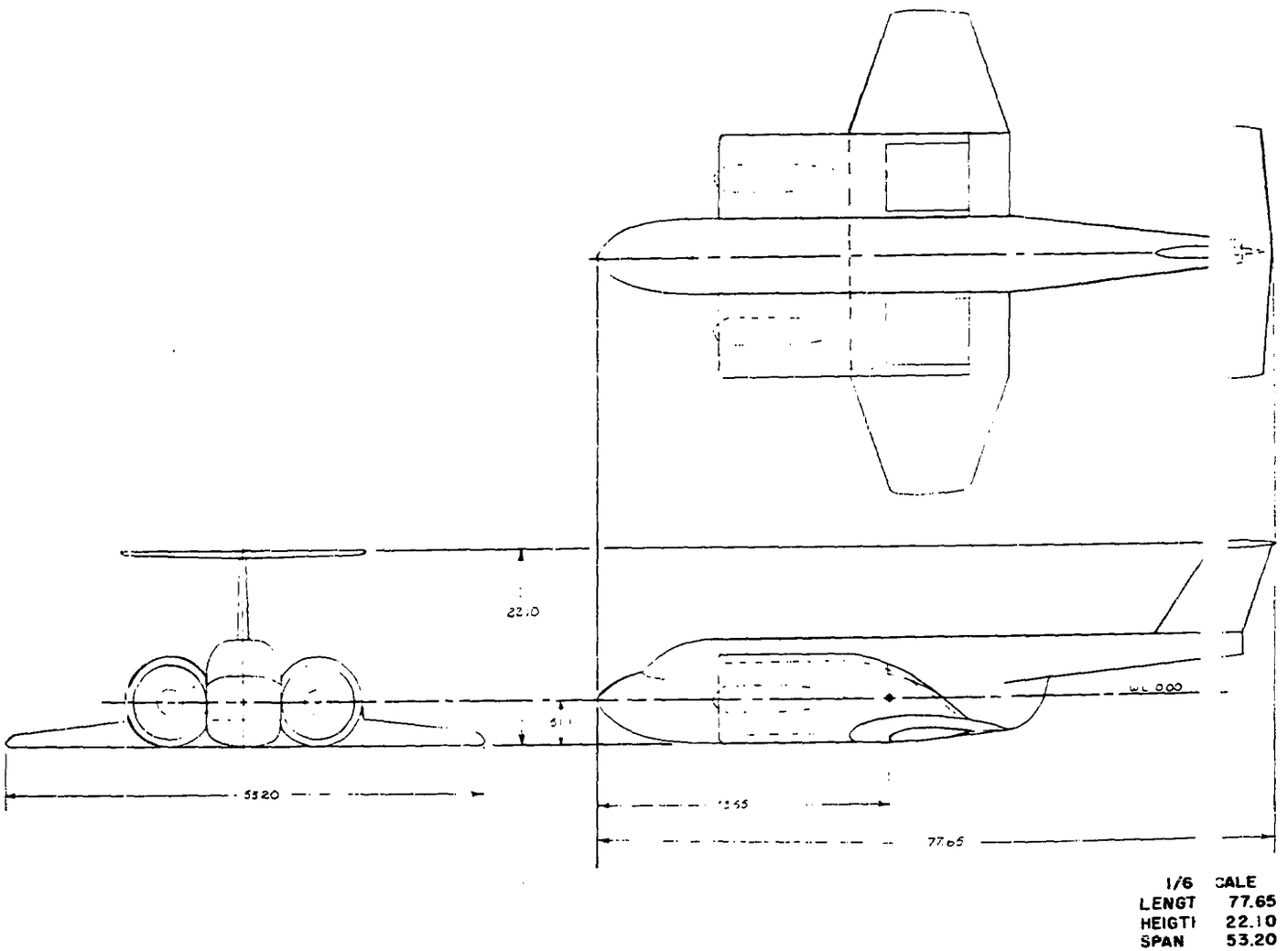

Figure 3. Configuration of the GETOL Wind Tunnel Model

made to facilitate installation of instrumentation. Analyses were conducted to determine the power required for the range of variables that needed to be investigated.

Wind Tunnel Model

The wind tunnel model was designed as a one-sixth scale of the Preliminary Flight Research Vehicle (FRV). This configuration has been selected to fulfill both a "general data" program for GETOL and an "aircraft design data" program for the final Flight Research Vehicle (FRV). Certain aspects of the test philosophy had to be eliminated to accomplish the overall task in the specified amount of time that was allotted for the test program. An example of this was that the spanwise flow in the slots was not eliminated by using slot vanes. These vanes would improve hovering ability but would cause many complications in the testing variations of slot arrangements.

It should be stressed once more that the main purpose of the wind tunnel model was to serve as a tool to determine the feasibility and potential of the GETOL concept in general. The model itself as seen in Figure 4 has a wing span of 53 inches and two 8.5 inch diameter fans. External contours are formed from a 1/8 inch fiberglas shell that is mounted to a basic frame. This frame is comprised of two main beams to which a balance is attached and from which the model is supported.

Basic variables built into the model to be investigated were slot exit angle, slot thickness ratios, slot area and nacelle door opening. All of these model variables with the exception of the nacelle door opening were obtained by having interchangeable pieces that fit into the base of the wing to form the contours of the peripheral slot. Door opening was obtained by removing the bolts from the brackets on the door and relocating them in the required holes.

The propulsive system was a single stage fan with variable inlet guide vanes. Power for the fan was provided by high pressure air.

Planform (Wing)

The planform of the wing was selected as a compromise between hovering and forward flight requirements. Princeton and Toronto Universities conducted tests with models having a planform similar to that of the Boeing-Vertol wind tunnel model. The model tested at Princeton (Figure 5), discussed in greater detail on Page 37, has an Aspect Ratio of 3.35. Lift augmentation and pitching moment were measured to establish basic trends.

Tests conducted at Princeton and Toronto University indicate a design problem with the slot flow. By observing smoke patterns and pressure surveys, it was determined that the flow was separating from the nozzle walls. A redesign of the nozzles partially corrected this problem, thus improving the GETOL efficiency.

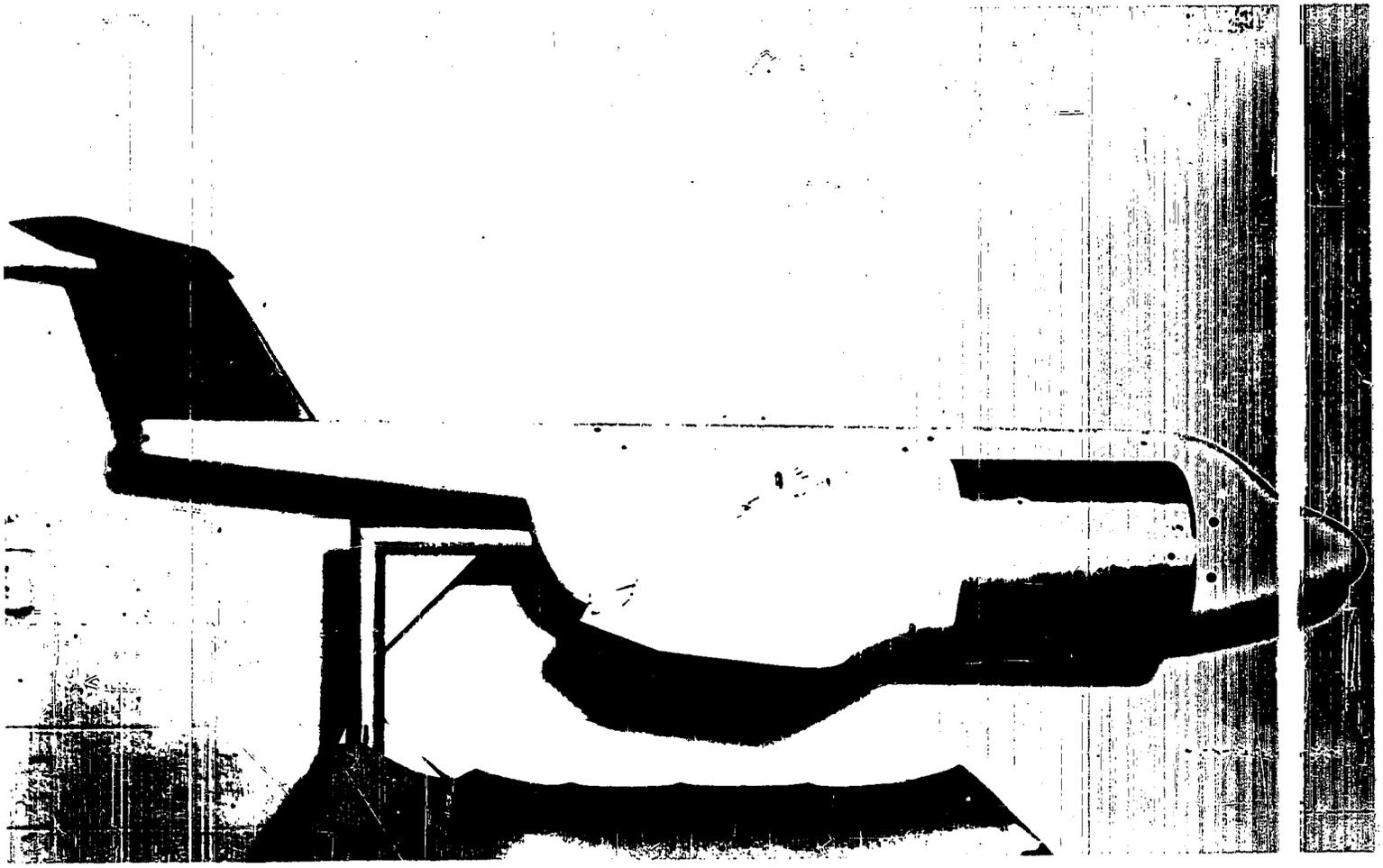

Figure 4. NASA Wind Tunnel Model

Figure 5. GETOL Planform (Wing)

TECHNICAL PROGRAM (PHASE I)

Fan

Aerodynamic design of the model fan was aimed at obtaining full scale flow velocities. The requirements of the model fan were a pressure rise of 100 lb/ft^2 for an inlet velocity of 200 ft/sec.

The propulsive system designed and manufactured by the Tech Development Company (see Figure 6) was a single stage fan with variable inlet guide vanes to provide a flexible design. Fan power was provided by high pressure air being supplied to the hub of the fan. This air then travelled out the hollow blade to a small orifice at the tip of the trailing edge of the blade thus providing a driving force to turn the fan.

A basic design objective was to have full scale velocities in the internal flow system and through the slot.

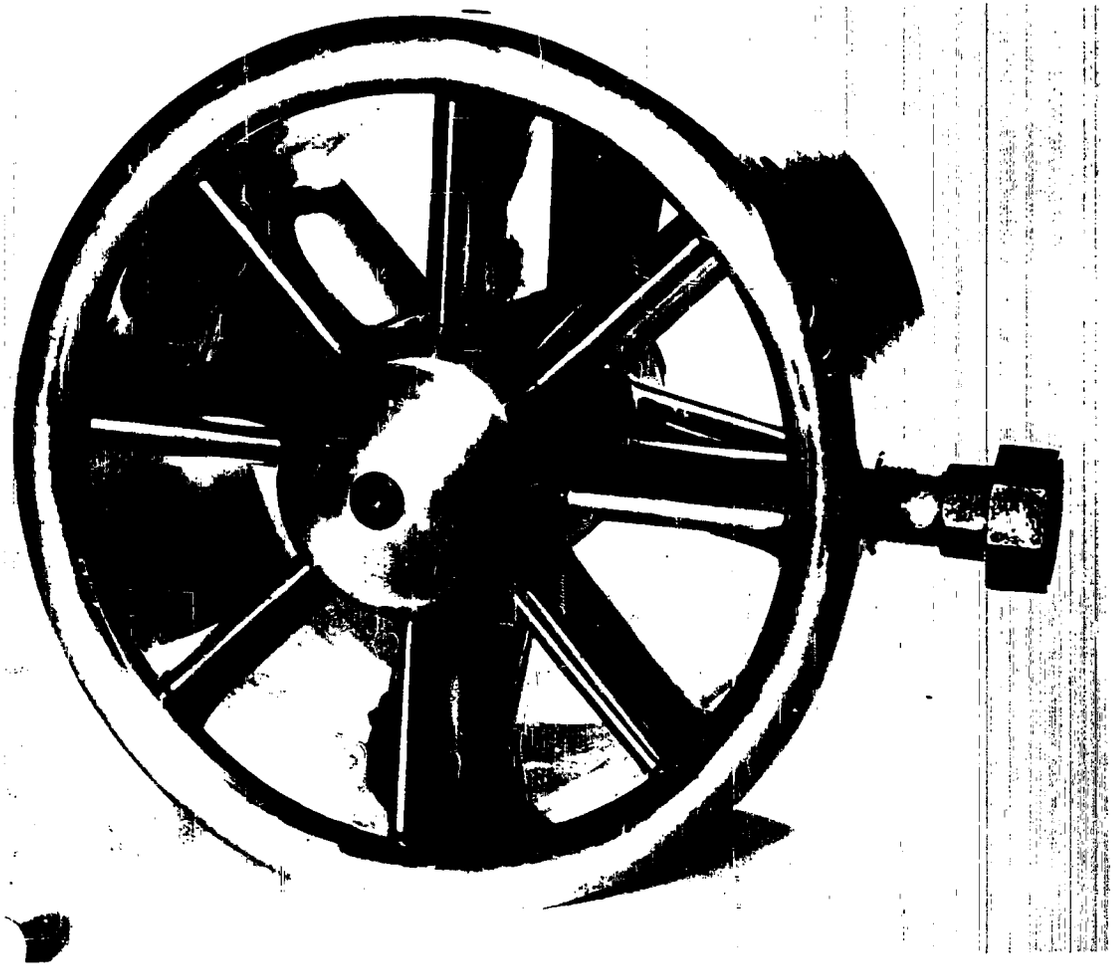

Figure 6. GETOL Fan

TECHNICAL PROGRAM (PHASE II)

Phase II – GETOL Model Testing And Data Analysis

This section describes the integrated test programs conducted to determine the feasibility and potential of Ground Effect Take-off and Landing (GETOL) aircraft. In addition, comparisons of data obtained from various development tests are made with data obtained from static room and wind tunnel testing performed by NASA. Further, final analysis of the data are made and serve as a basis for much of the design philosophy achieved from this analytical study program.

Boeing-Vertol Preliminary Tests

Preliminary Flow Tests

From the Performance Analyses described under Phase I on Page 11, a basic unknown was the internal losses incurred by having air from behind the fan turned down into the wing and turned again to flow spanwise out the wing to the peripheral slot. An internal flow test program was established to measure the overall pressure loss in a particular GETOL model shape to determine the nacelle flow area needed, areas of high loss, methods of decreasing flow losses by flow area corrections and internal velocity distributions. Investigation of the variation of nacelle flow area and wing entry opening did not permit the use of conventional model motors and fans. To eliminate this problem it was decided to draw air through the model with a large centrifugal blower and achieve the same results with a minimum amount of model change.

Figure 7 shows the basic internal flow test configuration and Figure 8 gives a pictorial view of the overall test setup. The model had two nacelles; one simulating the single fan configuration, the other simulating the two fan configuration. These were attached to the top of the plenum which was a hollow wing with peripheral slots (see Figure 9). The base plate was adjustable to obtain the effect of varying the front and rear slot thickness. Air was drawn through the model and flow visualizations were made by observing tufts through plexiglas windows in the top of the wing and the side of the plenum. A typical example of the flow visualization is shown in Figures 10 and 11.

A list of the pertinent data and the configurations tested are in Table II and are also illustrated in Figure 12. For each of these tested configurations, an investigation was made of the pressure drop of the air as it entered the wing to flow in a spanwise direction (see Figure 11). Figure 13 shows a Typical Pressure Profile at this measuring station for two configurations (No. 1 and 8). A summary plot presents the average pressure drop (see Table II) and the diffusion from the nacelle into the wing (see Figure 14).

After obtaining all the information at the various stations, a graph was prepared showing the pressure losses through the model for the design configuration shown in Table II (see Figure 15).

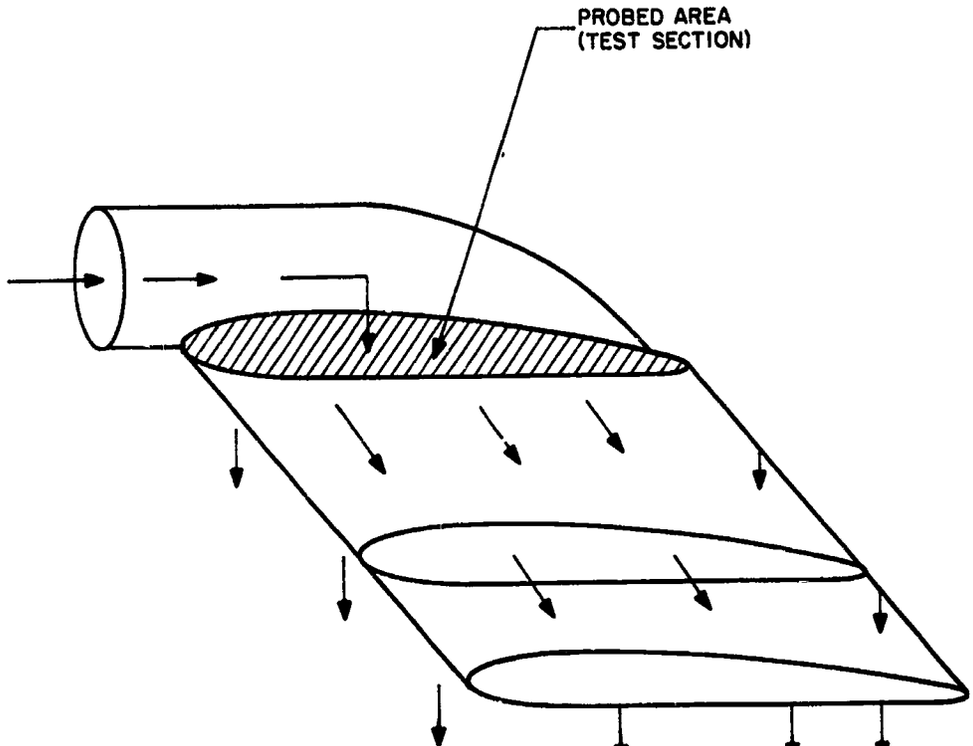

Figure 7. Internal Flow Test Configuration

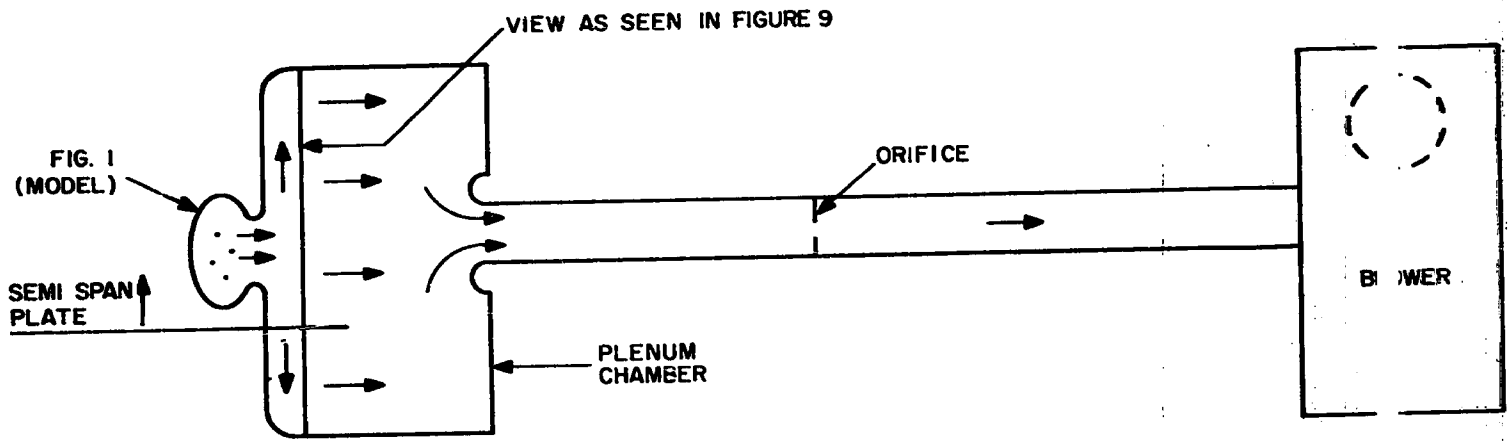

Figure 8. Overall Test Set-up

Figure 9. Plenum Chamber and Wing Slot

Figure 10. Flow Visualization of Bellmouth Duct with Blower On (Gap 3:1)

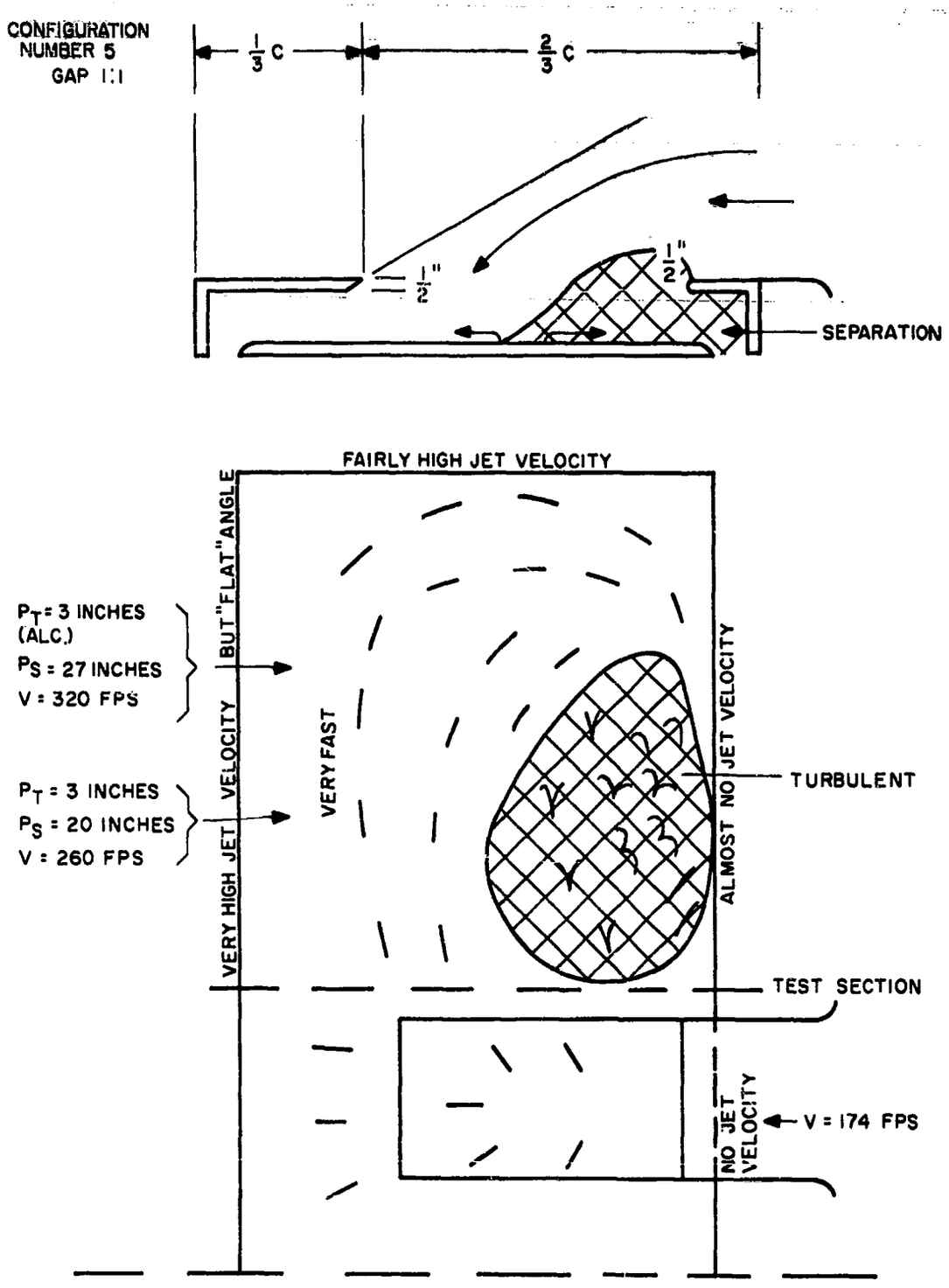

Figure 11. Typical Internal Flow Visualization

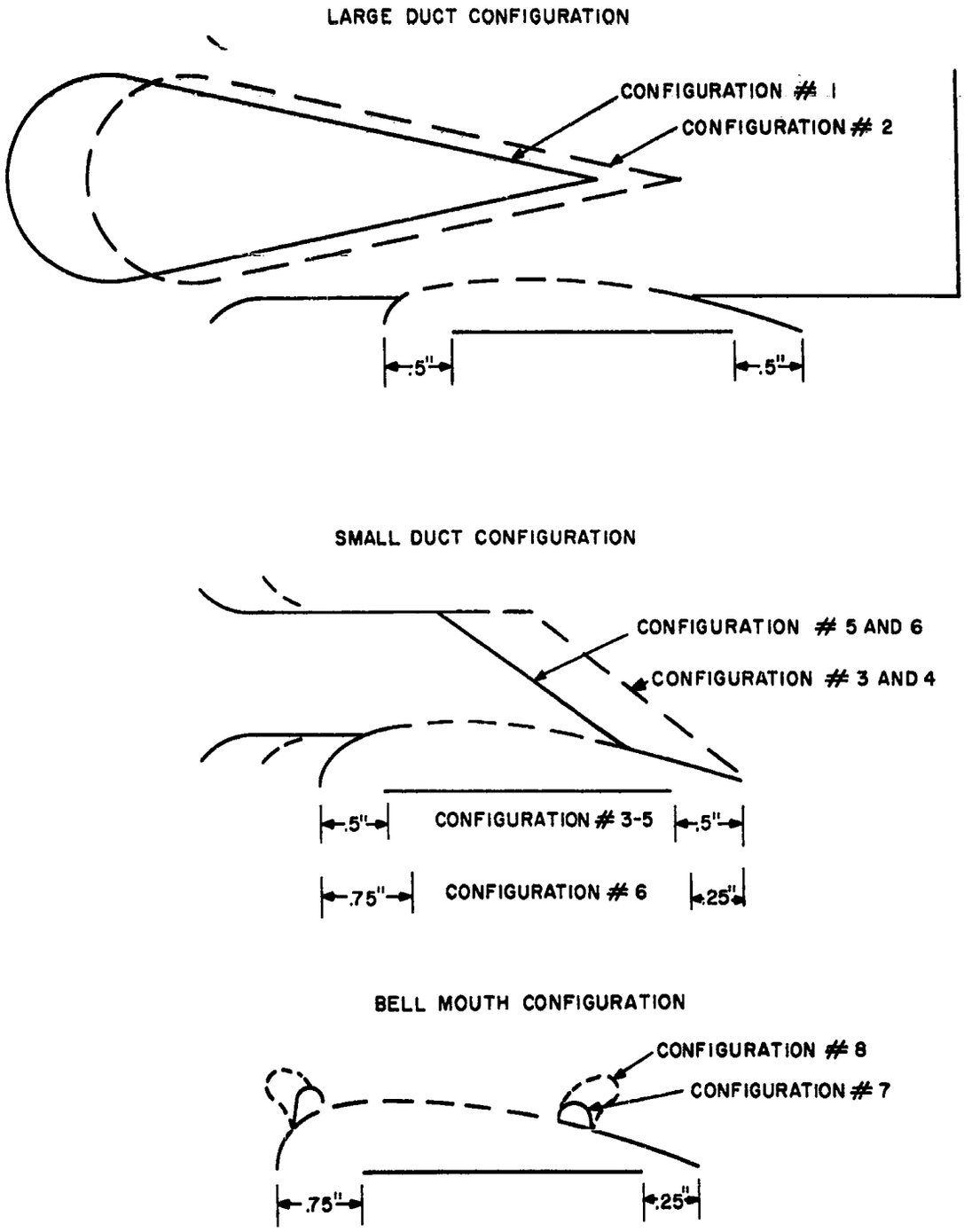

Figure 12. Tested Internal Flow Configurations

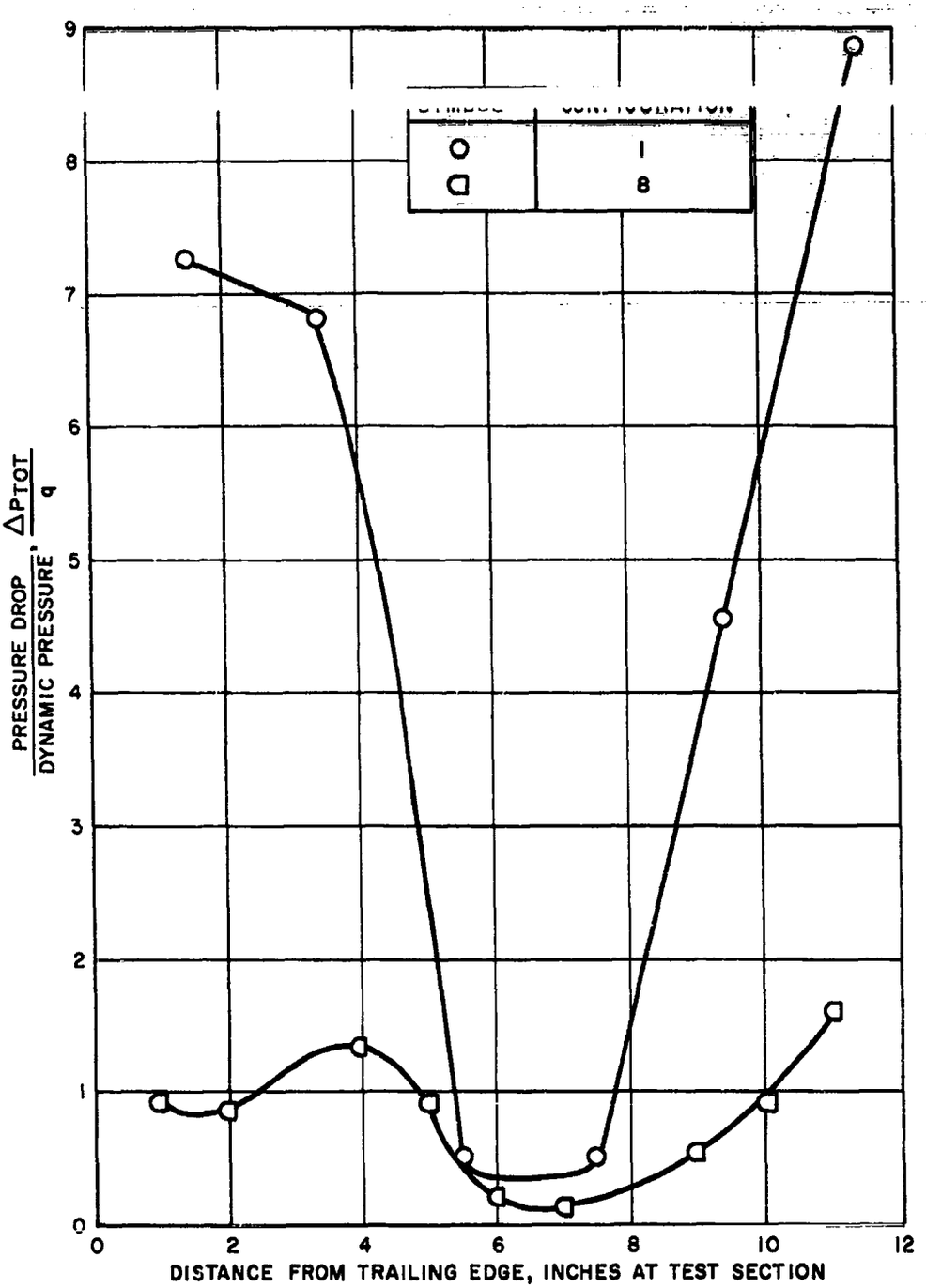

Figure 13. Typical Pressure Profiles (Configuration Nos. 1 and 8)

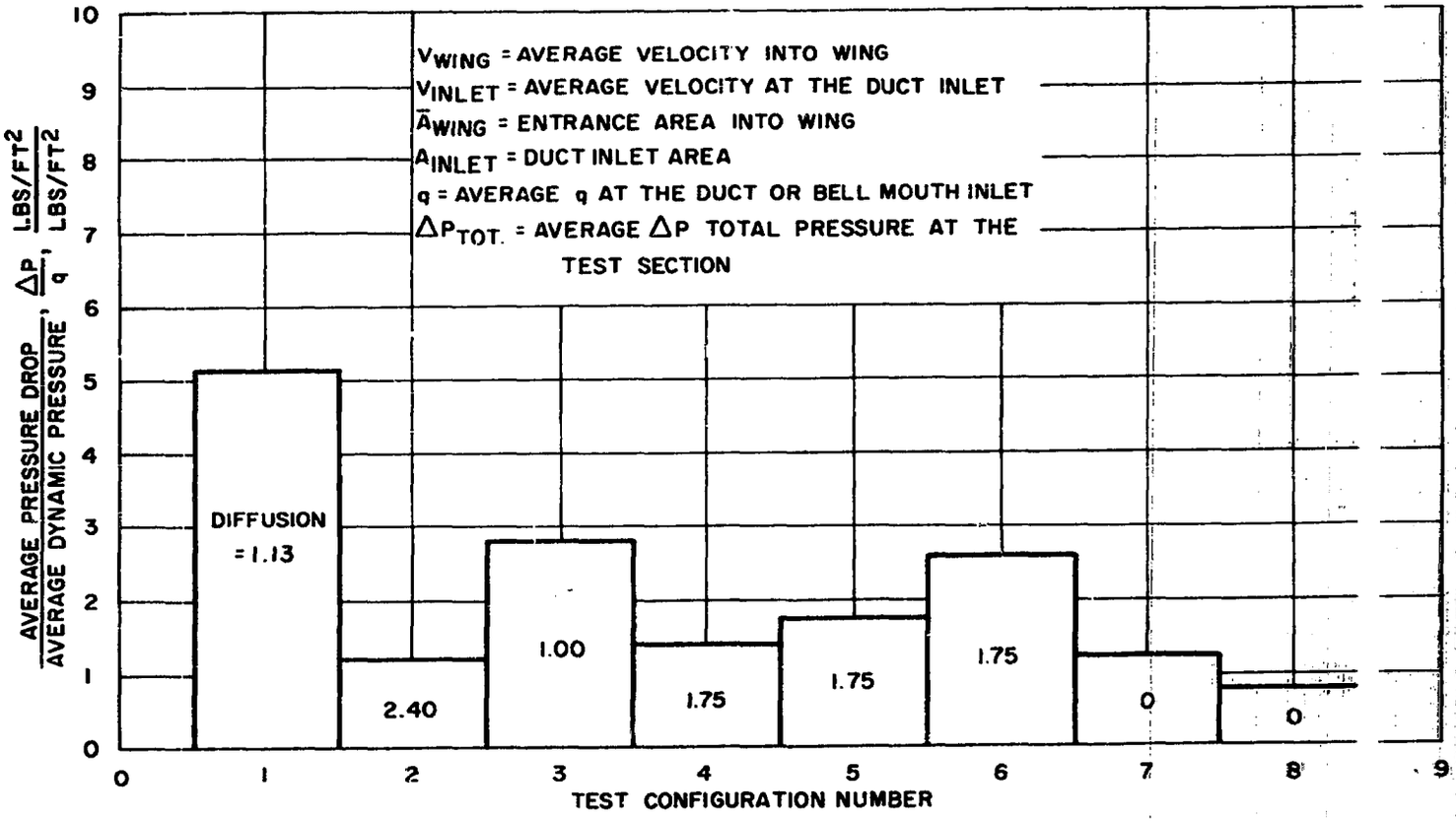

Figure 14. Average Pressure Drop and Diffusion for the Various Configurations

TABLE II

INTERNAL FLOW CONFIGURATION AND TEST RESULTS

Configuration Number	Inlet	Inlet Area (Ft^2) (A inlet, Ft^2)	Inlet Velocity (Ft/Sec)	Flow Q (CFM)	$\frac{\Delta P \text{ Tot}}{q}$ ($\leq$ aug)	Diffusion $\frac{\text{(A wing)}}{\text{(A inlet)}}$	Gap Ratio
1	Large Duct	.440	94	2,480	5.1	1.13	1:1
2	Large Duct	.207	182	2,260	1.2	2.4	1:1
3	Small Duct	.139	148	1,230	2.8	1.0	1:1
4	Small Duct	.139	189	1,580	1.38	1.74	1:1
5	Small Duct Forward	.139	174	1,450	1.75	1.74	1:1
6	Small Duct Forward	.139	126	1,050	2.60	174	3:1
7	Bellmouth 1	.243	144	2,100	1.25	0	3:1
8	Bellmouth 2	.243	159	2,320	.8	0	3:1
Model Design	Small Duct	.33	200	4,000	.5	2	-

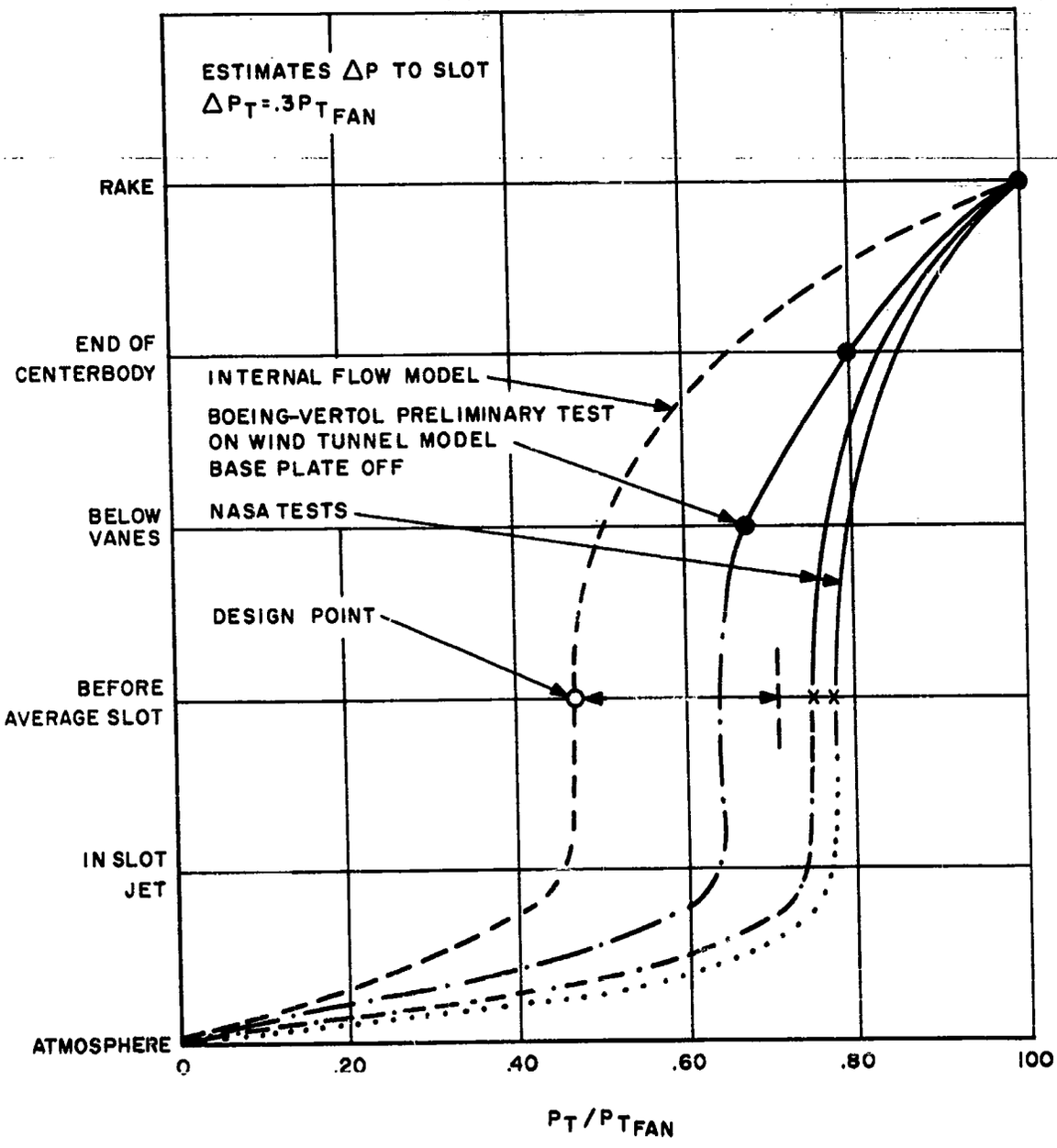

Figure 15. Pressure Loss at Various Stations Within the GETOL Model

From the results of the test it can be stated that with a high diffusion aft of the inlet (i.e. $\frac{A \text{ wing}}{A \text{ inlet}} = 2.0$) the pressure loss, relative to the inlet q, decreases. This occurred in configuration 2 and 4 and was relative to 1 and 3 respectively. Proper wing inlet distribution is extremely important for two following reasons:

1. With poor inlet distribution, the gap velocity may be non-uniform (see Figure 11).
2. With poor inlet distribution, the losses into the wing are high (Configuration No. 7 is better than Configuration No. 6 because of even inlet distribution.)

The corner radius of turn from the nacelle into the wing introduces a large percentage of the losses because of the high velocity air separation as it turns a sharp corner. Proper distribution reduces the high corner velocity and a large corner radius reduces the turning losses (note change in from Configuration No. 7 to Configuration No. 8 (see Figures 12 and 14) when the turning was reduced).

This testing shows that a $\frac{\Delta P}{q} = .5$ can be achieved with proper wing inlet distribution (inlet guide vanes) and large smooth turning radius.

Preliminary GETOL Model Testing

After model delivery to Vertol from the University of Wichita, the GETOL wind tunnel model (see Figure 4) was mounted on its test stand over a four by eight foot tufted ground board. A balance for measuring forces was not installed at this time and no force measurements were made. At this time (late March, 1961) functional and flow survey tests were conducted and operation of the model was satisfactory. The maximum fan drive air pressure available was 40 pounds/inch^2, while subsequent testing at NASA was conducted over the range of 100 to 200 pounds/inch^2. These tests permitted reasonable flow studies to be accomplished.

The first step taken was to set the turning vanes from the nacelle to the wing. They were adjusted to achieve minimum flow separation over the vanes. The windows in the wing base plate were used to observe the tufted vanes with flow through the model. Following this a flow survey around the peripheral slot was made. Using protractors and tufts, flow directions were determined and skirts were developed to provide the required jet directions, especially at the trailing edge. Total pressure distribution around the slot was considered quite uniform.

An investigation of the pressure levels was performed and losses at various stations within the model were measured at this time. Figure 15 provides this information as well as the results of the initial internal flow tests conducted at Boeing-Vertol. The conclusion is that the wing entry vanes provide

uniform turning so that the losses at this point (and for the whole flow system) are low.

Princeton University Tests (Planform)

General

In a parallel effort to the Boeing-Vertol GETOL Feasibility Study, initial work done by Princeton University has been utilized in the following manner:

1. As a guide for initial sizing of a GETOL aircraft and design of the wind tunnel model for NASA.

2. As a source of additional fundamental information on the significance of planform shape and flow distributions.

Princeton's interest in GETOL aircraft stemmed from their work in GEM's under ALART (Army Low Speed Aircraft Research Task) funding from TRECOM. They had been evaluating the lifting and trim variations of various basic planform shapes, from square through rectangular to triangular.

Although limitations in the information have been discovered, the results of this work are reported herein since much of Vertol's NASA model concept was based on this work.

A second data group from Princeton University was obtained from their test of an additional planform which represents the first generation GETOL with a straight tapered wing planform. This work uncovered two significant facts:

1. That for a given planform, varied slot flow distributions resulted in varied moment characteristics;

2. That all of Princeton's GETOL planform tests had been done with a two component balance (lift force and pitching moment, no thrust force) and consequently, although lift forces were proper, moments had not been correctly resolved.

With the discovery of flow distribution significance and after discussions with Princeton, Wichita, and Toronto Universities and with TRECOM it was agreed that a second generation GETOL planform (that being the Boeing-Vertol wind tunnel planform) should be tested to:

1. Measure forces and moments with a three component balance.

2. Specifically evaluate and determine some fundamental trends for the effect of slot flow distribution. Unfortunately this effort was not fully realized.

TECHNICAL PROGRAM (PHASE II)

The final task at Princeton University was their undertaking of an evaluation of a cruciform planform. The shape of a GETOL wing and fuselage naturally suggests such a slot shape possibility. This would represent an improvement in longitudinal stability as well as the ability to shift forward the hovering Center Of Pressure. To this end, a fairly simple cruciform model test was conducted by Princeton (under ALART funds) and the test data were made available to Boeing-Vertol. Flow distribution problems were inherent in this model (reverse flow for some portions of the slot was observed) but some general trends were obtained.

Testing Under The ALART Program

Four types of tests were performed at Princeton University and are described below.

Initial Planform Tests. Information from preliminary planform tests conducted by Princeton University was received early in 1960. The following characteristics of hovering were parametrically investigated:

1. Performance as a function of planform.
2. Static stability (longitudinal and lateral as a function of planform).
3. Center of Pressure location as a function of peripheral slot widths (wider at the leading edge).
4. The effect upon performance and stability of non-peripheral jet wings added to a GEM fuselage.

Six planforms have been tested (see Figure 16). The models were self-powered to obviate plumbing interference with the force measuring equipment, but this advantage was offset by difficulties with accurate mass flow measurement in a self-powered model.

The information, presented in the non-dimensional forms of Augmentation Ratio ($\frac{L}{mV_J}$) and height parameters ($\frac{h}{mac}$), illustrated the effect of Aspect Ratio on the Augmentation Ratio for constant values of height.

To obtain a forward Center of Pressure, the width of the front slot was increased and that of the rear slot was decreased. This effect is shown in the variation of pitching moment coefficient (C_m) with angle of attack for specific values of height to mean aerodynamic chord ratio.

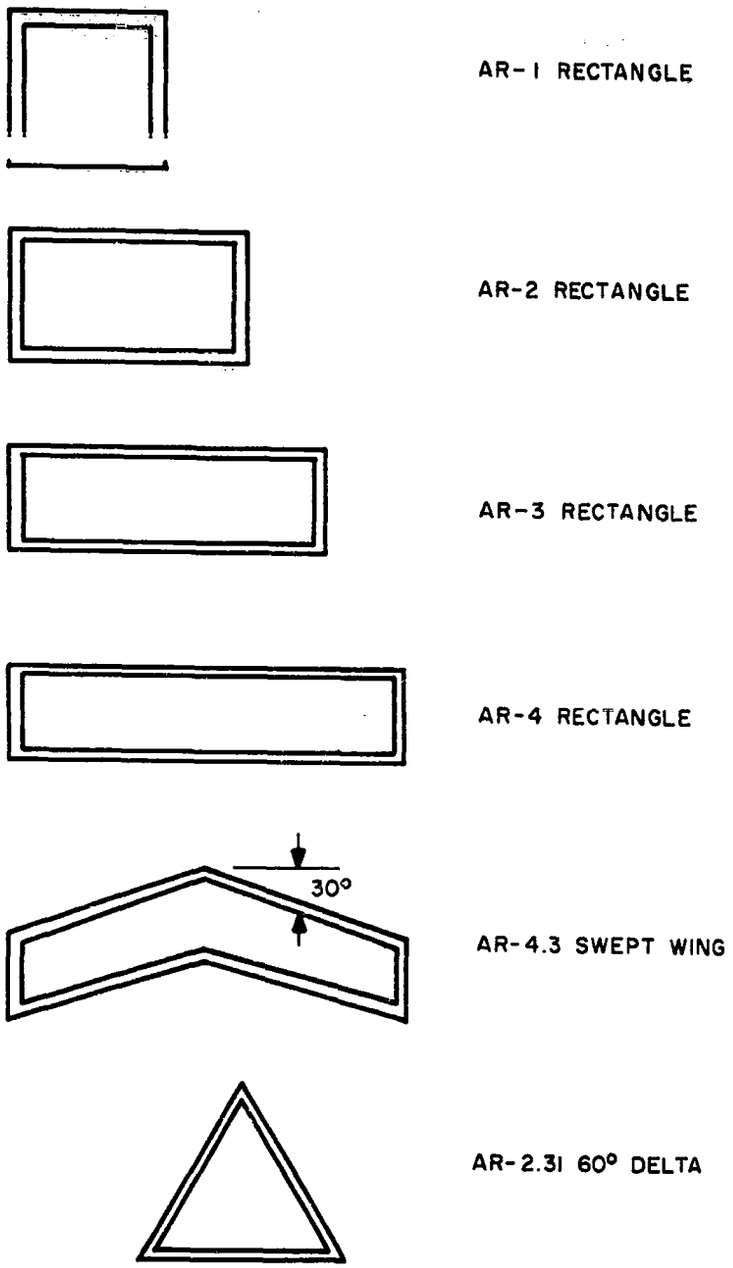

NOTE:

TOTAL AREA OF EACH PLANFORM = $1^{\square'}$(S)

S_j/S EACH CASE = .063 ± 3%

θ_0 = 0°, ALL CORNERS SHARP

NOT DRAWN TO SCALE

Figure 16. Schematic Diagram of Planform Models

Two of the planforms, the 30° swept planform and the 60° delta, exhibited a close shape in fact seems superior to the rectangle of the same Aspect Ratio. In comparing various planforms, Augmentation Ratio is not a valid means of comparison and is discussed in greater detail on Page 84. Figure 17 presents the hovering height attainable for various Aspect Ratio wings with the same wing area for specific values of Augmentation. This shows the hovering height for the 60° delta shape is approximately the same for the lower Augmentation Ratio but becomes less as the Augmentation Ratio increases. Simulated non-peripheral jet wing panels were added to the 60° delta shape in subsequent testing; the loss of hovering performance was suprisingly small when the advantage of increased L/D during transition, resulting from wing proximity to ground, is considered.

Pitching Moment Coefficients were incorrect since the drag force and its contribution to the moments were neglected. The balance used measured the vertical forces in front and rear, and only these individual forces were used to calculate the Pitching Moment.

The Aspect Ratio for the large wind tunnel model to be tested at NASA was selected from the variation of Augmentation Ratio with Aspect Ratio for constant values of Height to Chord Ratio. Augmentation Ratio, defined as $\frac{L}{mV_J}$, is a questionably accurate means of performance, since Jet Momentum (mV_J) is defined in the Princeton Report (see Reference 6, Page 193) by the experimentally derived relation $J = mV_J = \Delta Phc$. This latter relationship would appear valid only under the condition that there is no vortex flow induced by the peripheral jet.

Wind Tunnel Planform Tests. Initially, the primary purpose of this test was to determine the effect of changing the slot flow distribution on the stability characteristics of the GETOL planform. This was to be accomplished by using a model with a planform the same as the GETOL wind tunnel model and be of such design that the thickness of the cross-sectional flow area could be varied to obtain the following three basic chord-wise sections:

1. Type 4418 airfoil.
2. "Semi-plenum" - a thickness of approximately 50% of the chord.
3. Plenum - a thickness of approximately one chord.

Forces, moments, mass flow, and peripheral slot flow distribution were to be measured for the hovering condition. It was expected that the plenum would result in an even flow distribution around the periphery and possibly a more desirable operating condition. As the thickness of the planform is decreased, the uniformity of the flow distribution presumably would also decrease.

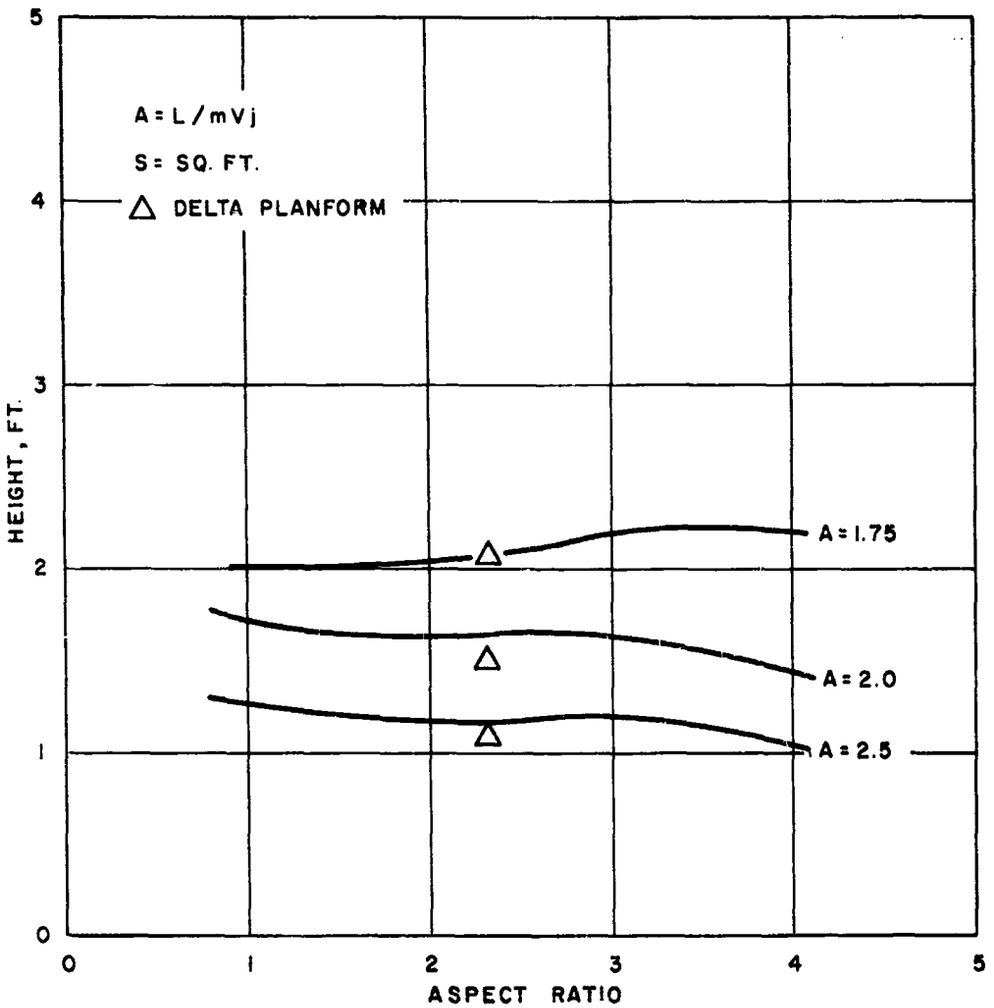

Figure 17. Height vs. Aspect Ratio

with the resulting data, the effect of distribution on forces, moments, and mass flow would be established and from the performance and stability requirements it was planned that a determination of the desirable degree of uniformity could be attained.

As additional information, the effect of altitude, gap ratio (leading edge thickness/trailing edge thickness) and angle of attack was to be investigated.

The model was a box with an internal contoured planform which simulated the GETOL wind tunnel model wing. In the upper surface there were two circular openings, at approximately the same position as on the wind tunnel model, for the passage of air into the wing cavity. The ducts, placed over these openings, were four inch aluminum pipes perpendicular to the upper surface and had wooden inlets with one-fourth inch radii. These pipes were in two pieces, one piece being an extension added to provide a section to measure the pressure distribution across the duct far enough ahead of the fan to eliminate the effect of pre-rotation of the air. The pressure distribution was for the determination of mass flow through the system. In the ducts were commercial model fans with a high solidity and hub diameter-to-tip diameter ratio. Fan power was supplied by small D.C. motors operating at forty volts and eight amps. The base plate was fastened to four posts being adjusted from the upper surface of the box. Slots in the base provided adjustability for the variation of the gap ratio. The geometric slot flow angle (θ) was fixed at -30° (measured from a line normal to the base, negative angles inward toward the center of the base). A one-fourth inch trailing edge flap was added for a portion of the test to provide additional directional control of the jet. Additional semi-plenum and plenum models were not provided and the planned distribution effect tests were not conducted.

A three component balance (lift, drag and pitching moment) was used. This balance was of the strain gaged, cantilevered-beam type and was used in conjunction with three carrier amplifiers with milliammeters for readout. Fluctuating aerodynamic loads hampered accurate reading of the meters because the damping factors were low.

There was a definite interaction of the lift and drag forces requiring an elaborate calibration and complicating the data reduction.

Before the primary objectives of the test could be accomplished, preliminary data on this model had to be obtained to determine the effect of altitude and leading edge/trailing edge gap ratio on the lift, thrust and pitching moment characteristics.

Calibration of the balance was the first step in the program. Variation of the gap ratio and angle of attack at an altitude of three inches was the first item to be investigated. Next was a small variation on height from the basic three inches at the same gap ratios and angles of attack. The third step in the test consisted of varying the height from one half inch to six inches for a gap ratio

of 3:1. A rerun of some of the data, to check doubtful test points and the addition of the trailing edge flap was the fourth step. Flow measurement and tuft and smoke studies constituted the final portion of the test. The following table summarizes the total test on the GETOL planform flow model.

TABLE III

TEST PROGRAM FOR BOEING-VERTOL WIND TUNNEL PLANFORM

Run No.	Gap Ratio Calibration	Height (h)	Angle of Attack (α)	Incremental Angle of Attack ($\Delta\alpha$)
1	$t_{LE}/t_{TE} = 1$	3 in	± 20°	2°
2	$t_{LE}/t_{TE} = 2$	3 in	± 20°	2°
3	$t_{LE}/t_{TE} = 3$	3 in	± 20°	2°
4	$t_{LE}/t_{TE} = 3$	3 in	±12°	2°
5	No good			
6	$t_{LE}/t_{TE} = 3$	2 in	± 10°	2°
7	$t_{LE}/t_{TE} = 3$	4 in	± 10°	2°
8	$t_{LE}/t_{TE} = 2$	4 in	± 10°	2°
9	$t_{LE}/t_{TE} = 2$	2 in	± 10°	2°
10	$t_{LE}/t_{TE} = 1$	4 in	± 10°	2°
11	$t_{LE}/t_{TE} = 3$	.5 6 in	0°)	
12	$t_{LE}/t_{TE} = 3$	.5 6 in	+ 5° (	Inlet extensions
13	$t_{LE}/t_{TE} = 3$	.5 6 in	- 5°)	plus trailing
14	$t_{LE}/t_{TE} = 3$	.5 6 in	0° (	edge flap
15 (1a)	$t_{LE}/t_{TE} = 3$	3 in	± 5°	5°)
	$t_{LE}/t_{TE} = 3$	2 in	0°	(
(6)	$t_{LE}/t_{TE} = 2$	3 in	± 5°	5°) inlet
	$t_{LE}/t_{TE} = 2$	4 in	± 6	2° (
	$t_{LE}/t_{TE} = 2$	2 in	± 5	5°)exten-
(7)	$t_{LE}/t_{TE} = 1$	3 in	± 5	5° (sions
	$t_{LE}/t_{TE} = 1$	2 in	± 5°	5°)
	$t_{LE}/t_{TE} = 1$	4 in	± 5°	5° (

Investigations on the Vertol planform model demonstrated that no specific height and gap ratio the lift increased with angle of attack. The thrust remained relatively constant with height after a height of two inches was attained. Pitching Moment remained constant as the angle of attack varied.

A typical illustration of the Augmentation Ratio is shown in Figure 18. Changing the gap ratio from 1:1 to 3:1 was done to obtain a forward shift in the Center of Pressure while keeping the magnitude of the lift constant. Figure 19 indicates a trend towards forward shift in the Center of Pressure* for an angle of attack of zero degrees and various heights. As the tests were conducted qualitative tuft and smoke studies were made of the flow under the wing.

Flow measurement was made and the following effects were investigated:

1. Inlet Extensions
2. Trailing Edge flap
3. Gap Ratio
4. Height
5. Angle of Attack

Upon comparing the results, no measurable difference was noted.

Gauzed Wind Tunnel Planform Test. This type test was conducted solely by Princeton University for Boeing-Vertol in an attempt to provide a uniform flow distribution. Gauze was placed over the slot to increase the uniformity of flow. One layer of gauze was applied around the periphery and the uniformity was checked by using a hand-held total pressure probe. Another layer of gauze was then applied at the wing tips and on the leading and trailing edge of the main center section of the wing.

Since the mass flow was not measured, this data can only be used qualitatively in looking at gap ratio and Center of Pressure shift and angle of attack effect. In trying to create a uniform flow, the Center of Pressure has been shifted forward for the same heights as in the non-uniform case. Variation of the angle of attack has a very little effect on thrust or Pitching Moment for all gap ratios and heights.

*Later tests with the large (5 foot) model at NASA did not substantiate this Center of Pressure shift.

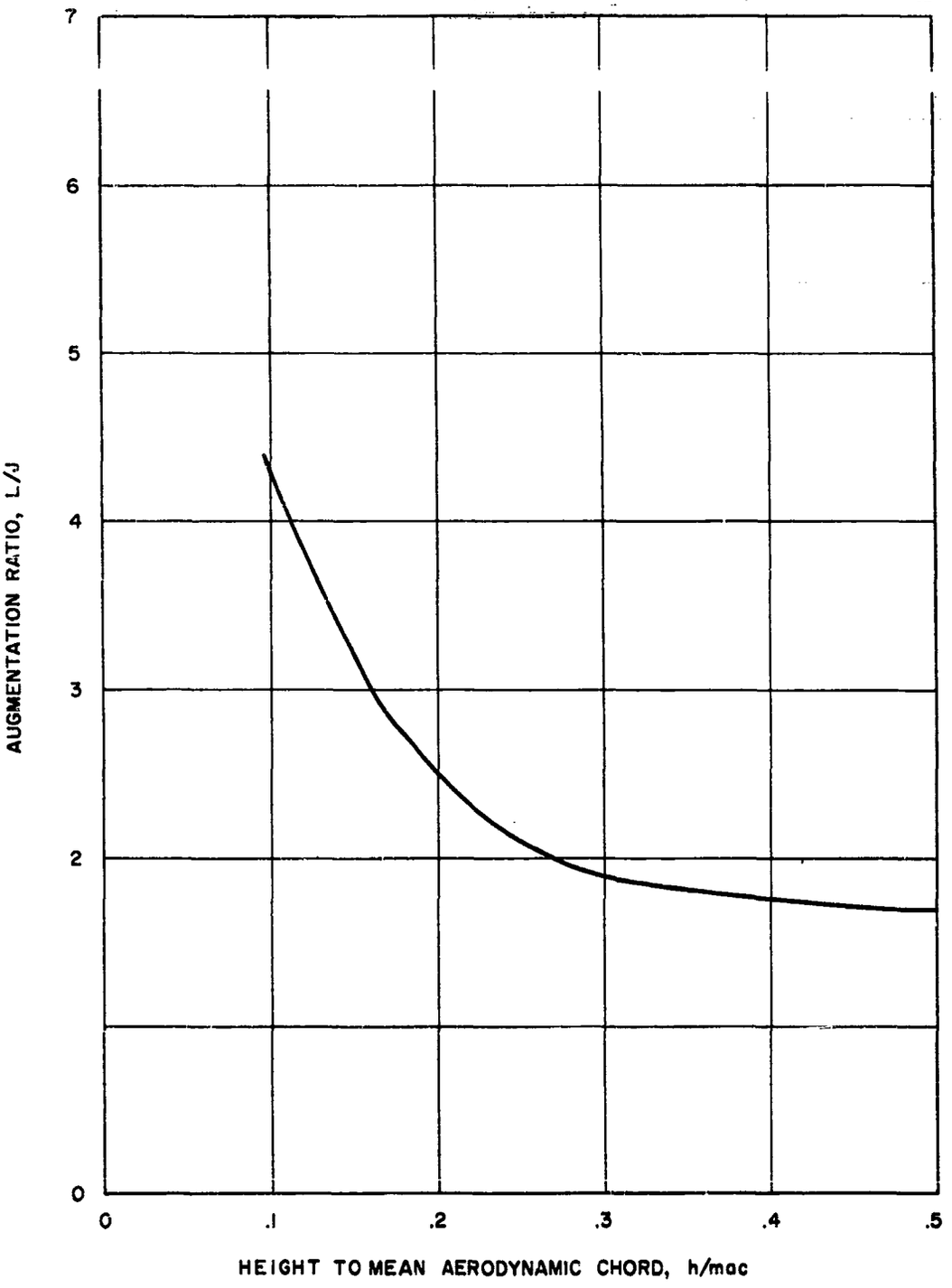

Figure 18. Augmentation Ratio vs. Height to Mean Aerodynamic Chord

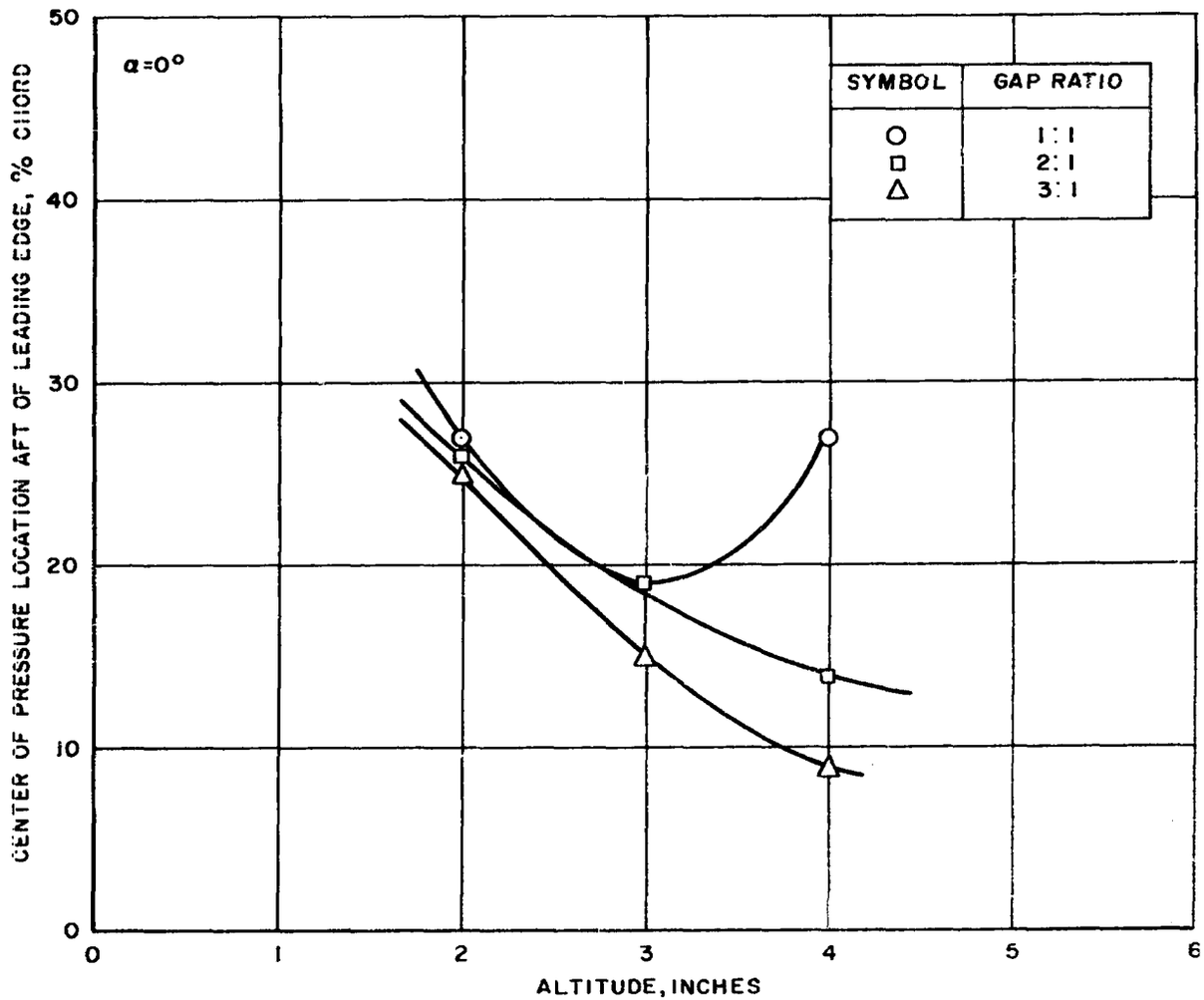

Figure 19. Center of Pressure Location vs. Altitude (α = 0°)

Cruciform Test. As the aspect ratio of a GETOL wing increases, the static to this problem would be to take two rectangular shapes and place them perpendicular to each other. Such a model was built by Princeton University. The fuselage was a large box-like plenum with a fan in the center. The wing volume was small in comparison to the fuselage volume and the passage from the fuselage to wing was small with sharp edges. For this reason, most of the flow issued from the fuselage slots.

An investigation of the stability characteristics was the primary purpose of this test. A comparison of the cruciform to the wing slots only, can be seen in Figures 20 and 21 for values of h/mac = .16 and .32. These two configurations show moderate pitch and roll stability at h/mac = .16. As the height increases, pitch and roll stability becomes neutral. No definite improvement in the longitudinal stability was demonstrated and can possibly be explained by the strange flow distributions occurring in this model.

Since the mass flow was not measured, a comparison of the lift for various configurations could be made only by non-dimensionalizing lift in ground effect by lift out of ground effect. This does take into account the change in internal resistance and its corresponding effect on mV_J caused by taping some of the slots but does not include the effect of height on these two terms which may not be as minor as in other configurations investigated in the past. One conclusion that can be made is that the ratio of lift in ground effect/lift out of ground effect ($L/L\infty$) for this model is higher with fuselage blowing than without it as illustrated in Figure 22.

University of Toronto Tests (Dynamic Model)

General

It was learned from discussions at the University of Toronto that they were conducting test programs and constructing a test facility to test aircraft flying close to the ground. It was further discovered that a co-operative study program could be established to complete the construction of this facility and test a dynamic GETOL model similar to the Bocing-Vertol wind tunnel to be tested at NASA.

The following program was developed:

1. Complete construction of the track and carry out development work necessary to put it into operating condition.

2. Construct a GETOL model similar to the Boeing-Vertol wind tunnel model.

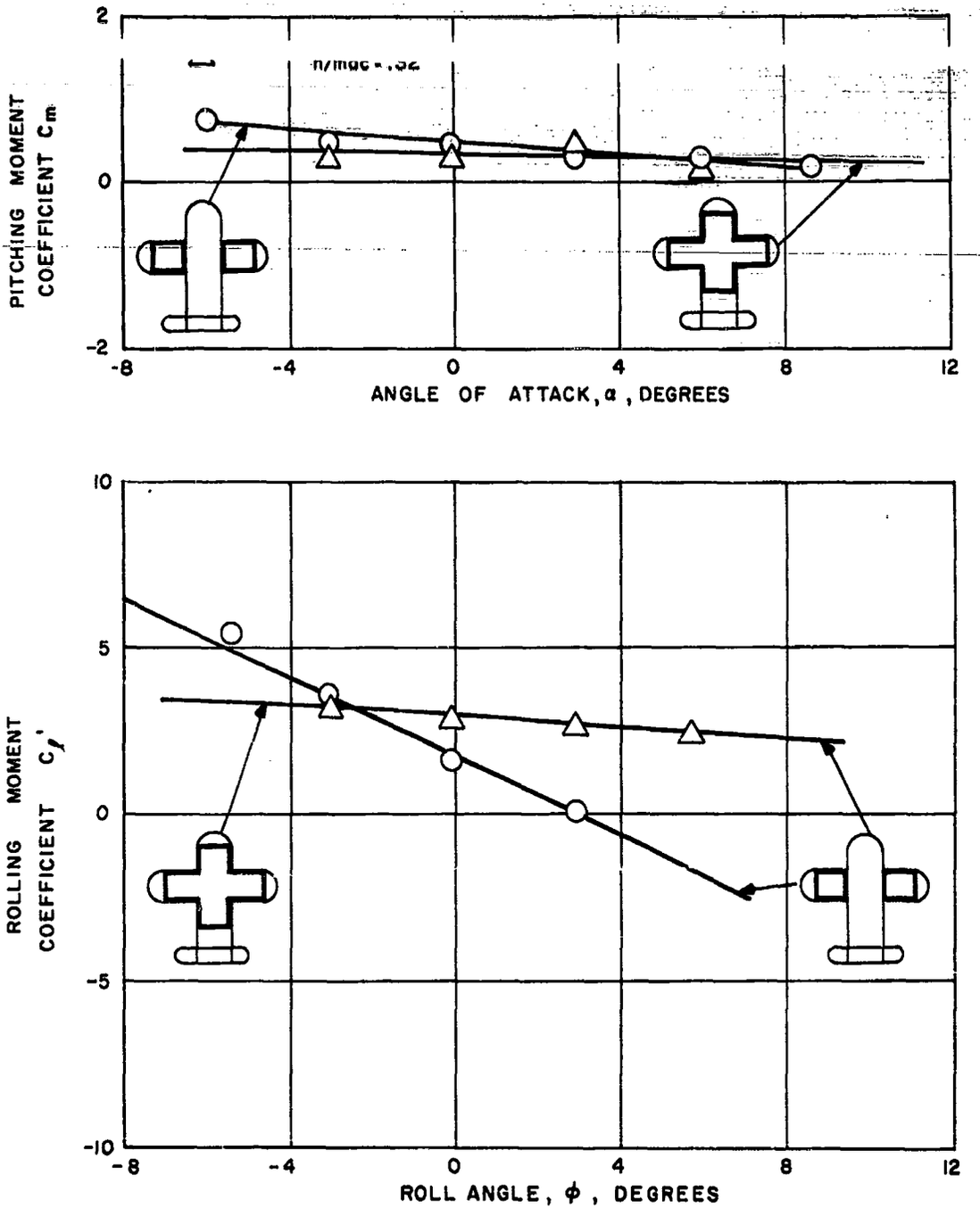

Figure 20. Lateral and Longitudinal Static Stability Characteristics (h/mac = .32)

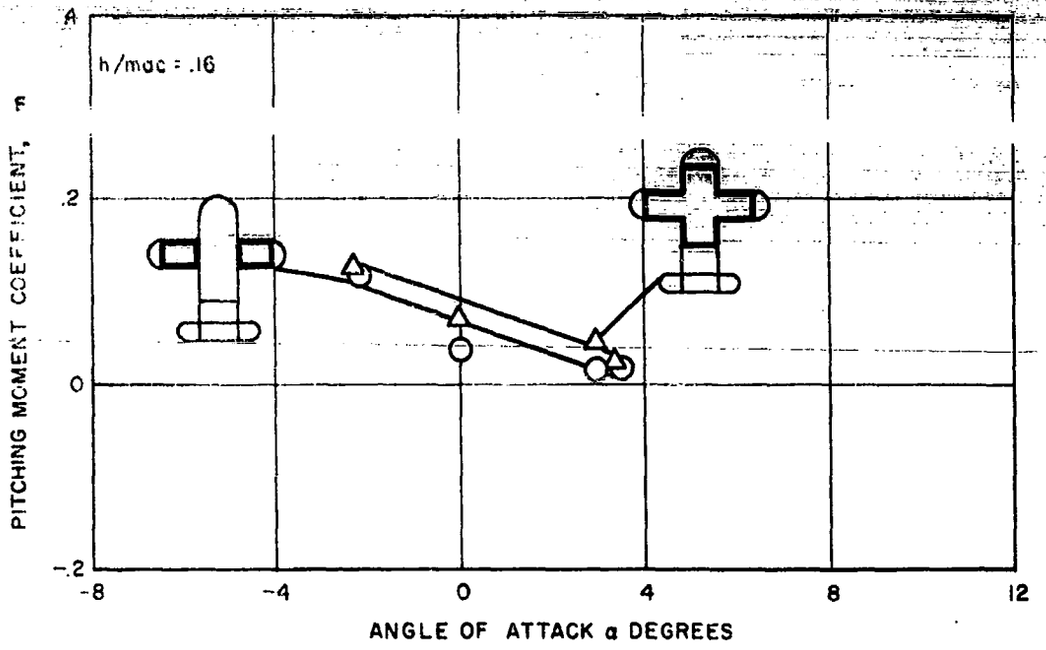

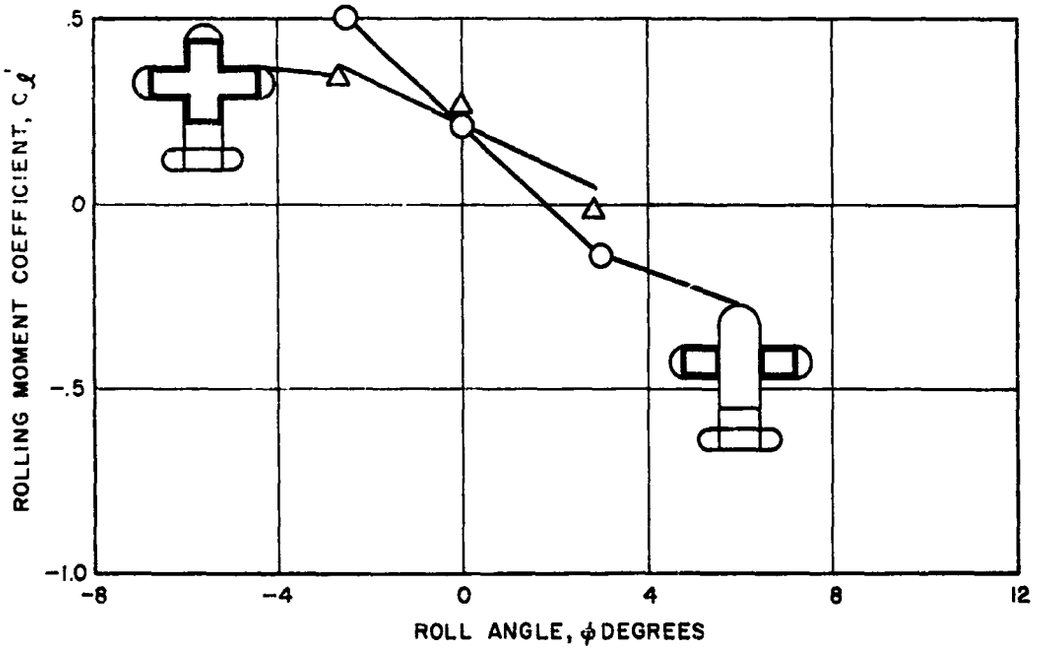

Figure 21. Lateral and Longitudinal Static Stability Characteristics (h/mac = .16)

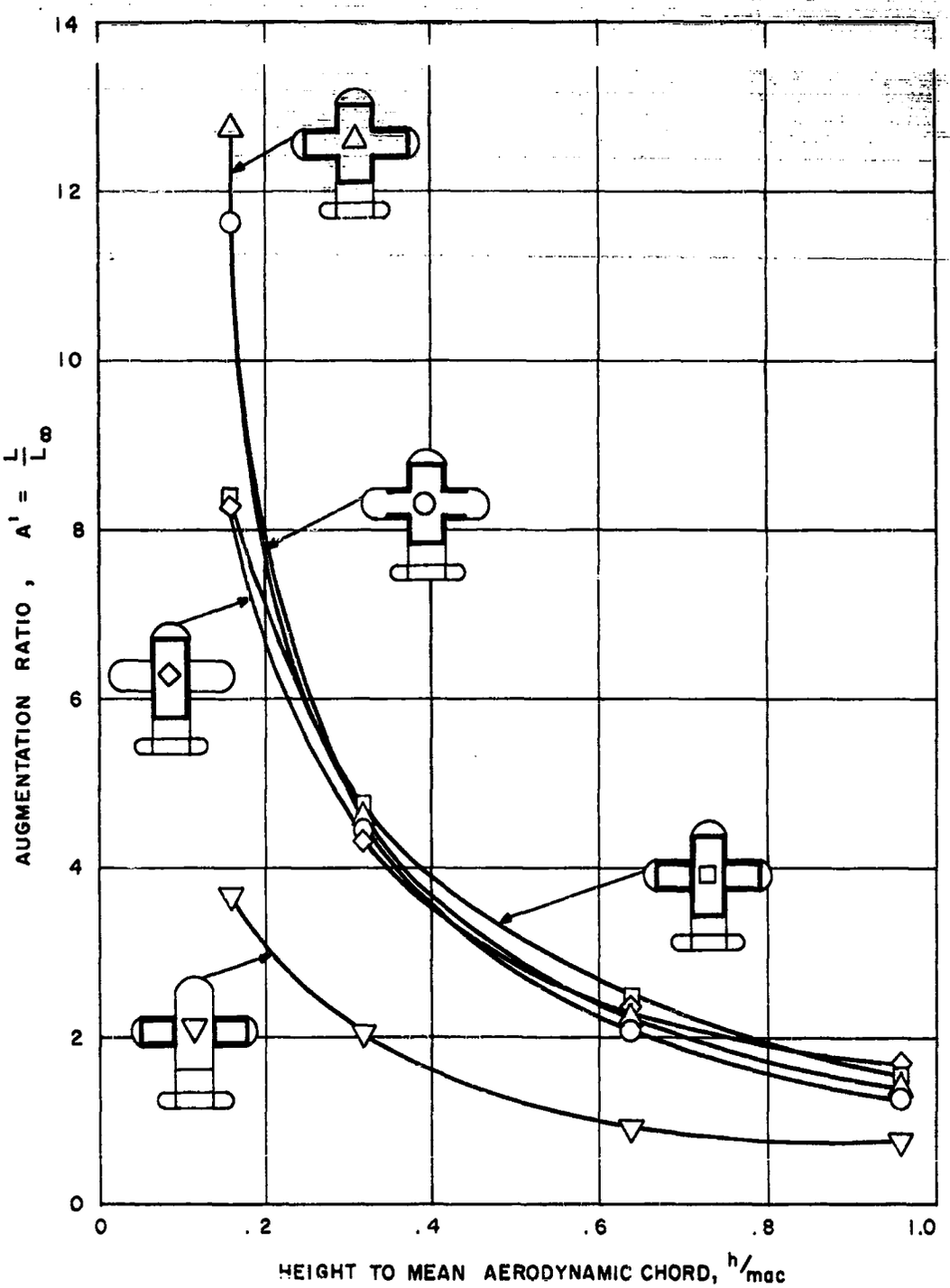

Figure 22. Augmentation Ratio vs. h/mac

3. Carry out a program of tests on the model within the time limits of the

4. Provide Boeing-Vertol with data from the Aspect Ratio of 4 peripheral jet wing being tested in the wind tunnel.

Circular Track Tests

Owing to the dearth of information on aircraft flying in close proximity to the ground, a circular track facility was constructed at the University of Toronto. Testing on this type of test facility eliminates the possibility of the problem of boundary layer on the ground board encountered in wind tunnel testing. A circular track also permits harnessing the model to suppress any undesirable motions such as roll and yaw, and also allows the possibility of continuous recording of flight attitude.

Arrangements were made by Boeing-Vertol with the University of Toronto to fund an effort to complete construction of their track facility, perform development effort and place it into operating condition, and construct and test a model, as shown in Figure 24, similar to the Boeing-Vertol wind tunnel model. Testing on this model was conducted in two phases: (1) dynamic tests, performed on the track and shown in Figure 25, and (2) static tests. These two areas of testing are described in great detail in Appendix E, Volume II. A typical sample of data obtained from testing on the track is shown in Figure 26 and shows a velocity of 27 ft/sec at an average height of one half inch.

From the results obtained from this study, it appears that this method of testing was very useful and resolved the dynamic characteristics of the GETOL type aircraft quickly and easily. A major achievement was that this crude, simple model demonstrated that the peripheral jet GETOL can operate at a relatively constant height and transist from hover to forward flight very easily on fixed slot angles using the door in the rear of the nacelle to obtain propulsive force. The static tests, a survey of the pressure distribution across the slot and around the periphery, demonstrated that distribution was not uniform and remains a problem area.

Wind Tunnel Tests Aspect Ratio -- Wing with Peripheral Blowing Slots

Generally, these experiments were an application of the ground effect concept to conventional airplane flight; previous efforts had been restricted to vehicles designed for operation close to the ground throughout their flight regime. Thrust in this improved vehicle would be furnished either by the trailing edge jet directed back or by a separate propulsion unit.

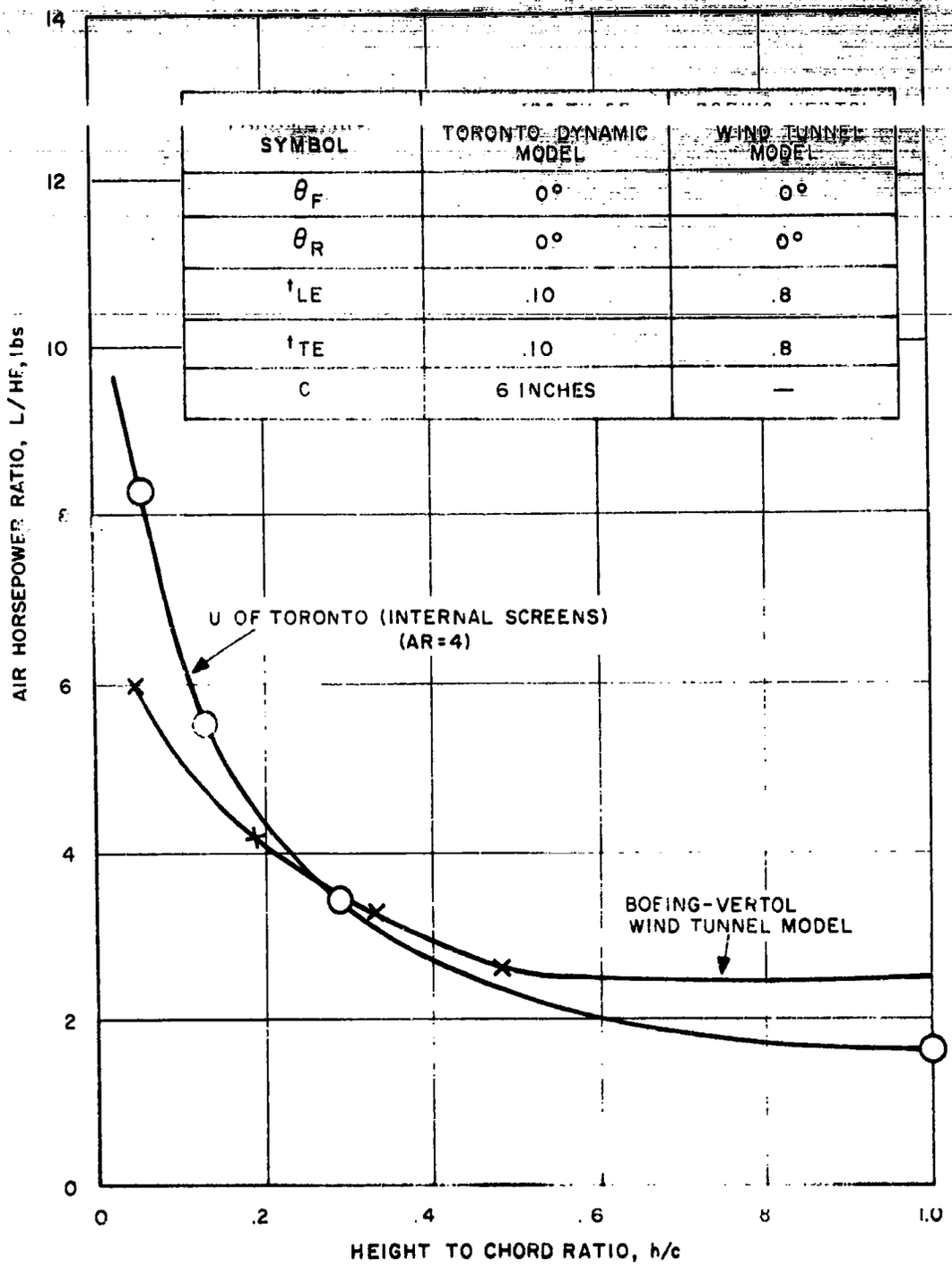

Figure 23. Variation of Lift Per Air Horsepower Ratio to Height to Chord Ratio (Aspect Ratio 4)

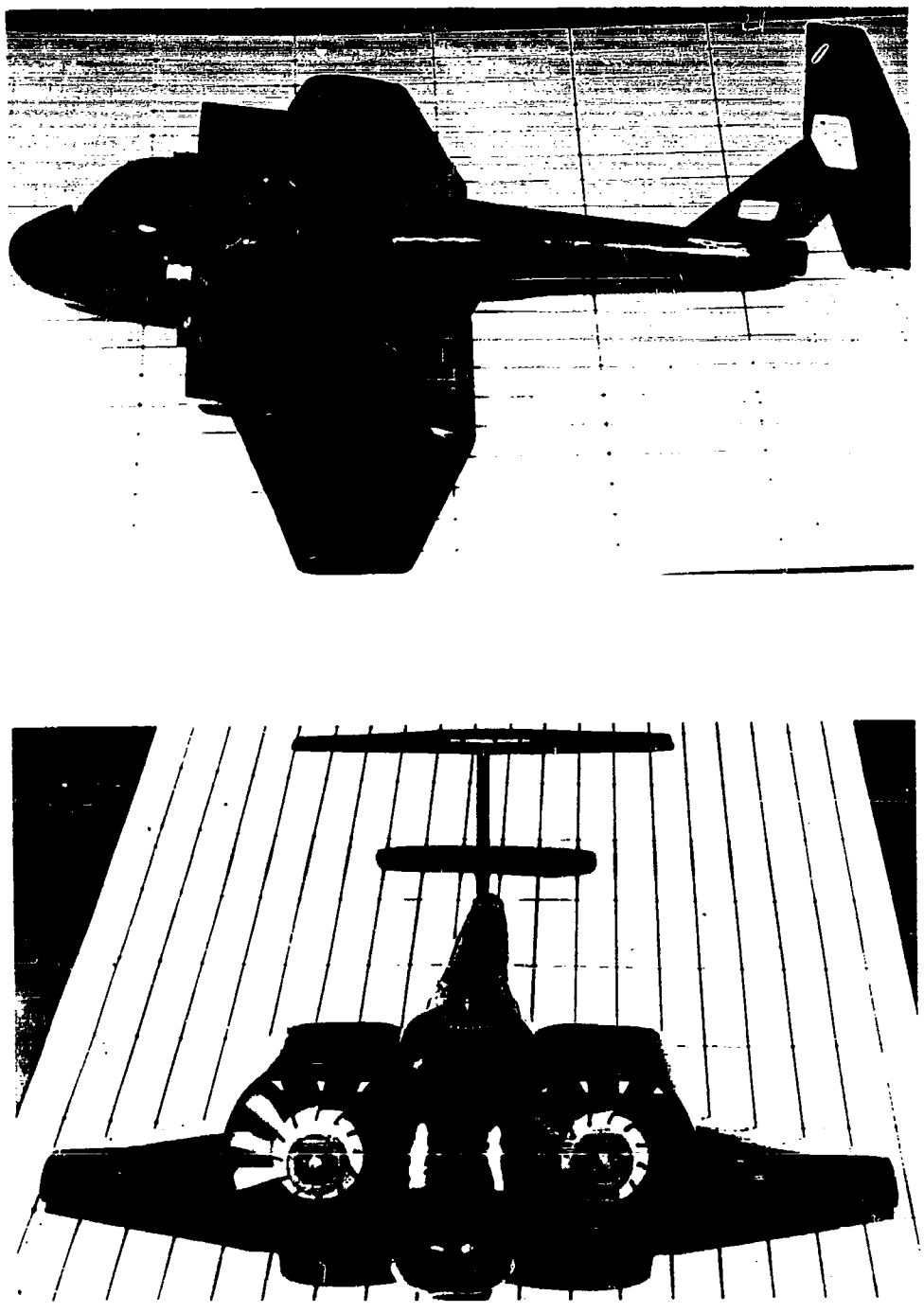

Figure 24. University of Toronto Dynamic Track Model

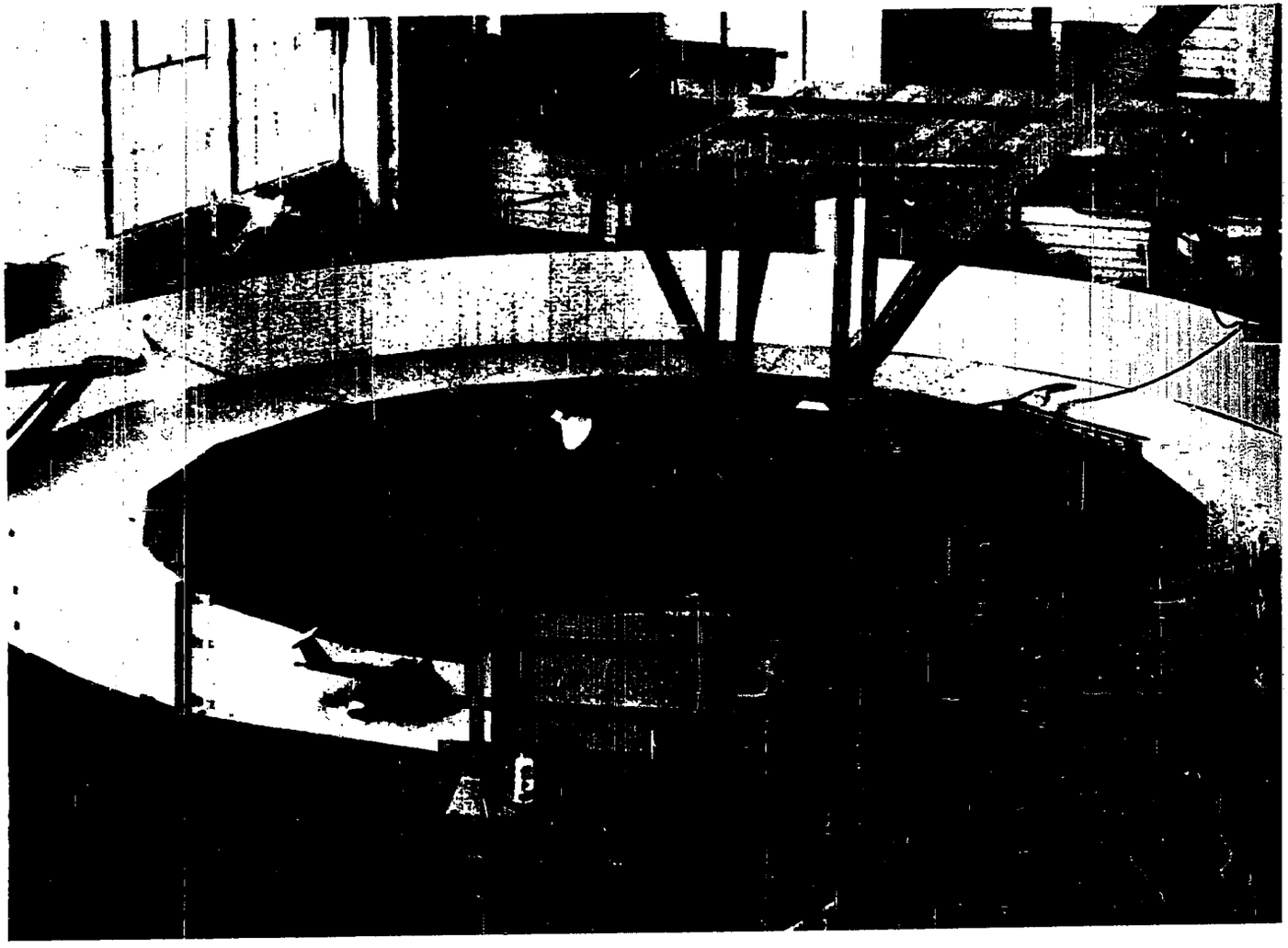

Figure 25. Typical Test Run of Track Model

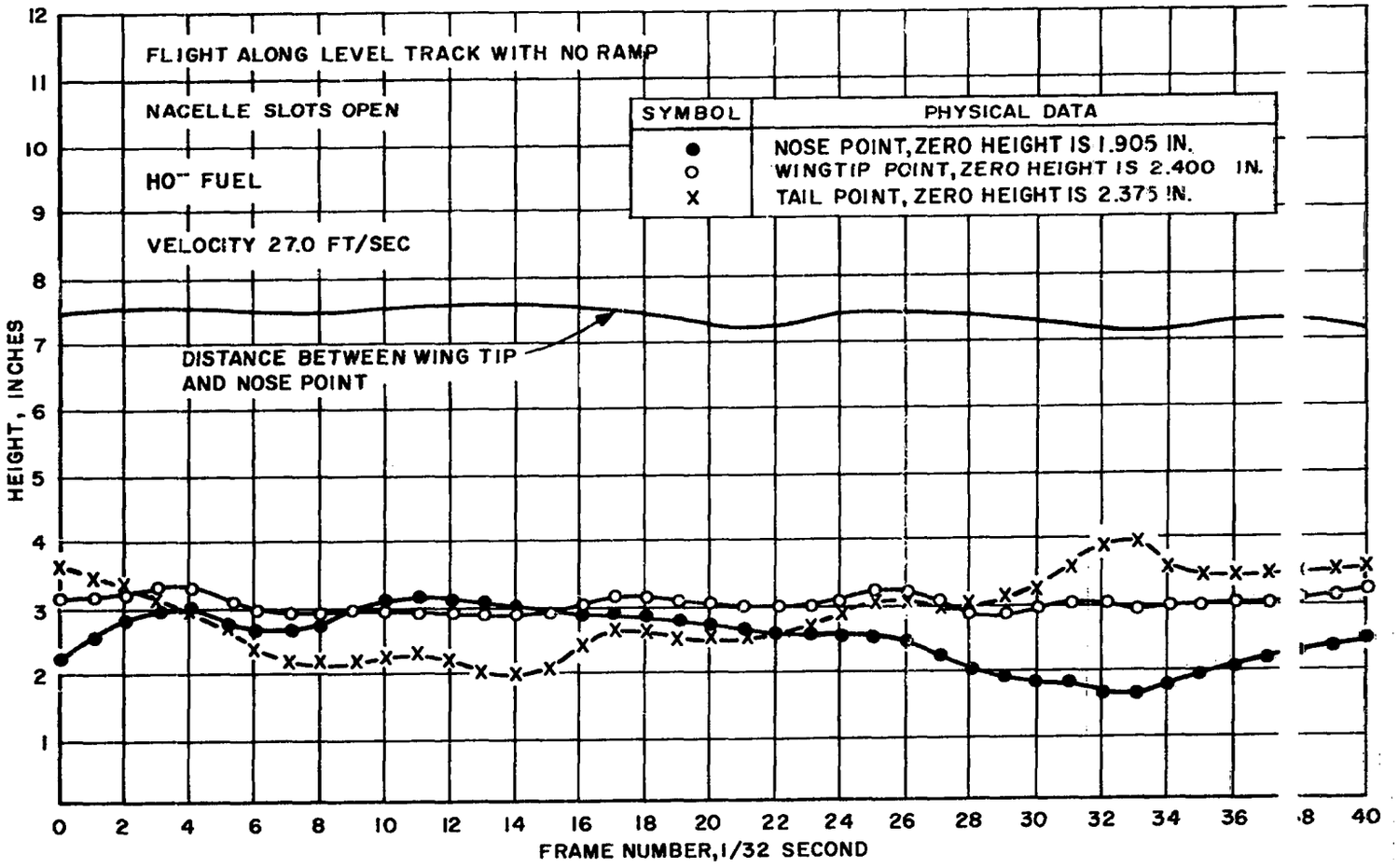

Figure 26. Typical Test Result from University of Toronto Track Test

TECHNICAL PROGRAM (PHASE II)

The specific objective of these tests were to determine the lift [illegible] pitching moment characteristics of a rectangular wing equipped with a peripheral jet for various heights above the ground, forward speed, and angles of attack. The circular planform, more suitable for a conventional GEM, was replaced by a planform with an Aspect Ratio of 4 since the wing would have to be efficient also in cruising flight remote from the ground.

Some information obtained from this testing is shown in Figure 23. This demonstrates the variation of lift per air horsepower variation with Height to Chord Ratio. Superimposed on this figure is the same variation for the Boeing-Vertol wind tunnel model with similar slot angles and slot flow area. There is a deviation between the two curves; at the lower Height to Chord Ratio, the Boeing-Vertol model achieves a lower lift per air horsepower but at the high Height to Chord Ratio the trend reverses. This difference could be attributed to a difference in planform shape and Aspect Ratio. However it is thought that flow distribution is the major cause for this difference, since the Toronto model had almost uniform flow distribution and the Boeing-Vertol model had a non-uniform distribution.

NASA Tests (Static, Track and Wind Tunnel)

General

The NASA testing of the large 5 foot span GETOL model was conducted in the 17 foot section of the Langley 7 x 10 foot tunnel. In addition, most preliminary functional checks and static tests were conducted in their 30 x 60 foot Static Room.

Beside the tunnel tests about fifty runs were performed on the NASA tow track facility, recording data as the model passed over a sixty foot ground board section.

Description of Model and Instrumentation

A brief description of the 5 foot model is given here and shown in Figure 27. This figure is an overall view of the model showing the major components. One of the possible methods of obtaining forward propulsive force is the use of doors in the nacelle (see Figure 28) to permit the air to flow straight through the nacelle thereby acting as a ducted fan. For the hovering regime the vertical lift is generated by air issuing from a peripheral slot in the wing base (see Figure 29). To turn the air passing through the fan into the wing, turning vanes are required as shown in Figure 30.

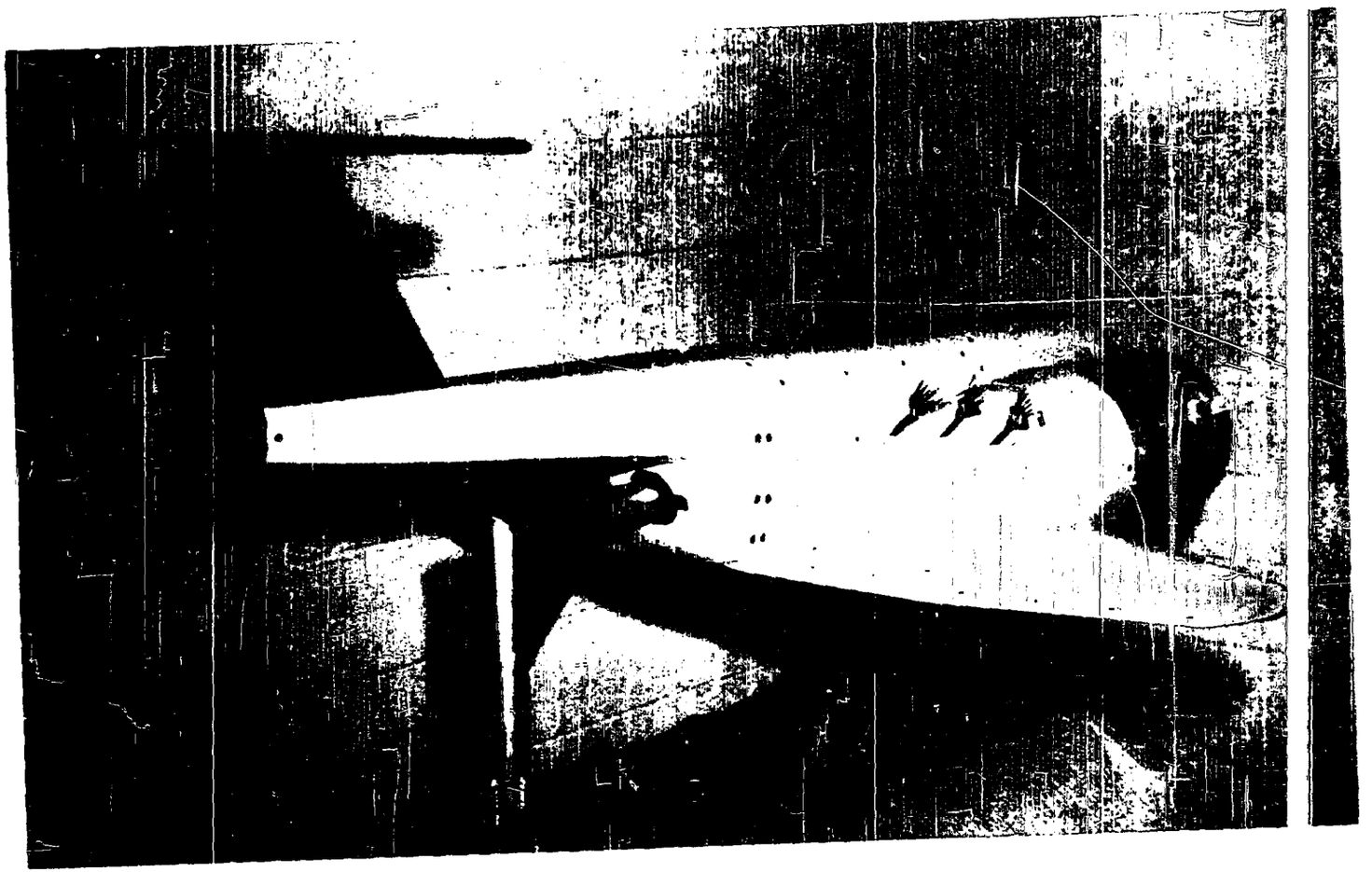

Figure 27. GETOL Wind Tunnel Model

Figure 28. GETOL Wind Tunnel Model (Nacelle Door)

Figure 29. GETOL Wind Tunnel Model (Wing Base with Slot Opening)

Figure 30. GETOL Wind Tunnel Model (Wing Turning Vanes)

sensors, and a recording system.

Fan flow and pressure were sensed by a three-armed five probe total pressure rake in each nacelle. On each rake arm was located one static pressure probe and a static pressure orifice, the latter flush with the nacelle outer wall (see Figure 39).

No slot probes were installed on the model due to the variability of the base plate slot inserts and the inability to provide flow alignment assurance for each test configuration; neither were probes used on the base itself since prior attempts to measure base pressure (e.g., Princeton) had shown that these pressure levels are normally low and readily obscured by swirl of the flow beneath the wing.

The nacelle exit was provided with total and static pressure rakes. This arrangement was not used since testing showed the total pressure at the nacelle exit to be the same as the fan rake total and the static to be the ambient static. From these, the flow was known.

The model was mounted on a NASA six-component #710 strain gaged balance (see Figure 31). NASA personnel provided the necessary calibration for the instrument which was designed to measure the six components of interest. These included lift, drag and side forces, and the pitching, rolling, and yawing moments.

Pressure recording consisted of the photographing of manometer boards and the simultaneous registration of pressure on IBM cards through the use of scanner valves, with Brown balancing of the scanner valve transducer output. This automatic readout system was obtained from, and installed at NASA, by personnel of The Boeing Company. The apparatus is pictured in Figures 32 and 33.

Force data readings from the #710 balance were recorded manually from Brown dials.

One additional item was recorded, fan rpm, by stroboscopic alignment of pulses from a transducer mounted on the nacelle wall. The pulses obtained were the result of the compressed air from the fan tip passing over the transducer.

During track tests, all data recording were made with an oscillograph. Since there was a limitation on the number of channels available, a minimal quantity of data were obtainable. Subject to this limitation, the data selected for recording were as follows: six components of force and moment (lift, drag, side force, pitching, rolling and yawing moments), four pressures (one total pressure and one static pressure behind each fan), and forward velocity.

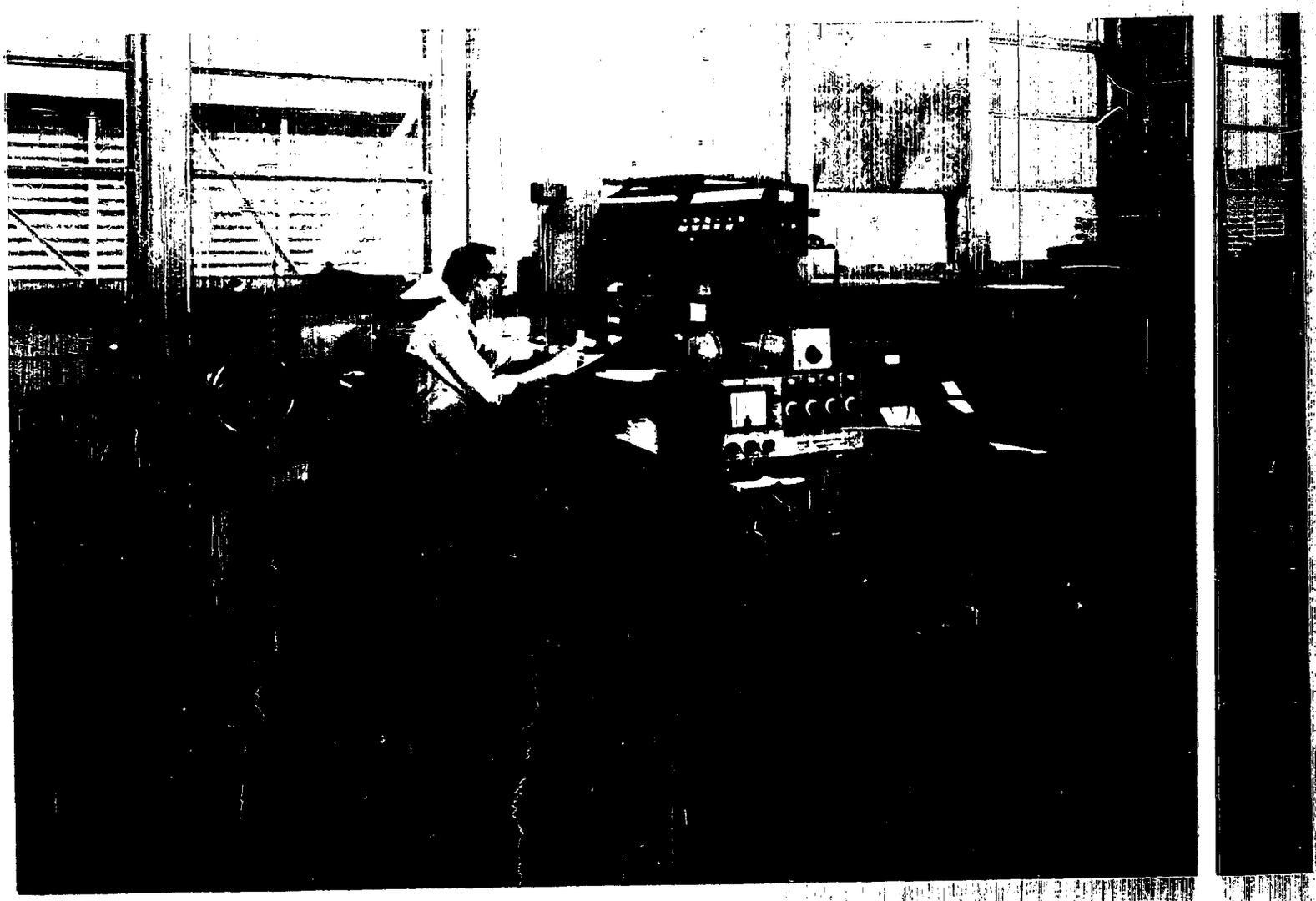

Figure 31. Force Measurement Equipment

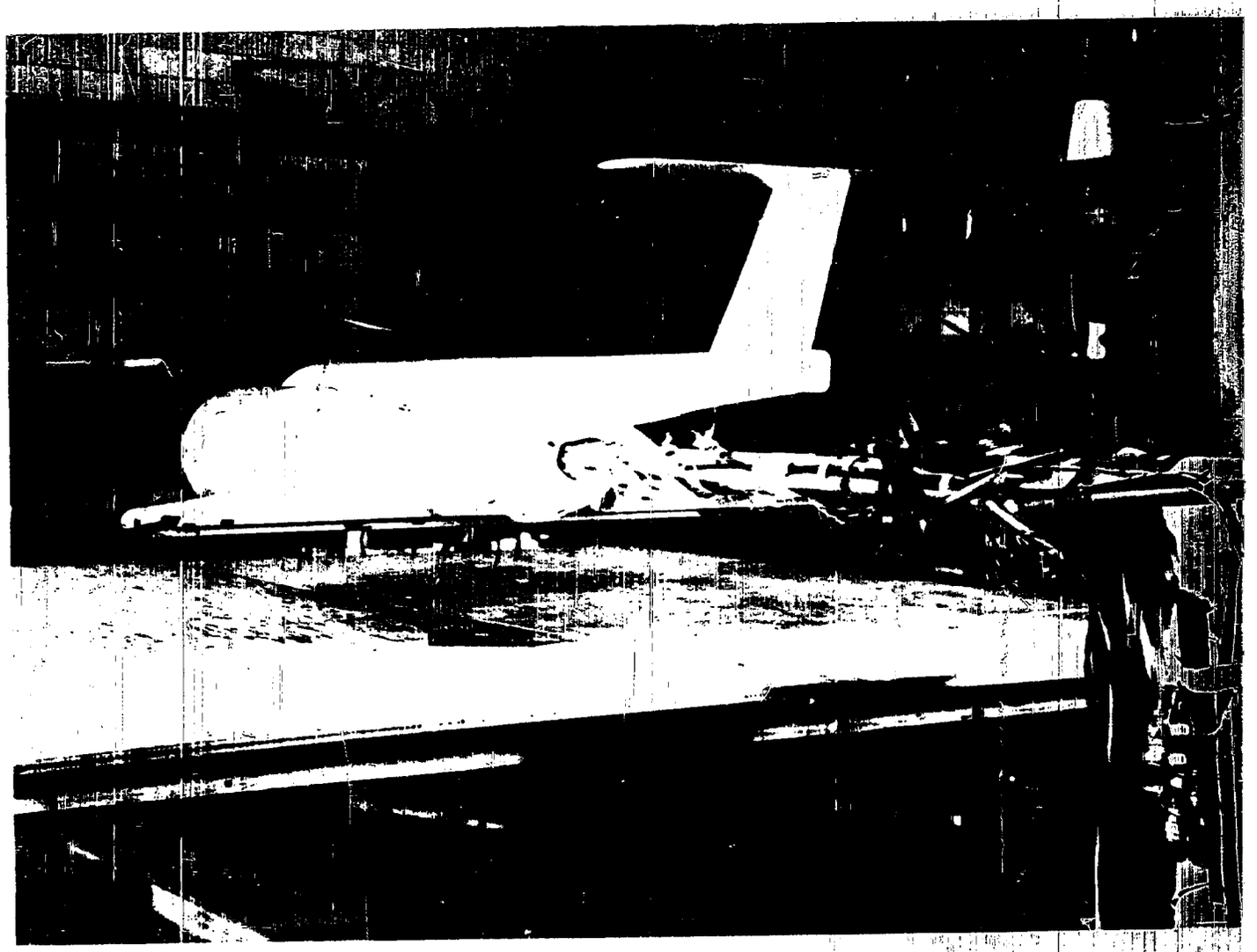

Figure 32. Pressure Measurement Equipment

Figure 33. Automatic Digital Pressure Data Recording System

from these transducers were then amplified, together with those from the six balance, to give moderate trace deflections at normal operating conditions. Recording of the data were thus simple and rapid, though the data itself proved subsequently useless; the carriage, bouncing the model, contributed such large and random amplitudes that any analysis of the data would be futile.

NASA Test Program

Static Room Tests at NASA: Static room testing extended through the two month period from April 21 to June 29, 1961, with an interruption from May 31 to June 9 for tow track tests. This phase of the operation had the following objectives:

1. To determine the functional response of the model to full (200 psi) fan drive air;
2. To investigate the flow through the model by calibrating the fan rake;
3. To perform all necessary testing of the forces present in the hovering situation.

Installation of the model was in a 30 x 60 foot room. Height adjustments were made by raising or lowering the ground board on platform lifts and the ground board was blocked to provide angles of attack of -5, 0, 5 and 10 degrees relative to fuselage centerline. Figure 34 shows the static room installation.

After the initial few days of installation difficulties and the customary period of mutual familiarization of personnel with the model, testing was begun.

Fan flow calibration was the first effort. The procedure was to rake carefully with manually inserted probes across the permanent fan rake station. The results of these measurements are graphically illustrated in Figure 40.

Fan swirl, due to the tip driving jets, caused a skewed high velocity jet ring in the measuring section. This ring caused substantial inaccuracies in flow measurement. To eliminate the fan tip swirl, a honeycomb was manufactured and was located behind the fan (see Figure 34).

Recalibration with the honeycomb provided further flow calibration curves which have been included with those of Figure 40. This latter calibration was considered satisfactory, since the permanent instrumentation average pressure then agreed with the calibrated average pressure.

Actual force testing, which did not begin until after return from the track, consisted of 1050 test points encompassing the following range of hovering geometries:

1. h 3.6 to 17 inches
2. α -5 to +10 degrees
3. 3 fan rpms per configuration

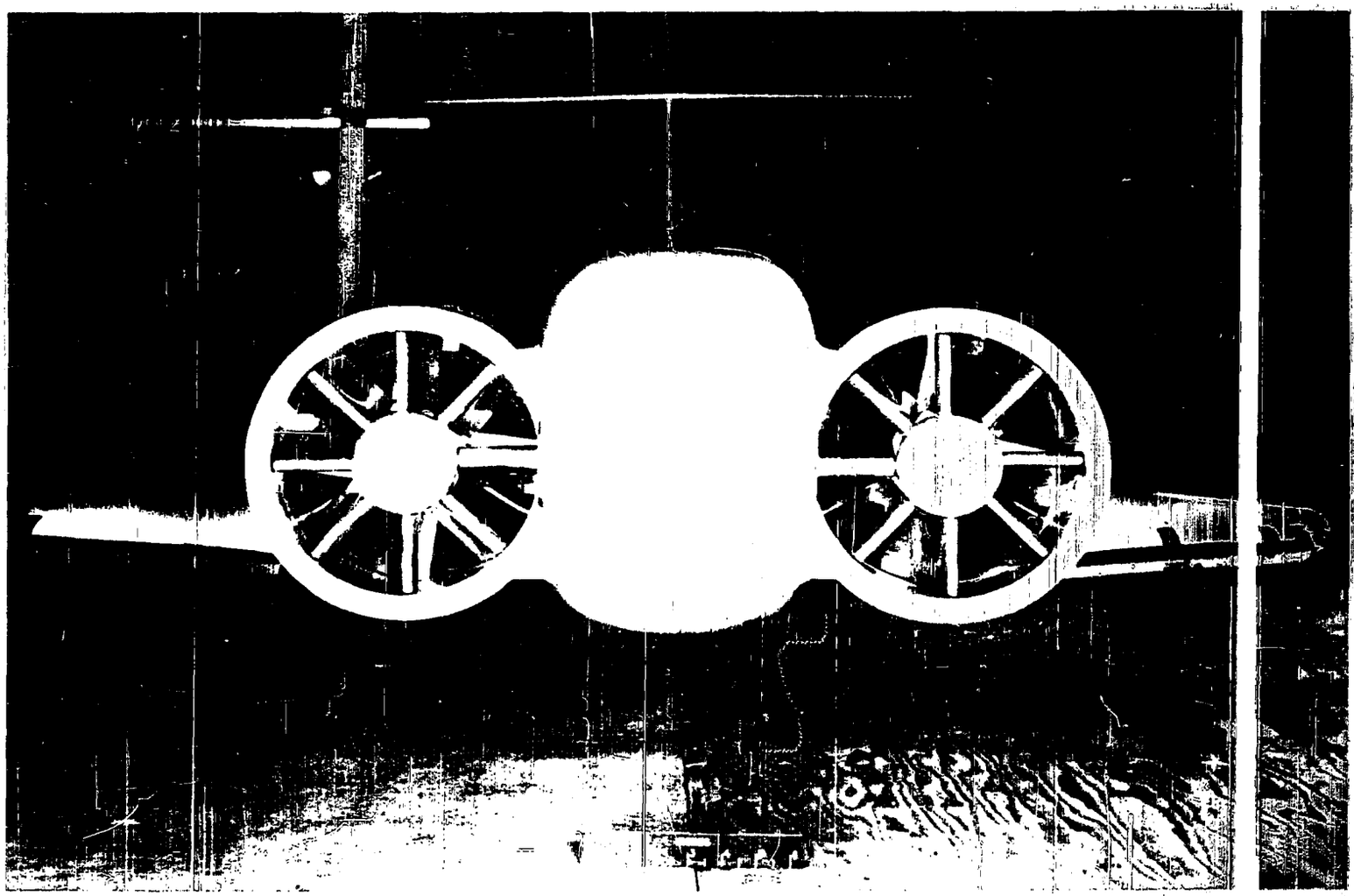

Figure 34. Front View of GETOL Model Over Ground Board

4. Range of slot angles and gaps

5. Doors open and shut

6. Roll ± 5 degrees

A complete tabulation of the static room tests is presented in Table IV.

A comprehensive survey and interpretation of the results of the static room testing is made on Page 84.

Track Testing at NASA: During the course of the static room program, when the calibrations were almost completed, the instrumentation was disconnected and the model taken to the tow track facility. This portion of the test required two weeks, from May 31 to June 12, 1961. A total of 54 data points, as listed in Table V, were obtained. The carriage from which the model was suspended can be seen in Figure 35 and 36. Flat spots on the tires and small gaps in the rails gave rise to periodic oscillations of the carriage as it was moved along the track. This resulted in vibration of the carriage and was transmitted to the model. Diagonal support struts were added to eliminate the lateral movement and a viscous damper installed to damp the vertical oscillations (see Figure 35). Operation of the model now appeared satisfactory; dirt from the compressed air system, however, subsequently ruined a set of bearings.

Recording of data, by means of the oscillograph, were simple, rapid and semi-automatic. Each run down the track corresponded to one test point, the compressed air bottles being refilled after each two or three run interval. The work at one end of the track was approximately two feet lower than the level of the ground board so that modifications of the slot geometry were made quite easily. The only problem encountered in the course of these tests were a recurrent tendency of the leading edge tapes and those on the tip slots to blow off.

The data taken at the tow track had neither the honeycomb flow straighteners behind the fan nor skirts around the slots. No evaluation of the data will be made in this section, but will be included in the comprehensive analysis of the NASA program on Page 83.

Tunnel Tests at NASA: Tunnel tests were conducted during the three week period from July 7 to July 28, 1961. Two shifts were maintained for the latter half of this time. The tunnel installation is shown in Figures 37 and 38.

Approximately 2000 test points were obtained, and are logged in Table VI. The model operation during the tunnel test period was very satisfactory. Fan bearing problems, attributed to the contaminated supply air, were significantly improved and fan bearing life was extended to periods of 100 hours or more.

TABLE IV

TABULATION OF STATIC ROOM TESTS

				RUN NO.					
				ANGLE OF ATTACK (α)					
Θ_F	Θ_R	t_{LE}	t_{TE}	-5	0	+5	+10	h/c	Comments
-30X	-30X	.8	.8	49	46	-	52	.2	-
↓	↓	↓	↓	48	45	44	51	.33	-
				50	47	42	53	.5	-
				56	55	-	57	1.0	-
				-	54	43	-	∞	-
-30X	-30X	.8	.8	-	-	58	-	.2	ROLL +5°
↓	↓	↓	↓	-	-	59	-	.33	ROLL +5°
				-	-	60	-	.5	ROLL +5°
				-	-	61	-	1.0	ROLL +5°
-30X	-30X	.8	.8	-	-	62	-	.2	ROLL -5°
↓	↓	↓	↓	-	-	63	-	.33	ROLL -5°
				-	-	64	-	.5	ROLL -5°
				-	-	65	-	1.0	ROLL -5°
-30X	-30X	.8	.8	-	-	-	204	.33	AFT NAC.
↓	↓	↓	↓	-	-	201	205	.5	AFT NAC.
				-	-	202	206	1.0	AFT NAC.
-30V	-30X	.8	.8	-	-	207	-	.2	1/2 AFT NAC.
↓	↓	↓	↓	-	-	208	-	.33	1/2 AFT NAC.
				-	-	209	-	.5	1/2 AFT NAC.
				-	-	210	-	1.0	1/2 AFT NAC.
-30X	-30X	.8	.8	-	-	179	-	.2	DOOR = .2
↓	↓	↓	↓	-	-	180	-	.33	DOOR = .2
				-	-	181	-	.5	DOOR = .2
				-	-	182	-	1.0	DOOR = .2
				-	-	183	-	.2	DOOR = 1.05
				-	-	184	-	.33	DOOR = 1.05
				-	-	185	-	.50	DOOR = 1.05
				-	-	186	-	.33	DOOR = .55
				-	-	188	-	.33	DOOR = 1.94
-30X	-30X	.8	.8	190	194	199	-	.2	AFT NAC.
↓	↓	↓	↓	191	195	200	-	.33	AFT NAC.
				192	196	-	-	.5	AFT NAC.
				193	197	-	-	1.0	AFT NAC.
				-	198	-	-	∞	AFT NAC.

TABLE IV

TABULATION OF STATIC ROOM TESTS (Continued)

				RUN NO.					
				ANGLE OF ATTACK (α)					
Θ_F	Θ_R	t_{LE}	t_{TE}	-5	0	+5	+10	h/c	Comments
-30	-30	.8	.8	-	70	-	-	.2	TAIL OFF
				-	71	-	-	.33	TAIL OFF
				-	72	-	-	.5	TAIL OFF
				-	73	-	-	1.0	TAIL OFF
				-	74	-	-	∞	TAIL OFF
0X	-30X	.8	.8	137	141	146	150	.2	-
				138	142	147	151	.33	-
				139	143	148	152	.5	-
				140	144	149	153	1.0	-
				-	145	-	-	∞	-
-30X	-30X	1.07	.53	245	249	254	258	.2	-
				246	250	255	259	.33	-
				247	251	256	260	.5	-
				248	252	257	261	1.0	-
				-	253	-	-	∞	-
-30X	-30X	1.2	.4	262	266	271	275	.2	-
				263	267	272	276	.33	-
				264	268	273	277	.5	-
				265	269	274	278	1.0	-
				-	270	-	-	∞	-
-30X	-30X	1.0	1.0	279	283	288	292	.2	-
				280	284	289	293	.33	-
				281	285	290	294	.5	-
				282	286	291	295	1.0	-
				-	287	-	-	∞	-
-30X	-30X	1.33	.67	-	-	296	-	.2	-
				-	-	297	-	.33	-
				-	-	298	-	.50	-
				-	-	299	-	1.0	-
				-	300	-	-	∞	-
-30X	-30X	1.5	.5	-	-	301	-	.2	-
				-	-	302	-	.33	-
				-	-	303	-	.50	-
				-	-	304	-	1.0	-
				-	305	-	-	∞	-

TABLE VI

TABULATION OF STATIC ROOM TESTS (Continued)

				RUN NO.					
				ANGLE OF ATTACK (α)					
Θ_F	Θ_R	t_{LE}	t_{TE}	-5	0	+5	+10	h/c	Comments
-30X	-30X	.6	.6	306	310	315	-	.2	-
↓	↓	↓	↓	307	311	316	319	.33	-
				308	312	317	320	.50	-
				309	313	318	321	1.0	-
				-	314	-	-	∞	-
-30X	-30X	.8	.4	-	-	323	-	.2	-
↓	↓	↓	↓	-	-	324	-	.33	-
				-	-	325	-	.50	-
				-	-	326	-	1.0	-
				-	327	-	-	∞	-
-30X	-30X	.9	.3	-	-	328	-	.2	-
↓	↓	↓	↓	-	-	329	-	.33	-
				-	-	330	-	.50	-
				-	-	331	-	1.00	-
				-	332	-	-	∞	-
-30X	+30X	1.07	.53	-	-	333	-	.2	-
↓	↓	↓	↓	-	-	334	-	.33	-
				-	-	335	-	.50	-
				-	-	336	-	1.00	-
				-	337	-	-	∞	-
-30X	-30X	.8	.8	-	-	66	-	.2	NO LE SKIRT:
↓	↓	↓	↓	-	-	67	-	.33	TIP & REAR ONLY.
				-	-	68	-	.5	↓ ↓
				-	-	69	-	1.0	
+30X	0X	.8	.8	211	215	220	224	.2	-
↓	↓	↓	↓	212	216	221	225	.33	-
				213	217	222	226	.5	-
				214	218	223	227	1.0	-
				-	219	-	-	∞	-
+30X	-30X	.8	.8	154	158	163	167	.2	-
↓	↓	↓	↓	155	159	164	168	.33	-
				156	160	165	169	.5	-
				157	161	166	-	1.0	-
				-	162	-	-	∞	-

TABLE IV

TABULATION OF STATIC ROOM TESTS (Continued)

				RUN NO.					
				ANGLE OF ATTACK (α)					
Θ_F	Θ_R	t_{LE}	t_{TE}	-5	0	+5	+10	h/c	Comments
-30X	0X	.8	.8	86	90	95	99	.2	-
				87	91	96	100	.33	-
				88	92	97*	101	.5	*POSSIBLY H = 11"
				89	93	98	102	1.0	-
				-	94	-	-	∞	-
-30X	+30X	.8	.8	103	107	112	116	.2	-
				104	108	113	117	.33	-
				105	109	114	118	.5	-
				106	110	115	119	1.0	-
				-	111	-	-	∞	-
0	0X	.8	.8	-	-	171	-	.2	NO LE SKIRT
				-	-	172	-	.33	
				-	-	173	-	.5	
				-	-	174	-	1.0	
				-	175	-	-	∞	
0X	0X	.8	.8	228	232	237	241	.2	-
				229	233	238	242	.33	-
				230	234	239	243	.5	-
				231	235	240	244	1.0	-
				-	236	-	-	∞	-
-30	+30	.8	.8	-	75	-	-	.2	-
				-	76	-	-	.33	-
				-	77	-	-	.5	-
				-	78	-	-	1.0	-
				-	79	-	-	∞	-
CLOSED	+30	0	.94	-	81	-	-	.2	-
				-	82	-	-	.33	-
				-	83	-	-	.5	-
				-	84	-	-	1.0	-
				-	80	-	-	∞	-
-30X	+30X	1.20	.40	-	-	338	-	.2	-
				-	-	339	-	.33	-
				-	-	340	-	.50	-
				-	-	341	-	1.00	-
				-	342	-	-	∞	-

TABLE IV

TABULATION OF STATIC ROOM TESTS (Continued)

				RUN NO.					
				ANGLE OF ATTACK (α)					
Θ_F	Θ_R	t_{LE}	t_{TE}	-5	0	+5	+10	h/c	Comments
-30X	-30X	.90	.30	343	344	329	345	.33	-
↓	↓	.80	.40	346	347	324	348	.33	-
		1.33	.67	349	-	296	-	.20	-
				350	351	297	352	.33	-
		1.5	.5	353	354	302	355	.33	-
-30X	+30X	1.07	.53	356	357	-	358	.33	-
		1.20	.40	359	360	-	361	.33	-
-30X	-30X	.8	.8	-	-	362	-	.33	β = 20 (1 GV)
				-	-	364	-	.33	β = 25 (1 GV)

TECHNICAL PROGRAM (PHASE II)

TABLE V

Run No.	Θ_F	Θ_R	t_{LE}	t_{TE}	h/c	Rpm	Velocity (fps)
9128	-30	-30	.8	.8	∞	F_4 - 27	0
9129	↓	↓	↓	↓	↓	C_5 - 50	↓
9130	↓	↓	↓	↓	↓	F_5 + 15	↓
9131	↓	↓	↓	↓	↓	I_5 + 21	↓
9134	-30	-30	.8	.8	.33	F_4 - 30	0
9135	↓	↓	↓	↓	↓	C_5 + 15	↓
9136	↓	↓	↓	↓	↓	F_5 + 32	↓
9137	↓	↓	↓	↓	↓	I_5 + 27	↓
9229	-30	+30	.8	.8	∞	F_4 - 25	0
9230	↓	↓	↓	↓	↓	C_5 + 5	↓
9231	↓	↓	↓	↓	↓	F_5 + 30	↓
9232	↓	↓	↓	↓	↓	I_5 + 10	↓
9235	-30	+30	.8	.8	.33	F_4 - 5	0
9236	↓	↓	↓	↓	↓	C_5 + 11	↓
9237	↓	↓	↓	↓	↓	F_5 + 22	↓
9238	↓	↓	↓	↓	↓	I_5 + 30	↓
9245	-30	+30	.8	.8	.33	F_4 + 20	60
9248	↓	↓	↓	↓	↓	C_5 - 14	60
9251	↓	↓	↓	↓	↓	F_5 + 12	60

TABLE V

TABULATION OF TRACK TESTS (Continued)

Run No.	Θ_F	Θ_R	t_{LE}	t_{TE}	h/c	Rpm	Velocity (fps)
9257	-30	+30	.8	.8	.33	I_5 - 10	45
9260	↓	↓	↓	↓	↓	I_5 + 34	22.5
9277	-	+30	-	.8	∞	F_4 - 22	0
9278	↓	↓	↓	↓	↓	C_5 - 38	↓
9279	↓	↓	↓	↓	↓	F_5 + 15	↓
9280	↓	↓	↓	↓	↓	I_5 - 8	↓
9283	-	+30	-	.8	.33	F_4 - 56	0
9284	↓	↓	↓	↓	↓	C_5 - 49	↓
9285	↓	↓	↓	↓	↓	F_5 + 10	↓
9287	↓	↓	↓	↓	↓	I_5 + 15	↓
9318	-	+30	-	.94	.33	F_4 - 19	0
9319	↓	↓	↓	↓	↓	C_5 - 35	↓
9320	↓	↓	↓	↓	↓	F_5 + 30	↓
9321	↓	↓	↓	↓	↓	I_5 + 11	↓
9326	-	+30	-	.94	∞	F_4 + 37	0
9327	↓	↓	↓	↓	↓	C_5 - 50	↓
9328	↓	↓	↓	↓	↓	F_5 - 14	↓
9329	↓	↓	↓	↓	↓	I_5 - 28	↓

TABLE V

TABULATION OF TRACK TESTS (Continued)

Run No.	Θ_F	Θ_R	t_{LE}	t_{TE}	h/c	Rpm	Velocity (fps)
9370	-	+30	-	.94	.33	F_4 + 10	60
9373	↓	↓	↓	↓	↓	C_5 - 5	60
9376	↓	↓	↓	↓	↓	F_5 - 50	60
9380	↓	↓	↓	↓	↓	I_5 - 32	45
9383	↓	↓	↓	↓	↓	I_5 - 47	22.5
9390	-30	-30	.8	.8	.33	F_4 - 8	60
9393	↓	↓	↓	↓	↓	C_5 + 40	60
9396	↓	↓	↓	↓	↓	F_5 - 5	60
9399	↓	↓	↓	↓	↓	I_5 + 25	45
9402	↓	↓	↓	↓	↓	I_5 + 21	22.5

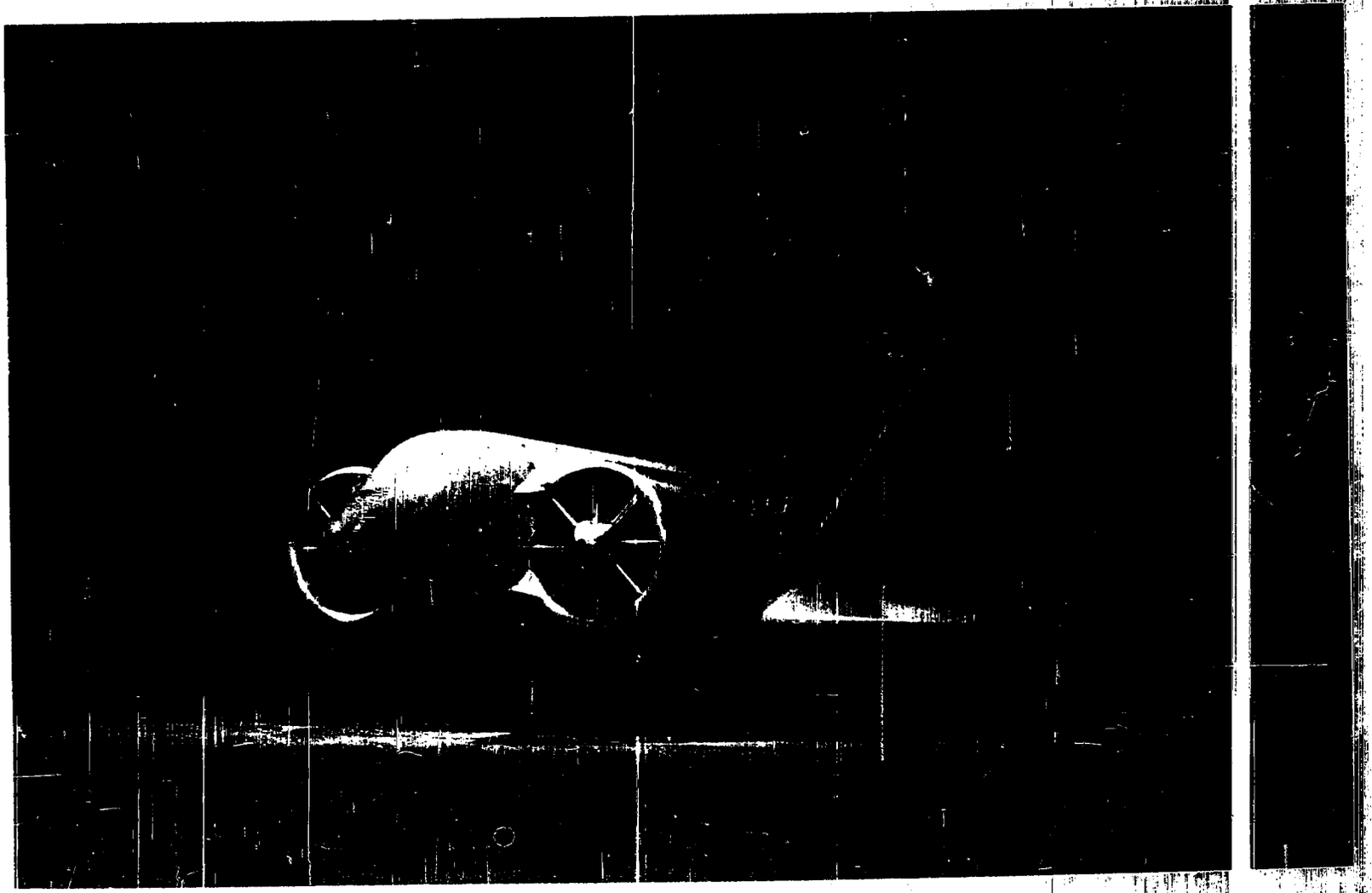

Figure 35. GETOL Model Suspended from Moving Carriage

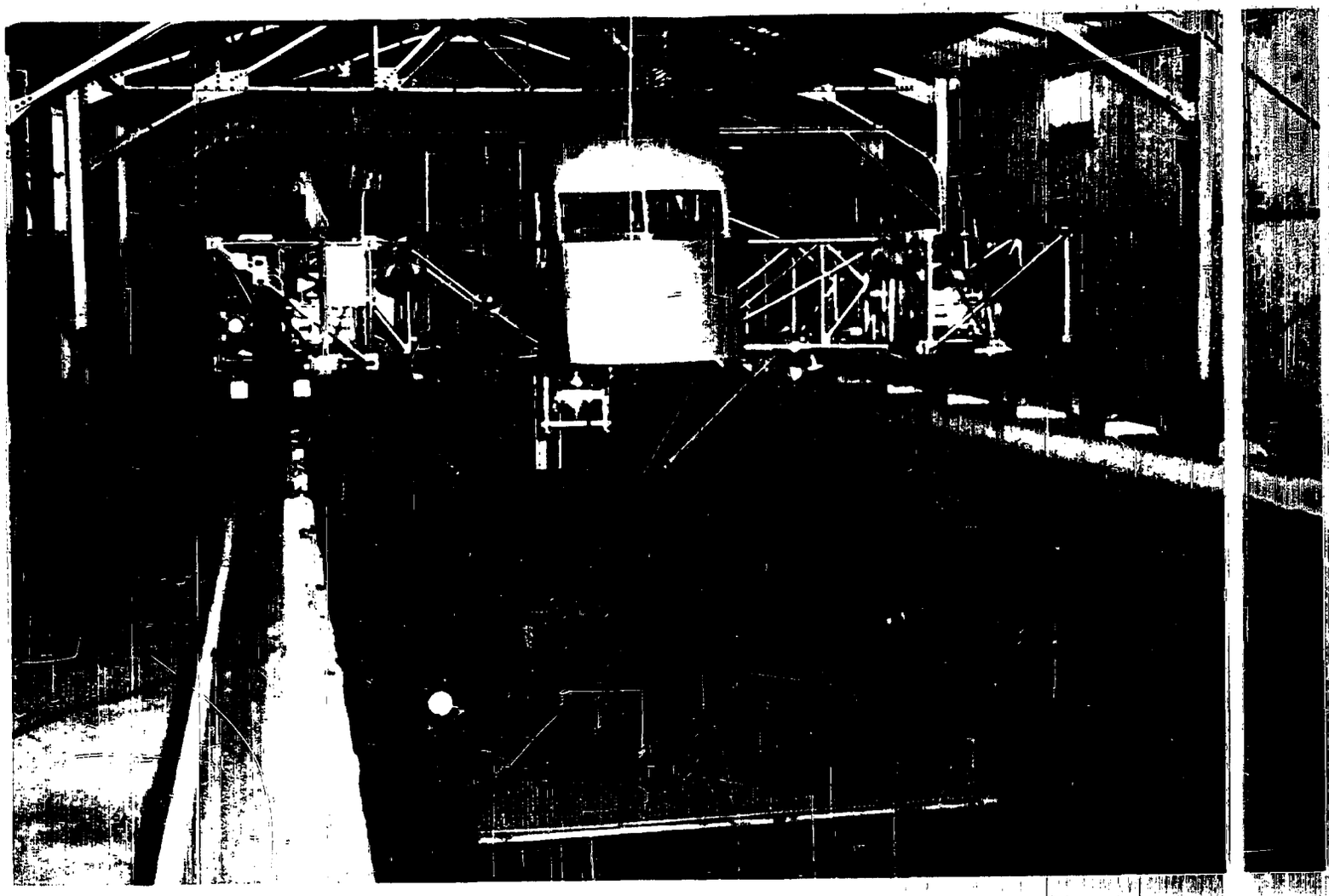

Figure 36. NASA Moving Carriage Installation

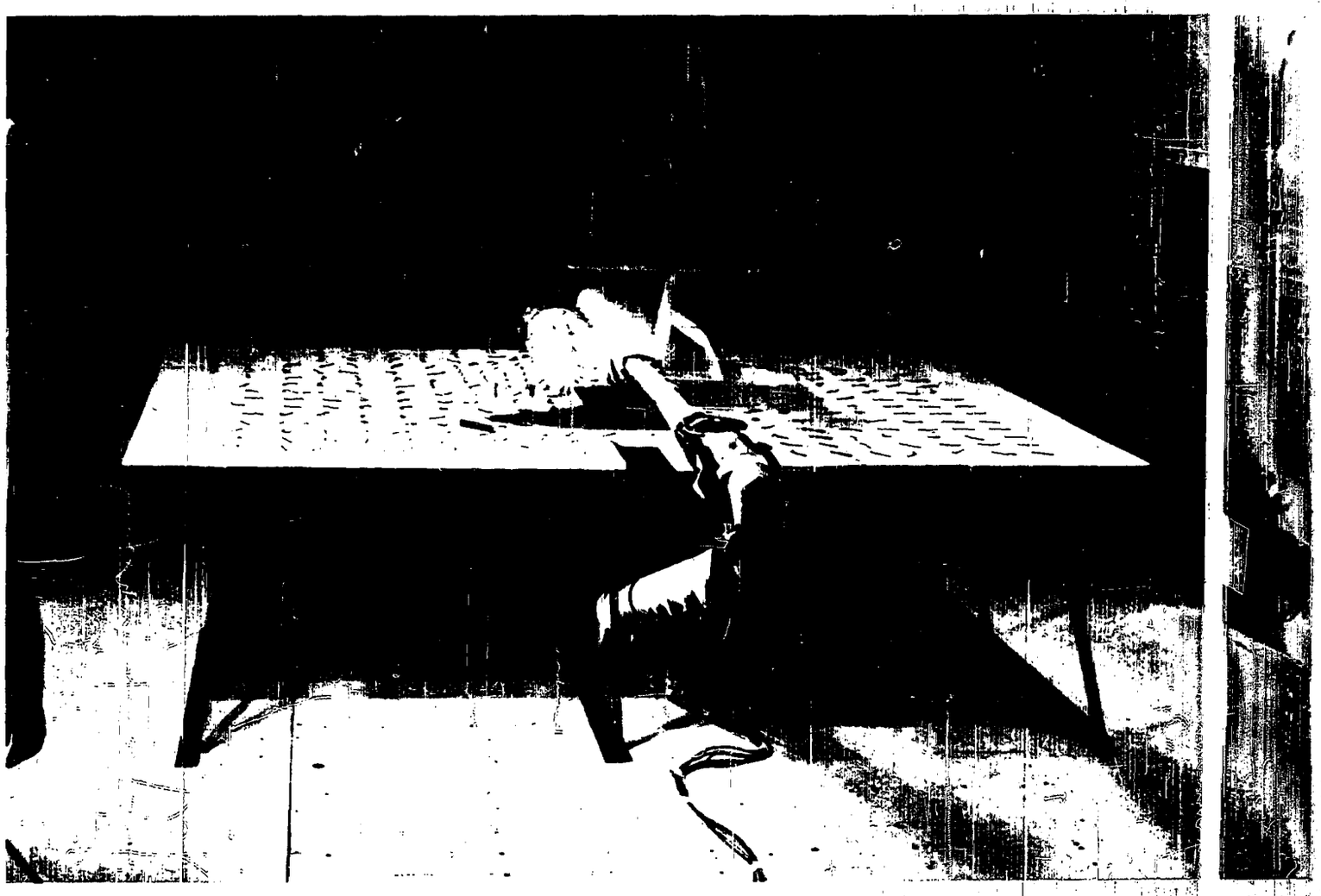

Figure 37. GETOL Model in NASA Test Section

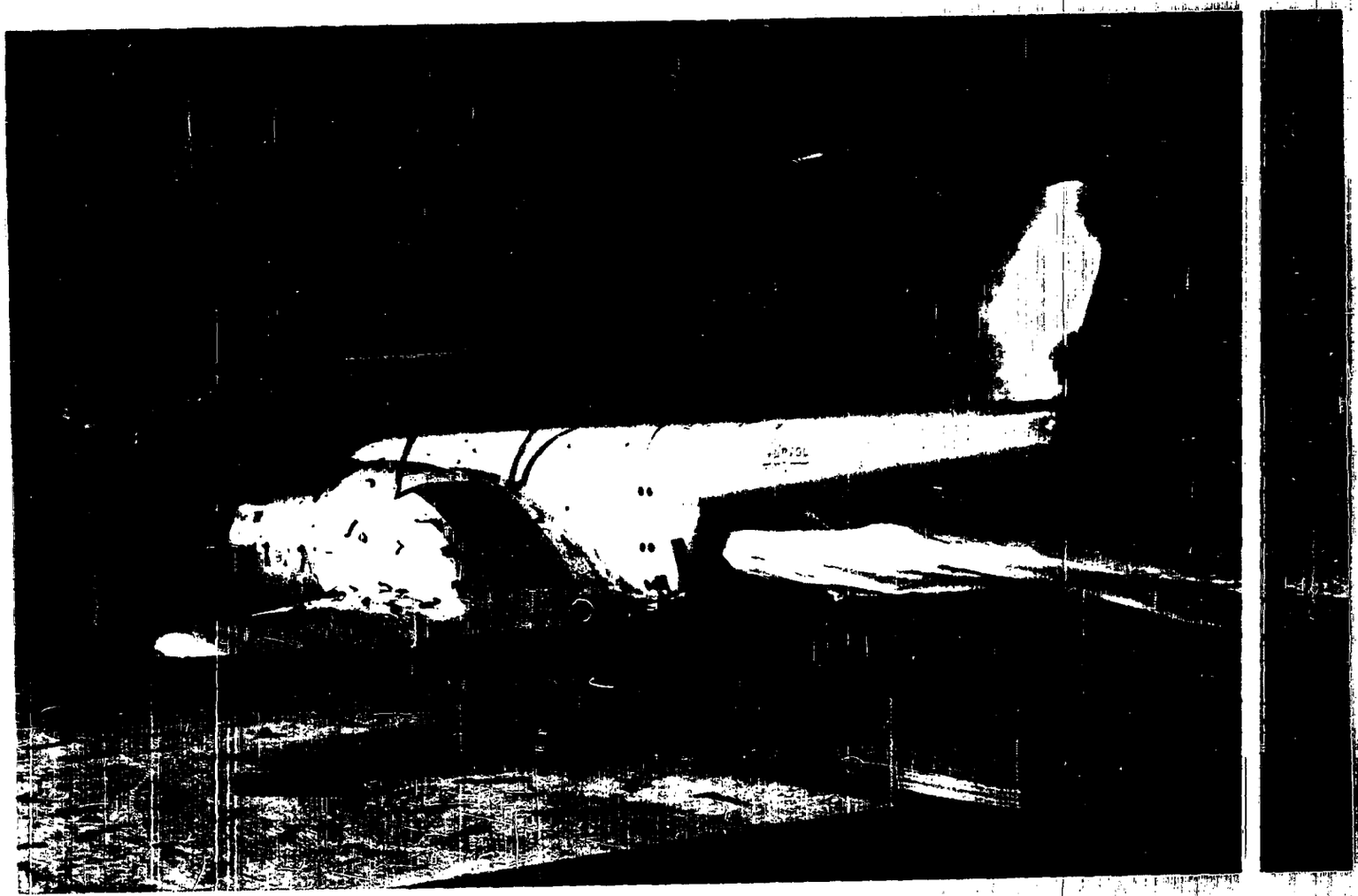

Figure 38. GETOL Model and Ground Board Installation

TABLE VI

TABULATION OF TUNNEL TESTS

Config. No.	Run No.	Θ_F	Θ_R	t_{LE}	t_{TE}	h/c	Door	Tail	Skirts	Comments
42	633-636	-30x	+30x	.8	.8	.2	0	OFF	YES	
43	637-640	-		.8	.8	.5	0	OFF	YES	
67	641-644			1.2	.4	.5	0	OFF	YES	
68	645-648			1.2	.4	.2	0	OFF	YES	
69	649-652			1.2	.4	.33	0	OFF	YES	
46	653-656			.6	.6	.33	0	OFF	YES	
47	657-660			1.0	1.0	.33	0	OFF	YES	
70	661-666			.8	.8	∞	0	OFF	YES	
71	667-670			.8	.8	∞	0	ON	YES	
27	671-674	-	+30x	-	.8	∞	0	ON	YES	
36	675-680	-		-	.8	∞	0	OFF	YES	
72	681	-		-	.8	∞	0	OFF	YES	V = 0
27	682	-		-	.8	∞	0	ON	YES	
73	683-688	-	+60x	-	.8	∞	0	OFF	YES	
74	689	-		-	.8	∞	0	OFF	YES	V = 0
26	690-693	-		-	.8	∞	0	ON	YES	
32	694-697	-	-30x	-	.8	∞	0	ON	YES	
33	698-703	-		-	.8	∞	0	OFF	YES	
75	704	-		-	.8	∞	0	OFF	YES	V = 0
76	705-710	-30x	+30x	.8	.8	∞	0	OFF	YES	
77	711-714	-30x	+30x	.8	.8	∞	0	ON	YES	
14	716-719	-	-	-	-	∞	OFF	ON	NO	Airplane
38	720	-	-	-	-	∞	0	ON	NO	Nacelles Blocked Long Fuselage
39	721	-	-	-	-	∞	0	OFF	NO	Nacelles Blocked Long Fuselage
40	722	-	-	-	-	∞	0	OFF	NO	Nacelles Blocked Short Fuselage
41	723	-	-	-	-	∞	0	ON	NO	Nacelles Blocked Short Fuselage
78	401	-	-	-	-	.33	0	ON	NO	
79	402	-	-	-	-	.20	0	ON	NO	
80	403	-	-	-	-	.33	0	OFF	NO	
81	404	-	-	-	-	.20	0	OFF	NO	
31	405-409	-30	-30	.8	.8	.33	0	OFF	NO	
82	410-414	-30	+30	.8	.8	.33	0	OFF	NO	
37	415-419	-	+30	-	.94	.33	0	OFF	NO	
12	420-425	-	+30	-	.94	.33	0	ON	YES	
54	428	-	+30	-	.94	.33	0	ON	YES	q = 0
55	429-430	-	+60x	-	.94	.33	0	ON	YES	

TABLE VI

TABULATION OF TUNNEL TESTS (Continued)

Config. No.	Run No.	Θ_F	Θ_R	t_{LE}	t_{TE}	h/c	Door	Tail	Skirts	Comments
56	437	-	+60x	-	.94	.33	0	ON	YES	q = 0
8	445-450	-30x	+30x	.8	.8	.33	0	ON	YES	
9	457-460	↓	↓	.8	.8	.33	.2	ON	YES	
11	463-468	↓	↓	.8	.8	.33	2.0	ON	YES	
10	469-474	↓	↓	.8	.8	.33	1.05	ON	YES	
28	481-486	-30x	-30x	.8	.8	.33	0	OFF	YES	
2	487-492	↓	↓	.8	.8	.2	0	ON	YES	
1	493-498	↓	↓	.8	.8	.33	0	ON	YES	
50	499-504	-60x	+60x	.8	.8	.33	0	ON	YES	
51	505-508	↓	↓	.8	.8	.2	0	ON	YES	
6	511-516	↓	↓	1.2	.4	.33	0	ON	YES	
4	517-519	-30x	-30x	.8	.8	.33	1.05	ON	YES	
5	520-522	↓	↓	.8	.8	.33	1.94	OFF	YES	
48	523-525	↓	↓	.8	.8	.33	0	OFF	YES	5° Roll (L. Wing Down)
49	526-528	↓	↓	.8	.8	.33	0	OFF	YES	10° Roll (L. Wing Down)
53	529-534	↓	↓	.8	.8	.2	0	OFF	YES	
3	535-540	↓	↓	.8	.8	.5	0	OFF	YES	
7	541-543	↓	↓	1.2	.4	.5	0	OFF	YES	
15	544-546	↓	↓	1.2	.4	.2	0	OFF	YES	
13	547-549	↓	↓	1.2	.4	.33	0	OFF	YES	
52	550-552	↓	↓	1.1	.5	.33	0	OFF	YES	
30	553-555	↓	↓	.6	.6	.33	0	OFF	YES	
29	556-558	↓	↓	1.0	1.0	.33	0	OFF	YES	
57	559	↓	↓	.8	.8	.33	0	OFF	YES	Asymetric Power L-I_5 R-off
58	560	↓	↓	.8	.8	.33	0	OFF	YES	Asymetric Power L-I_5 R-C_4
59	561	↓	↓	.8	.8	.33	0	OFF	YES	Asymetric Power L-I_5 R-L_4
60	563-565	↓	↓	.8	.8	.33	0	OFF	YES	Yaw Control LF +30 RR +30
44	575	-	-30x	-	.8	.33	2.0	OFF	YES	
45	576-577	-	-30x	-	.8	.50	2.0	OFF	YES	
61	586	+30x	-30x	.8	.8	.33	0	OFF	YES	
18	587-589	↓	↓	.8	.8	.20	0	OFF	YES	
16	590-592	↓	↓	.8	.8	.50	0	OFF	YES	
19	593-596	0x	-30x	.8	.8	.50	0	OFF	YES	

TABLE VI

TABULATION OF TUNNEL TESTS (Continued)

Config. No.	Run No.	Θ_F	Θ_R	t_{LE}	t_{TE}	h/c	Door	Tail	Skirts	Comments
21	597-600	0x	-30x	.8	.8	.20	0	OFF	YES	
62	602	↓	↓	-	-	.50	0	OFF	NO	Nacelles Closed, Power Off
20	603-606	0x	-30x	.8	.8	.33	0	OFF	YES	
63	607-610	↓	0x	.8	.8	.33	0	OFF	YES	
64	611-614	↓	↓	.8	.8	.2	0	OFF	YES	
34	615-618	↓	↓	.8	.8	.5	0	OFF	YES	Check
35	619-624	-30x	-30x	.8	.8	.33	0	OFF	YES	
65	625-628	↓	↓	.8	.8	.33	0	OFF	YES	β = -5° Roll
66	629-632	↓	↓	.8	.8	.33	0	OFF	YES	β = -10° Roll

of the tunnel ground board, which was mounted on parallelogram legs, and did not fold readily. After repeated efforts, a change in the wing slot inserts could be accomplished in about twenty minutes.

The analysis of the data for this section are evaluated on Pages 80 to 148.

Interface of GETOL Test Data

General

Data were obtained from tests at Boeing-Vertol, Princeton University, University of Toronto and at NASA's Langley Field facility. To achieve a comprehensive picture, a concatenation of the separate sources of data are required. Since the majority of the data obtained are from NASA and are the bases upon which most of the conclusions were obtained, this section of the GETOL final report will show the interface of the data from the above tests.

Interface of Boeing-Vertol and NASA Flow Data

From the preliminary testing in the static room at NASA, it became evident that the rotation of the air at the measuring station caused by the high pressure air used to drive the fan would present problems in flow calibration, force measurement and internal losses. Figure 40 presents the maximum total and static pressure distribution across the duct as obtained from surveys made with hand-held probes and from fixed rakes at the measuring station.

Before the honeycomb behind the fan was installed, there was a large difference in the pressure readings obtained from the survey and fixed rakes. This was caused by reading the maximum pressure (essentially the supply pressure near the duct wall) at its skew angle from the axial direction of the duct for the survey and measuring the axial component for the fixed rakes. After the honeycomb was installed there was good agreement between the survey and the fixed rakes thus indicating that the swirl problem was eliminated. From the data obtained from the static room testing of the model (with the honeycomb), an estimation of the losses from the measuring station behind the fan to the peripheral slot was made for various configurations. Shown on Figure 15 is the total pressure at specific station through the model referred to the total pressure measured behind the fan. It can be noted that there is a narrow band formed by the various peripheral jet configurations investigated. Also there is a significant difference in the losses between the preliminary Boeing-Vertol tests made on the wind tunnel model (without honeycomb) and that from the NASA data. The magnitude of the losses up to the inlet to the peripheral slot was less than estimated from preliminary analysis and much less than that obtained from initial internal flow tests. This indicates that an internal flow system can be constructed to result in a small loss while having a complicated path through which the air must flow.

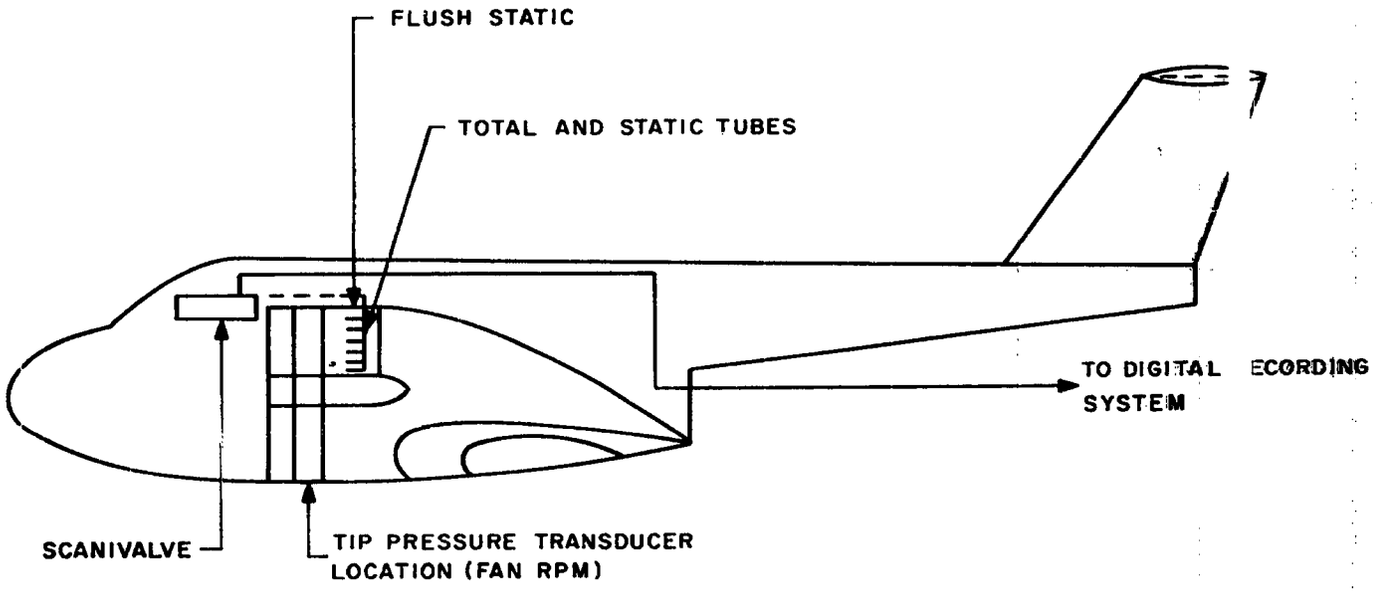

Figure 39. Fan Flow and Pressure Instrumentation

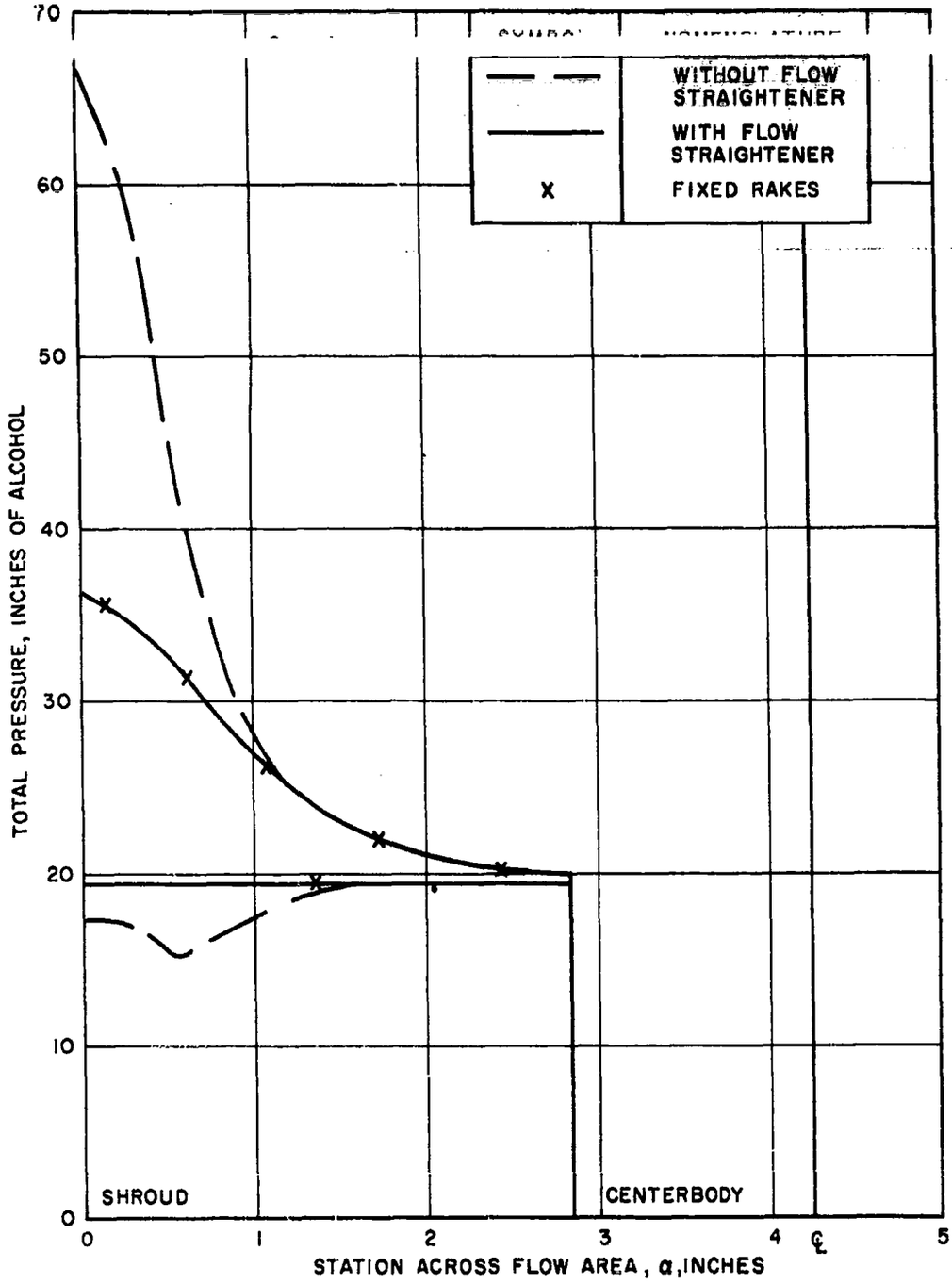

Figure 40. Fan Flow Calibration

TECHNICAL PROGRAM (PHASE II)

Interface of NASA Track And Wind Tunnel Force Data (Moving Boundary Layer)

The testing accomplished at the tow track facility, as described on Page 64, was not very significant. Force data were made vague by the random oscillation imposed on model by the supporting carriage which moved along the track. Flow data does not include the effects of the honeycomb. With these facts in mind, comparisons for three configurations were made with the NASA Static Room and Wind Tunnel Data. These comparisons are for the following configurations:

1. Figure 41: $\theta_F{}^2 = $ —— $\theta_R = +30°$
2. Figure 42: $\theta_F{}^2 = -30$ $\theta_R = -30$
3. Figure 43: $\theta_F{}^2 = -30$ $\theta_R = +30$

The method of presentation of the data used in this section is typical of a convenient form of non-dimensionalization. Shown is the conventional Lift Coefficient divided by the Momentum Coefficient plotted against the reciprocal of the Momentum Coefficient for a constant angle of attack. This presents the continuous variation of lift from hover through transition. For any specific conditions the Lift Coefficient can be obtained by dividing the ordinate by the abcissa. The abcissa is indicative of a forward speed scale where $1/C\mu$ is equal to zero. The velocity is zero and as $1/C\mu$ increase the velocity also increases. For the jet flap configuration (see Figure 41) there appears to be good agreement over the range of the reciprocal of the Momentum Coefficient tested. Figure 42 presents the hovering slot arrangement. This indicates close agreement in hover and low values of $1/C\mu$. As the speed is increased there is a deviation showing the track data resulting in a higher lift than the wind tunnel data. In Figure 43 there is still a different trend shown. In hover and low values of $1/C\mu$ there is poor agreement, and indicating the track data has developed a greater amount of lift than the tunnel data. As the speed is increased the trend is completely reversed; the tunnel data demonstrates higher lift than the track data.

These trends discussed cannot be taken as conclusive evidence as to what effect the moving or stationary boundary layer on the ground board has on the forces developed by the model in forward flight.

Interface of Princeton Planform And NASA Static Room Data

A planform for the GETOL wind tunnel model was determined from initial testing performed at Princeton University and preliminary analysis by Boeing-Vertol. This testing (see Page 35) was performed to give some qualitative insight into the performance to be expected from the model design. A standard performance comparison for Ground Effect Vehicles, shown in Figure 44, is the

relationship of Augmentation Ratio and the Height to Chord Ratio. In this figure

$t_{LE} = t_{TE}$). There is a small difference in the curves and can be attributed to the possible inaccuracies in flow measurement in the Princeton tests. These are limitations imposed upon the data by the low mass flow through the model and thereby results in extremely low pressure differentials that are difficult to obtain accurately.

With these factors in mind, the conclusion reached from the Princeton tests presented a good quantitative and qualitative representation of the basic hovering characteristics of the wind tunnel planform that can be made.

Analysis of NASA Data

General: The data obtained during the NASA tests incorporates so many facets that it has been difficult to determine a best method of presentation. Rather than discuss the data for each test phase (i.e. static room, track and tunnel), it has been decided to discuss by subject the findings of these tests. Occasionally, several items utilize data plotted on a given curve, so of necessity, curves and figures are collectively grouped. Cross reference or duplication in considerations (such as slot angles when discussing gap ratio or gap ratio when discussing trim moments) are unavoidable and necessary.

Some of the important factors that affect the data in this section are stressed here. The model had a lengthened fuselage and nacelles. A section of approximately twelve inches was added to facilitate in measuring the flow behind the fan. With this lengthened section there was the possibility of developing vortex flow and have a negative lift and nose down pitching moment increment. It became evident from some exploratory investigations that these effects were of minor magnitude and therefore are not included in this report.

Slot extensions and skirts were used in almost all of the static room and wind tunnel testing, but unfortunately none were used at the track test. Honeycomb flow straighteners were used in the static room and wind tunnel testing but were not installed at the time of the track tests.

Development of Performance Parameters (Augmentation or Lift/HP): To evaluate the performance of any of the tested GETOL configurations, it was first necessary to determine a parameter which would truly reflect such performance. Classically, ground effect vehicles have used "Augmentation" termed "A", as a measure of performance

$$\text{"A"} = \frac{\text{total lift}}{\text{jet lift}} = \frac{L}{mV_j}$$

Many other definitions have been proposed such as:

$$\text{"A"} = \frac{\text{lift in Ground Effect}}{\text{lift out of Ground Effect}}$$

or

$$\text{"A"} = \frac{\text{Lift}}{mV_{\text{equivalent}}}$$

Use of mV_J (mass flow rate x average slot jet velocity) seems most logical, but the ability to know V_J is the problem. Princeton has used Chaplin's theory of thin jets to determine V_J from a measurement of base pressure, but this base pressure measurement is so dependent on the location of such measurement that errors are almost inevitable.

Knowledge of the total pressure within the wing (or plenum) and the calculation of the resultant jet velocity is another possibility but depends on (usually known) slot orifice characteristics.

A third method is to define V_J from the Quantity Flow and the slot area. This, too, depends on the slot orifice coefficient, but if the slot flow area is considered to be the geometric slot area, at least a consistent set of numbers can be obtained.

Figure 45 presents the results of the NASA tests on the GETOL model as Augmentation Ratio (A) versus Height to Chord Ratio (h/c), where V_J is defined as the Quantity Flow divided by the geometric slot area ($Q/A_{\text{slot geom}}$). Inspection of this curve shows the design Augmentation Ratio attained at a Height to Chord Ratio of .33 is 1.60. Further, this method of obtaining mV_J shows an advantage in Augmentation Ratio for a wider gap and is illustrated in Figure 46 for three power levels tested in the static room. The first conclusion drawn from these two figures is that the wider gap is better. However, Figure 47 presents the Quantity Flow for these same gap areas and it is apparent that as the slot is widened the flow does not proportionately increase; the flow is not filling the slot gap and defining actual V_J as $Q/A_{\text{slot geom}}$ is in error.

Looking further, Figure 48 presents the same model configurations in terms of lift per air horsepower (L/HP). Here, no unknowns are involved (not to say that test inaccuracies might not exist). L/HP is considered a very valid measure of performance. However, note that no particular advantage is shown for any gap ratio; if any, there is a slightly better power required situation for the smaller and larger slot, certainly contradictory to Figure 46.

To evaluate another definition of V_J, where:

$$V_J = \sqrt{\frac{2P_{T\text{slot}}}{\rho}}$$

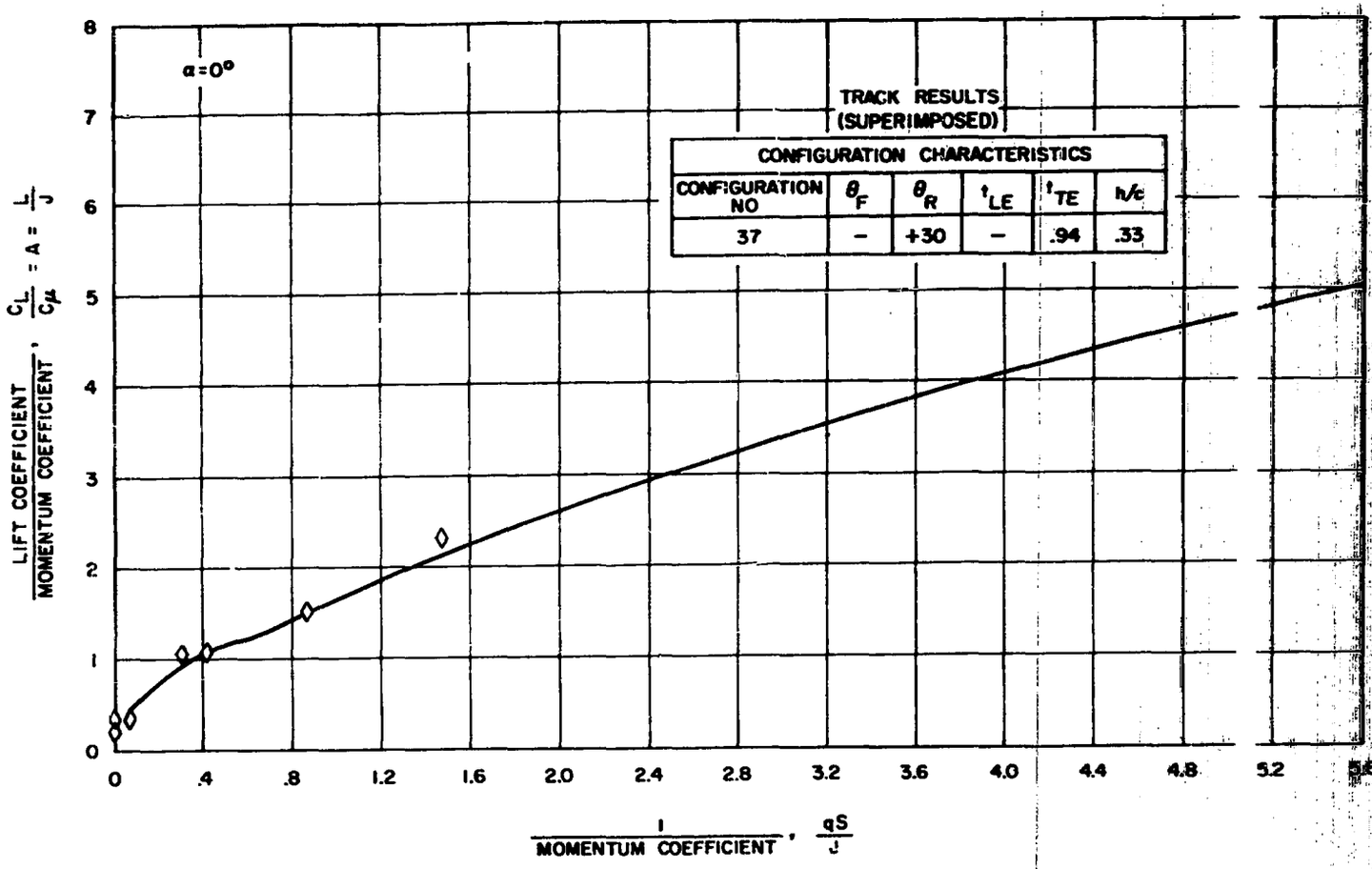

Figure 41. $\frac{\text{Lift Coefficient}}{\text{Momentum Coefficient}}$ vs. $\frac{1}{\text{Momentum Coefficient}}$ ($\alpha = 0°$)

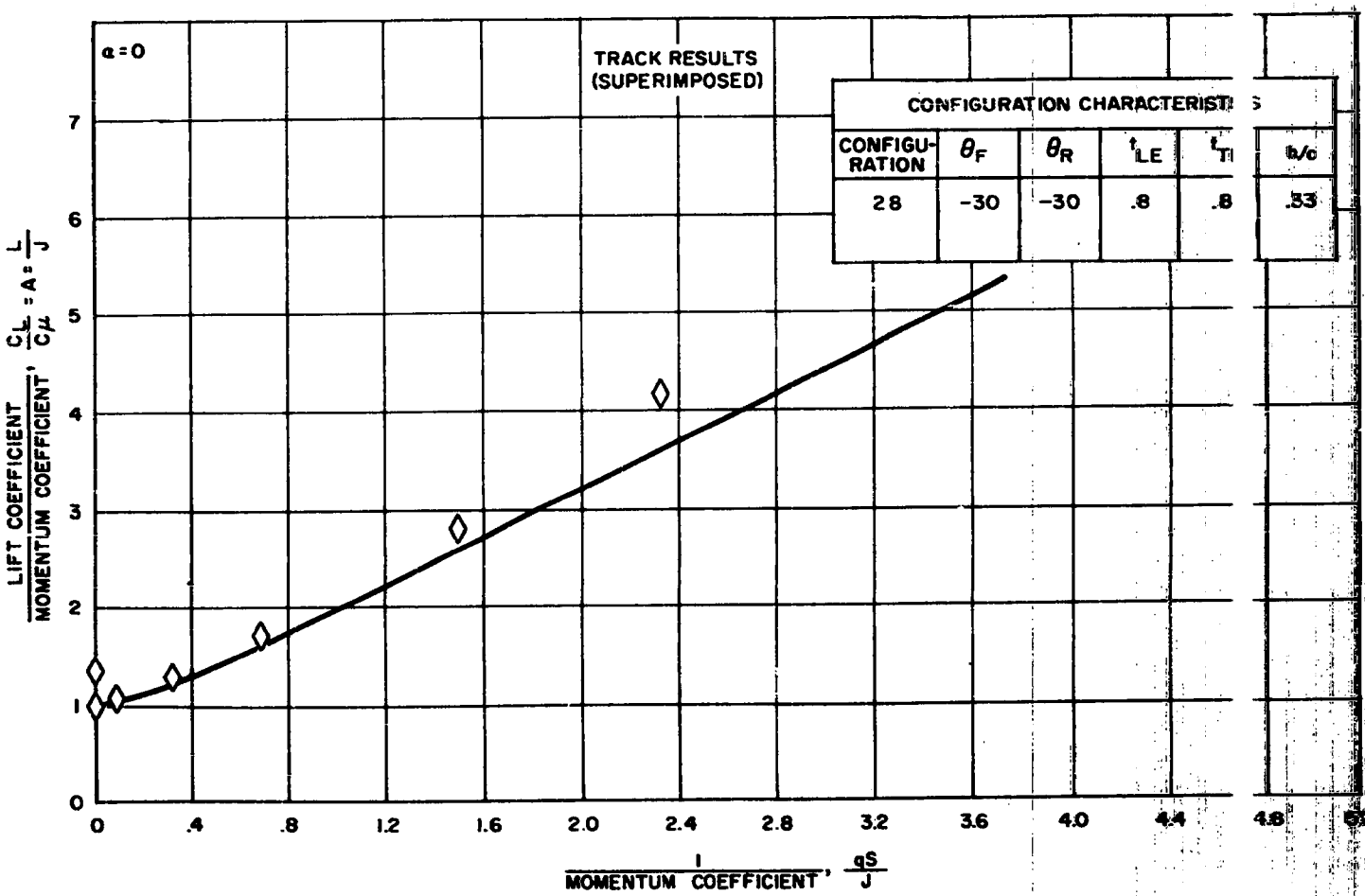

Figure 42. $\frac{\text{Lift Coefficient}}{\text{Momentum Coefficient}}$ vs. $\frac{1}{\text{Momentum Coefficient}}$ ($\alpha = 0°$)

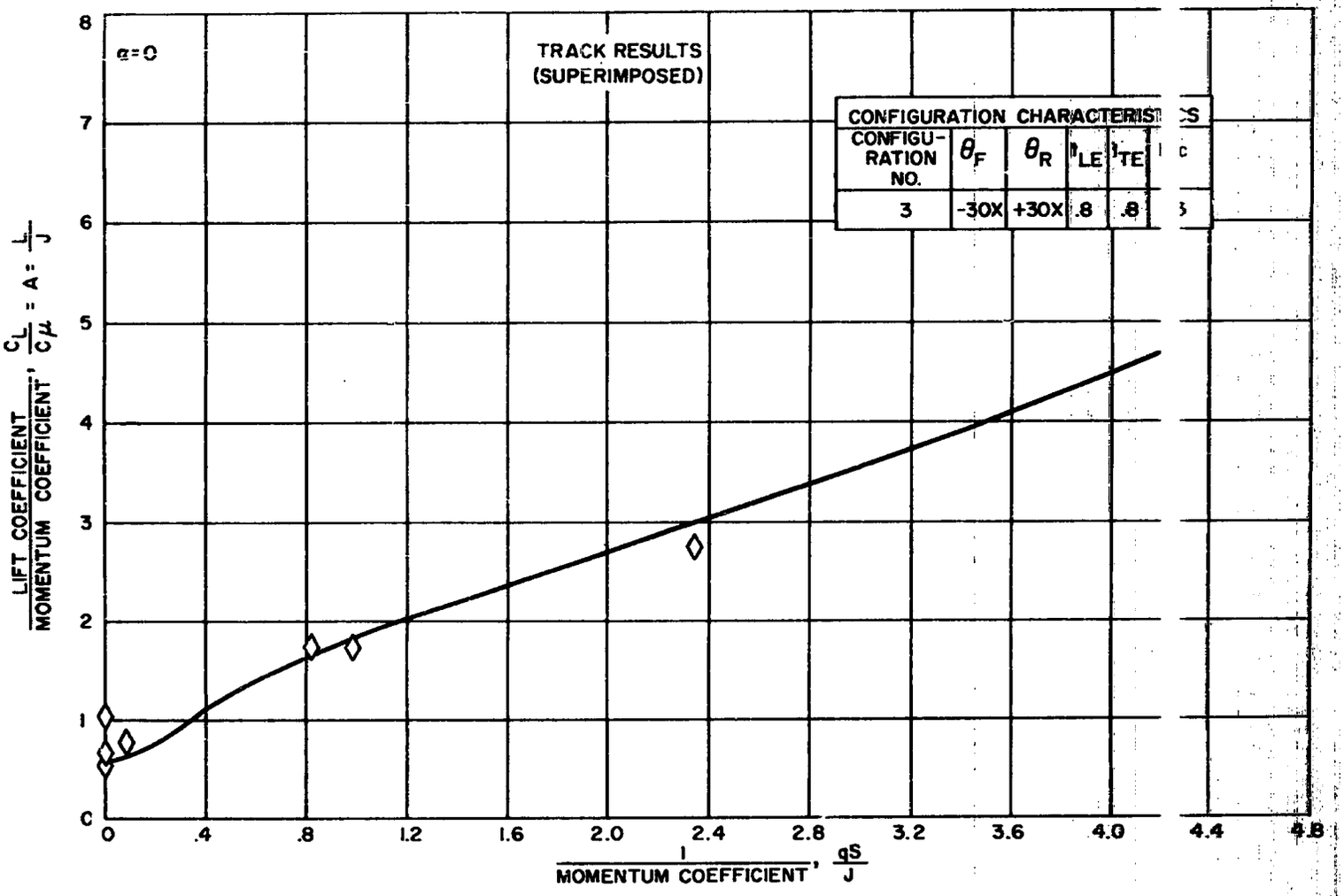

Figure 43. $\frac{\text{Lift Coefficient}}{\text{Momentum Coefficient}}$ vs. $\frac{1}{\text{Momentum Coefficient}}$ ($\alpha = 0°$)

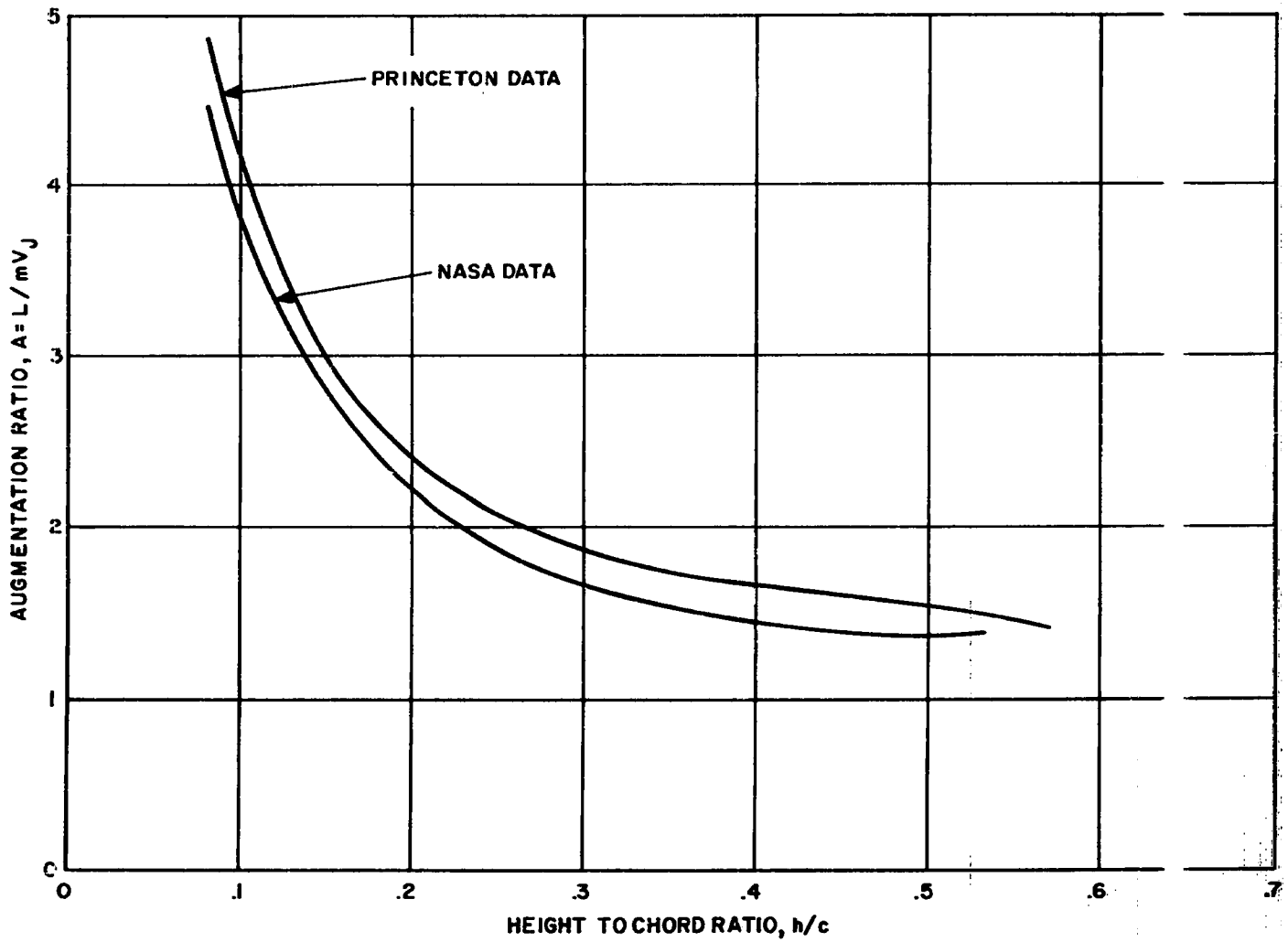

Figure 44. Augmentation Ratio vs. Height to Chord Ratio

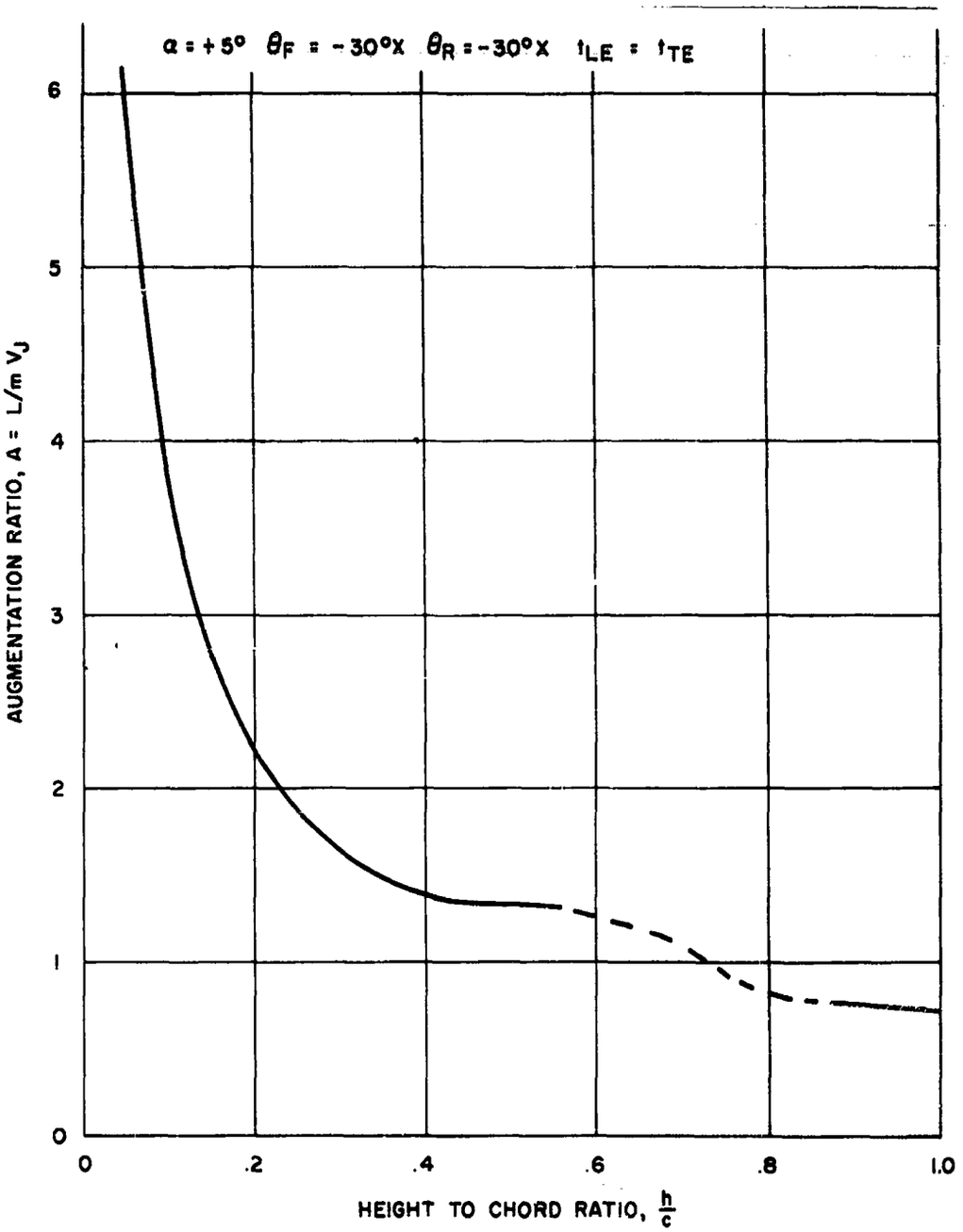

Figure 45. Augmentation Ratio vs. Height to Chord Ratio

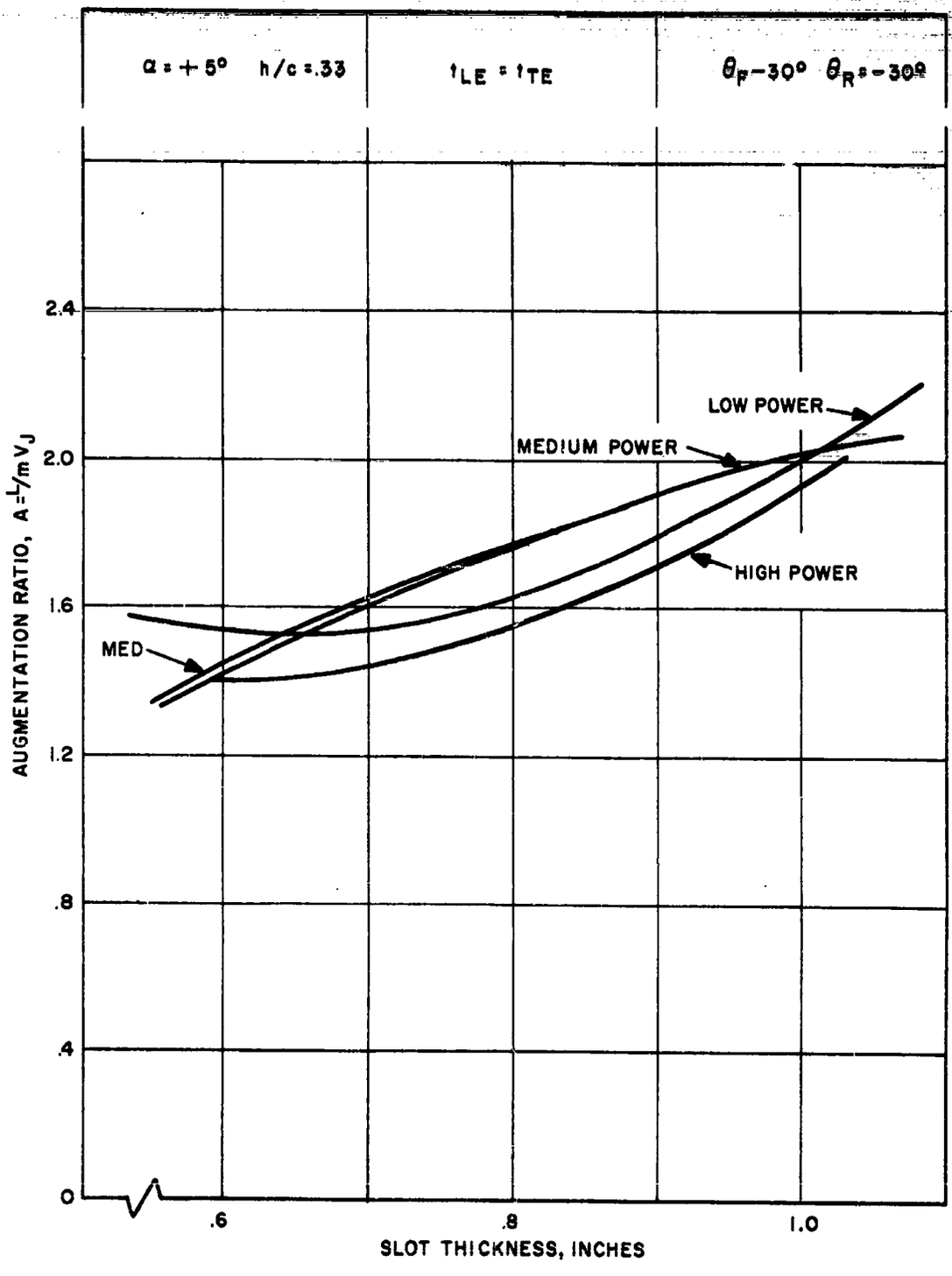

Figure 46. Comparison of Augmentation Ratio for Three Gap Areas and Three Power Levels (h/c = .33, α = +5°)

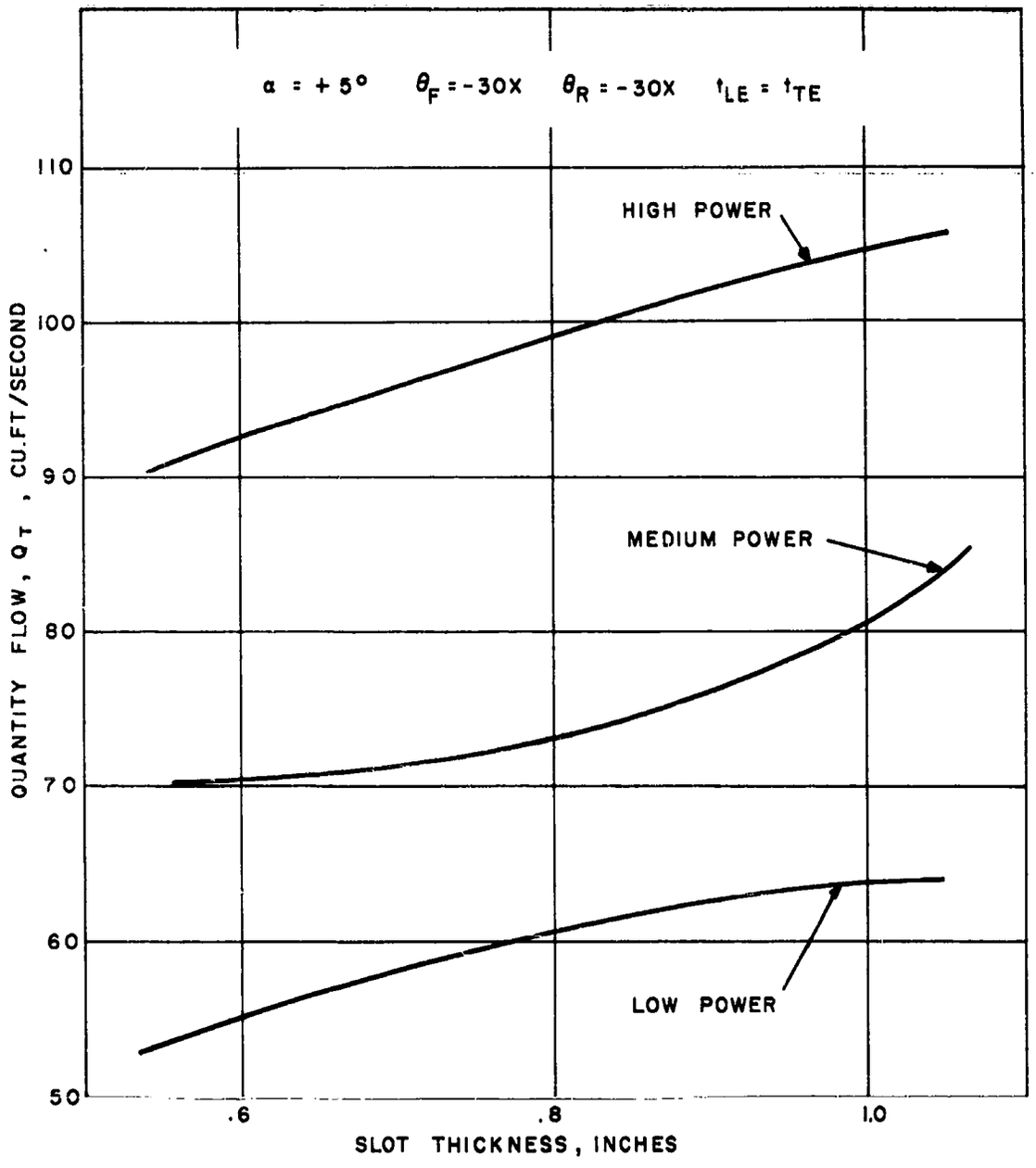

Figure 47. Quantity Flow vs. Gap Area for Three Power Levels

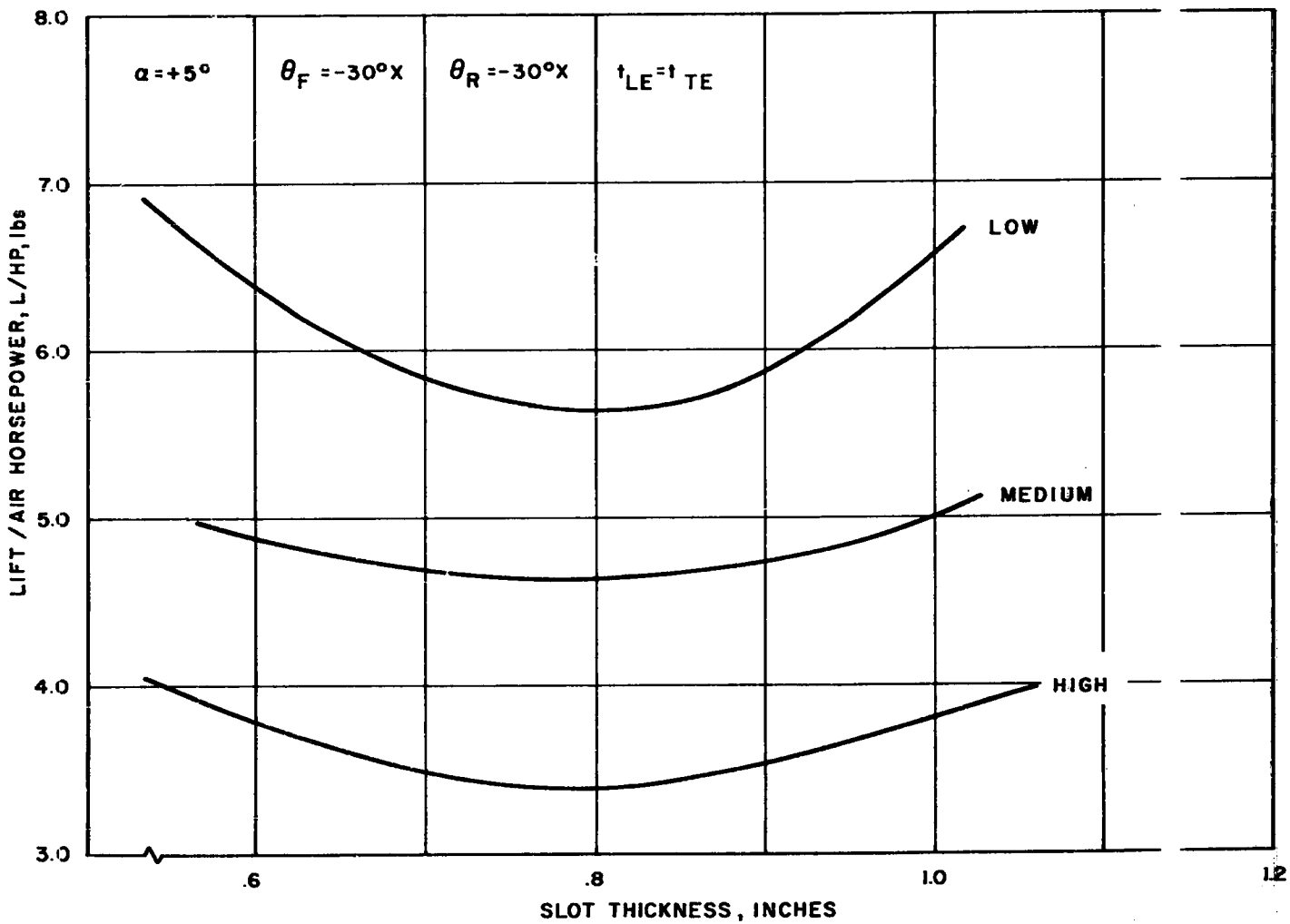

Figure 48. Lift Per Air Horsepower vs. Gap Area ($\alpha = +5°$)

Table VII presents the Augmentation Ratio based upon:

$$\text{"A"} : V_J = Q/A_{slot} \quad \text{or} \quad \text{"A}_2\text{"} : V_{J_2} = f\,(P_{T_{slot}})$$

TABLE VII

COMPARISON OF AUGMENTATION RATIO

Configuration (GAP - $t_{LE} = t_{TE}$)	Slot Velocity (VT) (Ft/Sec)	Slot Velocity (V_{J_2}) (Ft/Sec)	Augmentation Ratio ("A")	Augmentation Ratio ("A_2")
.6	151	169	1.4	1.11
.8	124	173	1.8	1.14
1.0	114	171	2.0	1.17

"A_2" seems about constant with changing gap area, "A" of course varies.

The solution to this problem is as follows:

1. To evaluate hovering capabilities of various model geometries, we must use L/HP.

2. To conveniently compare hovering capabilities for the same geometry but at different heights or attitudes, this is consistent with flow data discussed in subsequent sections where heights, angle of attack and even forward velocities tested make no significant difference in slot flow rate. The only available parameter (besides fan RPM, of course) which significantly changes flow rates is gap geometry. We may use Augmentation Ratio and we will define "A" in terms of the most easily measured test information as $Q/A_{slot\ geom}$.

The previous discussion concerns itself, primarily with the hovering regime. For the transition and forward flight regimes, L/HP appeared to be the best method of comparison since it has been shown that no unknowns are involved and is a valid measure of performance. This is so if the comparison of L/HP versus forward speed are made for specific design parameters (especially wing loading, ω). In an attempt to make the following analysis applicable to any "size" aircraft of this general configuration it was necessary to determine an additional performance parameter.

As can be seen in Volume II, Appendix C, this non-dimensional form of presentation for the force data is applicable to any wing loading.

Power data can be handled in a similar manner but not non-dimensionally. To see this relationship, it is first necessary to look at the fan characteristics; this is done in detail on Page 96 but it can be stated that for one configuration there is a fixed resistance and a relationship between the total pressure behind the fan and the quantity flow that exists. Since air horsepower is essentially the product of the total pressure and Quantity Flow, and jet slot momentum (jet lift) is a function of Quantity Flow, there is a definite correlation between air horsepower and jet slot momentum.

For a given set of conditions, equilibrium flight (Drag = 0) and a specific angle of attack, the reciprocal of the Momentum Coefficient is determined and hence the Lift Coefficient Over the Momentum Coefficient ($\frac{C_L}{C_\mu} = \frac{L}{mV_J} = A$), results in an effective Augmentation Ratio through transition being obtained. By dividing a specific wing loading by the effective Augmentation Ratio, the jet slot momentum per unit of wing area is determined and thereby specifies the power per unit of wing area.

Therefore, the following statements can be made:

1. $\frac{\text{Jet slot momentum}}{\text{Wing area}} = \frac{\text{Wing loading}}{\text{Effective Augmentation Ratio}} \quad \left[\frac{mV_j}{S_\omega} = \omega/(L/J)\right]$
2. $\frac{\text{Air horsepower}}{\text{Wing area}} = \text{Constant} \left(\frac{\text{jet slot momentum}}{\text{wing area}}\right)^{3/2} \quad \left[\frac{HP}{S_\omega} = K * \left(\frac{mV_J}{S_\omega}\right)^{3/2}\right]$
3. $\frac{\text{Lift}}{\text{Air horsepower}} = \frac{\text{Wing Loading}}{\text{Air horsepower/wing area}} \quad \left[\frac{L}{HP} = \frac{\omega}{HP/S}\right]$
4. $\therefore \frac{L}{HP} = \frac{\omega}{K\left(\frac{\omega}{L/J}\right)^{3/2}}$ for a specific wing loading.

Wing loading is the only variable in the above equation; thus to eliminate this dependence upon wing loading, both sides of the equation are multiplied by the square root of the wing loading and the result is:

$$\frac{L}{HP}\sqrt{\omega} = \frac{(L/J)^{3/2}}{K}$$

which is a constant for a given configuration for any wing loading.

* K is a function of the resistance of the flow system

Since this term varies with forward velocity and this is also dependent upon the wing loading, the velocity must be converted to dynamic pressure and then divided by the wing loading. This results in a plot showing the variation of $\frac{L}{HP}\sqrt{\omega}$ with q/ω.

Flow and Fan Characteristics. Using a peripheral jet for hover and transition, the Ground Effect Take-off and Landing (GETOL) aircraft's basic characteristics are dependent upon the flow and fan characteristics. These are separated into the following three distinct sections:

1. Fan and Model Flow
2. Fan Pressure Effects
3. Flow Distribution

Fan and Model Flow: Consideration here must be given to two specific flow items:

1. The validity of the model fan flow measurements.
2. The resulting model flow rates for the various geometrical configurations.

The first item, validity of the model fan flow measurement, was presented on Pages 80 and 82. Figure 40, the resulting curve, showed that the installed pressure rakes behind the fan would provide accurate flow measurement by simple arithmetic average.

The second item, model flow rakes and pressure requirements, as shown in Figure 49 is the variation of Quantity Flow with fan RPM for various slot geometries. The band for each configuration is a combination of data scatter, Height to Chord Ratio and forward speed. A straight line would be expected for the fan except that the tip jet air used for power might provide a nonlinear characteristic. However, the curve, except for scatter, is linear and provides adequate knowledge of the model flow for a given geometry.

Shown on Figure 50 is a plot of the pressure behind the fan versus the Quantity Flow for various slot configurations. The band shown is a function of scatter Height to Chord Ratio and angle of attack. For an ideal fan the variation of total pressure behind the fan would be a function of the square of the Quantity Flow. The plotted curves and their equations (included in Figure 50) provide excellent support to the following facts:

1. For a given geometry, the flow-pressure relationship does not vary with height.
2. Flow measurements are quite accurate.

2. Ram pressure increases the flow along the same resistance line defined in hovering.

Fan Pressure Effects: To be assured of proper parametric expressions, it was important to make certain that no parameter vary with flow rate (except for the possibilities of secondary effects such as internal flow Reynolds numbers). To this end, the hovering Lift Coefficient, Augmentation Ratio ("A"), was specifically evaluated early in the static room phase for possible variance with fan pressure (hence V_J). Figure 51 presents this investigation and shows the consistency of Augmentation Ratio with jet velocity (V_J).

Thus, all coefficients forms used in this GETOL analysis were similarly constant with respect to fan total pressure, except the one dimensional parameter of great importance, L/HP. The dependence of L/HP on the lifting fluids velocity is elementary and of necessity results in the requirement that power evaluation of the GETOL type aircraft had to account for specific wing and fan pressure loadings. To eliminate this requirement, the slightly revised parameter of $\frac{L}{HP}\sqrt{\omega}$ was used for certain areas of investigation. The reasons for using this parameter are described on Page 84.

Flow Distributions: No specific variations of slot flow distributions were imposed on the model tested at NASA, but as mentioned in other sections of this report, the measured characteristics of this model, especially trim moment and stability results, were a function of the flow distributions which this model possessed.

Measurements of the slot total pressure described on Page 33 were quite uniform. If at a future date, when criteria becomes available, some correction to force and moment data may be possible. The importance of flow distribution is that it must be known for the detail design of an actual GETOL Flight Research Vehicle (FRV).

The significance is that any GETOL capability which may be predicted from the results of this GETOL Feasibility Study are limited to that which would occur based upon further analysis of the slot flow distributions. Possible estimations of improvement may be obtained but specific improvements require further testing.

Slot Geometry Effects

The term "Slot Geometry" represents a broad area that must be subdivided into the following items of major importance:

1. Slot Angles
2. Slot Skirts
3. Gap Area
4. Gap Ratio

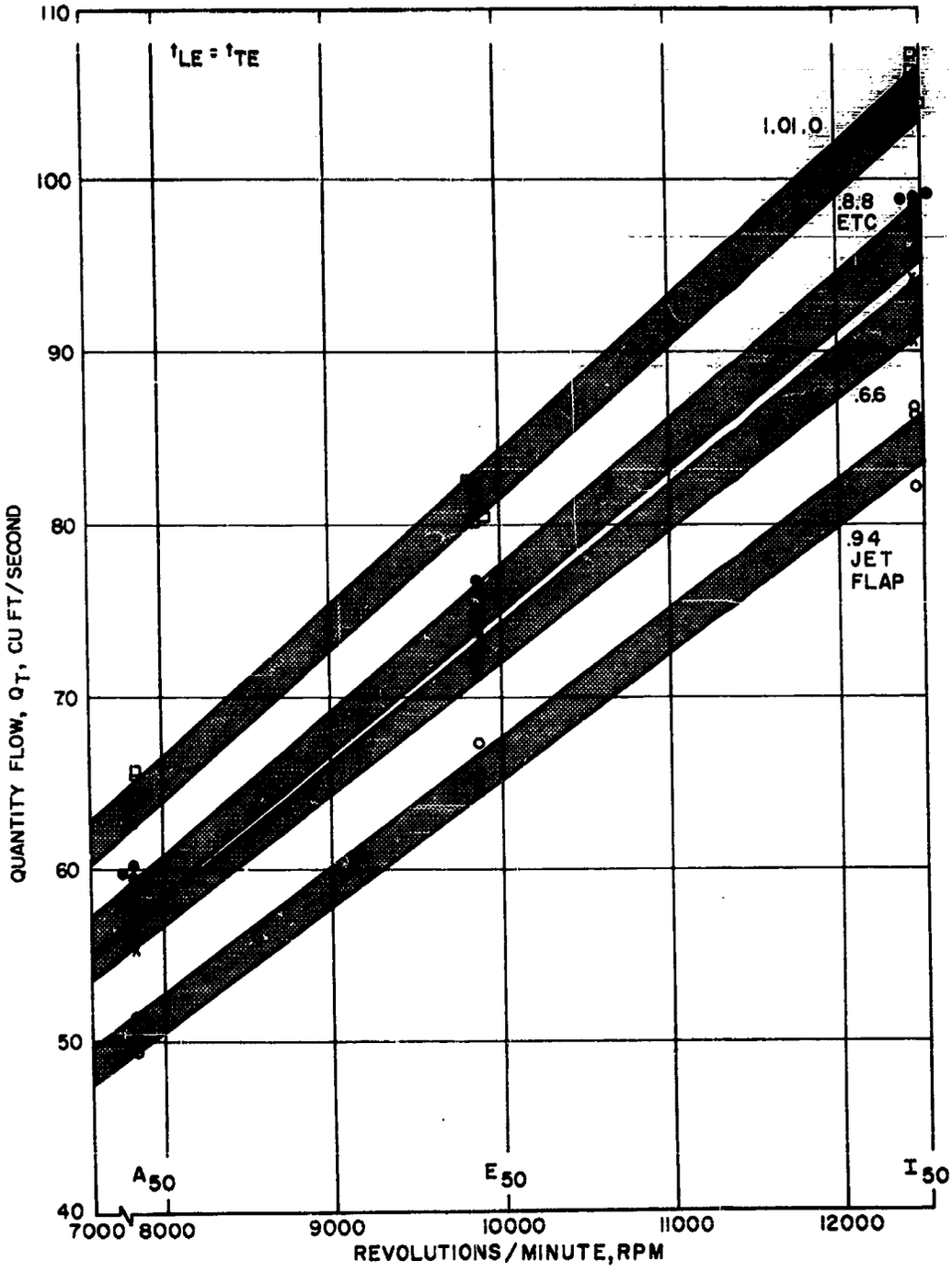

Figure 49. Quantity Flow vs. Fan RPM for Various Slot Configurations

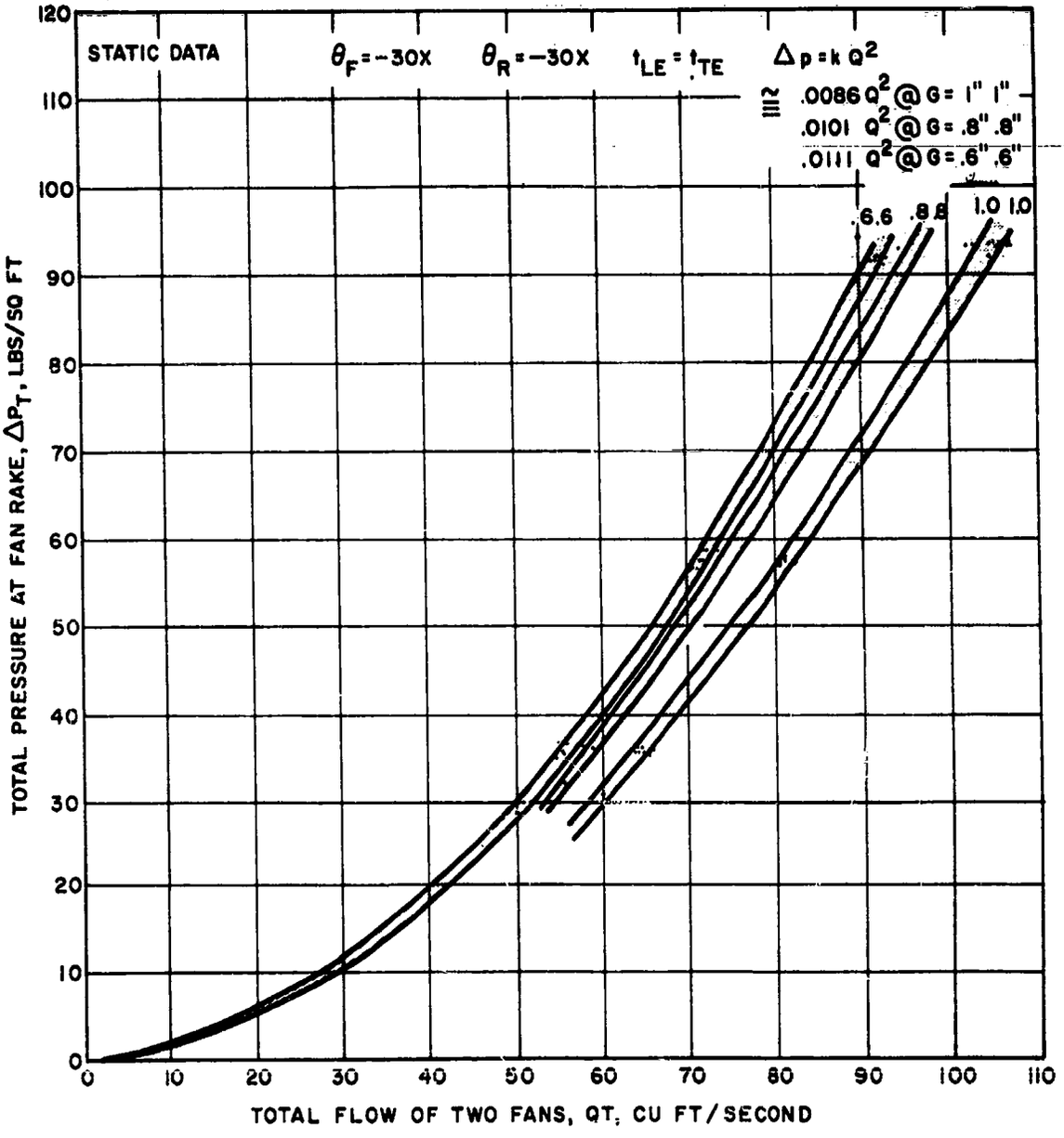

Figure 50. Total Pressure Behind Fan vs. Quantity Flow (Static Data)

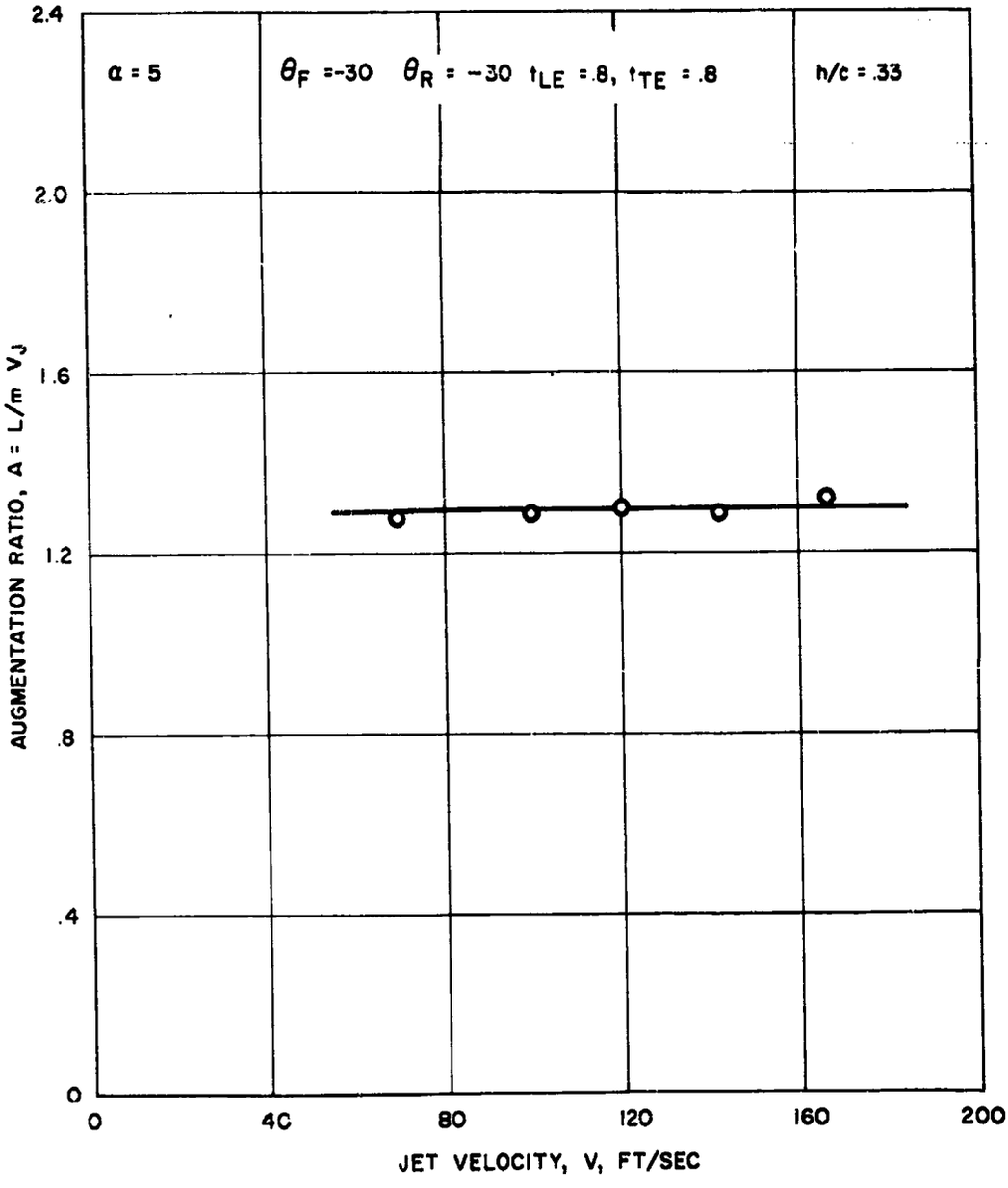

Figure 51. Variation of Augmentation Ratio with Jet Velocity

Each of these items are interrelated, but to analyze the specific effects of one item, one is varied while the others remain constant. The effect of Slot Geometry variations must be considered on performance, stability and trim in hover and transition. Each of the following terms of major importance are discussed in this manner:

Slot Angles: Hovering Performance — Figure 56 presents the performance for several possible hovering slot arrangements with equal gap as shown below:

θ_F	θ_R
-30x	-30x
-30x	+30x
0x	-30x

Note that L/HP is the compared parameter as it must be when comparing different geometries. Although magnitudes of difference are small, there is a superiority in hovering performance for the θ_F -30° x θ_R = -30°x configuration.

Hovering Stability — In the determination of the effect of slot angles on hovering stability the variation of pitching moment with angle of attack was plotted and is shown on Figure 55 for the significant slot angles tested. It should be noted that on this figure negative pitching moment is up. Two configurations exhibit very slightly stable characteristics; they are θ_F = -30° x θ_R = -30° x and θ_F = -30° x θ_R = 0° x. Actually all configurations have what seems to be a mild slope and are about neutrally stable, but a slight advantage may exist for the two geometries previously mentioned.

Hovering Trim — All slot angles (see Figure 55) show a large nose down trim moment about the model balance which was at the 25% root chord on the thrust line. Only the θ_F = -30° x θ_R = +30° x configuration shows a reduction in this trim moment, but this geometry suffers excessive performance loss as shown in Figure 56.

Transition Performance — As stated previously on Page 84, when comparing different geometries $\frac{L}{HP}\sqrt{\omega}$ variation with q/ω should be used to make the resulting comparisons applicable to any wing loading. In the transition regime, a comparison of $\frac{L}{HP}\sqrt{\omega}$ was made with the nacelle doors closed, the model at a constant Height to Chord Ratio and drag equal zero for three slot arrangements shown in Table VIII. (see Figure 56)

For the θ_F = 0°x θ_R = -30°x configuration power required constant increases. For the other two configurations, there is a small difference in the power required in hover and the low speed regime. As the speed is increased, the difference becomes much more significant. Although the difference is minimal at

TABLE VIII

CONFIGURATIONS FOR SLOT ANGLE INVESTIGATION

Configuration No.	θ_F	θ_R	t_{LE}	t_{TE}
(1)	-30°x	-30°x	.8 in	.8 in
(8)	-30°x	+30°x	.8 in	.8 in
(20)	0°	-30°x	.8 in	.8 in

extremely low speeds there is a definite advantage at higher velocities for the θ_F = -30°x θ_R = -30°x configuration.

Transition Stability — To compare the stability in transition for three slot angle configurations, a variation of the Pitching Moment Coefficient (C_m) with angle of attack is shown for three values of the reciprocal of the Momentum Coefficient (a measure of the state of transition between hover and forward flight). Figure 57 presents this variation for three slot angle configurations. They demonstrate marginal stability characteristics, but the θ_F = -30°x θ_R = -30°x and θ_F = -30°x θ_R = +30°x configurations are neutrally stable.

Transition Trim — Figure 58 shows a large nose down trim moment in the low speed range about the model balance which was at the 25% chord. This Center of Pressure is approximately at the 50% chord. As the velocity is increased the trim moment decreases to zero. The difference between the θ_F = -30°x θ_R = -30°x and θ_F = -30°x θ_R = +30°x configuration is of minor significance. A general trend similar to this was noted for all configurations tested.

Slot Skirts: Slot skirts were developed as extensions to the outer edge of the slot contours to better effect the desired flow directions. A typical skirt installation is shown on Figure 59. Skirts were screwed to the wing when possible, or taped when necessary. Visually, these skirts improved flow directions, especially for the trailing edge slot. Most significant testing at NASA was therefore conducted with the skirts on. In Tables IV, V and VI, skirted slot angles are referred to as θ x i.e. -30°x. A limited number of runs were made with the skirts off as in the tow track tests which were conducted without them. It is the intent of this section to show the effect of skirts on performance, stability and trim.

Hovering Performance — Figure 59 shows the improvement in Augmentation Ratio which resulted from the skirt installation. In reasonable ground clearance situations the improvement in lifting ability is about 45%. Figure 60 presents the same skirt on-off situation in terms of lift per air horsepower due to the fact that "A" can be misleading when comparing different Slot Geometries and that the addition of skirts to a given Slot Gap and angle is effectively a Slot Geometry change. Here, too, the skirt improvement is noted, but is about 35%.

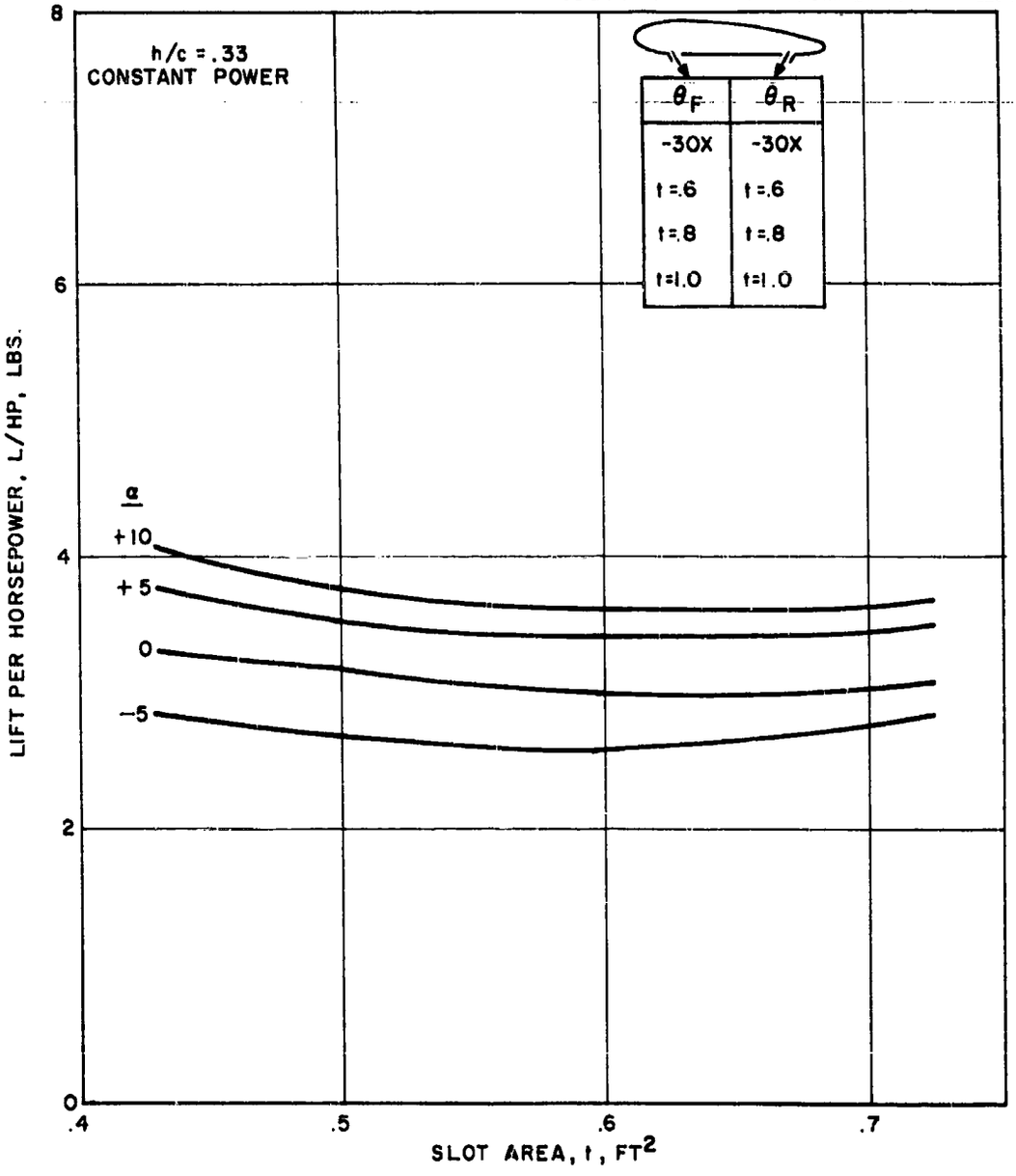

Figure 52. Lift Per Air Horsepower vs. Slot Area (Gap 1:1)

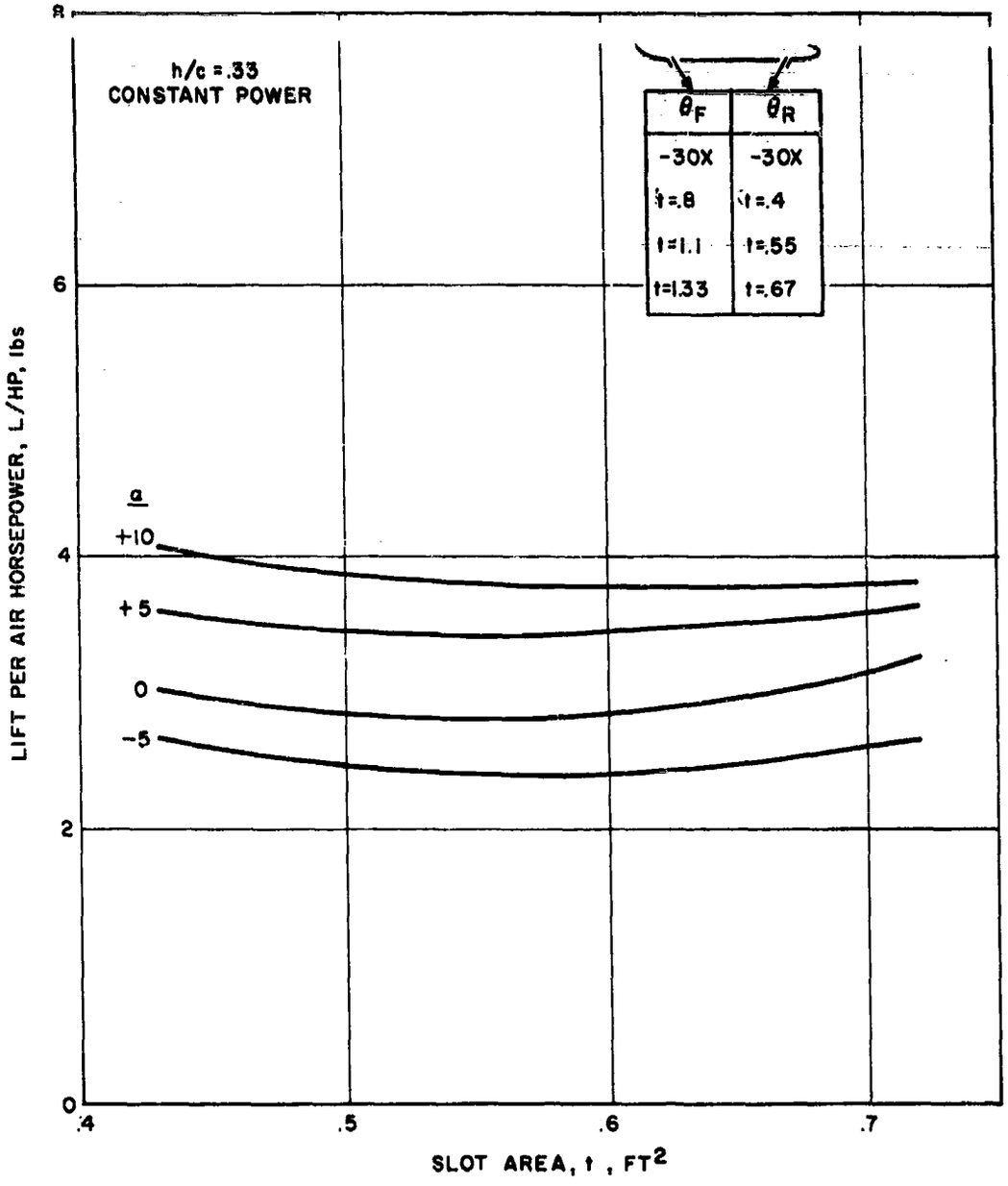

Figure 53. Lift Per Air Horsepower vs. Slot Area (Gap 2:1)

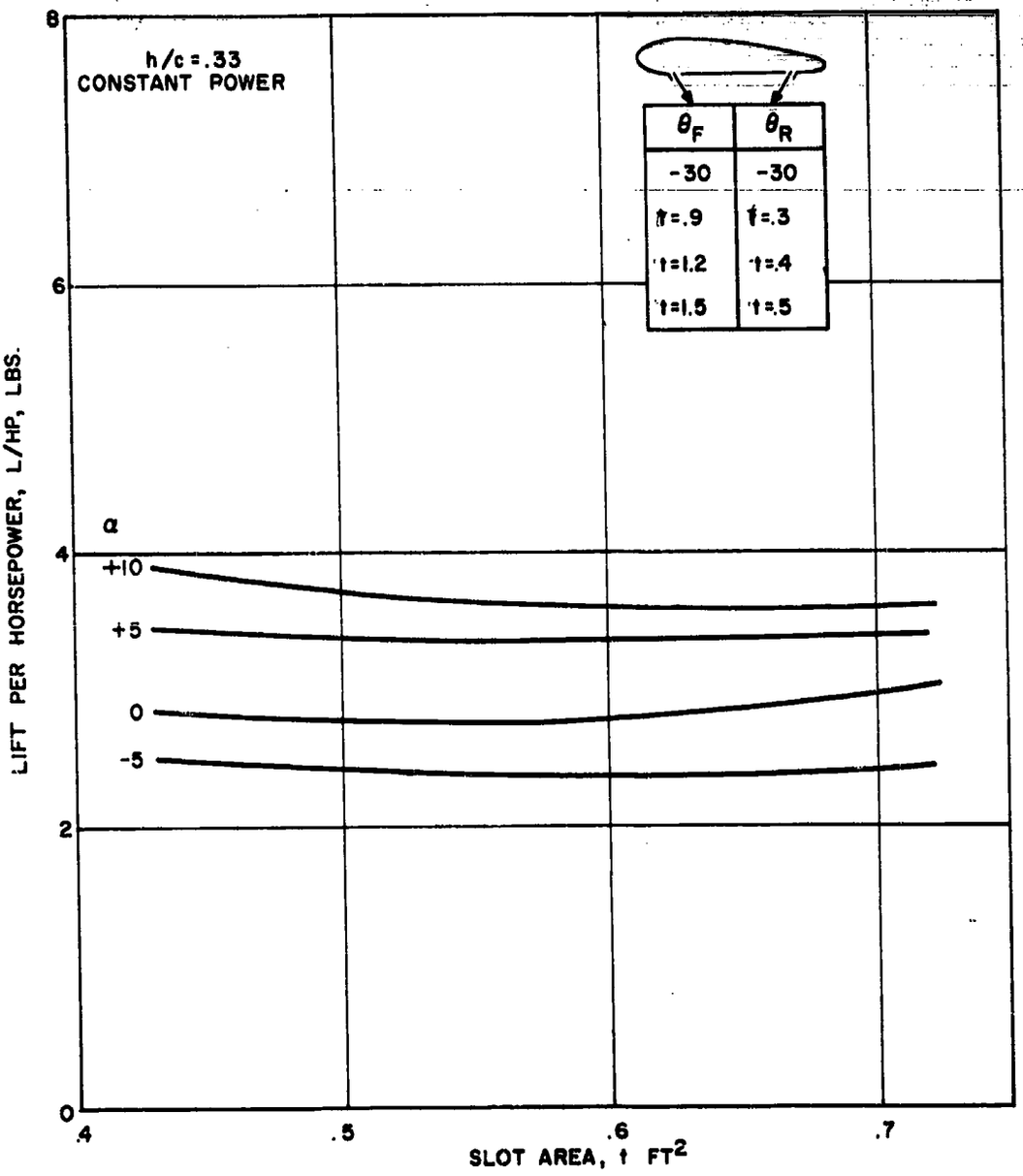

Figure 54. Lift Per Air Horsepower vs. Slot Area (Gap 3:1)

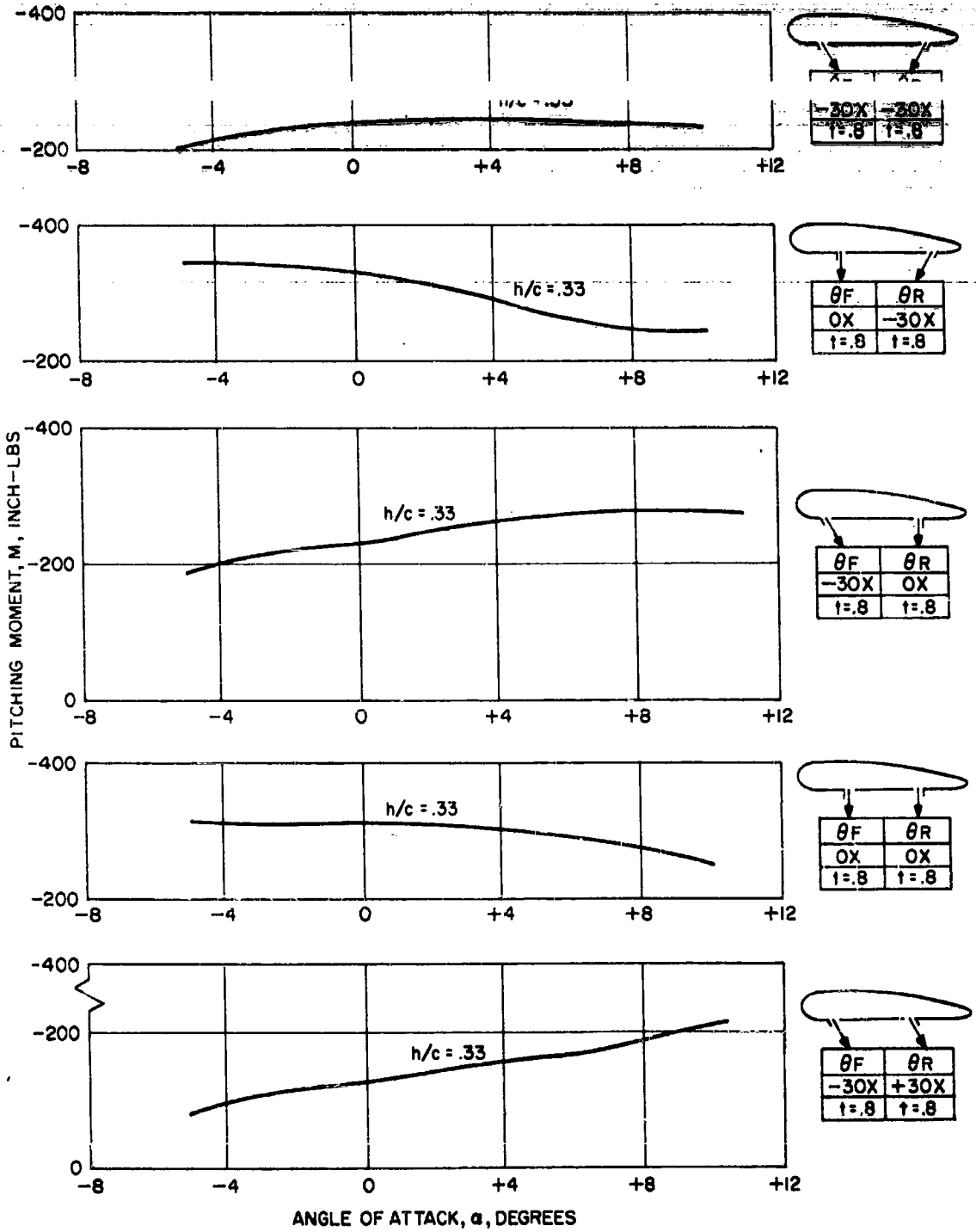

Figure 55. Hovering Stability Characteristics for Various Slot Arrangements

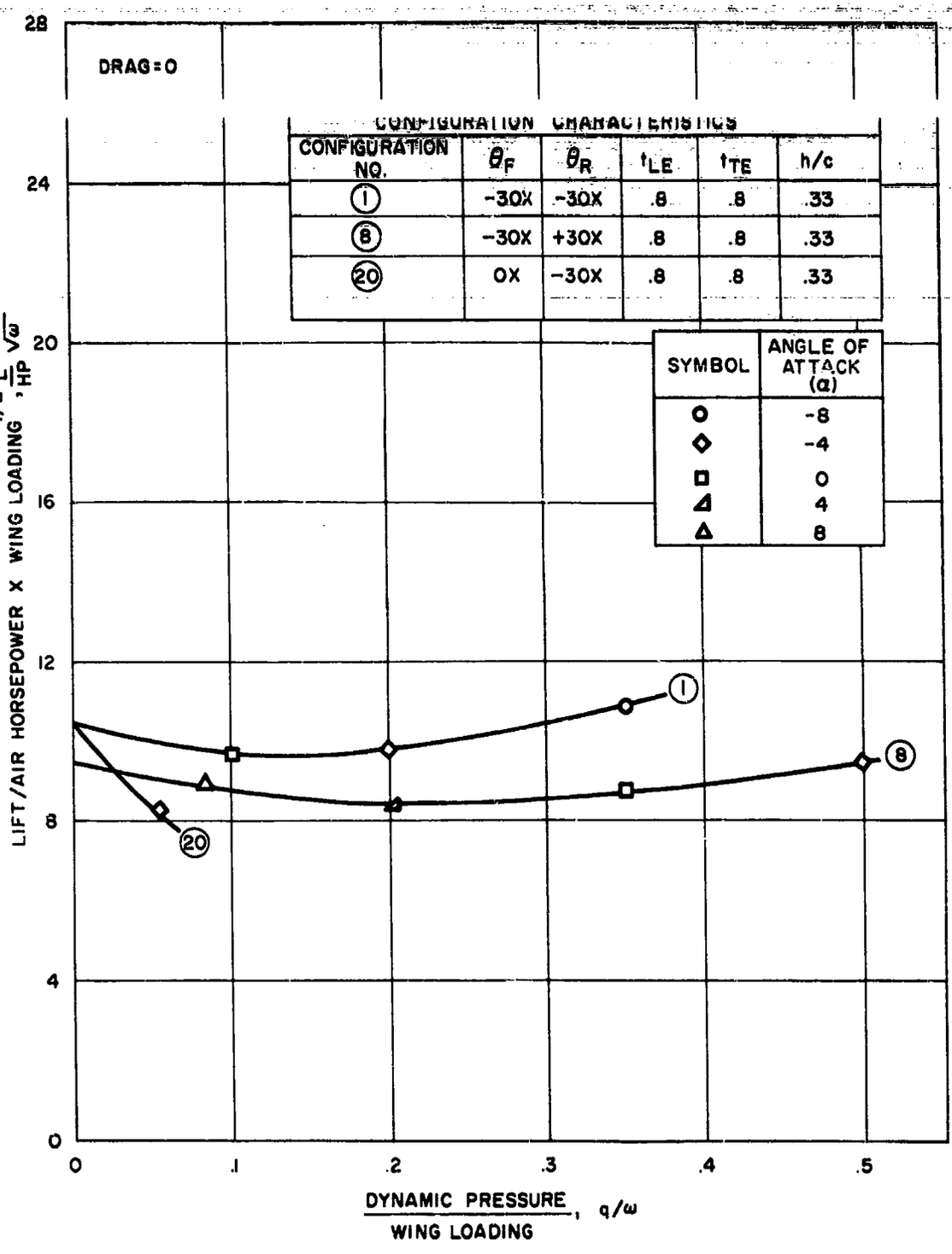

Figure 56. Effect of Slot Angle on Lift Per Air Horsepower in Transition

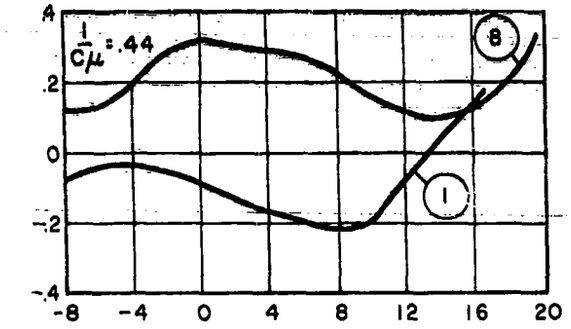

CONFIGURATION CHARACTERISTICS					
CONFIG.	θ_F	θ_R	t_{LE}	t_{TE}	h/c
8	-30X	+30X	.8	.8	.33
1	-30X	-30X	.8	.8	.33

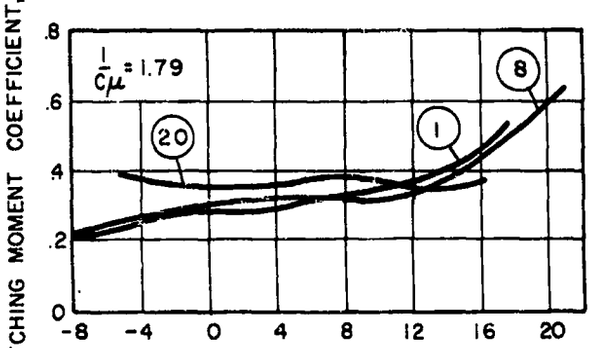

CONFIGURATION CHARACTERISTICS					
CONFIG.	θ_F	θ_R	t_{LE}	t_{TE}	h/c
8	-30X	+30X	.8	.8	.33
1	-30X	-30X	.8	.8	.33
20	0X	-30X	.8	.8	.33

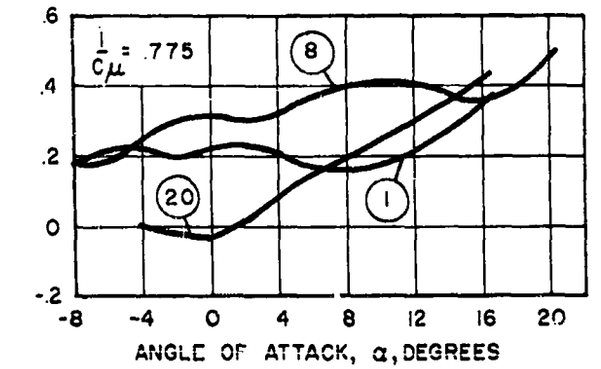

CONFIGURATION CHARACTERISTICS					
CONFIG	θ_F	θ_R	t_{LE}	t_{TE}	h/c
8	-30X	+30X	.8	.8	.33
1	-30X	-30X	.8	.8	.33
20	0X	-30X	.8	.8	.33

PITCHING MOMENT COEFFICIENT, C_m.

Figure 57. Pitching Moment Coefficient vs. Angle of Attack for Various Slot Angles

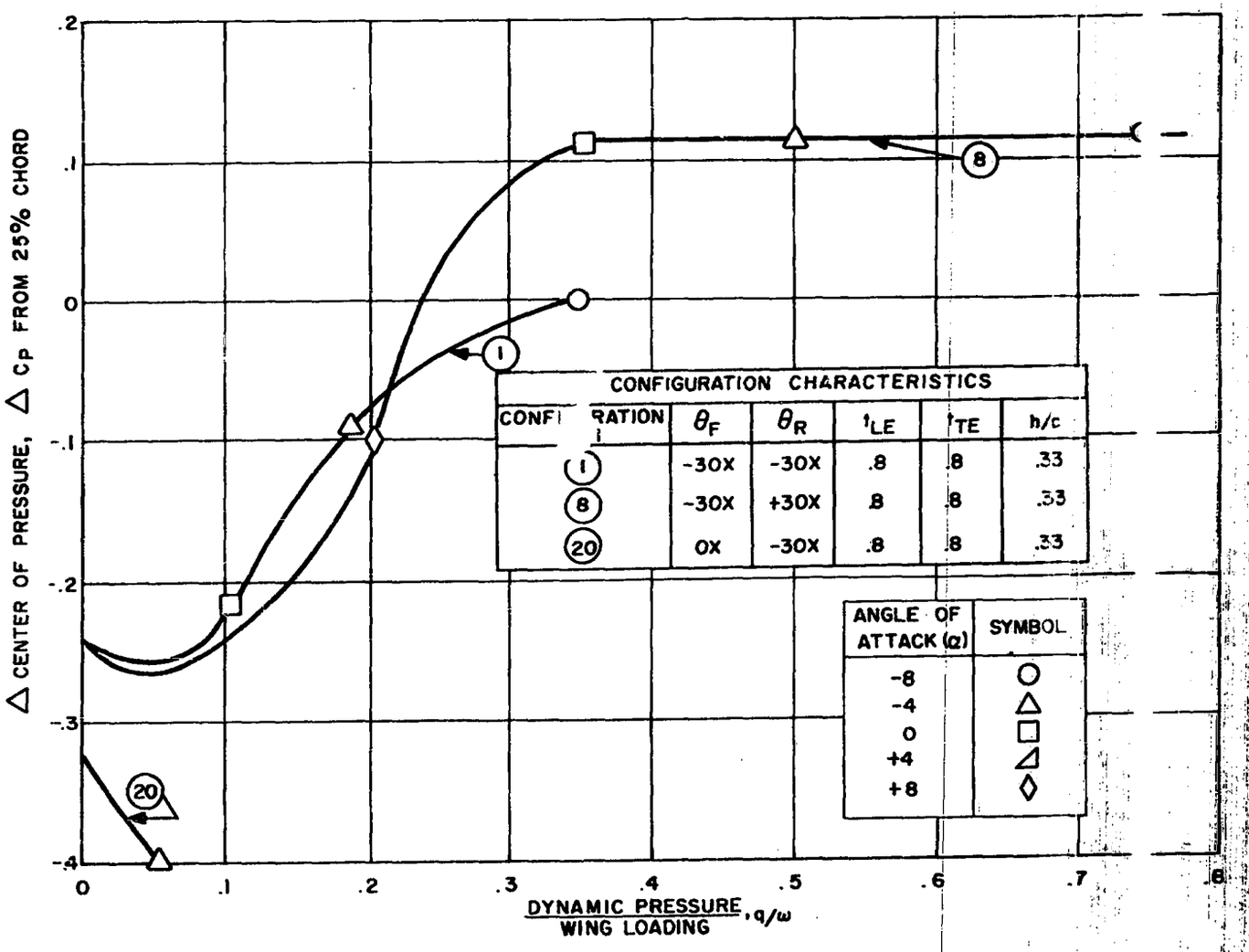

Figure 58. Center of Pressure Travel in Transition for Various Slot Angles

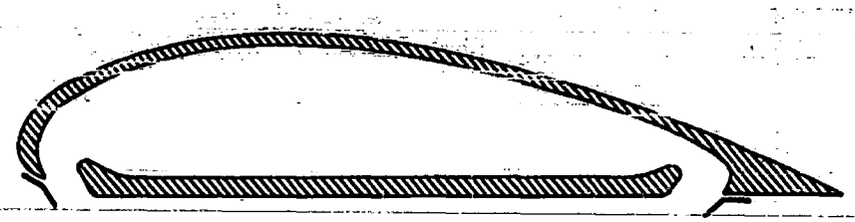

TYPICAL SKIRT INSTALLATION

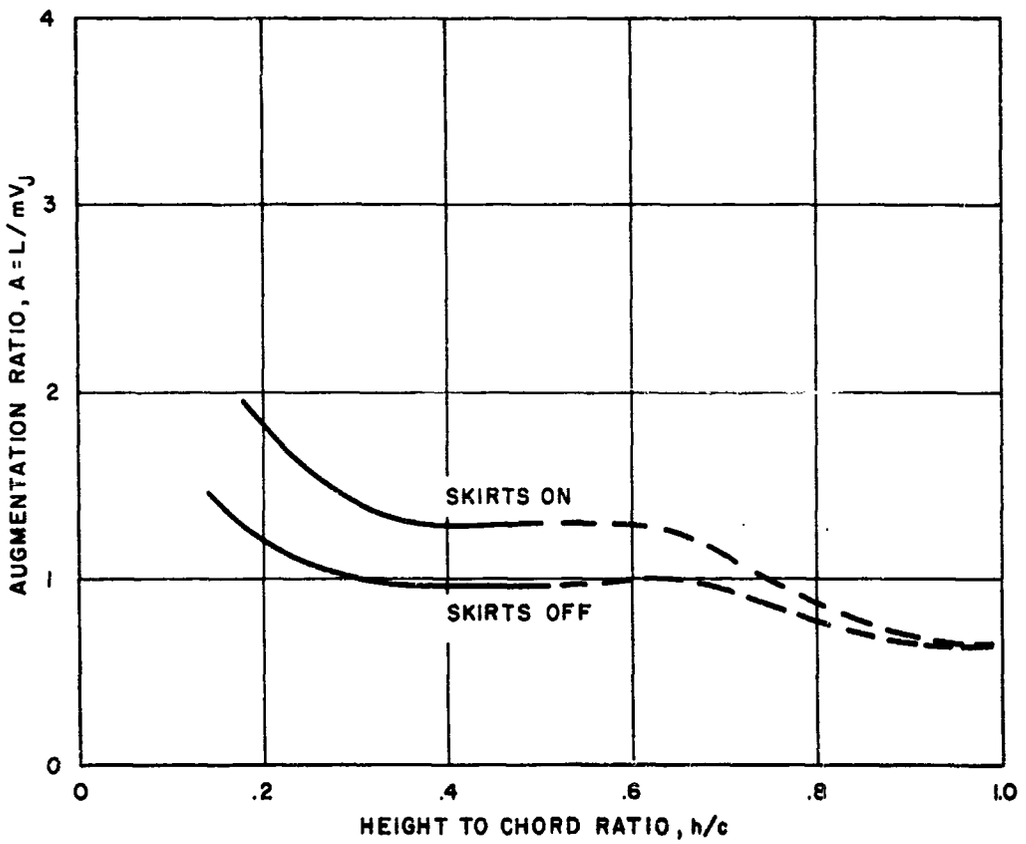

Figure 59. Effect of Slot Skirts on Augmentation Ratio

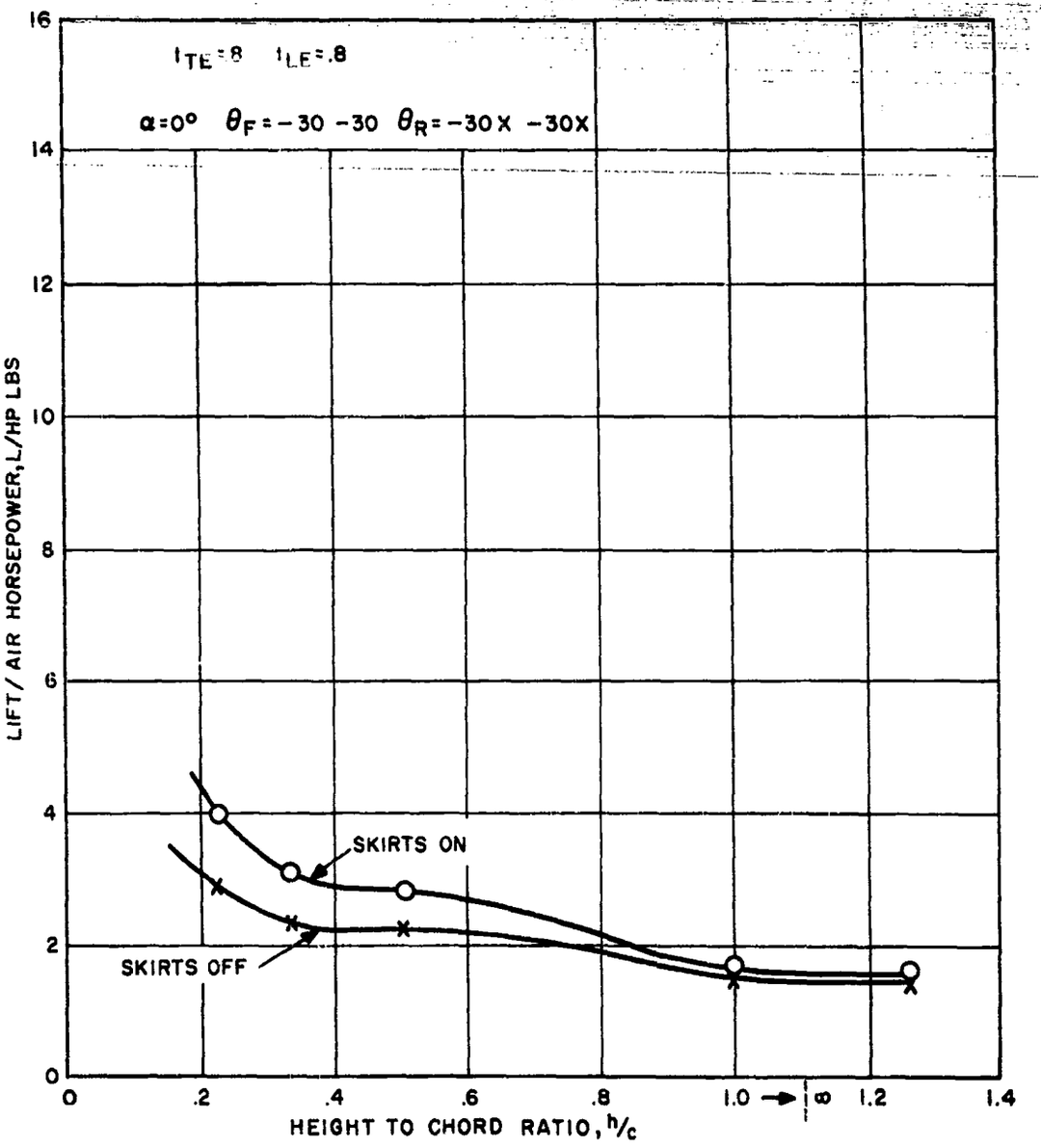

Figure 60. Effect of Slot Skirts on Hovering Performance (α = 0°)

Certainly, an improvement in hovering capability of about 40% is clearly demonstrated.

Hovering Stability — The effect of slot skirts on hovering stability cannot be determined. Unskirted tests which provide such data were within the first forty static room test runs for which data are not available. This lack of data is due to fan swirl (before installation of honeycomb flow straighteners) limitations.

Hovering Trim — Only four test points exist to suggest the trim change in hovering due to skirts. These points are shown on Figure 61. At Height to Chord Ratios of 1.0 and .5 there seems to be no moment change; at a Height to Chord Ratio of .33 a slightly less severe nose down moment was recorded; at a Height to Chord Ratio of .20 about 20 percent decrease in nose down moment occurred. Although this information is meager, certainly it is in favor of the skirts and adds evidence to their desirability.

Transition Performance — The effect of the addition of skirts to the $\theta_F = -30°$ $\theta_R = -30$ slot angle in transition is shown in Figure 62. This configuration had the same slot area and Height to Chord Ratio with the doors closed and zero drag. There is a constant decrement in power (approximately 20 percent) attained by the addition of skirts over the range tested. As can be noted for the angle of attack through transition, the configuration with skirts achieves any speed at a lower angle of attack thus indicating that better flow direction is achieved by the use of skirts.

Transition Stability — To illustrate the effect of the addition of the skirts to the slots on the stability characteristics, the Pitching Moment Coefficient variation with angle of attack is shown in Figure 63. For the low speed regime ($1/C_\mu \leq .50$) there are definite stable trends for angles of attack of less than +4 degrees but above that there are definite unstable characteristics. As the speed is increased, the characteristics become only marginally stable. There is no major difference in the trends, only in the magnitude of the trim moment.

Transition Trim — A comparison of the Center of Pressure through transition for skirts on and skirts off can be seen in Figure 64. There is a negligible difference noted and the variation of location with speed follows the general trend previously stated without any definite advantage shown for either configuration.

Gap Area:* Gap area was one of the basic test variables in the program, and runs were made at three basic slot gaps.

$T_{LE} + T_{TE}$	S_J/S_W
1.2 inches	.075
1.6 inches	.10
2.0 inches	.125

Note: Gap area ratio is not considered here where the leading edge gap was larger than the trailing edge gap.

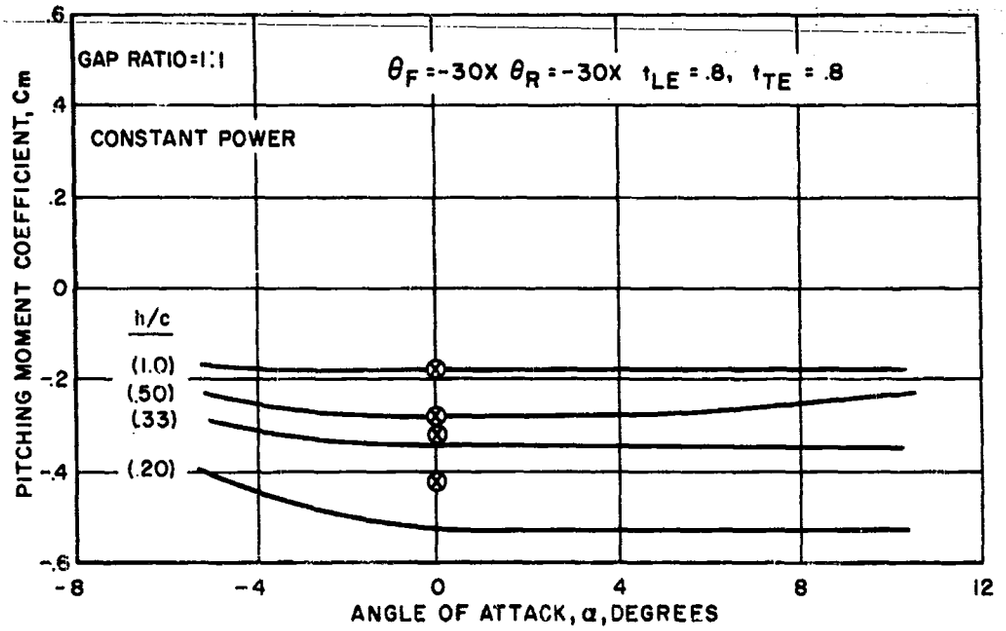

Figure 61. Effect of Height on Hovering Trim (Gap 1:1)

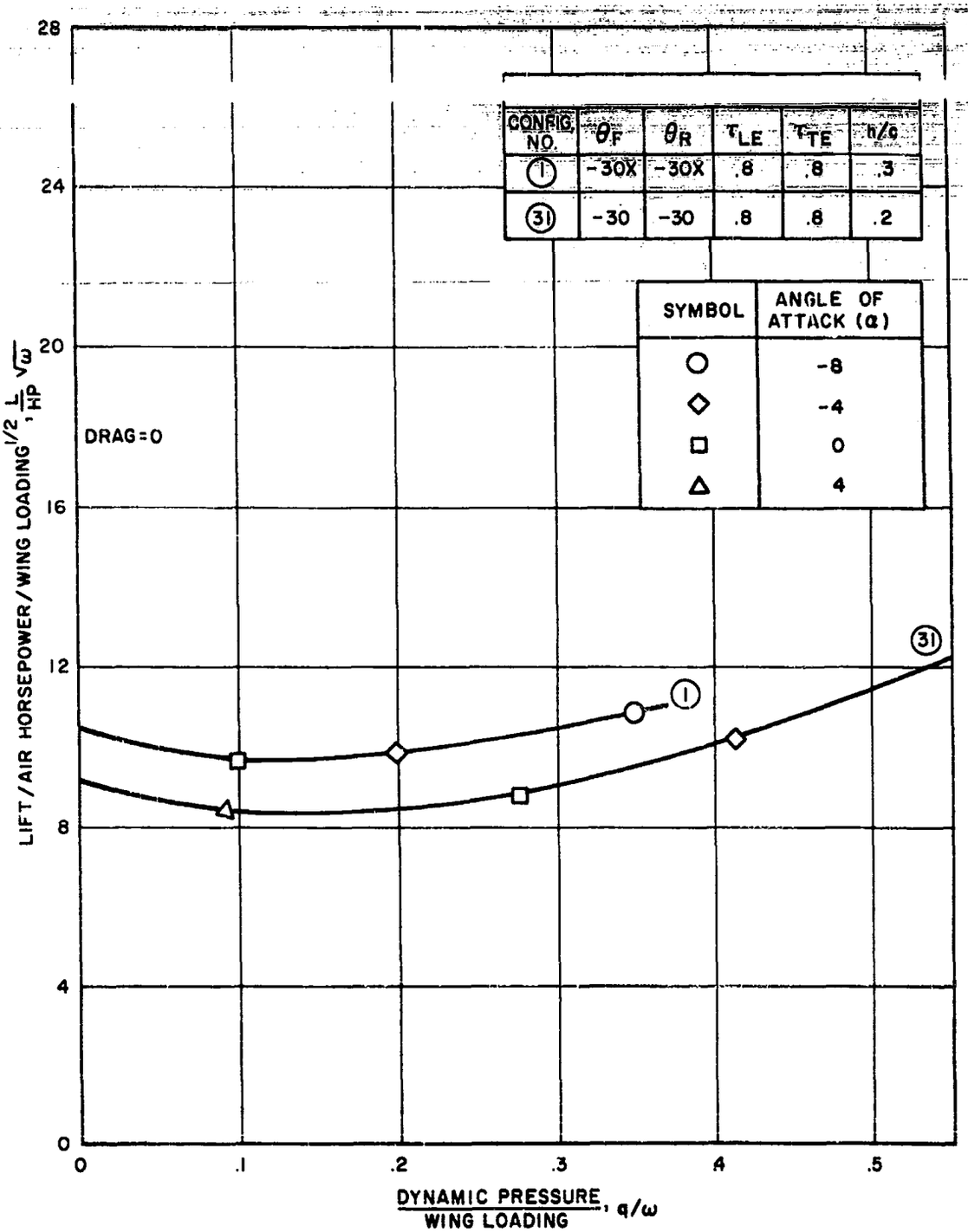

Figure 62. Effect of Slot Skirts on Lift Per Air Horsepower Variation in Transition

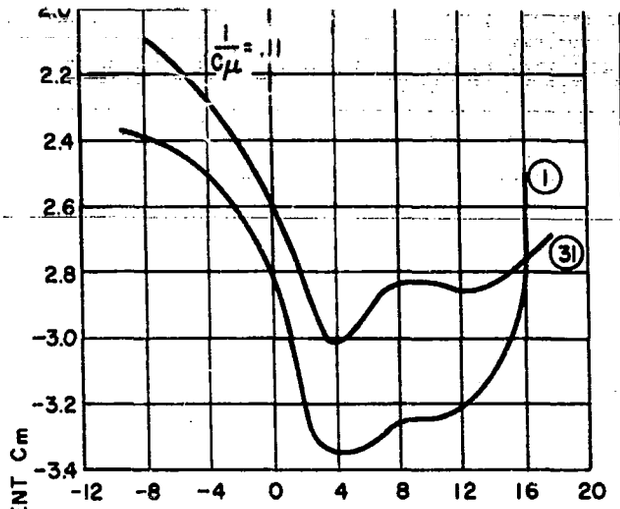

CONFIGURATION CHARACTERISTICS					
CONFIGURATION NO.	θ_F	θ_R	t_{LE}	t_{TE}	h/c
1	-30	-30	.8	.8	.33
31	-30X	-30X	.8	.8	.33

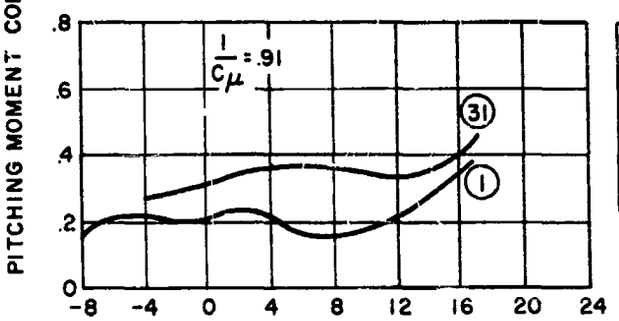

CONFIGURATION CHARACTERISTICS					
CONFIGURATION NO.	θ_F	θ_R	t_{LE}	t_{TE}	h/c
31	-30	-30	.8	.8	.33
1	-30X	-30X	.8	.8	.33

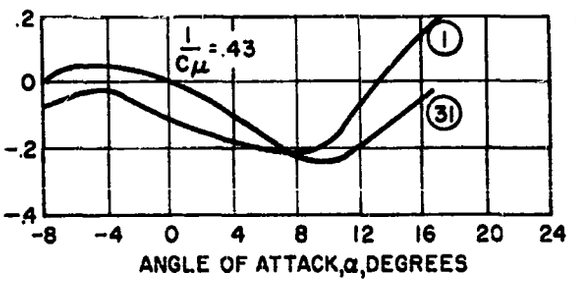

PITCHING MOMENT COEFFICIENT Cm

ANGLE OF ATTACK, α, DEGREES

CONFIGURATION CHARACTERISTICS					
CONFIGURATION NO.	θ_F	θ_R	t_{LE}	t_{TE}	h/c
31	-30	-30	.8	.8	.33
1	-30X	-30X	.8	.8	.33

Figure 63. Pitching Moment Coefficient vs. Angle of Attack for Skirts On and Off the GETOL Model

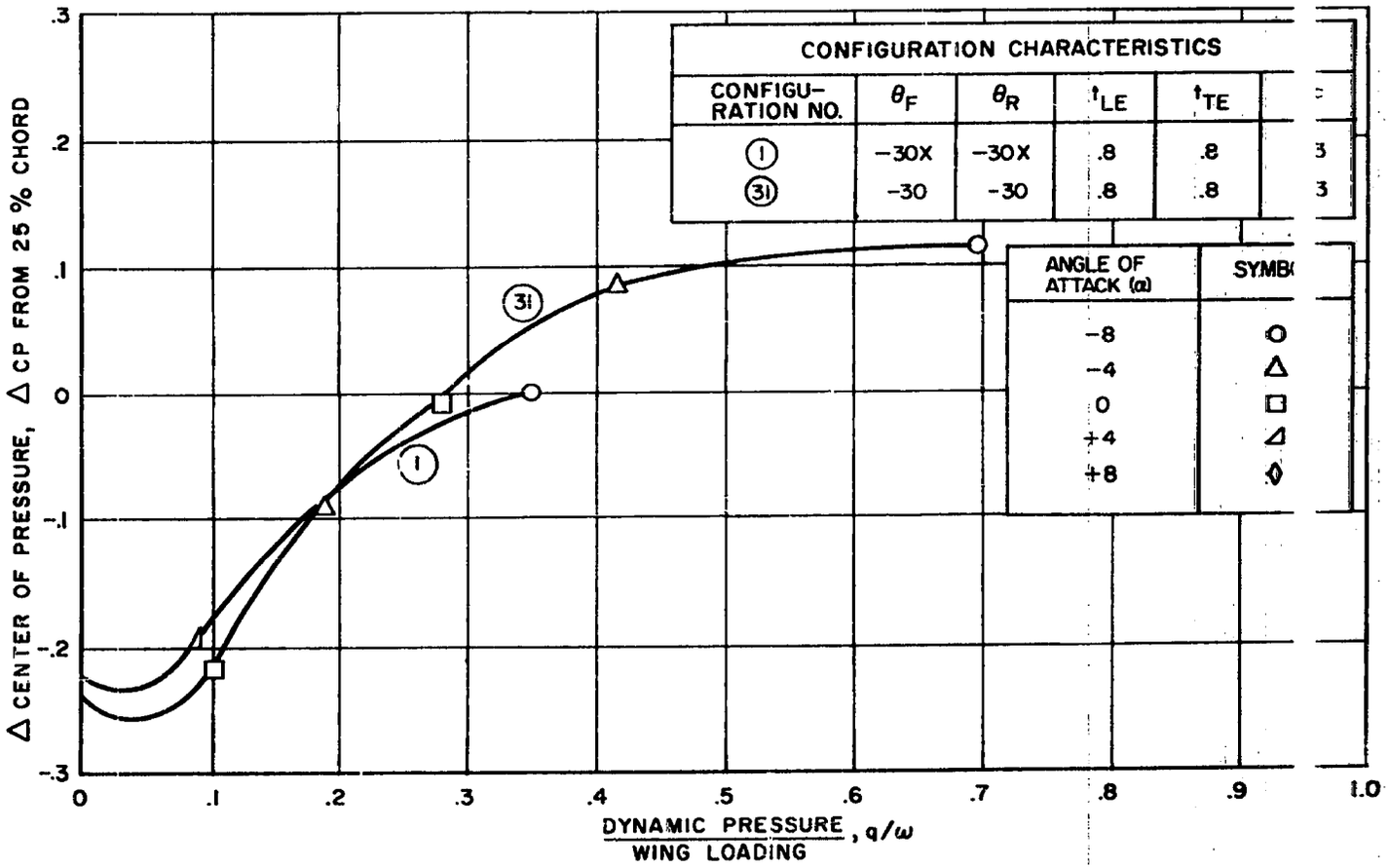

Figure 64. Center of Pressure Travel in Transition for Skirts On and Off the GETOL Model

Ratio or lift per air horsepower (see Page 84) Figures 46, 47 and 48 were developed. Referring again to these figures, Augmentation Ratio suggests the larger gap area but Augmentation is an incorrect parameter when comparing gap variances. Lift per air horsepower (Figures 48 and 52) suggests a possible slight performance advantage for a gap area either larger or smaller than the nominal S_J/S_W of .10 gap for which most of the testing was conducted.

Figures 52, 53, 54, 65, 66 and 67 add more information for gap area variations at various angles of attack, Height to Chord Ratio: (h/c) and gap ratio (t_{LE}/t_{TE}) configurations.

Here the trends seem to favor the smaller gap areas, showing a small increase in lift per air horsepower for the smaller gap area ($\frac{S_J}{S_W} = .075$) over the medium gap area ($\frac{S_J}{S_W} = .10$)

Hovering Stability — Figures 65, 66 and 67 present the moment characteristics at the three gap areas. Inspection reveals that the variation of Pitching Moment Coefficient with angle of attack ($dCm/d\alpha$) is approximately neutral for any of the three gap areas tested and may be slightly stable for the smaller area. The conclusion, if any, is again in favor of the smaller area.

Hovering Trim — This is also shown on Figures 65, 66 and 67 for three gap areas. No significant change in the trim moment was effected at any variation in gap area.

Transition Performance — Since there is some uncertainty about Augmentation Ratio, it appears that the best method of comparison, as stated on Page 84, is the product of lift and (wing loading)$^{1/2}$ divided by air horsepower. Figure 68 represents the variation power required with velocity. This indicates that of the three configurations shown, the smallest gap area is somewhat better throughout transition. There is a power decrease with this configuration at low speed that increases to zero and then decreases again as the speed continues to increase when compared with the basic configuration ($F = -30x\ \theta_R = -30x\ \frac{S_J}{S_W} = .10$). The largest gap area, defined by the ratio $\frac{S_J}{S_W} = .125$, when compared to the basic configuration shows a small decrease in power in hover but as the velocity is increased the power required becomes greater for a major portion of transition. It then decreases as the velocity is further increased and approaches the power required by the smallest gap area. This results in the selection of the smallest slot area as best for transition.

Transition Stability — The effect of varying gap area on the stability characteristics is shown in Figure 69. For the three gap area ratios investigated ($S_J/S_W = .075; .10$ and $.125$) there is no definite decrease or increase in stability. Neutrally stable characteristics are noted up to angle of attack of 8 degrees

and as this is increased, there is a change to a slight instability. This indicates no distinct advantage is obtained by varying gap ratio.

Transition Trim — The effect of gap area on trim is shown on Figure 70. For the large gap area (S_J/S_W = .125) there is a more aft Center of Pressure location than for the medium and small gap area, but the overall trend is basically the general trend of the Center of Pressure located near the fifty percent chord in hover and extremely low speed and moving to the 25% chord. Again no definite advantage is shown.

Gap Ratio: Gap ratio was another basic variable in the NASA test program. Tested were: t_{LE}/t_{TE} = 1:1, 2:1 and 3:1. The primary intent of making the leading edge slot larger than the trailing edge slot was to shift the Center of Pressure in hovering forward to a position near the quarter chord, where the forward flight (airplane configuration) Center of Pressure would be expected. Princeton planform work (see Page 41) produced data where the Center of Pressure had been shifted forward when the gap ratio was increased from 1:1 to 3:1.

In any event, these NASA tests were expected to define a forward Center of Pressure shift with gap ratio.

Hovering Performance — Whether a significant performance penalty would occur with gap ratio variation was a primary question that would determine the potential of this possible method of gaining a forward shift in the Center of Pressure. The effect of changing the gap ratio on the lift per air horsepower is shown in Figure 73. There is no significant power penalty observed whether the gap ratio is 1:1, 2:1 or 3:1.

Hovering Stability — Referring to Figures 65, 66 or 67, the near neutral stability of any gap ratio is apparent; no improvement nor decrement to hovering stability would occur with variation in gap ratio up to 3:1.

Hovering Trim — The effect of gap ratio on hovering was the main answer being sought of this variable. Referring to Figures 65, 66 and 67 the Pitching Moment Coefficient is about constant with gap ratio; finding the Augmentation Ratio for this configuration in Figures 71 and 72 permits the Center of Pressure location to be calculated as shown in Table IX:

TABLE IX

VARIATION OF CENTER OF PRESSURE WITH GAP RATIO (α = +5°)

Configuration θ_F = -30x θ_R = -30x	t_{LE}/t_{TE}	A	C_m	ΔC.P. (from 25%c)
$t_{LE} + t_{TE}$ = 1.6"	1:1	1.75	-.30	-.17
h/c = .33	2:1	1.52	-.30	-.198
α = +5°	3:1	1.48	-.30	-.202

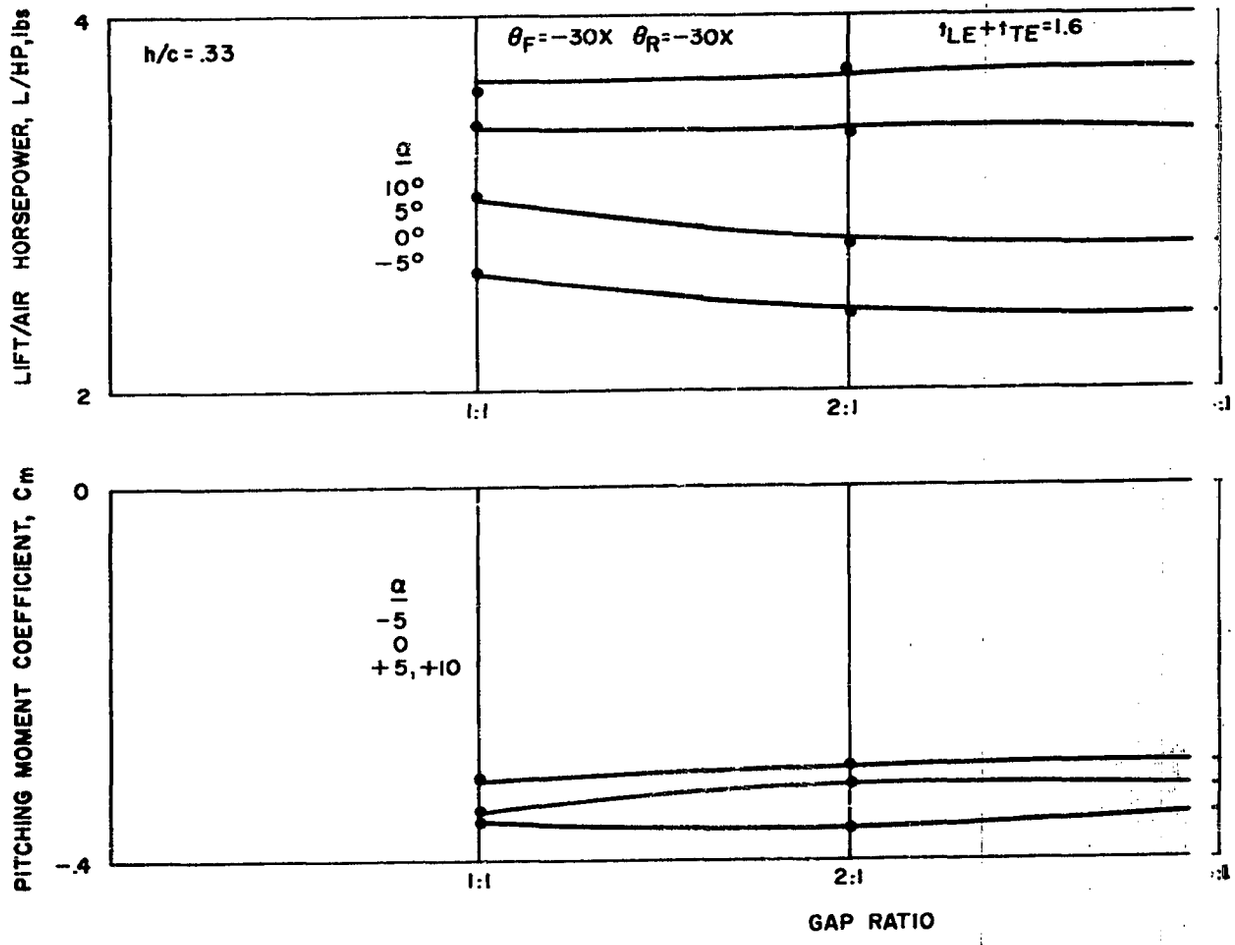

Figure 65. Variation of Hovering Performance and Stability for Three Gap Areas ($t_{LE} + t_{TE} = 1.6$)

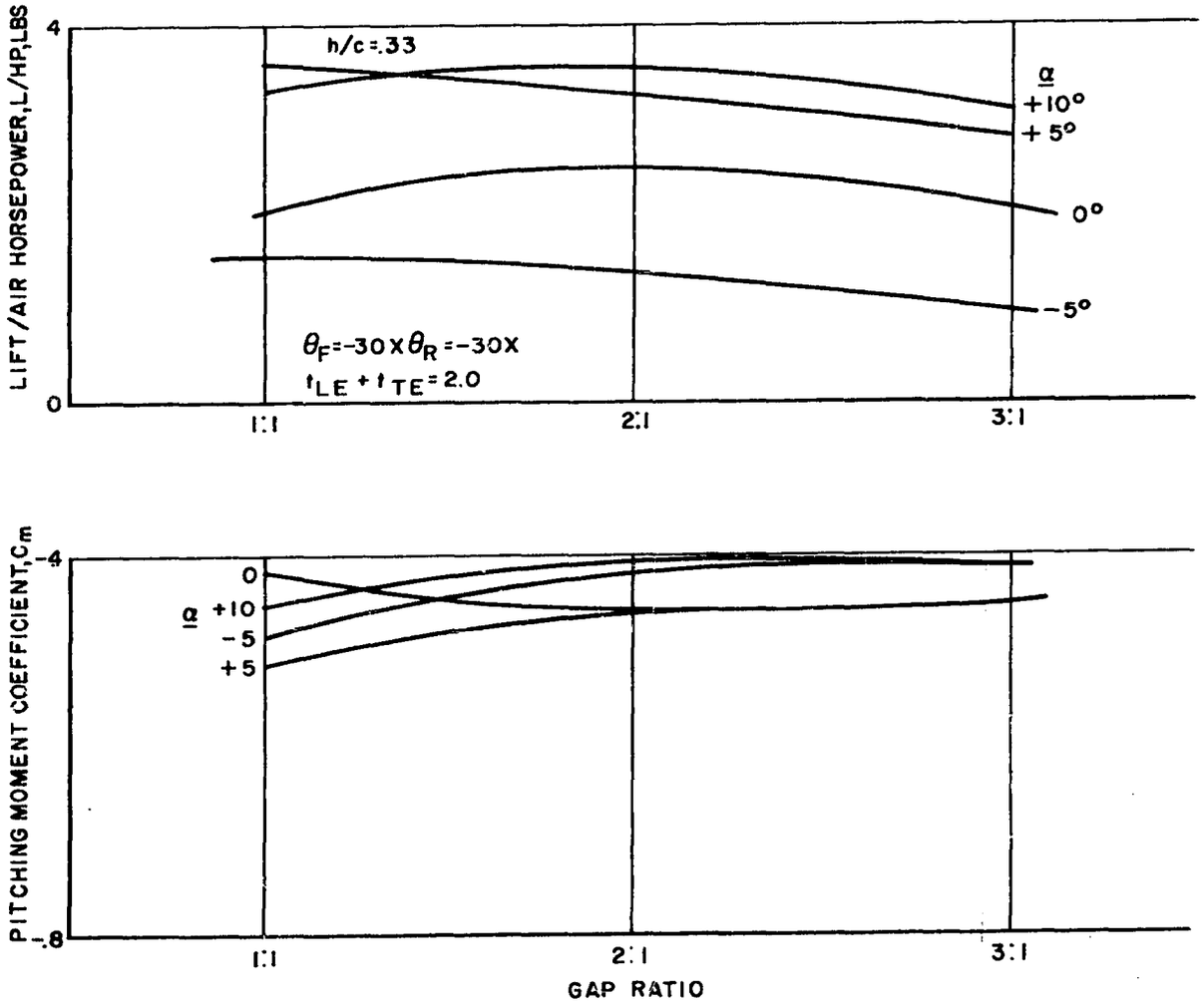

Figure 66. Variation of Hovering Performance and Stability for Three Gap Areas ($t_{LE} + t_{TE} = 2.0$)

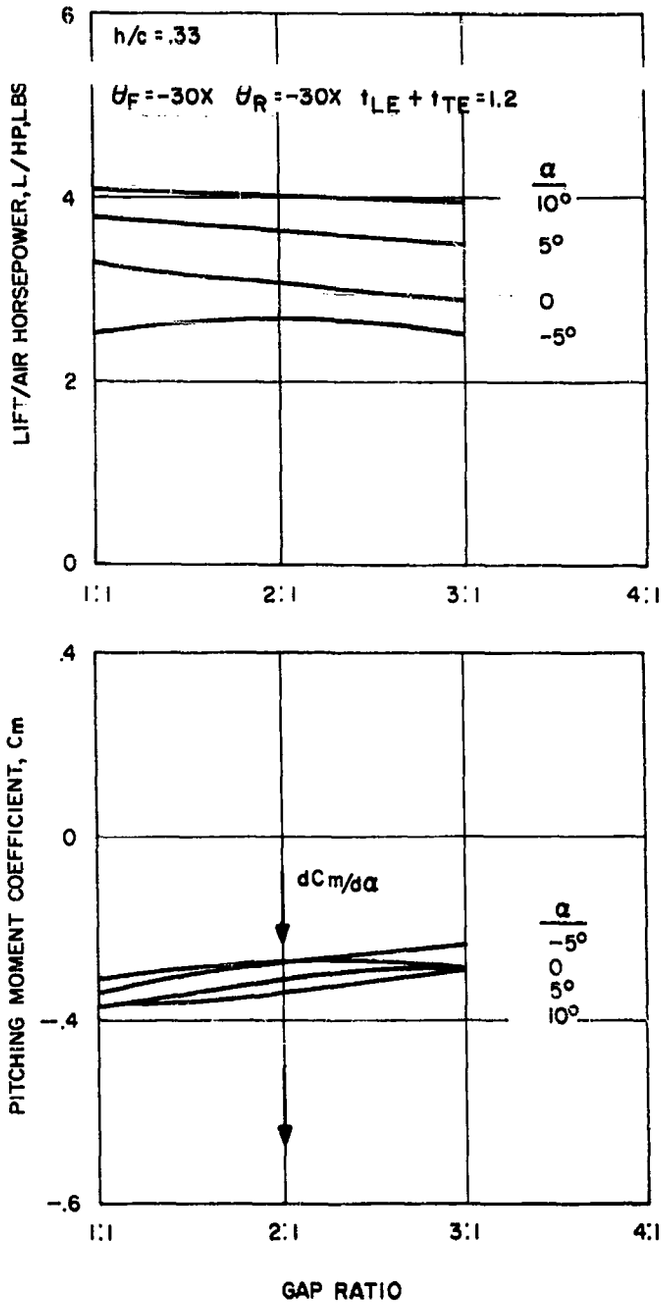

Figure 67. Variation of Hovering Performance and Stability for Three Gap Areas ($t_{LE} + t_{TE} = 1.2$)

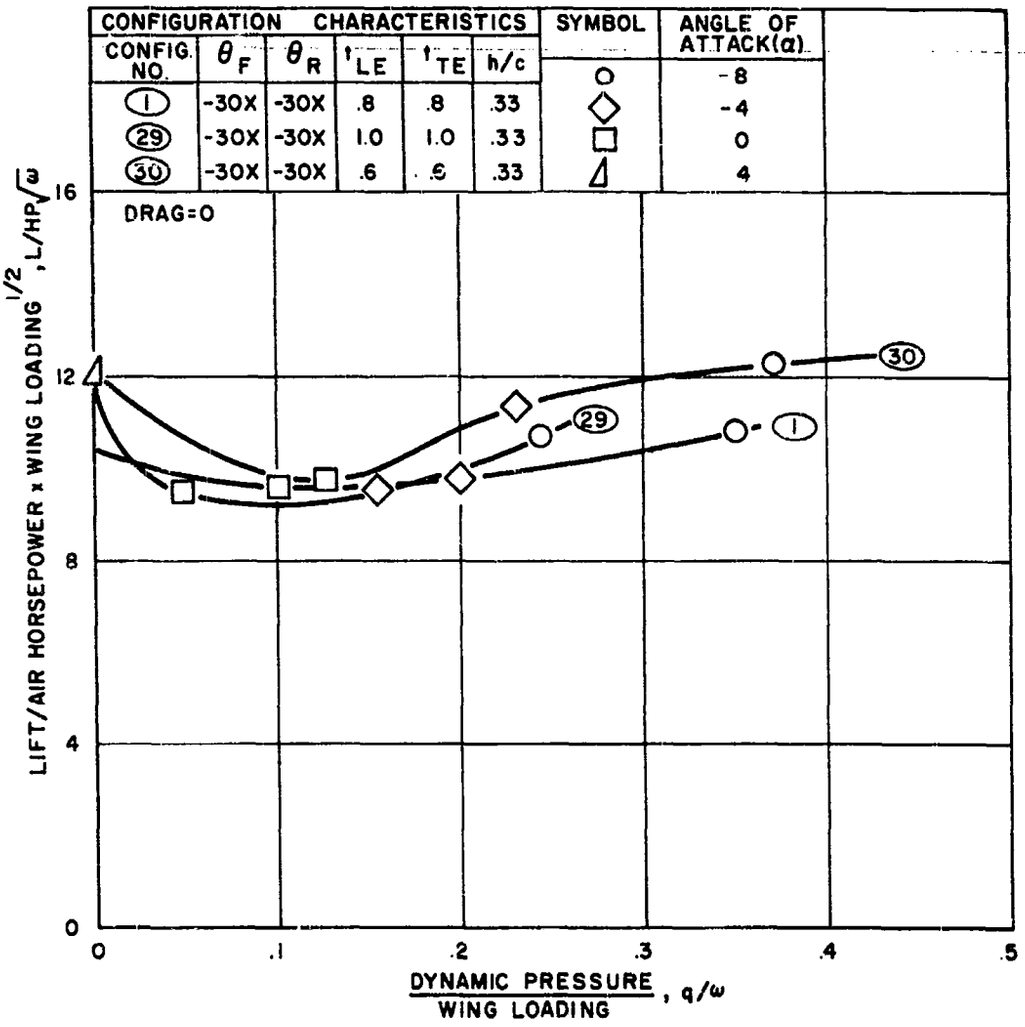

Figure 68. Effect of Gap Area on Lift Per Air Horsepower in Transition

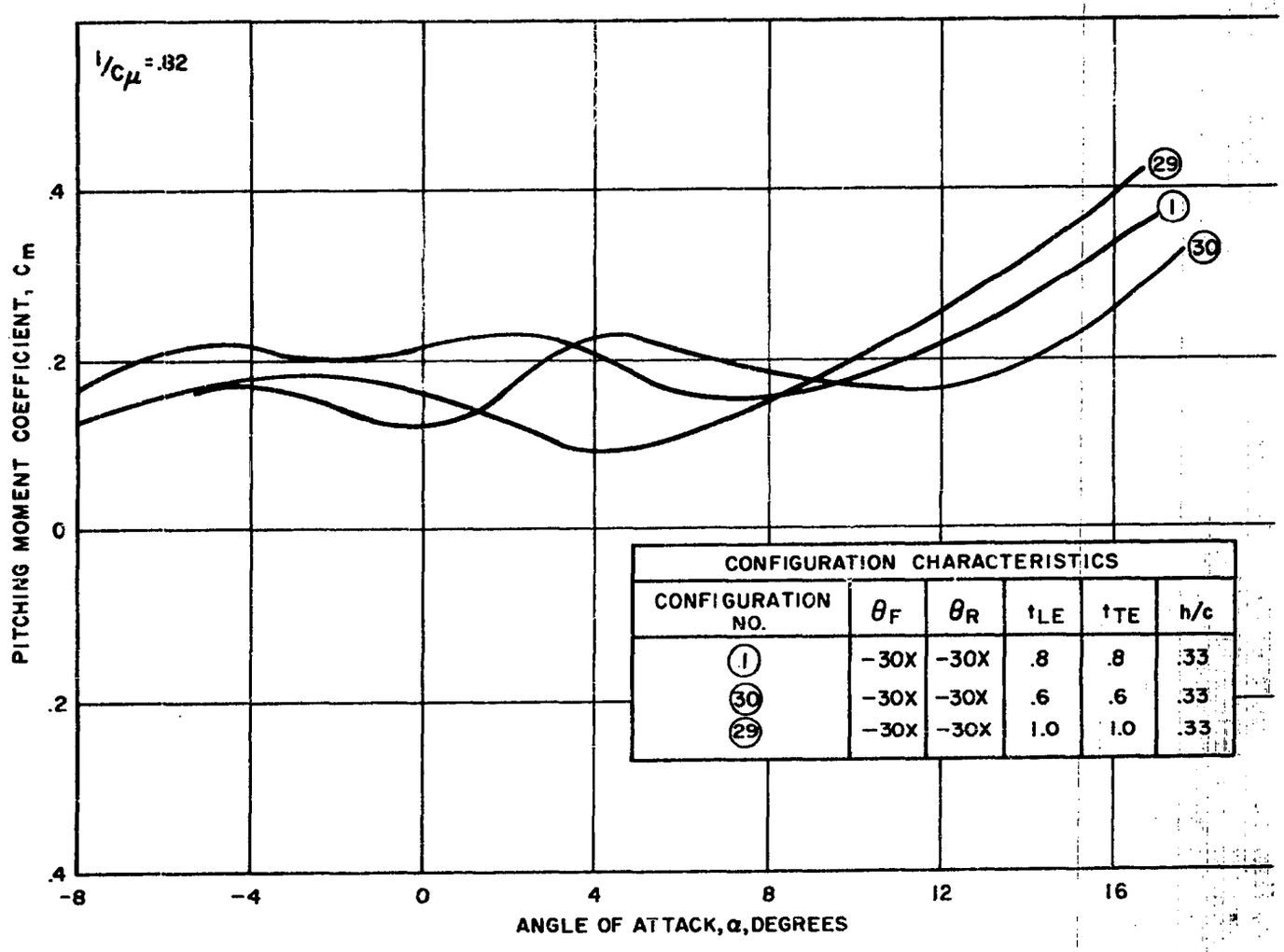

Figure 69. Pitching Moment Coefficient vs. Angle of Attack for Three Gap Areas ($1/C_\mu = .82$)

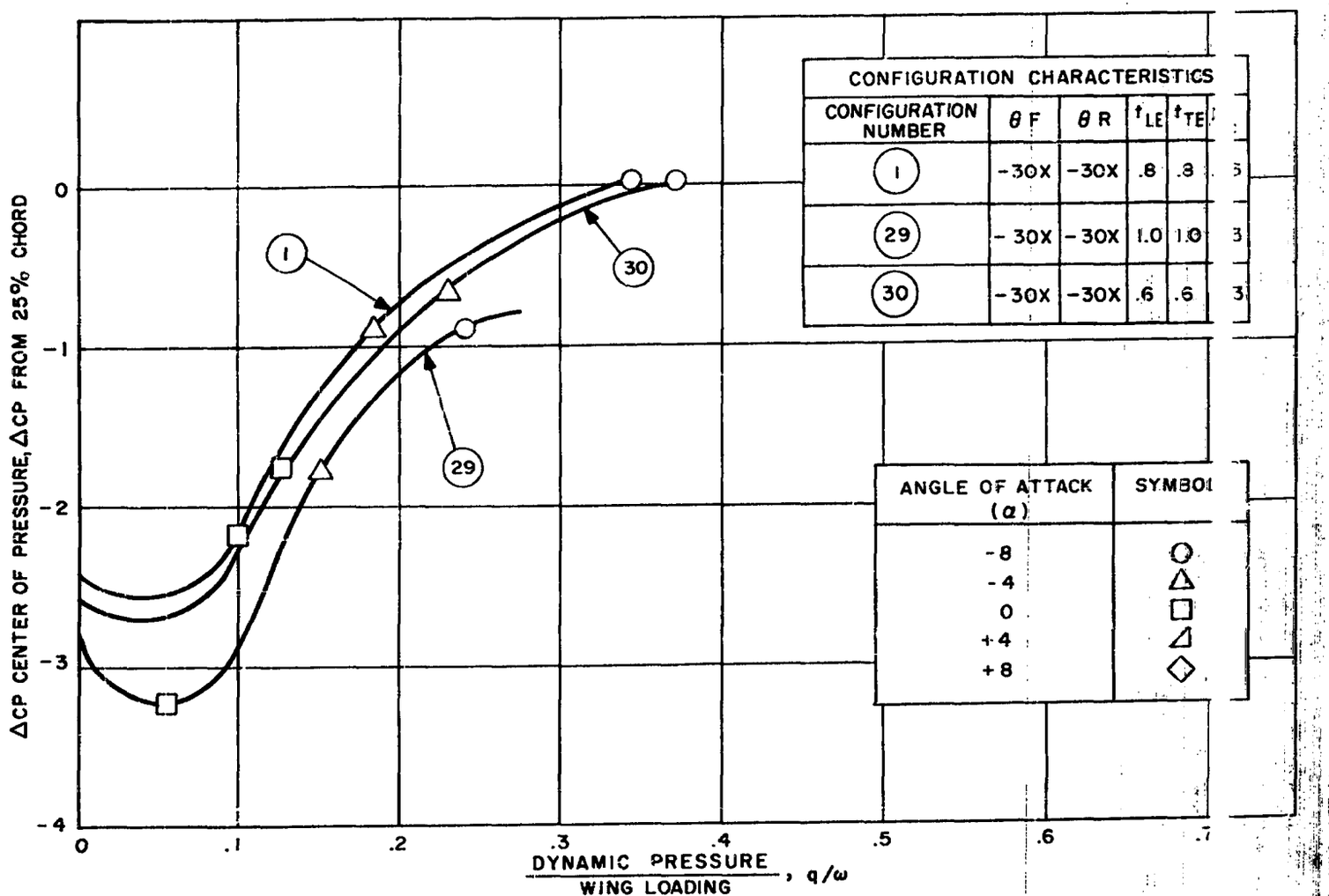

Figure 70. Center of Pressure Travel in Transition for Three Gap Areas

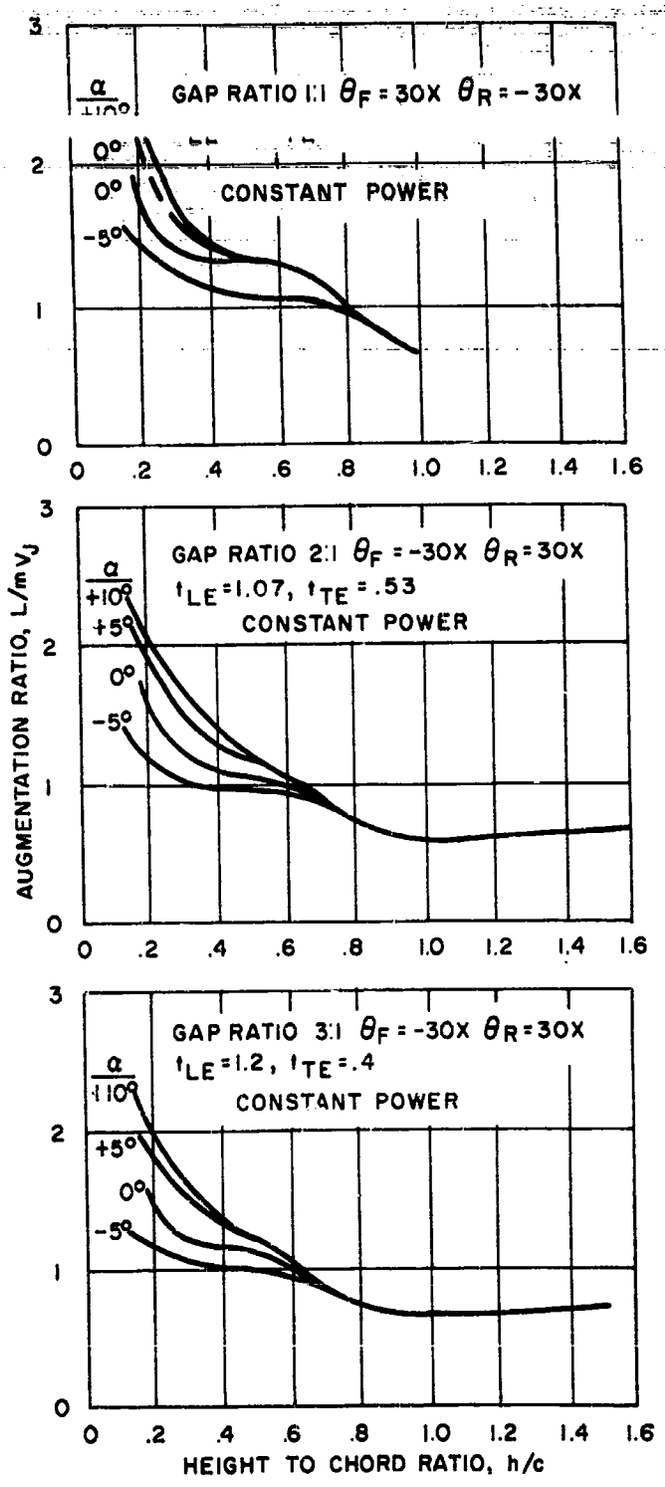

Figure 71. Variation of Augmentation Ratio with Height to Chord Ratio for Various Gap Ratios

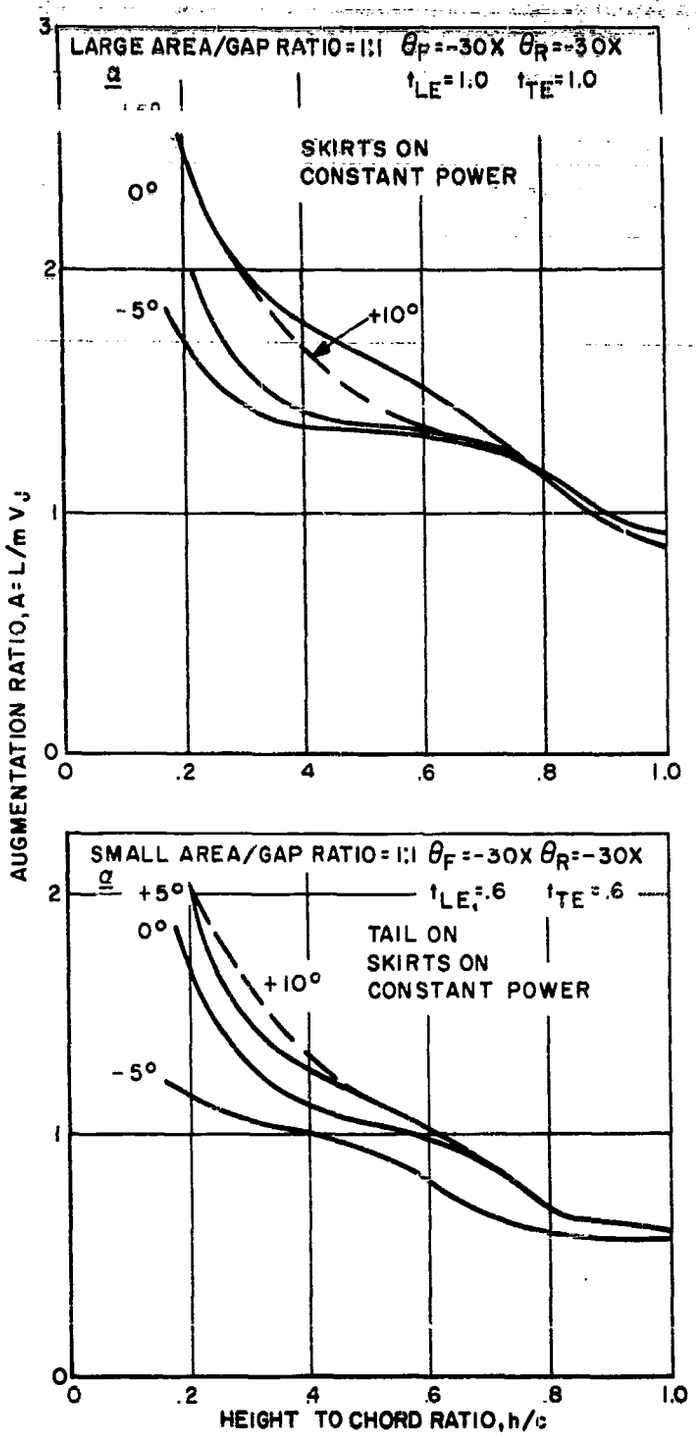

Figure 72. Variation of Augmentation Ratio with Height to Chord Ratio for Varied Areas of Equal Gap Ratios

As the leading edge gap was increased, no change in Center of Pressure occurred (the slight shift rearward in the previous calculation is not significant) for another angle of attack the same trend occurs in Table X.

TABLE X

VARIATION OF CENTER OF PRESSURE WITH GAP RATIO ($\alpha = -5°$)

Configuration $\theta_F = -30x$ $\theta_R = -30x$	t_{LE}/t_{TE}	A	C_m	C.P. (from 25%c)
$t_{LE} + t_{TE} = 1.6$	1:1	1.28	-.36	-.28
h/c = .33	2:1	1.05	-.36	-.34
$\alpha = -5°$	3:1	1.03	-.36	-.35

Note that the Center of Pressure does shift with angle of attack, which is explained in greater detail on Page 131. The significance of this section is that the shift of gap ratio to a larger slot at the leading edge does not effect a forward Center of Pressure shift (the small aft shift actually calculated is a surprise, and may be explained by a very small suck down on the nacelle and fuselage). This area was investigated and the amount of difference in lift or Pitching Moment obtained could possibly be the result of small data inaccuracies.

Transition Performance — To obtain the effect of gap ratio on the transition performance, the model was tested for three gap ratios (1:1, 2:1 and 3:1) at a Height to Chord Ratio of .33, nacelle doors shut and zero drag. This information is shown in Figure 73. A negligible difference in power is noticed at extremely low velocities but this difference becomes greater as the speed increases. Further increasing the speed decreases the increment of power between the three gap ratios to a negligible amount. This indicates that the peripheral curtain is being effected by the dynamic pressure of the free stream acting on it. The conclusion is that the basic gap ratio of 1:1 is best from the performance consideration.

Transition Stability — As the velocity increases through transition, the change in stability obtained by varying the gap ratio from 1:1 to 3:1 was not appreciable (see Figure 74). The near neutral stability obtained from the 1:1 gap ratio is representative for all gap ratios.

Transition Trim — The basic idea of obtaining a forward Center of Pressure in hover and transition, thus making it compatible with the forward flight regime, was not realized. Figure 75 presents the variation of Center of Pressure with velocity for the three gap ratios tested. There is no significant difference in trim among the three gap ratios and it follows the general trend with velocity.

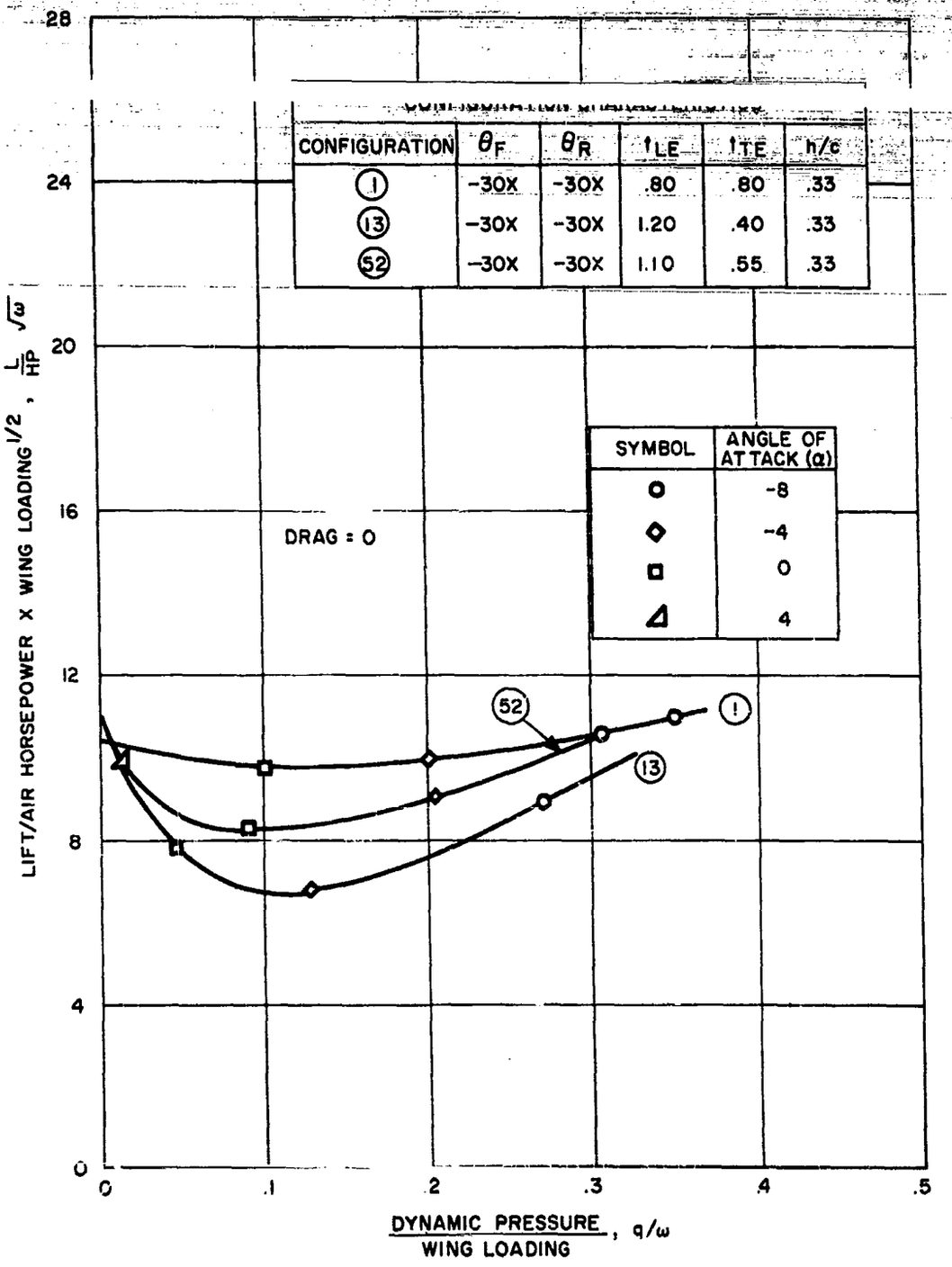

Figure 73. Effect of Gap Ratio on Lift Per Air Horsepower in Transition

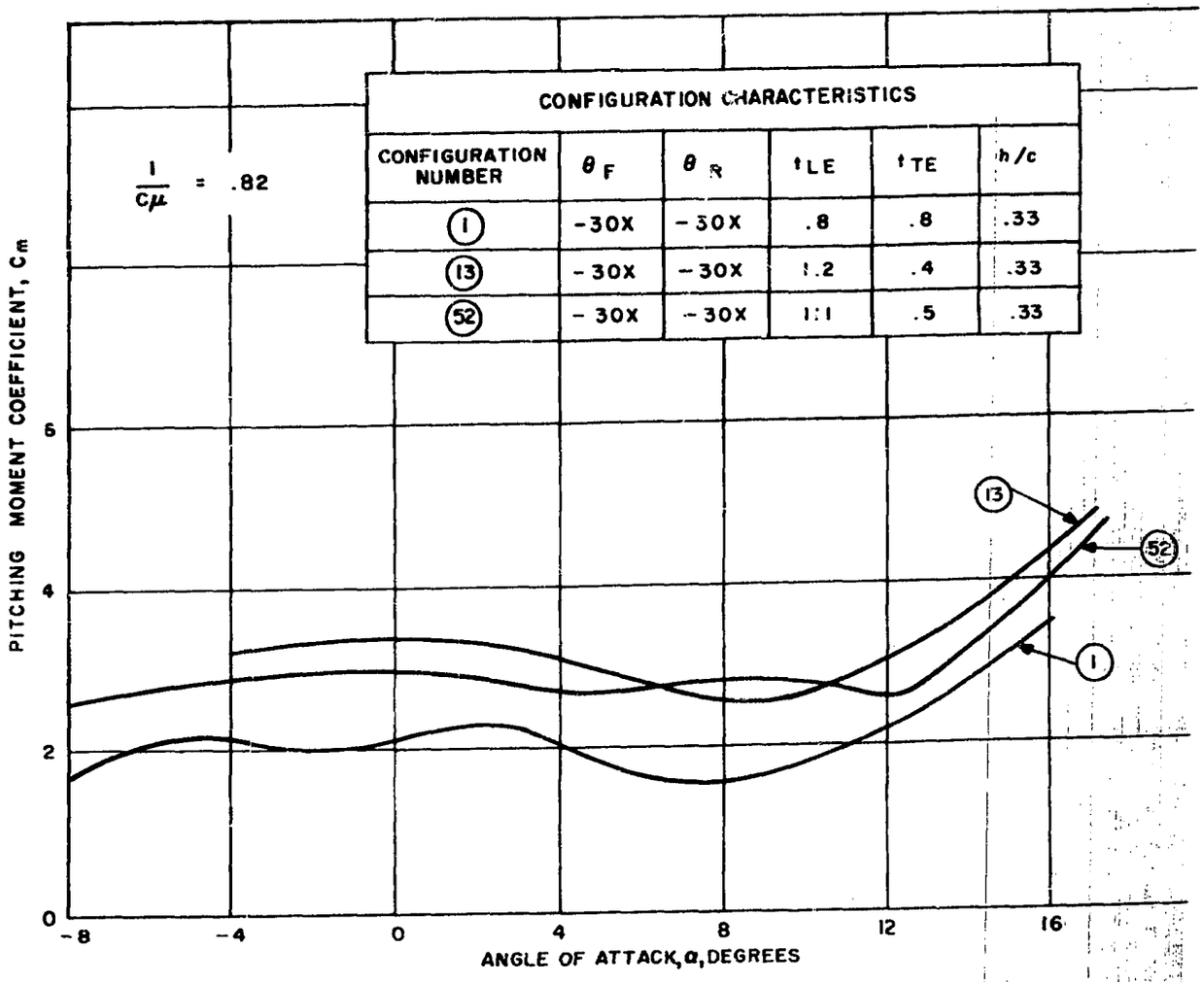

Figure 74. Pitching Moment Coefficient vs. Angle of Attack for Three Gap Ratios ($1/C_\mu = .82$)

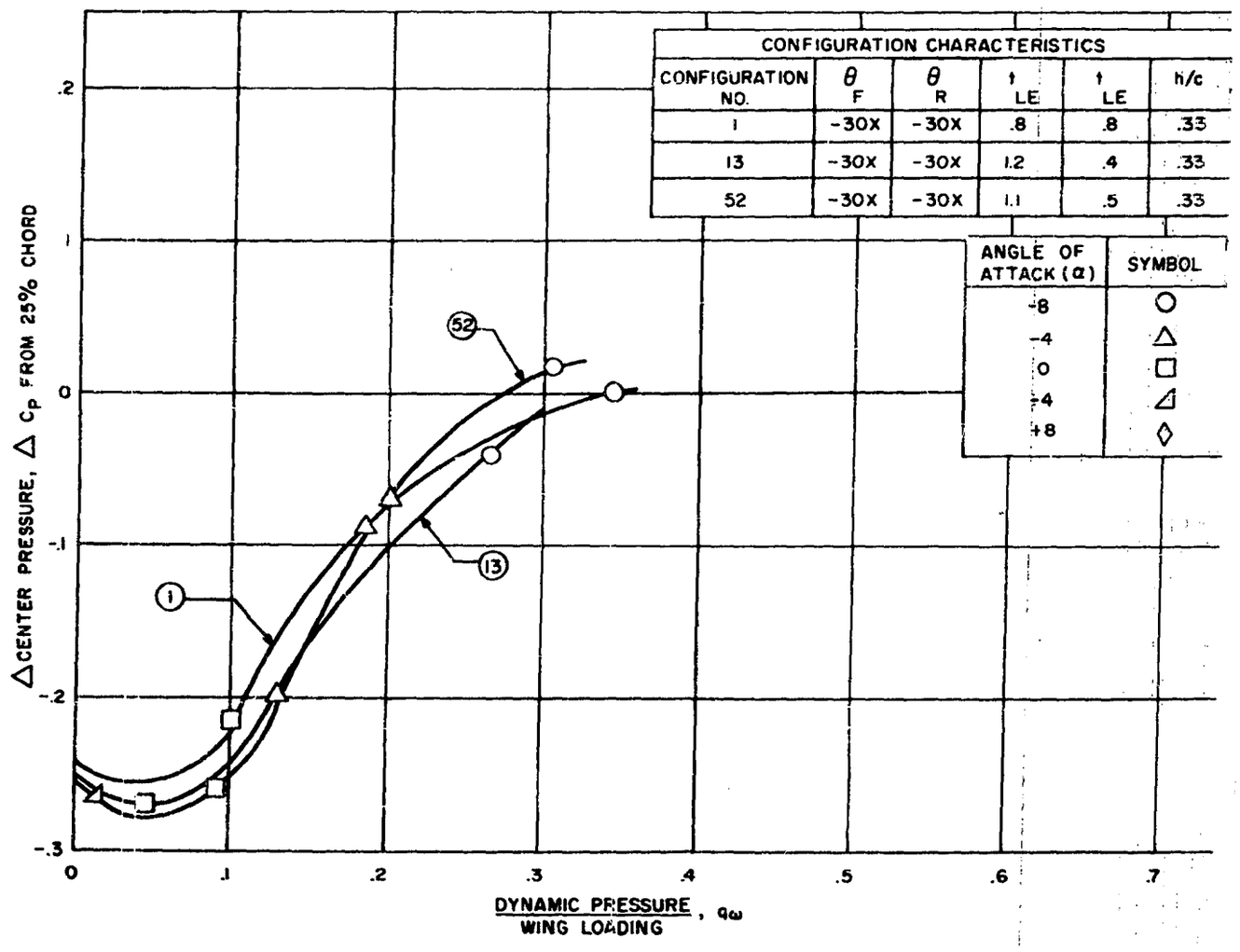

Figure 75. Center of Pressure Travel in Transition for Three Gap Ratios

Stability Characteristics

Forward Speed Effects: To facilitate handling of the hover and transition data, the conventional lift, drag and pitching moment coefficients ($C_L = \frac{L}{qS_\omega}$ $C_D = \frac{D}{qS_\omega}$, and $C_m = \frac{M}{qS_\omega C}$) where divided by the momentum coefficient ($C_\mu = \frac{mV_J}{qS}$) and plotted against $1/C_\mu$ (see Volume II, Appendix C) for constant angles of attack. This simplifies the determination of the aerodynamic coefficients while independently varying the dynamic pressure and jet slot momentum. As the forward speed increases, $1/C_\mu$ increases, the lift and drag coefficients (C_L/C_μ and C_D/C_μ) increase showing the aerodynamic effect. The pitching moment coefficient (C_m/C_μ) increases or decreases with $1/C_\mu$ depending upon the angle of attack. An almost linear relationship between CL/C_μ, C_D/C_μ, C_m/C_μ can be seen; therefore, demonstrating that for the higher speed range, mV_J has no major effect on these coefficients.

Aerodynamic Characteristics

One of the major influencing parameters on the aerodynamic coefficients is angle of attack. For example, as the angle is increased the lift coefficient increases up to a point where flow becomes separated over the leading edge and stall occurs. Similarly in GETOL, angle of attack has a great influence on the coefficients in hover, transition and forward flight. In hover, air issues from the bottom surface of the wing at some fixed angle to it; the angle of attack change results in changing the angle of the jet to the ground reference plane and hence a changed distribution of horizontal and vertical forces caused by the jet. This also results in an effective change in the base pressure trapped by the peripheral jet curtain. In transition and forward flight this is compounded by the aerodynamic effect. Therefore, an evaluation of the characteristics as affected by the angle of attack is required.

Angle of Attack Effects: Hovering Performance - There was a definite variation in hovering lifting ability with angle of attack. Figure 76 shows the Augmentation Ratio at several angles of attack for various slot angle configurations, always revealing the greatest lift in nose high attitudes. This is partially explained by the fact that the installed wing incidence plus airfoil bottom curvature results in a horizontal wing base when the fuselage was at an angle of attack of approximately +7 degrees. Figure 77 cross plots Augmentation Ratio versus angle of attack for several geometries. The trend to a higher Augmentation Ratio at six to ten degrees is obvious.

Hovering Stability - The variation of pitching moment with angle of attack is the measure of longitudinal static stability for the preferred hovering geometries of $\theta_F = -30x$ $\theta_R = -30x$ or $\theta_F = Ox$ $\theta_R = Ox$. Other slot angles exhibit positive or negative stability depending on the geometry, but all seem fairly neutral.

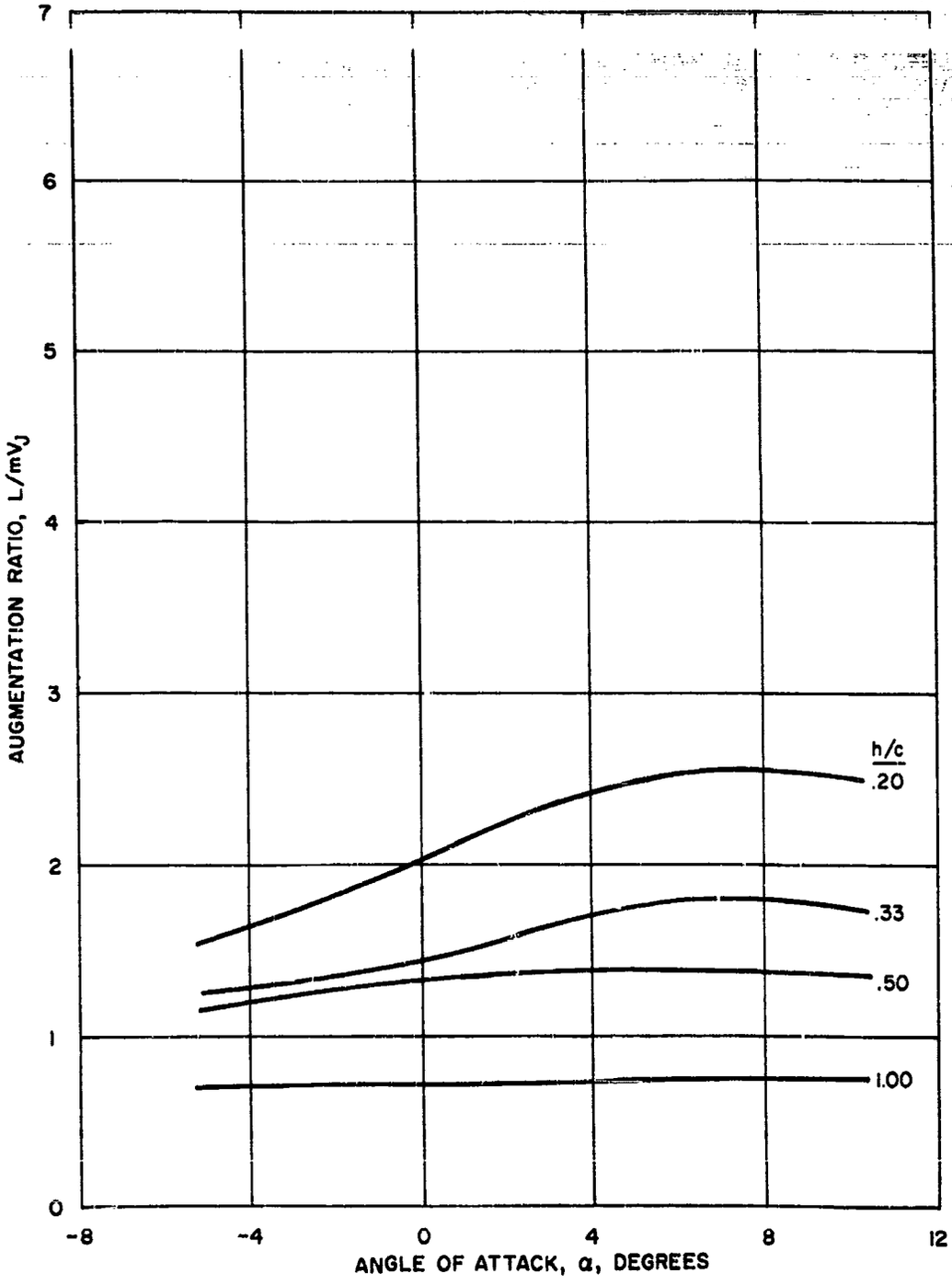

Figure 76. Variation of Augmentation Ratio with Angle of Attack for Various Height to Chord Ratios

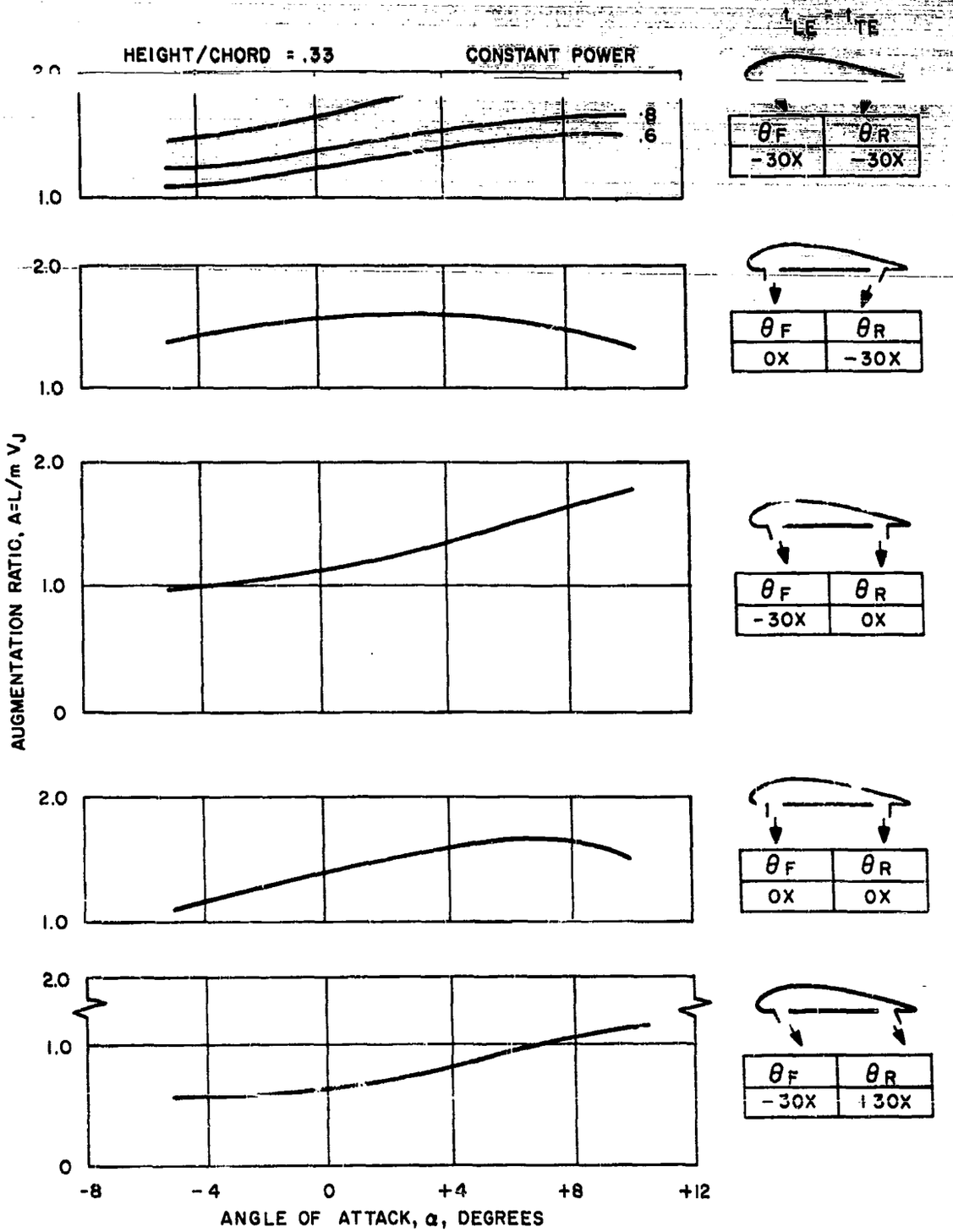

Figure 77. Variation of Augmentation Ratio with Angle of Attack for Various Slot Angle Configurations

neutral.

Hovering Trim - No angle of attack was discovered for the hovering configuration where the trim moment would be zero about the 25% chord. But, from Figure 83 there seems to be the least trim moment at approximately +7 degrees angle of attack. The conclusion is that from power, stability and trim considerations hovering at +7 degrees angle of attack is recommended.

Transition Performance - Figure 84 shows the variation of equilibrium power required through transition for typical slot angle - height configurations. With the drag equal to zero condition established, it can be noted that the angle of attack required decreases as the speed increases; as the forward speed increases the aerodynamic lift increases thereby requiring a lower lift coefficient to maintain a specified wing loading. The variation of lift coefficient with angle of attack is illustrated in Volume II, Appendix C and indicates decreasing lift with decreasing angle of attack.

Transition Stability - The effect of angle of attack on the Pitching Moment demonstrates the longitudinal stability. For the slot configuration, the trend of the stability characteristics is shown (see Figure 85) to be almost neutral or slightly positive. Stability is also a function of $1/C_\mu$ and as this value increases the stability changes from positive to negative (see Figure 193 of Volume II, Appendix C).

Transition Trim - As the velocity increases through transition, the angle of attack, established from the equilibrium condition, decreases as the velocity increases. A Center of Pressure variation with velocity is shown in Figure 86 following the general trend of hovering Center of Pressure at the 50% chord and moving forward to the 25% chord.

Jet Flap Characteristics: From many investigations it has been proven that the jet flap wing provides very high lift coefficients; thereby, making it very useful in the design of a Short-Take-off and Landing (STOL) aircraft. The GETOL aircraft, having air flow in the wing and through the peripheral slot, would lend itself to a jet flap configuration very easily by closing all but the trailing edge slot. With this capability available, it was felt that an investigation of this configuration with a jet flap should be investigated to determine its characteristics. To obtain this information, the leading edge and tip slots were closed and various trailing edge slot angles were tested.

Transition Performance - The effect of the jet slot angle on the performance in transition and forward flight is presented in Figure 78. The two configurations shown in Figure 78 are $\theta_F - \theta_R = +60$ x and $\theta_F - \theta_R = +30$ x as noted in GETOL terminology. In conventional terminology, the first is a jet flap deflection angle of 30 degrees and the second is a jet flap deflection angle of 60 degrees. In the low speed range there is a small difference in the L/HP between the two configurations, but as the speed increased there is a very significant difference in

that the $\theta_F = -\theta_R = +60x$ configuration becomes superior. Comparing the angles of attack to achieve any speed, the $\theta_F = -\theta_R = +30x$ configuration requires a lower angle. This indicates that a major portion of the lift is developed by the jet and poor turning of the air passing over the wing is obtained. From the performance demonstrated in the $\theta_F = -\theta_R = +60x$, it is the better configuration.

Transition Stability - Variation of the jet flap angle has no significant effect on the stability through transition (see Figure 79). Both configurations are slightly unstable and the increasing forward speed has changed only the trim moment.

Transition Trim - Figure 80 presents the variation of the Center of Pressure with speed. There is a small amount of shift incurred with forward speed. The $\theta_F = -\theta_R = +60x$ Center of Pressure is located at approximately the 15% chord and the $\theta_F = -\theta_R = +30x$ is near the 30% chord. Based upon trim, the $\theta_F = -\theta_R = +30x$ configuration would be most compatible with forward flight.

Performance Characteristics

Height Effects: One of the most powerful parameters for the Ground Effect Machine (GEM) is the operating height. Parametrically height is treated as height to diameter (h/d) for a circular planform. In this GETOL study height will be treated as Height to Chord Ratio (h/c), where c is the root chord (18 inches for the Boeing-Vertol wind tunnel model tested at NASA).

A requirement of TRECOM Contract DA44-177-TC-663, under which Boeing-Vertol has been conducting this GETOL feasibility study, was a three foot hovering height. For initial aircraft layouts the resulting Height to Chord Ratio was .33. For this reason most of the NASA testing was done at this Height to Chord Ratio of .33. However, considerable trend data points were obtained at h/c = .2, .5, 1.0 and ∞ so that this evaluation of the effect of hovering clearance may be conducted.

Hovering Performance — For comparisons of hovering performance variations with h/c, either lift per air horsepower or Augmentation Ratio may be used as long as model geometries are not wrongly compared. The purpose here being only to clearly determine the height-lift trend, Augmentation Ratio provides the most logical parameter. Referring to Figure 71, a variety of Augmentation curves are presented showing the increase in the lifting ability with decreased h/c. It is significant that, as a guide, dropping hovering h/c from the contemplated value of .33 to .20 will provide about 25 to 30% increase in lifting ability.

To obtain a feeling for the actual power requirements, Figures 81 and 82 should be used but it must be kept in mind that the lift per air horsepower attainable is a function of power loading; however, the same 25 to 30% lifting ability increase is shown for an h/c decrease from .33 to .20.

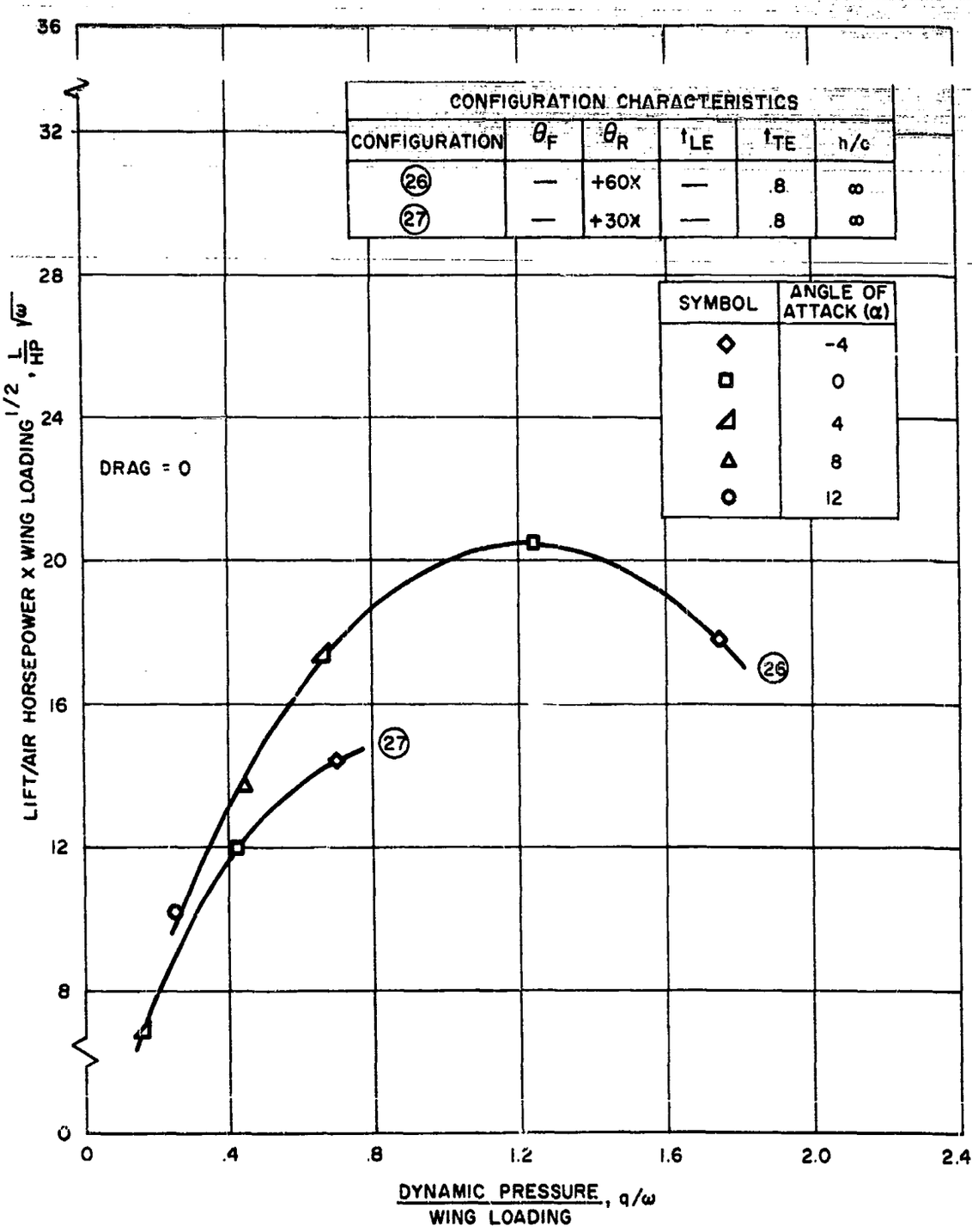

Figure 78. Effect of Jet Flap Angle on Lift Per Air Horsepower in Transition

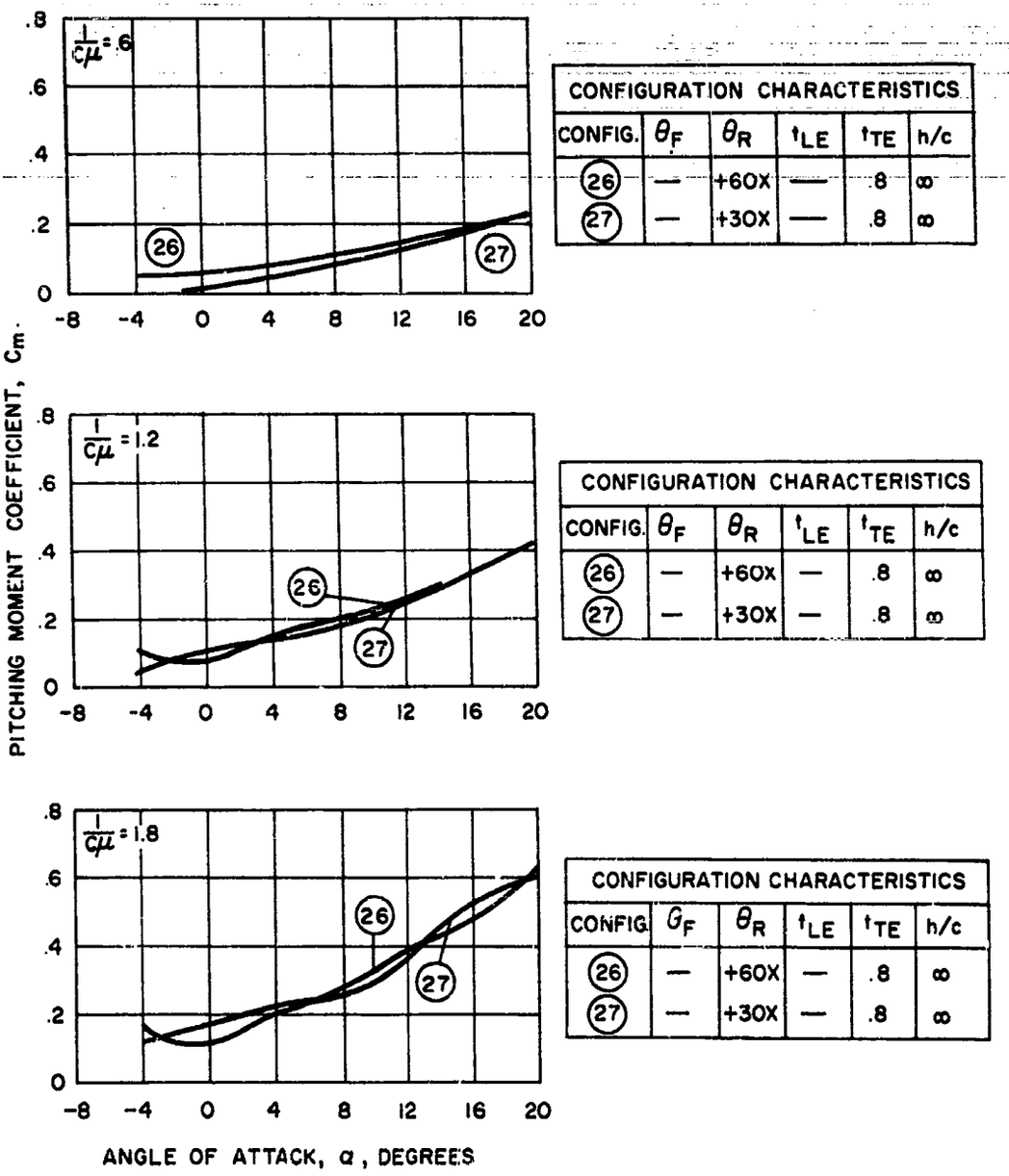

CONFIGURATION CHARACTERISTICS					
CONFIG.	θ_F	θ_R	t_{LE}	t_{TE}	h/c
㉖	—	+60X	—	.8	∞
㉗	—	+30X	—	.8	∞

CONFIGURATION CHARACTERISTICS					
CONFIG.	θ_F	θ_R	t_{LE}	t_{TE}	h/c
㉖	—	+60X	—	.8	∞
㉗	—	+30X	—	.8	∞

CONFIGURATION CHARACTERISTICS					
CONFIG.	θ_F	θ_R	t_{LE}	t_{TE}	h/c
㉖	—	+60X	—	.8	∞
㉗	—	+30X	—	.8	∞

Figure 79. Pitching Moment Coefficient vs. Angle of Attack for Various Jet Flap Angles

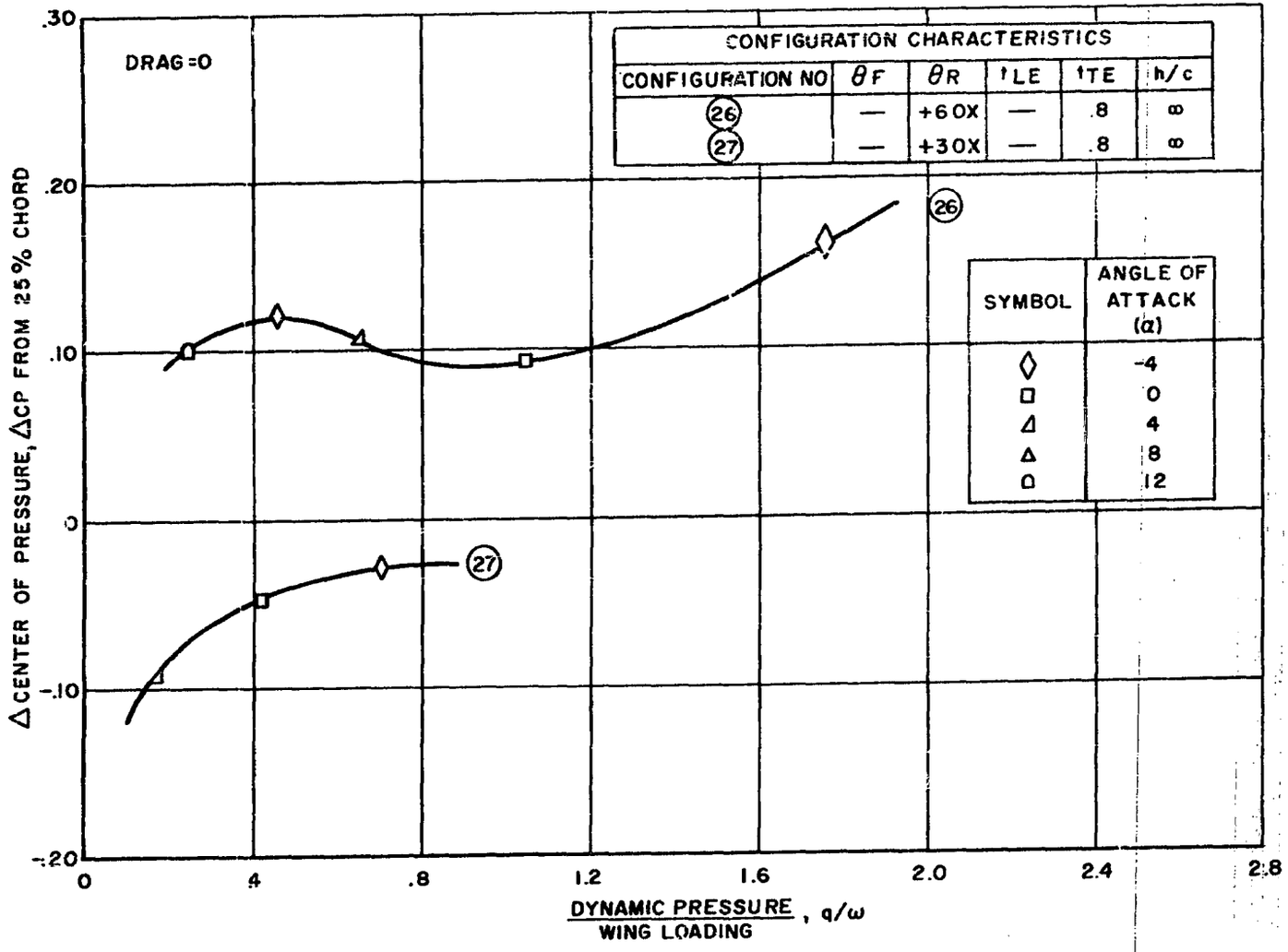

Figure 80. Center of Pressure Travel in Transition for Various Jet Flap Angles

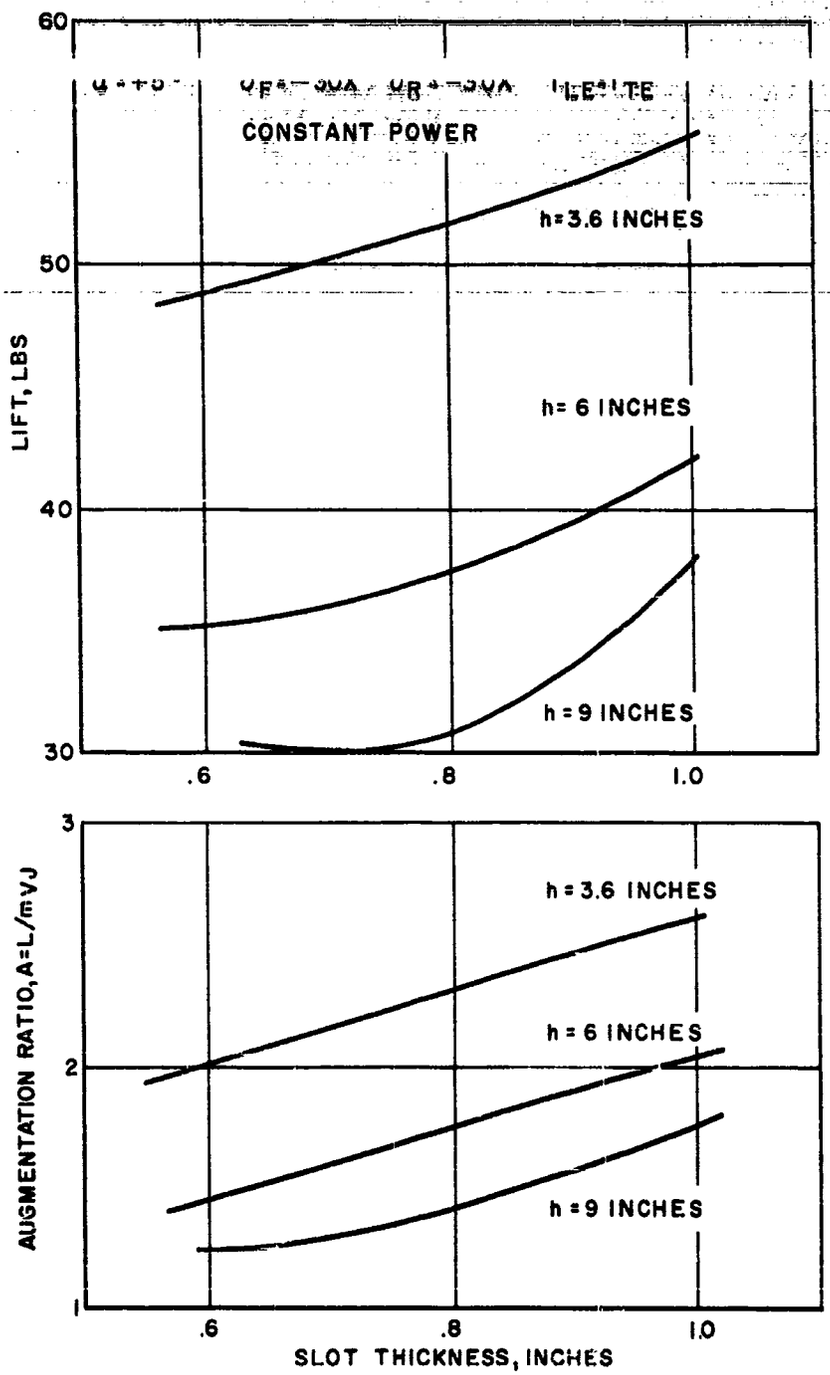

Figure 81. Force and Flow Parameters for θ_F = -30x θ_R = -30x Configuration (α = +5°)

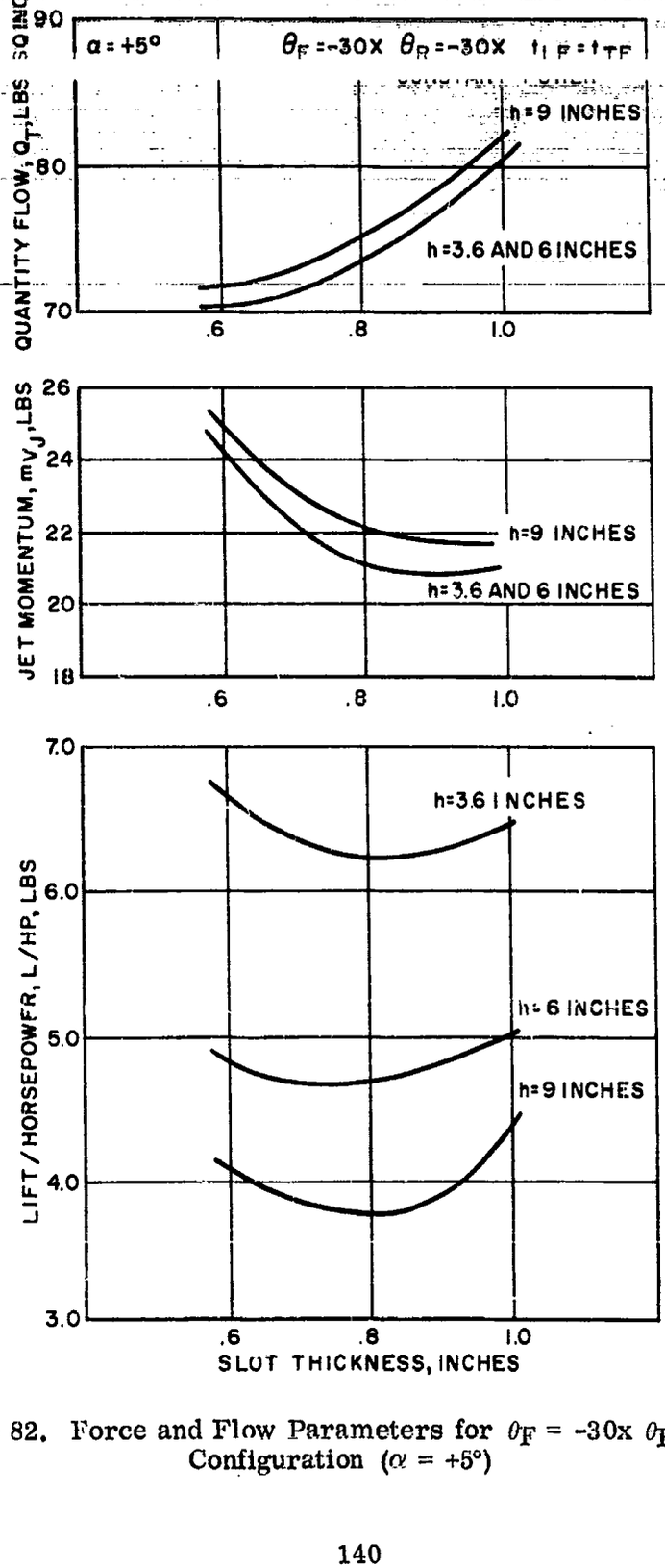

Figure 82. Force and Flow Parameters for θ_F = -30x θ_R = -30x Configuration (α = +5°)

Hovering Stability — Figure 83 presents Pitching Moment variation with angle of attack for three height ratios. These curves are typical of many plotted for hovering geometries and show about neutral longitudinal stability. As height is decreased no significant change in the slope occurs. The conclusion is that above h/c = .20 changing height makes no significant change in stability.

Hover Trim — Referring again to Figure 83 the trim moment is quite negative and certainly varies with height ratio. However, lift also decreases with increasing height and Table XI shows the actual shift of the center of the pressure.

TABLE XI

VARIATION OF CENTER OF PRESSURE WITH HEIGHT TO CHORD RATIO (α=0)

h/c	($\alpha = {}^{C_m}{}_0$)	($\alpha = {}^{C_L}{}_0$)	Δ C.P. (%) (from quarter chord)
.20	-.53	1.8	-29
.33	-.36	1.45	-24
.50	-.28	1.32	-21
Note: Negative percentage indicates aft center of pressure			

The conclusion is that any controlling trim moment will only vary slightly with height, but will be quite substantial, if the center of gravity must be located at the quarter chord. A front cruciform "T" may be needed just for moment balance (forward Center of Pressure shift) as well as for a possible stability improvement.

Transition Performance - To illustrate the effect of height on transition performance, a comparison of the parametric lift per air horsepower ($\frac{T}{HP}\sqrt{\omega}$) through transition is shown in Figure 84. There is a decrement in power required by reducing the Height to Chord Ratio from the basic value of .33 to .2 at low speeds. An increment in power required for the Height to Chord Ratio of .5 over that of .33 is obtained at very low forward speeds and decreases as the speed is increased. The power required for each of the three heights discussed converges as the speed is further increased. This indicates that the saving in power in the hovering regime decreased to the point of non-existence as the free stream dynamic pressure becomes great enough to deteriorate the augmented lift developed by the peripheral jet curtain.

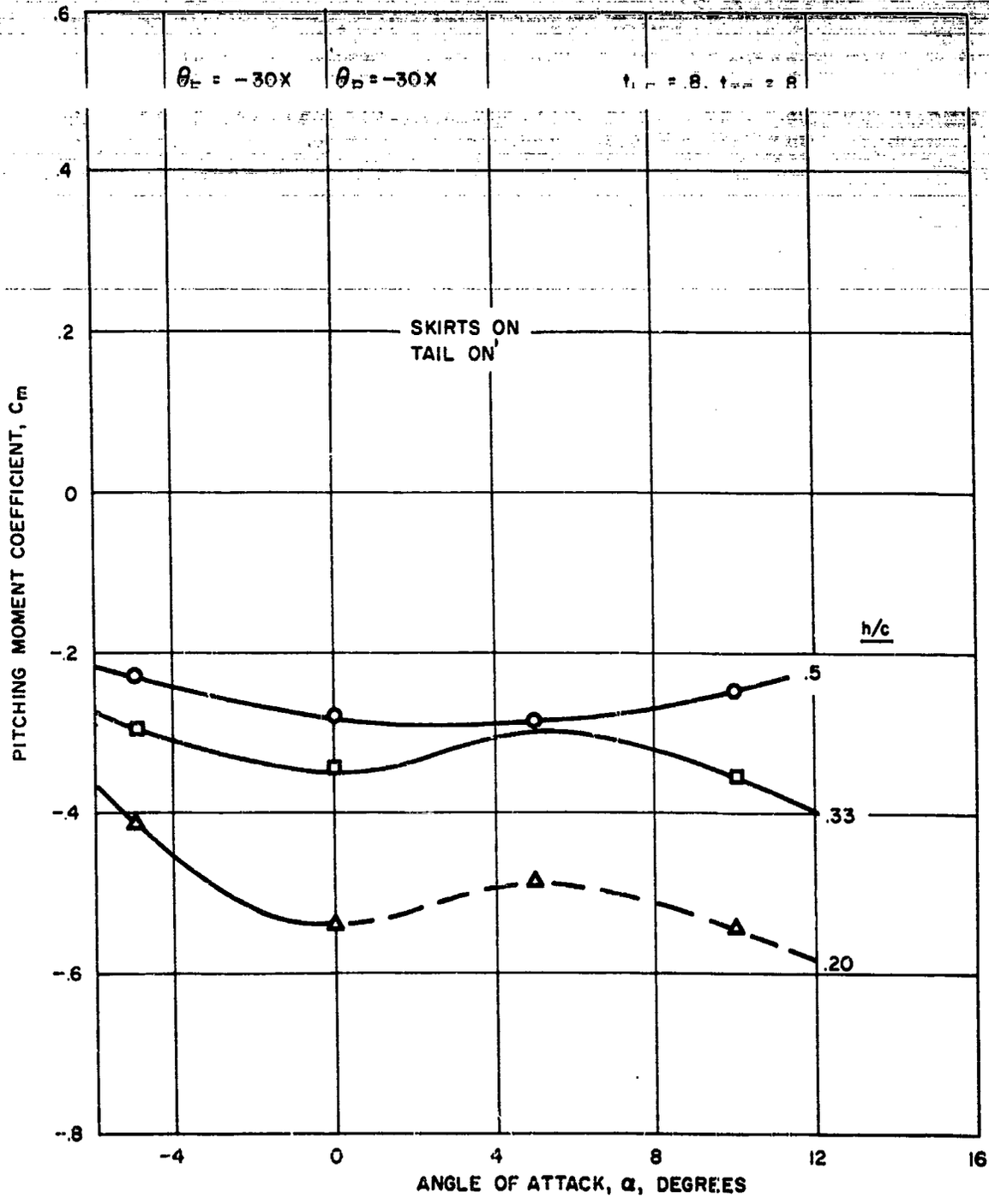

Figure 83. Pitching Moment Coefficient vs. Angle of Attack for Three Height to Chord Ratios

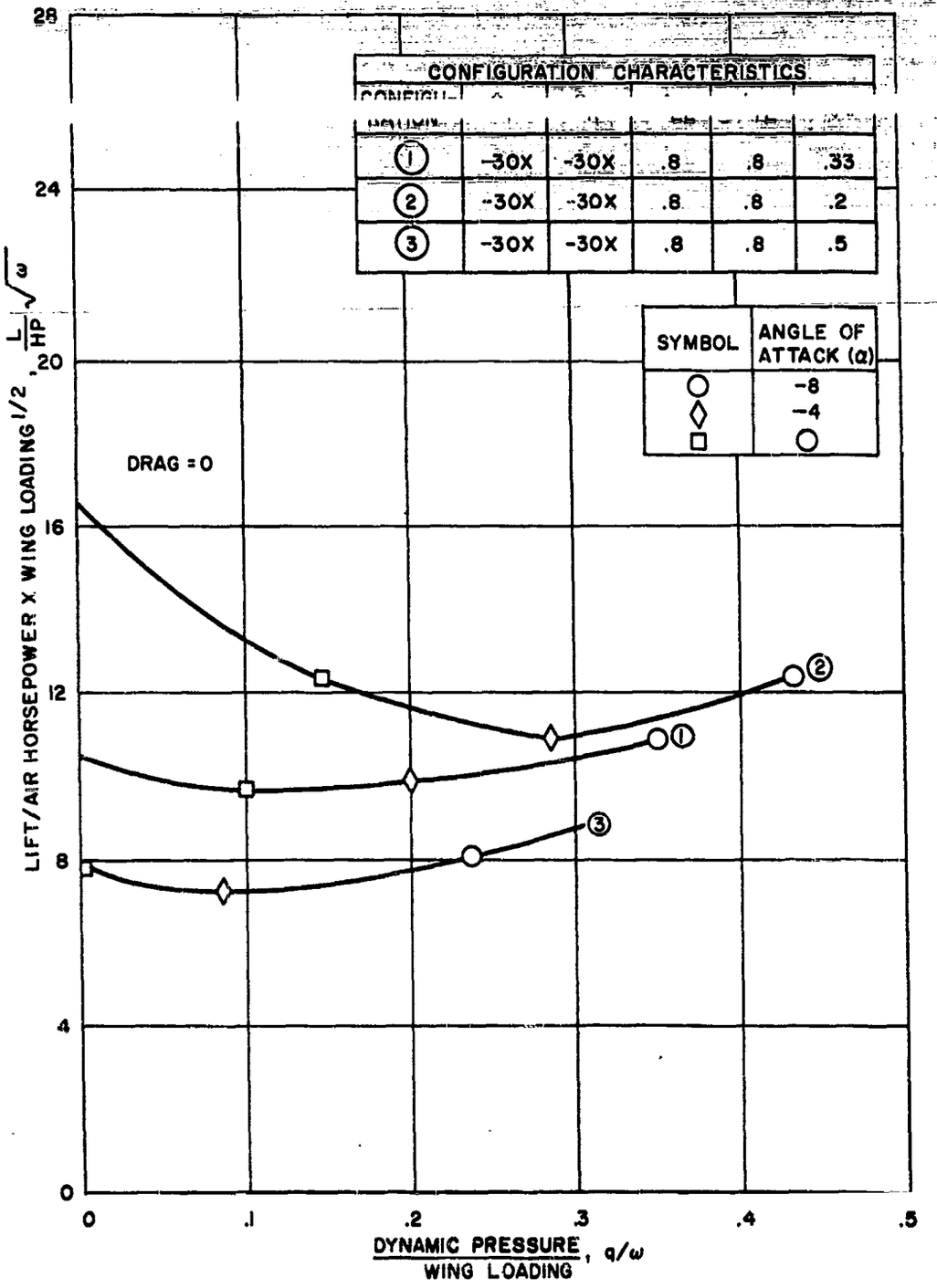

Figure 84. Effect of Height on Lift Per Air Horsepower in Transition

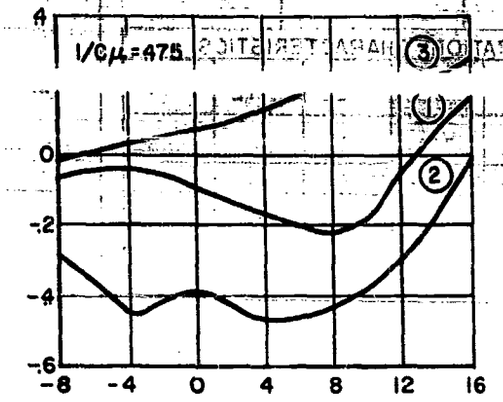

CONFIGURATION NO	θ_F	θ_R	t_{LE}	t_{TE}	h/c
②	-30X	-30X	.8	.8	.20
①	-30X	-30X	.8	.8	.33
③	-30X	-30X	.8	.8	.50

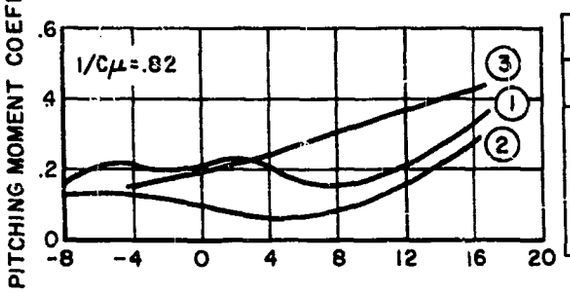

CONFIGURATION CHARACTERISTICS					
CONFIGURATION NO	θ_F	θ_R	t_{LE}	t_{TE}	h/c
②	-30X	-30X	.8	.8	.2
①	-30X	-30X	.8	.8	.33
③	-30X	-30X	.8	.8	.50

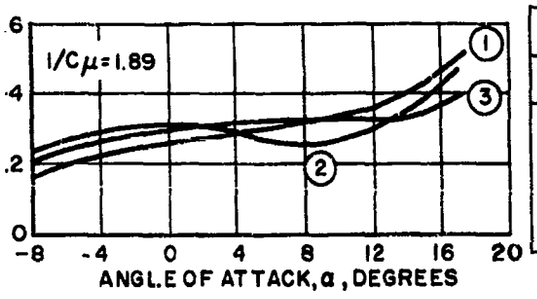

CONFIGURATION CHARACTERISTICS					
CONFIGURATION NO	θ_E	θ_R	t_{LE}	t_{TE}	h/c
②	-30X	-30X	.8	.8	.20
①	-30X	-30X	.8	.8	.33
③	-30X	-30X	.8	.8	.50

Figure 85. Pitching Moment Coefficient vs. Angle of Attack for Three Height to Chord Ratios

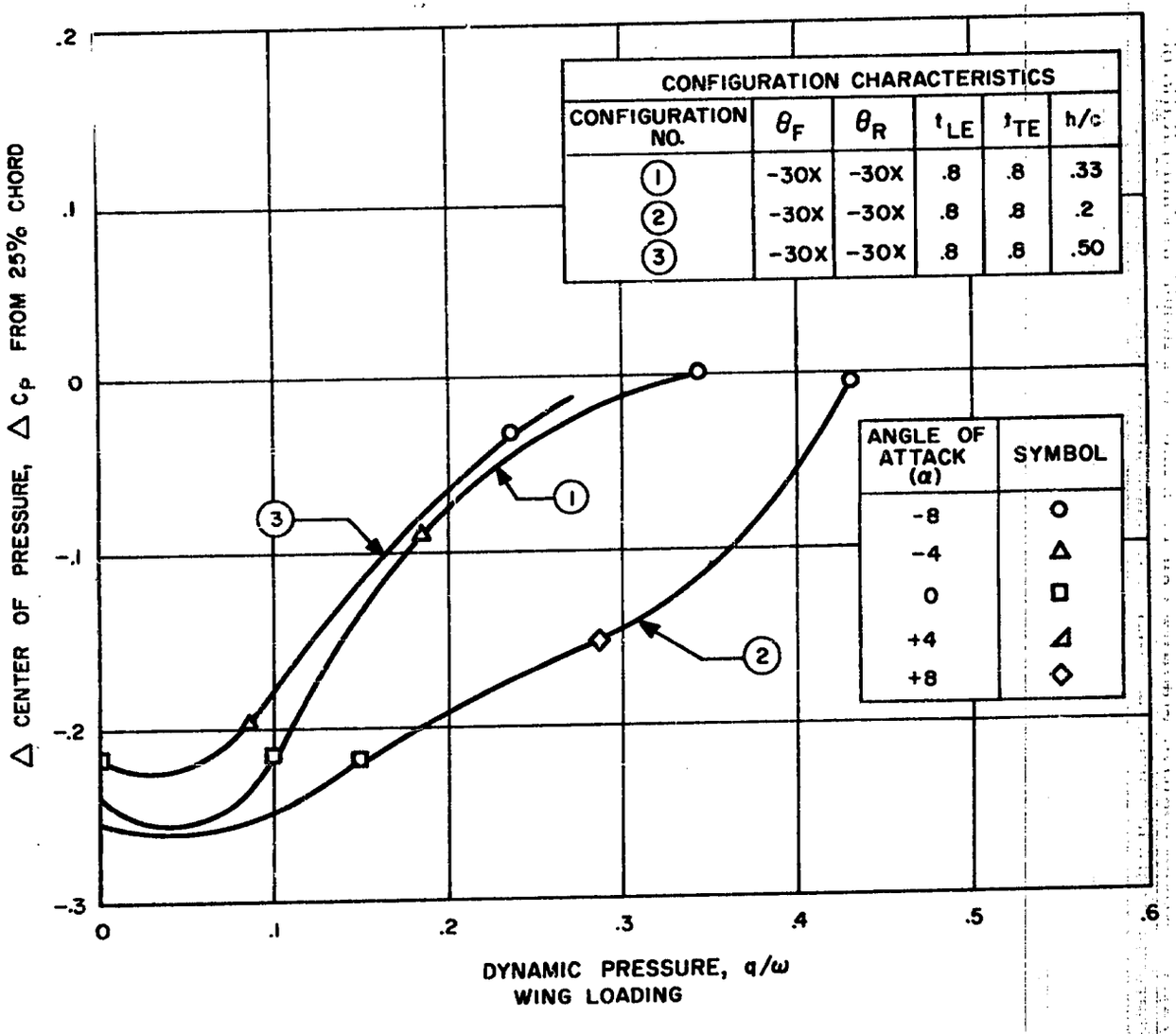

Figure 86. Center of Pressure Travel in Transition for Various Heights

transition is shown on Figure 85. For the Height to Chord Ratios of .20 and .33 neutral or slight positive stability can be seen. At a Height to Chord Ratio of .50 there is a slight unstable trend. This indicates that as the height increases the stability characteristics change from slightly stable to slightly unstable.

Transition Trim - Figure 86 shows the effect of height on the trim moment about the 25% chord through transition. There is a small effect caused by height at low speeds and beyond this the difference becomes very evident for the lower shaft. A cruciform "T" may be needed for stability improvement and correction of the large nose down Pitching Moment.

Propulsion Possibilities: Two basic concepts of propulsion were incorporated into the NASA testing:

1. Aft angled wing slots

2. Nacelle door opening

Propulsion is required to accelerate from hover, during transition, and in airplane flight. All three flight regimes were investigated, but Vmax was limited to 100 ft/sec.

Static Propulsion (Hovering) - Figure 87 presents the variation of lift with thrust of the model for two (angled slots or nacelle doors) methods of obtaining forward propulsion. To obtain a high acceleration both the forward and aft slots would be directed aft (θ_F = -30x θ_R = -30x); this condition demonstrates a small increase in thrust but a large decrease in lift. When the doors in the nacelle were opened there was a significant increase in thrust and only a small decrease in lift. The trend of this variation is not influenced by height. The superiority of the door thrust system is evident and the lift decrease is not nearly so severe as with the aft angled slots. This indicates that lift is developed by the slipstream passing over the door.

Transition Propulsion - To investigate the propulsion capabilities in transition, a comparison of the performance characteristics of various configurations was made. Shown in Figure 88 is this comparison in terms of the parametric lift per air horsepower ($\frac{L}{HP}\sqrt{\omega}$) required for an equilibrium transition (Drag = 0). For the two configurations (θ_F = -30x θ_R = -30x and θ_F = -30x θ_R = +30x) with the nacelle doors closed, forward propulsion was achieved by decreasing the angle of attack to obtain enough thrust to overcome the drag. The θ_F = -30x θ_R = -30x configuration results in a higher lift per air horsepower but at a lower angle of attack. These two configurations are again shown with the nacelle doors open two inches to obtain additional propulsive force. At low forward speeds the θ_F = -30x θ_R = +30x configuration has slightly better performance at a higher angle of attack. This indicates that a portion of the lift must be supplied by the propulsive force being at positive angles of attack. As the

librium and the difference in lift per air horsepower reversed. This further indicates that the $\theta_F = -30x$ $\theta_R = +30x$ requires a portion of the propulsive force to generate lift.

Included on Figure 88 are the jet flap and the airplane configurations to complete the overall picture of the flight regimes that the GETOL configuration must operate.

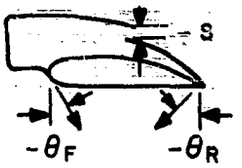

CONFIG.	θ_F	θ_R	r_{LE}	r_{TE}	h/c	S	SYM
	-30X	-30X	.8	.8	.20	0	∇_1
	-30X	0X	.8	.8	.20	0	∇_2
	-30X	+30X	.8	.8	.20	0	∇_3
	-30X	-30X	.8	.8	.20	1.05"	O_4
	-30X	-30X	.8	.8	.33	0	∇_5
	-30X	0X	.8	.8	.33	0	∇_6
	-30X	+30X	.8	.8	.33	0	∇_7
	-30X	-30X	.8	.8	.33	.20	O_8
	-30X	-30X	.8	.8	.33	.55	O_9
	-30X	-30X	.8	.8	.33	1.05	O_{10}
	-30X	-30X	.8	.8	.33	2.00	O_{11}

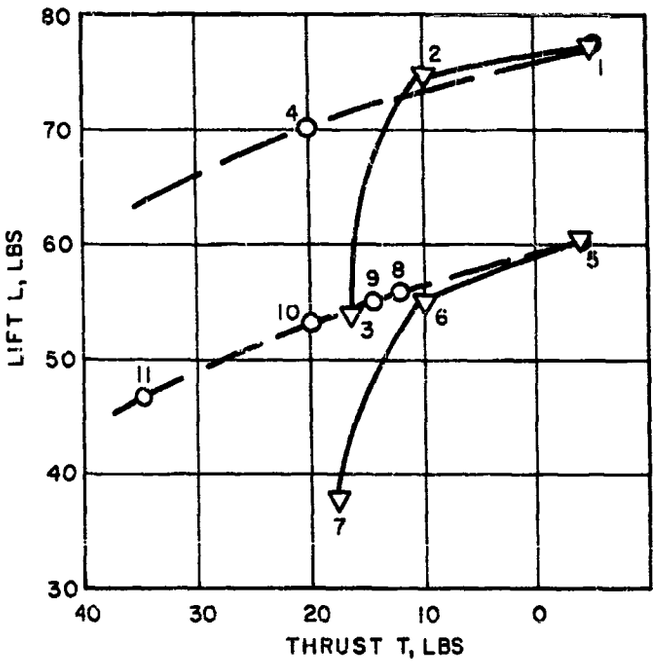

Figure 87. Lift vs. Thrust in Hovering from Doors or Slots

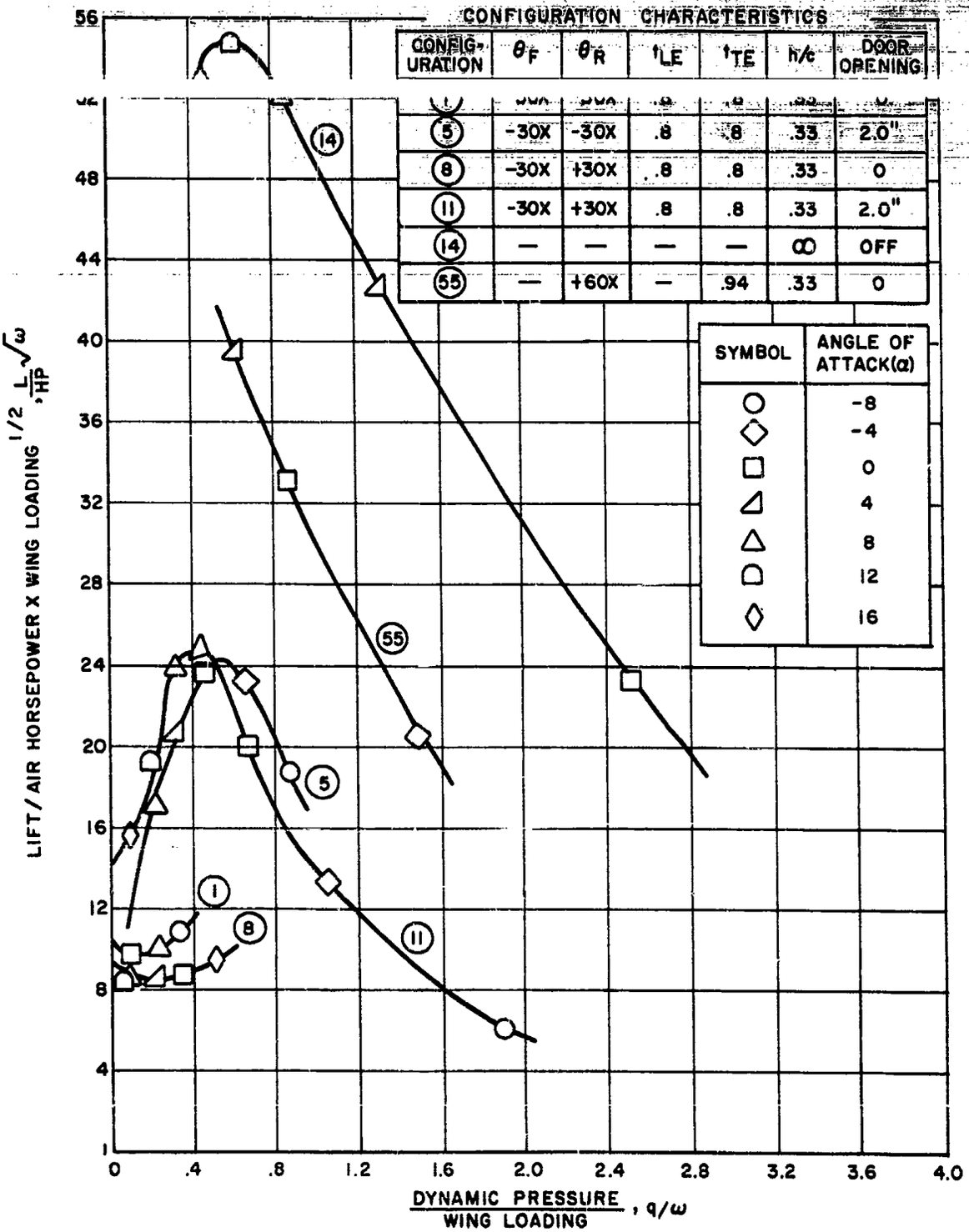

Figure 88. Effect of Slot Angles and Door Opening on Lift Per Air Horsepower in Transition

TECHNICAL PROGRAM (PHASE II)

To conclude Phase II of this report it is necessary to summarize the results of the analyses discussed herein. These analyses have been presented for the specific areas of investigation to determine the best combination of variables to achieve the design objectives. The results obtained are listed below:

1. A ground clearance of h/c = .33 can be obtained.

2. Satisfactory propulsion capabilities for take-off and forward flight can be obtained in the following manner:

   a) Nacelle doors open gradually, eventually converting to a ducted fan configuration in forward flight.

   b) The nacelle propulsion is better than aft angled wing slots and greatly reduces the mechanical complexity of the GETOL control system.

3. Internal flow losses were reduced to 20 to 30 percent by careful internal design.

4. In spite of the many design concessions forced by the GETOL system, L/D ratios indicated by tunnel tests promise a satisfactory airplane configuration.

5. STOL capability, based upon projected data, is acceptable.

6. Presently available data from this investigation indicates that the jet boundary layer on the ground has negligible effect on the wind tunnel data.

7. Inherent static stability and control in hovering appears marginal, but tests of a "T" shaped planform promise a satisfactory fix.

8. The relatively low lift per air horsepower of 3.0, obtained from the test data, are the result of poor flow distribution. It is thought that if flow distribution is improved that lift per air horsepower would also improve.

9. Compilation of broad GETOL data assembled in Volumes I and II represent basic GETOL knowledge which should be considered in itself as one of the most important results of this program.

From this summarization, it is evident that an aircraft of relative simplicity can be constructed to meet the design objectives. Two problem areas were indicated but they can possibly be solved by further development testing. These conclusions have thus indicated that the GETOL CONCEPT IS FEASIBLE.

TECHNICAL PROGRAM (PHASE III)

Phase III Recommended Program for the Construction of the Flight Research Vehicle (FRV)

General

The feasibility of Ground Effect Take-Off and Landing (GETOL) Aircraft has been proven by the completion of the test work and analyses presented in Volume I and Volume II of this report. In cooperation with Army and NASA personnel, studies by the Vertol Division of The Boeing Company have indicated the desirability of developing a Flight Research Vehicle (FRV) of this type for the evaluation of military applications.

Extensive engineering experience gained from the Integrated Study Program may be readily applied to the FRV. For example, important design parameters (Height to Chord Ratio, slot area to wing area ratio and slot angle) are either identical or very similar to those tested on the Boeing-Vertol wind tunnel model.

The basic features of the Flight Research Vehicle (FRV) are described in Phase III and shown in Figure 89. In addition, a discussion of the detail design is presented which also incorporates a recommended program to achieve the construction of a GETOL type aircraft. A weight and performance statement for this recommended vehicle is also shown in Table XII.

Major Design Features

The following items summarize the major design features of the Boeing-Vertol Ground Effect Take-Off and Landing Flight Research Vehicle (FRV):

1. Fuselage of monocoque construction.
2. Two interconnected, opposite rotating fixed pitch fans with variable pitch inlet guide vanes.
3. One (1) YT55-L-5 shaft turbine engine.
4. Two thousand (2,000) lb. fuel capacity.
5. Dual cockpit controls which operate in conventional sense for all regimes of flight.
6. Semi span external ailerons.
7. Slot flow nacelle door control for hover and transition control.

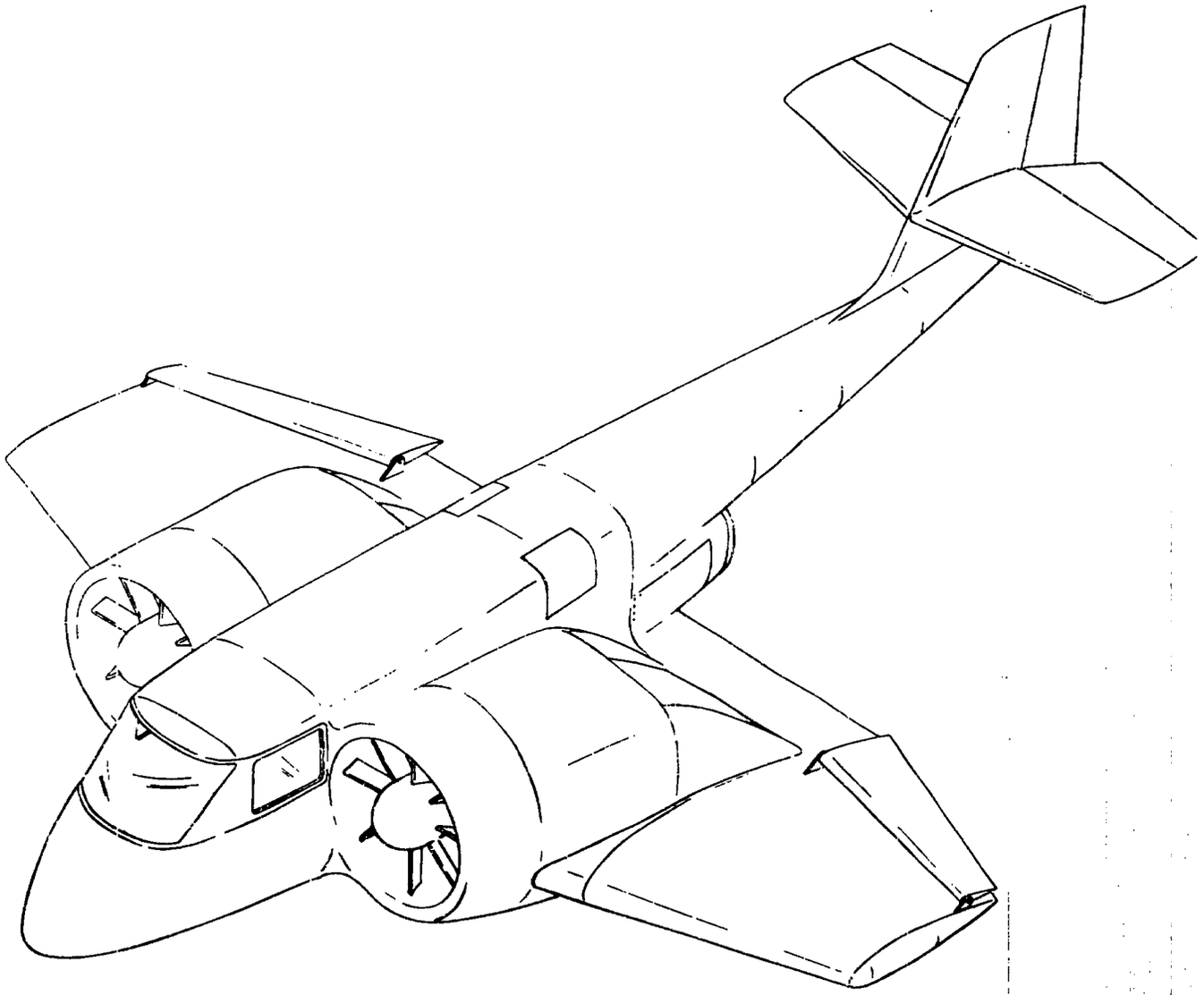

Figure 89. Isometric Sketch - GETOL Flight Research Vehicle (FRV)

TABLE XII

WEIGHT AND PERFORMANCE STATEMENT

Gross Weight, Std. Day, SL	8000 lb
Weight Empty	5167 lb
Fixed Useful Load	433 lb
Payload	400 lb
Span	32.00 ft
Length	42.75 ft
Height	14.00 ft
Wheel Thread	15.67 ft
Wheel Base	9.50 ft
Power Plant	1 Lycoming YT55-L-5
Fan Diameter	5.00 ft
Hub Diameter	2.00 ft
Blade Chord Root	.94 ft
Blade Chord Tip	.92 ft
Solidity Root	.600
Solidity Tip	.212
Disc Loading	
Wing Loading	26 lb/sq ft
Wing Area	307 sq ft
PERFORMANCE	
Sea Level, Standard Day	
Vmax (MIL)	260 mph
Vmax (NRP)	248 mph
h	3 ft
Take-Off Distance	500 ft over 50 ft obstacle
Endurance	1.5 hrs

TECHNICAL PROGRAM (PHASE III)

Aircraft Description

The Boeing-Vertol Model 129 is a twin fan hollow wing Ground Effect Take-Off and Landing Flight Research Vehicle powered by one Lycoming YT55-L-5 engine (see Figures 90 and 91). This engine has a military rating of 1970 shaft horsepower.

Fans

Two four-bladed fixed pitch fans are mechanically interconnected by drive shafting in the aft section of the nacelles and fuselage. This shafting is unloaded and has quick disconnect clutches. In front of each fan are the seven blade, variable pitch inlet guide vanes.

Nacelles

The two nacelles are an integral part of the fuselage that enclose the fans. At the aft end is a movable door to control the flow of air required for propulsion in transition and forward flight.

Fuselage

The fuselage, of semimonocoque stressed skin construction, has a single tail boom. A cabin, 52 inches wide, 54 inches high and 127 inches long provides adequate seating for six (four passengers, pilot and copilot) or for two (pilot and copilot) with a cargo area.

Wing Assembly

The wing is constructed in two pieces, the upper surface which is the main structure and the lower surface. Lower surface attachment to the upper surface is accomplished at the peripheral slot on the lower surface of the wing. A sandwich type honeycomb construction is used.

Ground Handling Wheels

A semi-submerged tricycle gear, incorporating a swiveling nose wheel, is provided for ground handling.

Controls

Dual controls for pilot and copilot are provided as shown in Figure 92.

Hover control is achieved by choking or closing the slots around the periphery to obtain pitch and roll. The outboard leading edge slot angles are varied in conjunction with choking for yaw.

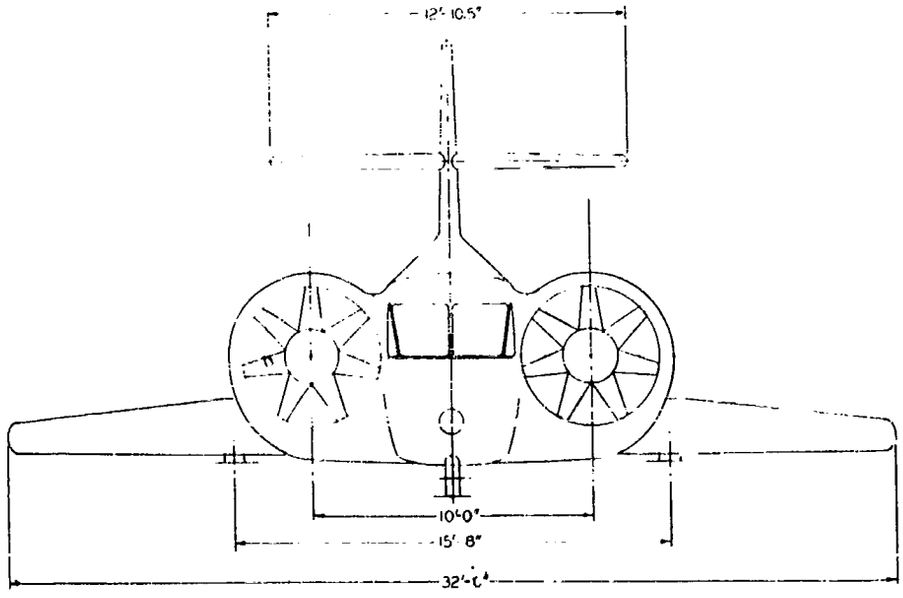
12'-10.5"
10'-0"
15' 8"
32'-0"

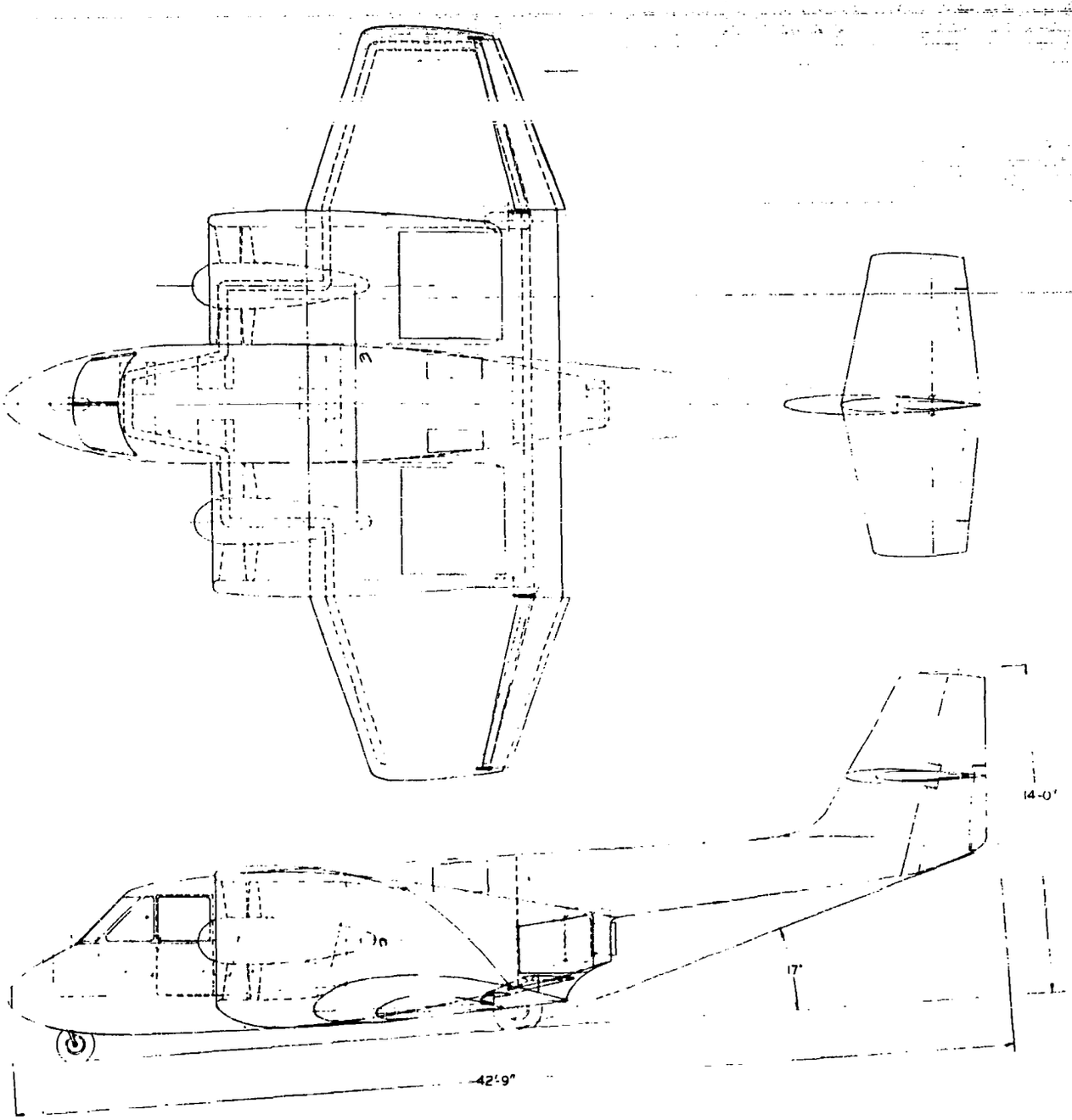

Figure 90. General Arrangement - GETOL Flight Research Vehicle (FRV) - Drawing No. SK11667

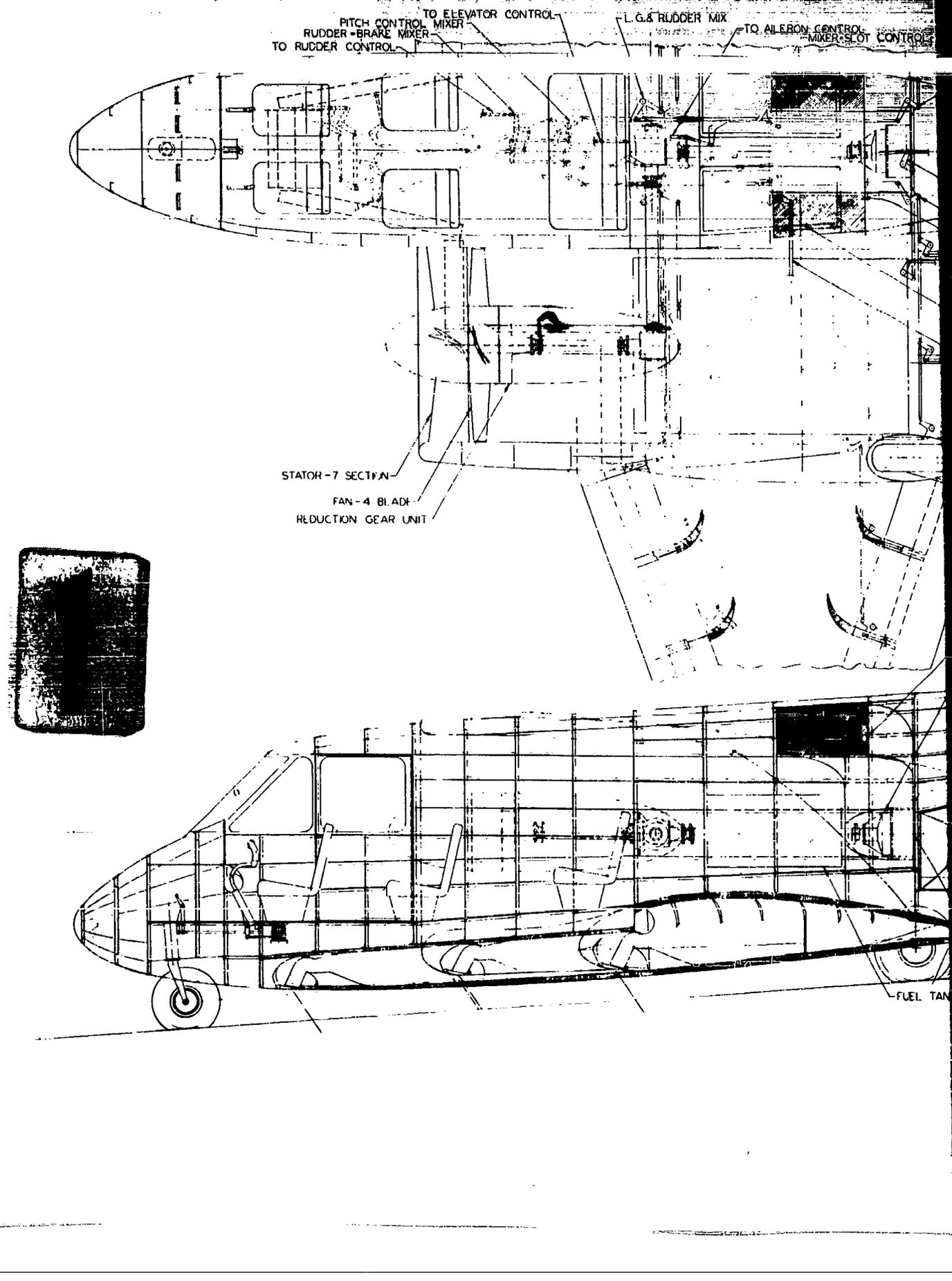
TO ELEVATOR CONTROL
PITCH CONTROL MIXER
RUDDER - BRAKE MIXER
TO RUDDER CONTROL
L.G. & RUDDER MIX
TO AILERON CONTROL
MIXER - SLOT CONTROL
STATOR - 7 SECTION
FAN - 4 BLADE
REDUCTION GEAR UNIT
FUEL TAN

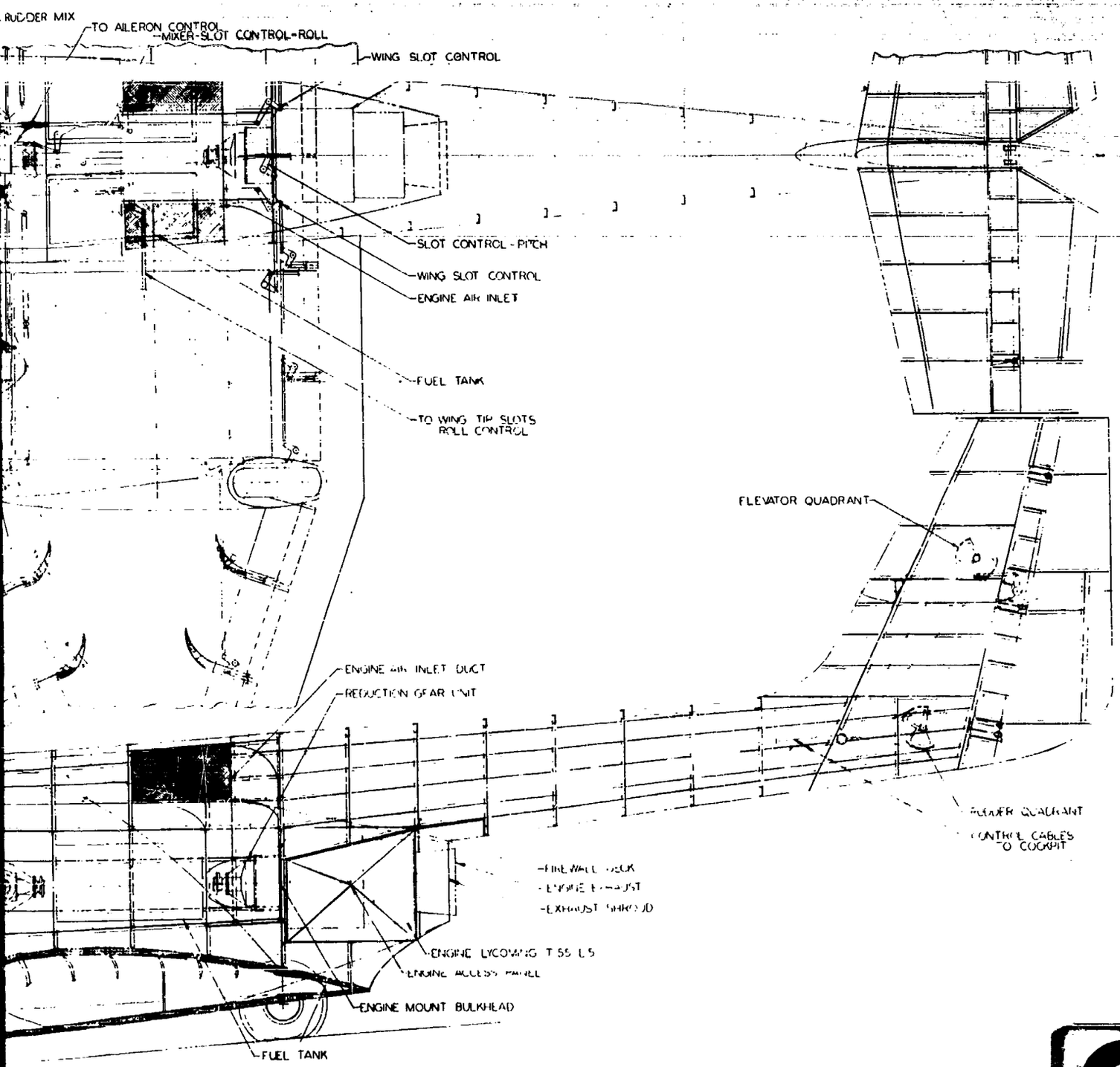

Figure 91. Inboard Profile - GETOL Flight Research Vehicle (FRV) - Drawing No. SK11668

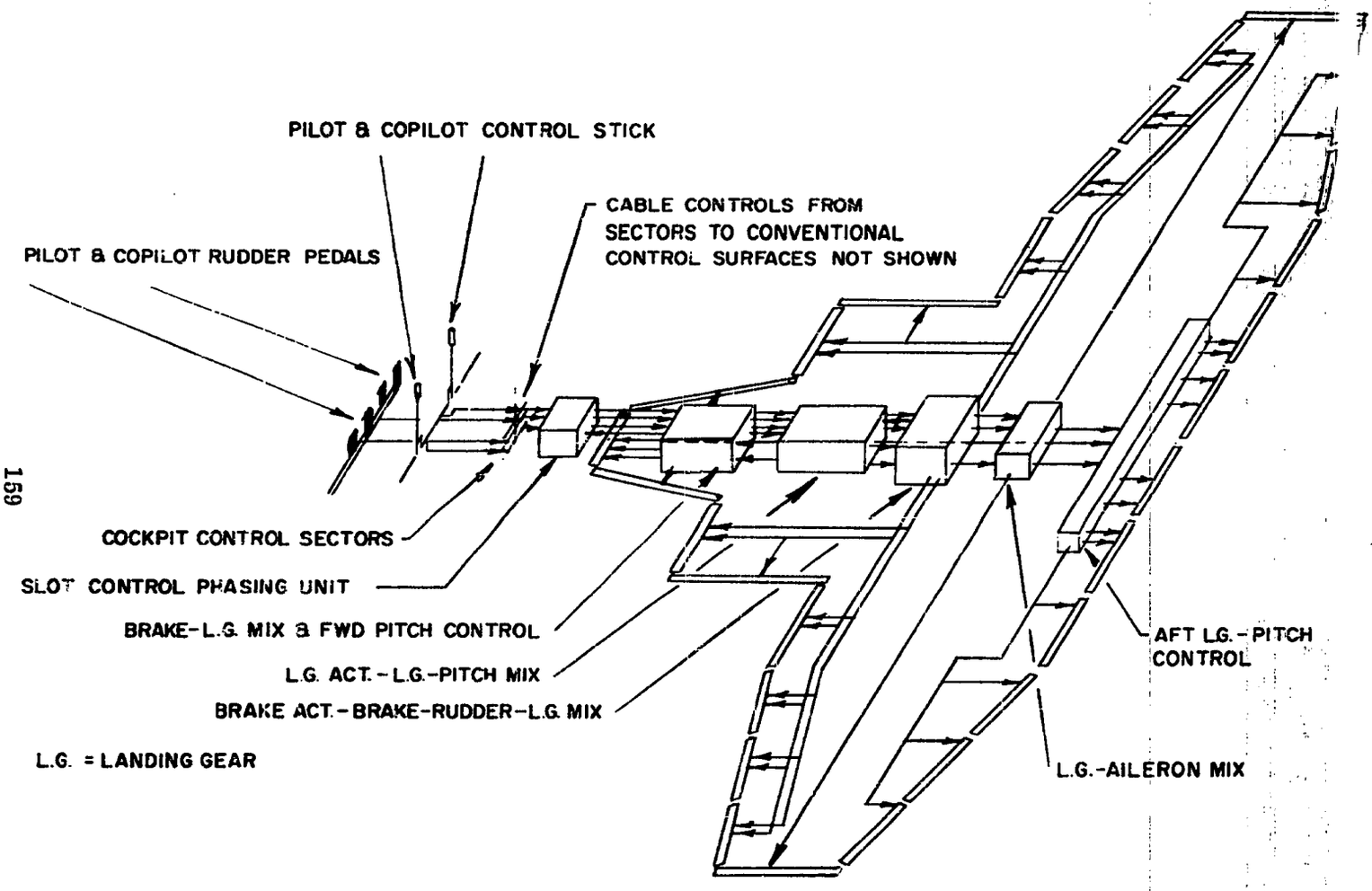

Figure 92. Slot Control Diagram - GETOL Flight Research Vehicle (FRV) - Drawing No. SK11669

During transition, control is achieved primarily through control vanes in the fan exit along with the aerodynamic controls used in forward flight. In the airplane flight regime the stabilizer provides pitch control, external ailerons provide roll control and the rudder provides yaw control.

Phasing of the control system is performed by a mechanical system which engages slot control to normal flight control.

Detailed Design

Aerodynamics

Performance: Drag Estimate - A component drag evaluation for the Ground Effect Take-Off and Landing (GETOL) Aircraft is shown below in tabular form for the cruise condition. From analyses of the drag of ducts, shrouds and "ring wings", an estimate of the effect of the ducts used in this configuration on drag has been incorporated. For the other more conventional components such as wing tail and fuselage, the drag was evaluated using a skin-friction wetted area coefficient modified for variation from non-optimum shape, surface irregularities and gaps. To provide a conservative analysis, these values were increased by an additional 20% as an interference.

ITEM	EQUIVALENT FLAT PLATE AREA
Fuselage	1.28
Ducts	1.60
Spinners	.22
Duct Struts	.16
Wing	1.99
Tail Boom	.40
Vertical Tail	.27
Horizontal Tail	.45
Interference	1.28
Total	7.65

From analyses of the wind tunnel data, summarized in Phase II of this report, the overall efficiency of the Boeing-Vertol wind tunnel model was marginal. Based upon these test results, it was evident that the performance was greatly affected by the poor distribution across and around the peripheral slot and the lack of directional control of this flow from the slot. In Phase II, it was shown that the losses from the fan to the slot were low, thus indicating that the losses were incurred in the slot.

It is believed that in the FRV these problems can be minimized by the use of vanes in the slot to obtain better flow direction and by improving slot shape to obtain better distribution. From other Vertol investigations, it was estimated that the overall efficiency could be improved from 33% (wind tunnel test data) to 70%. Gains due to this improvement in overall efficiency are shown in Figure 93 by the presentation of horsepower per square foot of wing area variation with jet slot velocity as obtained from wind tunnel tests and estimated for the FRV.

From the drag estimation of an aircraft of the FRV gross weight class and assuming optimum wing loading, the power required in forward flight was determined for several gross weights and selected speeds of flight (lower limits in Figure 94). It can also be seen from Figure 94 that a deviation of 50% from the optimum wing loading (upper limits of cross hatched area, Figure 94) results in a very small change in the power required in forward flight. This increase in wing area leads to a much higher hovering lift per horsepower at a given height from the ground. In this way a much better balance between power required in forward flight and that needed to obtain a three foot hovering height can be achieved. In order to better check this relationship, an analysis of the hover height attainable with the power installed was performed. The result of this analysis is shown in Figure 95 and indicates that the design objective of maximum velocity of 250 mph and a hover height of 3 feet are attainable. This conclusion is reached not only on the basis of the improved performance based on the NASA tests of the Boeing-Vertol wind tunnel model but also on Princeton data (Reference 6) and David Taylor Model Basin data (Reference 4 and 5). Figure 95 shows the hover height as calculated from the Princeton data and from the original Chaplin report (Reference 4). From further test work at David Taylor Model Basin, it was found that an assumption used in Reference 4 was incorrect and was revised in Reference 5. Figure 95, which includes this correction (broken line) as well as Princeton data, still gives better hovering height than those indicated by the "improved" vertol curve. On this basis, it may be assumed that hovering heights given by the improved curve should be attainable.

Investigation of the transition regime, in Phase II of this report, indicate that proper sequencing of the aft nacelle door with fixed slot angles is the best method to proceed from hover to forward flight. For the Flight Research Vehicle (FRV), a take-off analysis was performed with this transition schedule and it indicated that a take-off distance of 500 ft over a 50 ft barrier could be obtained.

Shown in Figure 96 is the power polar for the GETOL Flight Research Vehicle including the estimated improved performance.

These analyses show that the design objectives pertaining to performance of the FRV have been achieved.

Flying Qualities: Flying qualities are tailored to the special needs of each of the operational modes.

Hover — All lift and control are provided by the "T" shaped peripheral slot. Good hover flying qualities demand positive control force and moment producing devices, due to the fact that there isn't any slipstream dynamic pressure to provide forces from conventional surfaces. For safety, reliability and control power, the peripheral jet was selected as the source of control for moments and forces. Itemized below are controls for the various flight regimes:

1. Height Control - Inlet guide vanes
2. Longitudinal Control - Front and rear slot vanes
3. Directional Control - Front and rear slot vanes and front slot angles
4. Lateral Control - Tip slot vanes

Transition — Transition from hover to forward flight or vice versa is controlled primarily by the nacelle door opening and the two position forward slot. This functions as acceleration or deceleration control of forward speed. The important characteristics of this maneuver are as follows:

1. Net lift is derived from both the peripheral slot and the wing lift.
2. Control is partly from the peripheral jet and partly from conventional surfaces.

Control in transition is achieved through a combination of the airplane surfaces and the peripheral jet. The mixing is mechanically interconnected so the airplane surfaces are in operation at all times. Pitch control makes use of the front and rear slot valves plus elevator deflection to achieve the necessary moment. Roll control employs a combination of the tip slot vanes to obtain a differential thrust and external ailerons. Yaw control employs a combination of the front and rear slot vanes and the two position front slot angle with the rudder and external ailerons.

Conventional Flight — The conventional mode of flight is essentially similar to any low subsonic fixed wing aircraft. The principal difference is that no asymmetric power conditions can exist because of the interconnecting shaft.

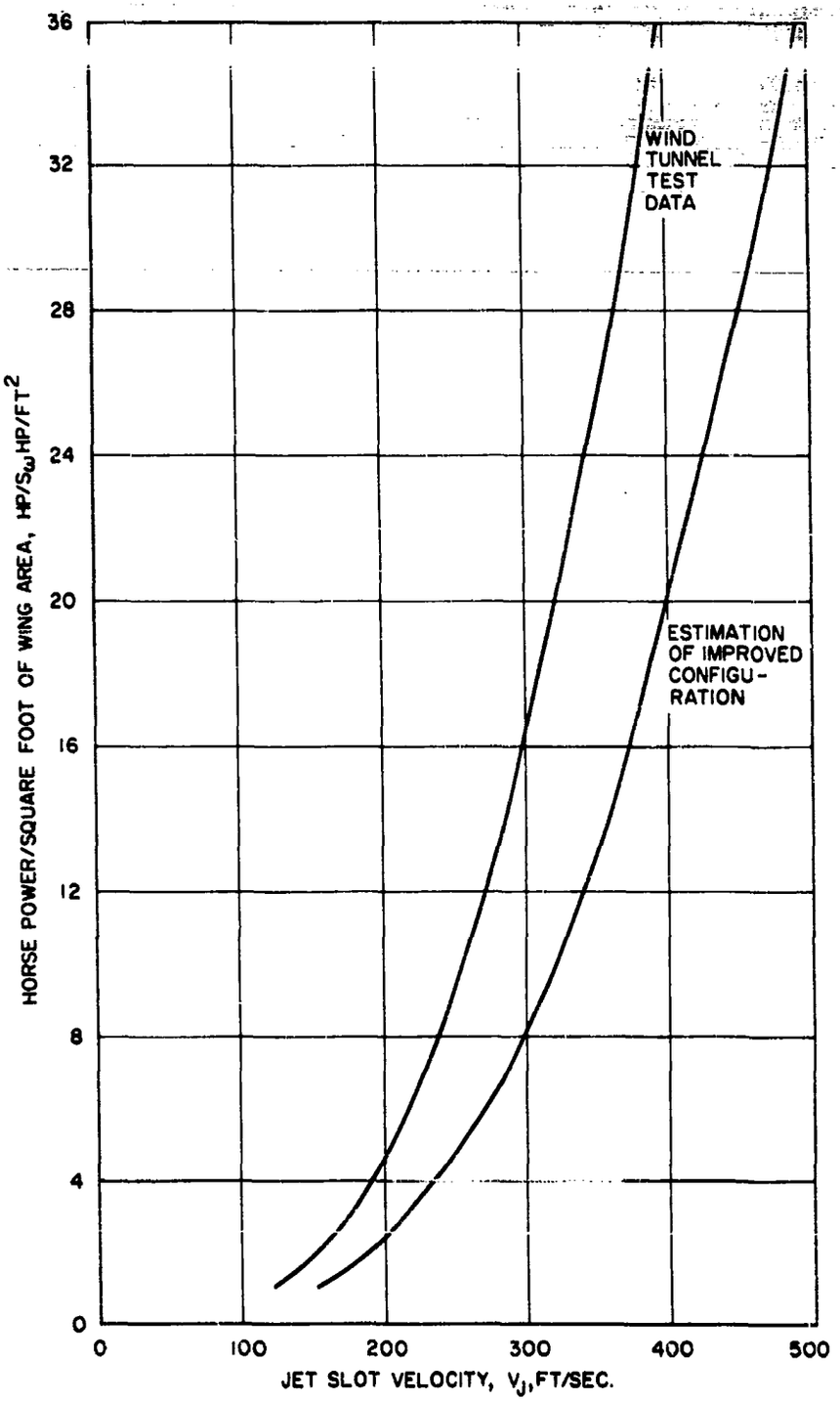

Figure 93. Horsepower Per Square Foot Wing Area vs. Jet Slot Velocity

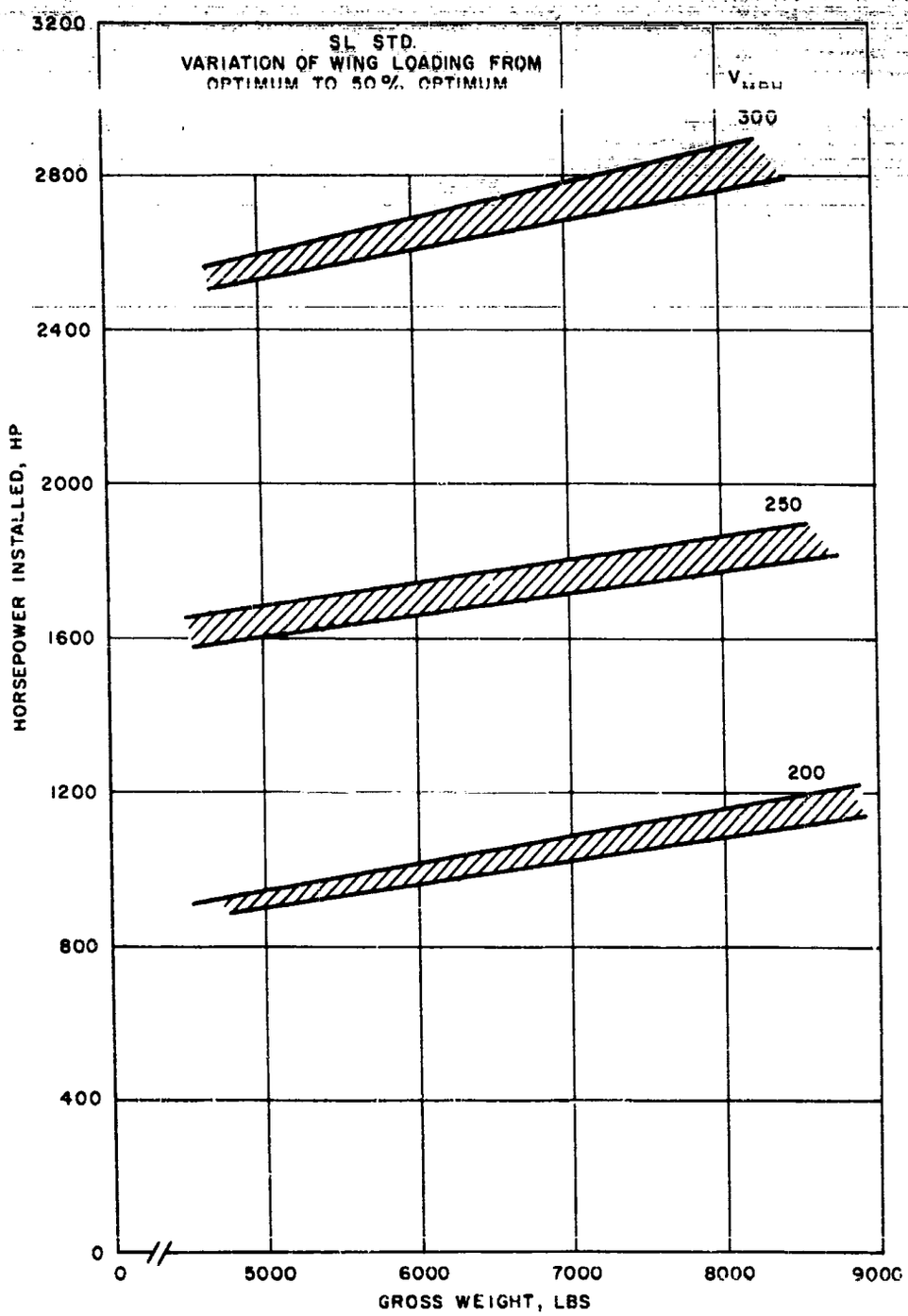

Figure 94. Horsepower Installed vs. Gross Weight

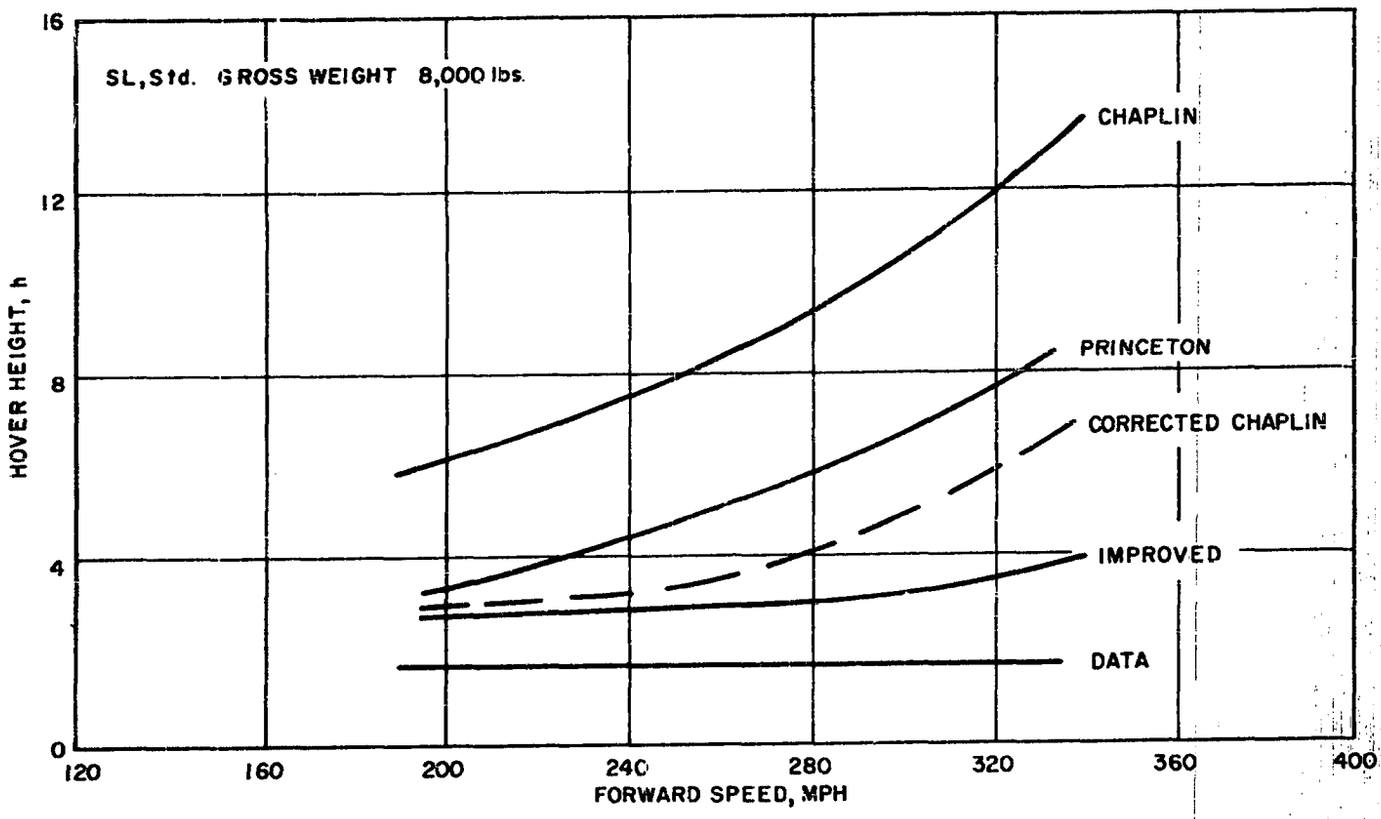

Figure 95. Hover Height vs. Forward Speed

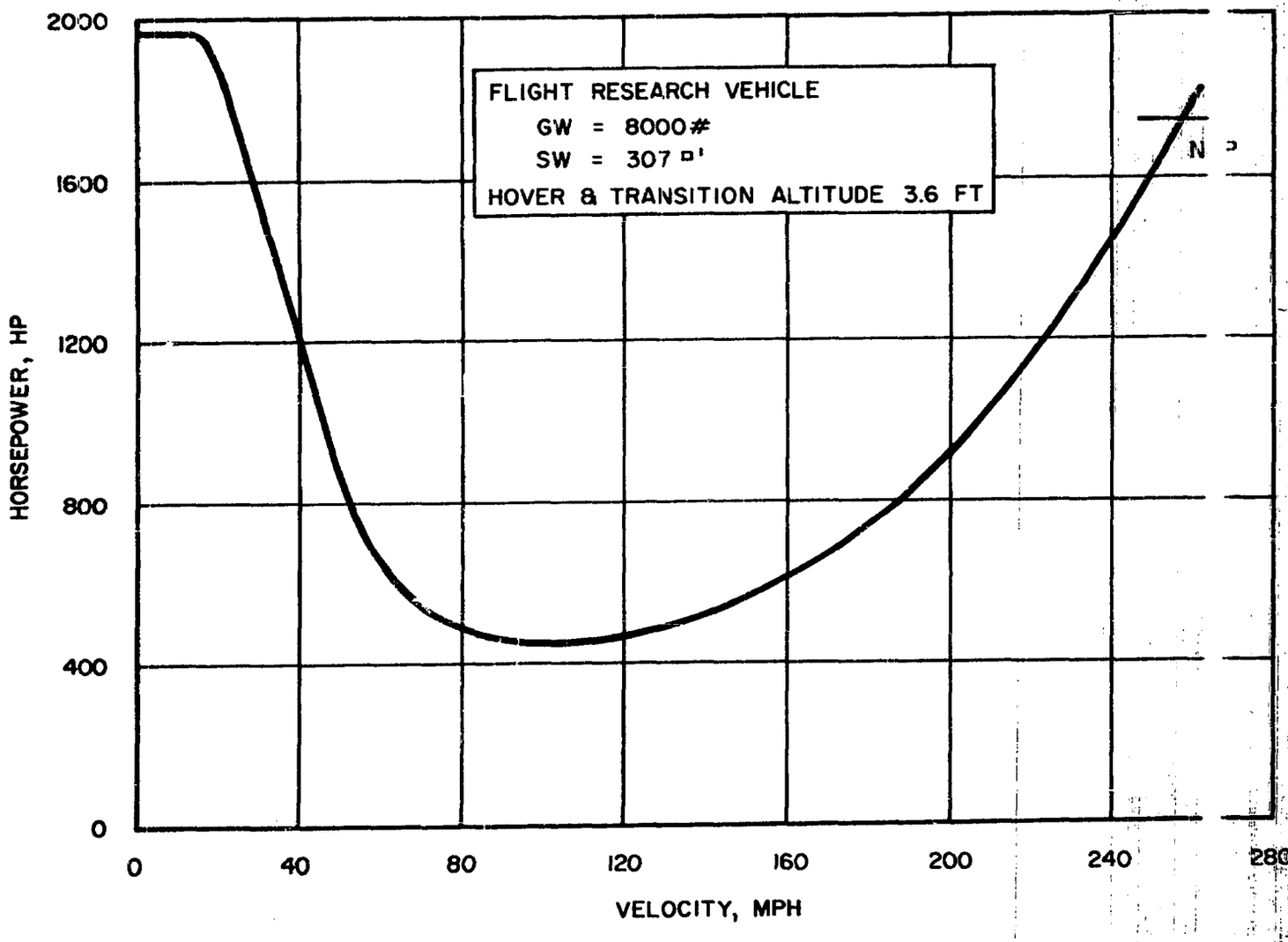

Figure 96. Installed Horsepower vs. Velocity

A summary of the operation of the hover and transition control system is shown in Figure 92 and itemized below:

SLOT CONTROLS

1. "Landing Gear" control opens slots uniformly all around.
2. "Brake" control diverts forward slots forward.
3. Rudder pedals, through phasing unit, divert forward slots in wing differentially, for yaw control.
4. Lateral stick motion closes slots in wing tips differentially, for roll control.
5. Longitudinal stick motion closes slots in fuselage and part of aft slots in wing differentially, for pitch control.
6. "Phasing" engages slot control with normal flight control system when "Landing Gear" is "Down" (Air Cushion operating).

Structural Design Criteria — Model 129

This section contains the Structural Design Criteria for the Boeing-Vertol Ground Effect Take-off and Landing (GETOL) aircraft. The structural criteria is defined in Table XIII to Table XX according to Military Specifications MIL-A-8860 to MIL-A-8870(ASG), MIL-S-8698(ASG) and MIL-F-9490B(USAF). The data contained in this section represents the criteria for the aircraft, fan, drive system, central system and other miscellaneous items.

BASIC AIRCRAFT DATA

Specifications: See References 1-13	
Aircraft Class: See Reference 10	
Basic Flight Design Gross Weight,	W = 8,000 lbs
Minimum Flying Weight,	W_L = 6,240 lbs
Take-off Weight,	$W_{T.O.}$ = 8,000 lbs
Level Flight Maximum Speed,	V_H = 250 mph = 217 kts
Limit Speed,	V_L = 1.4 V_H = 350 mph = 304 kts
Stalling Speed,	V_S = 70 mph = 61 kts
Military Power,	1970 SHP at 14,550 RPM
Normal Rated Power,	1740 SHP at 13,930 RPM
Aspect Ratio,	AR = 3.5
Wing Loading,	W/S = 26 lb/FT^2
Wing Section,	NACA 4418
Wing Span,	32.0 FT = 384 inches

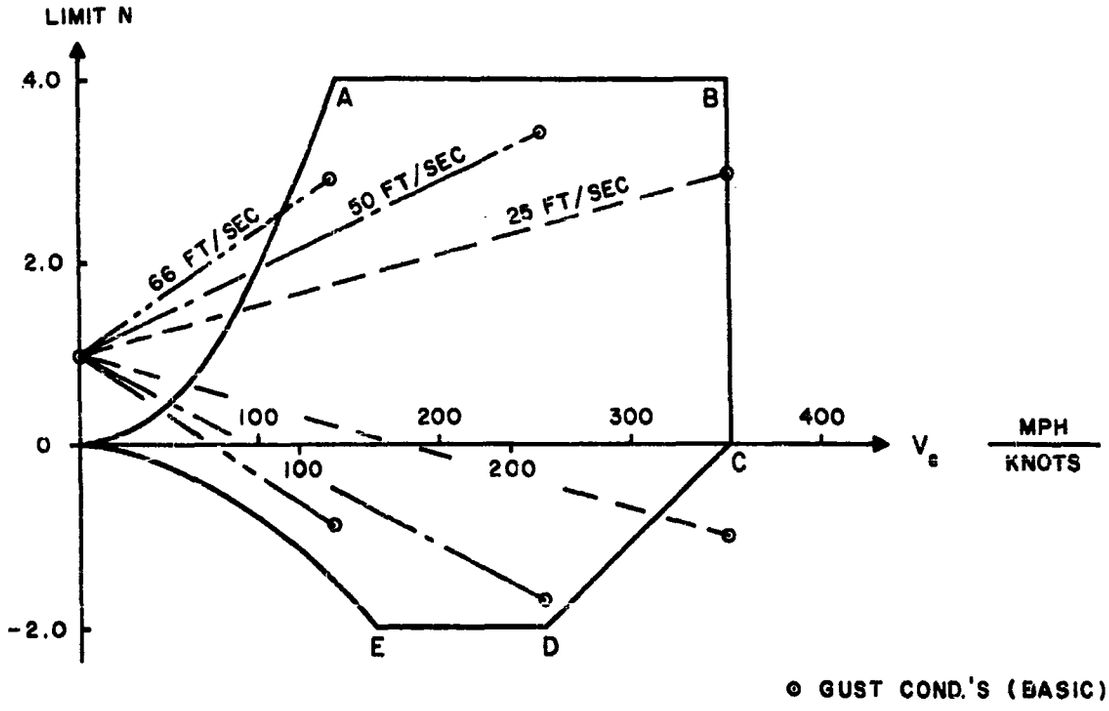

Figure 97. Symmetrical Flight V-n Diagram Limit

Fan Criteria: The loading conditions described in this criteria are in accordance with the requirements of MIL-S-8698 and MIL-A-8860 through MIL-A8870. The loading conditions for analysis of the fan are divided into the following four general groups:

1. Limit Maneuver Conditions - Conditions which provide the maximum inflight loadings on the fan, resulting from maneuver and gust loadings, are specified in Table XIII

2. Limit Gust Conditions

3. Fatigue Loading Schedule - Table XIV represents the design fatigue loading for the fan. Cumulative damage analysis will be performed using the Basic Fatigue Loading Schedule shown in Table XIV. All components shall be designed for a minimum of service life of 2500 hours. Bearings used in the fan shall be designed for a minimum service life of 1200 hours.

4. Special Conditions - Starting Torque represents the application of a starting shock torque applied to the blades while at rest (1.5 times the maximum torque resulting from the following starting procedure). With the free turbines at ground idle, the fans are brought up to idle speed. The throttle is then advanced to flight position accelerating the fans to normal RPM (N_n).

Drive System Criteria: Each element of the drive system shall be designed for the following loading conditions.

1. Fifty five (55) percent of design maximum power (1970 HP @14,430 RPM) to either fan in combination with the most critical fan shaft loads.

2. A limit load factor of 1.5 is applied to the torque load.

All drive system components except bearings shall be designed for a minimum service life of 2500 hours under the Basic Fatigue Loading Schedule of Table XIV. Bearings shall be designed for a minimum service life of 1200 hours. The following criteria, supplementing the Basic Fatigue Loading Schedule shown in Table XIV, shall apply in the design of the indicated components.

1. Transmissions and Intermediate Shafting (Exclusive of Gear Teeth and Bearings) - The cyclic torque in unaccelerated flight conditions shall be ±15% of steady power torque. In addition, these components shall be designed for unrestricted fatigue life at normal rated power (1,740 HP @ 13,930 RPM).

2. Propeller Shafts and Supports - Cyclic Torque is as specified in Item 2 of paragraph 1 of this criteria.

3 Bearings - Design of bearings for 1200 hours B-10 service life between overhauls shall be with considerations of a 60-40 distribution between fans at the basic design gross weight and the Basic Fatigue Loading Schedule of Table XIV.

4. Gear Teeth - In lieu of the Basic Fatigue Loading Schedule of Table XIV gear teeth shall be designed for unrestricted fatigue life under normal rated power (1,740 HP at 13,930 RPM), with 55% of power to either rotor.

Note:

Secondary loads arising from deflections and misalignments shall be considered for both limit and fatigue conditions

Miscellaneous Criteria: Crash loads - All items of which detachment might cause injury to crew or passengers shall be designed for the following ultimate load factors:

1. Eight (8) g Downward
2. Eight (8) g Forward
3. Eight (8) g Sideward

The load factors shall act separately.

In addition, the engines, transmission, and fuel tanks, as well as their supporting structures, will be designed to load factors of 20 g down, 20 g forward and 10 g side.

Crew Seats

The crew seats shall be designed for the following independent loading conditions (seats shall be at top limit of vertical adjustment either with normal seating angle or 15° aft tilt)

1. Down Load - A down load of 1,920 lbs. ultimate uniformly distributed over and normal to seat bottom.
2. Back Load - An aft. load of 1,000 lbs. ultimate uniformly distributed over and normal to the seat back.
3. Side Load - A side load of 1,920 lbs. ultimate applied at the crew members center of gravity and resisted by the safety belt, the shoulder harness and the seat structure.
4. Harness and Belt Loads - A load of 1180 lbs. ultimate applied to the lap belt mountings (equally distributed between the two) on the side of the seat in a direction forward and inclined 40 degrees up from the seat bottom. An ultimate load of 740 lbs. applied to the shoulder harness take-up mechanism in a forward direction parallel to seat bottom shall be applied simultaneously with the belt load.
5. Seat Attachment and Support Loads - Independently applied ultimate load factors of 8 g down, 8 g forward, 8 g lateral. The combined weight of the man, seat, and equipment shall be taken as 240 lbs.
6. Front Edge Load - A vertical load of 400 lbs. ultimate applied to the front edge of the seat bottom over a length extending 1-1/2 inches to each side of the center of the seat.

REFERENCE: MIL-A-8861 (ASG)

REF. PAR.	COND. NO.	CONDITIONS	FWD SPEED (EAS)	POWER SETTINGS	LOAD FACTOR			ANGULAR VELOCITY			ANGULAR ACC.			WING LOAD DISTRIBUTION %	HORIZONTAL TAIL		V
					VERT.	LAT.	LONG.	PITCH RAD/ SEC	ROLL RAD/ SEC	YAW RAD/ SEC	PITCH RAD/ SEC^2	ROLL RAD/ SEC^2	YAW RAD/ SEC^2		LOAD	LOAD % DISTRIB.	L
SYMMETRICAL FLIGHT CONDITIONS (BASIC CONFIGURATION)																	
3.2.1	1	POSITIVE LOAD FACTOR	ALL SPEEDS UP TO V_L	0-MILITARY RATED POWER	(1) n=4.0 max	0	AS CALC	$\dot{\Omega}_V$	0	0	0	0	0	50-50	NOTE (2)	(11) 50-50	
3.2.1	2	NEGATIVE LOAD FACTOR	ALL SPEEDS UP TO V_H	0-MILITARY RATED POWER	(1) n=-1.0 min	0	AS CALC	$\dot{\Omega}_V$	0	0	0	0	0	50-50	NOTE (2)	(11) 50-50	
3.2.2.2	3	MANEUVER-SPECIFIED CONTROL DISPLACEMENT	ALL SPEEDS UP TO V_L	0-MILITARY RATED POWER	(1)	0	AS CALC	AS CALC (10)	0	0	AS CALC (10)	0	0	50-50	AS CALC (10)	(11) 50-50	
3.5	4	GUST-66 FT/SEC - UP	V_G	0-MILITARY RATED POWER	AS CALC (6)	0	AS CALC	0	0	0	AS CALC (3)	0	0	50-50	AS CALC (6)	(11) 50-50	
3.5	5	GUST-66 FT/SEC - DN	V_G	0-MILITARY RATED POWER	AS CALC (6)	0	AS CALC	0	0	0	AS CALC (3)	0	0	50-50	AS CALC (6)	(11) 50-50	
3.5	6	GUST-50 FT/SEC - UP	V_H	0-MILITARY RATED POWER	AS CALC (6)	0	AS CALC	0	0	0	AS CALC (3)	0	0	50-50	AS CALC (6)	(11) 50-50	
3.5	7	GUST-50 FT/SEC - DN	V_H	0-MILITARY RATED POWER	AS CALC (6)	0	AS CALC	0	0	0	AS CALC (3)	0	0	50-50	AS CALC (6)	(11) 50-50	
3.5	8	GUST-25 FT/SEC - UP	V_L	0-MILITARY RATED POWER	AS CALC (6)	0	AS CALC	0	0	0	AS CALC (3)	0	0	50-50	AS CALC (6)	(11) 50-50	
3.5	9	GUST-25 FT/SEC - DN	V_L	0-MILITARY RATED POWER	AS CALC (6)	0	AS CALC	0	0	0	AS CALC (3)	0	0	50-50	AS CALC (6)	(11) 50-50	
SYMMETRICAL FLIGHT CONDITIONS (LANDING APPROACH CONFIGURATION)																	
3.2.3	10	LANDING BALANCED PULL-OUT	$V_{L_{JF}}$ (12)	0-MILITARY RATED POWER	0~2.0	0	AS CALC	$\dot{\Omega}_V$	0	0	0	0	0	50-50	(2)	(11) 50-50	
3.2.3	11	LANDING PULL-OUT SPECIFIED CONT. DISPL.	$V_{L_{JF}}$ (12)	0-MILITARY RATED POWER	0~2.0	0	AS CALC	AS CALC (10)	0	0	AS CALC (10)	0	0	50-50	AS CALC (10)	(11) 50-50	
3.5	12	GUST-50 FT/SEC - UP	ALL SPEEDS TO $V_{L_{JF}}$ (12)	0-MILITARY RATED POWER	AS CALC (6)	0	AS CALC	0	0	0	AS CALC (3)	0	0	50-50	AS CALC (6)	(11) 50-50	
3.5	13	GUST-50 FT/SEC - DN	ALL SPEEDS TO $V_{L_{JF}}$ (12)	0-MILITARY RATED POWER	AS CALC (6)	0	AS CALC	0	0	0	AS CALC (3)	0	0	50-50	AS CALC (6)	(11) 50-50	
UNSYMMETRICAL FLIGHT CONDITIONS (BASIC CONFIGURATION)																	
3.3.1(a) 3.3.1.1	14	ROLLING PULL-OUT ACCELERATED ROLL	ALL SPEEDS TO V_L	0-MILITARY RATED POWER	1.0 to .8n	AS CALC (10)	AS CALC (10)	AS CALC (10)	AS CALC (10)	AS CALC (10)	AS CALC (10)	AS CALC (10)	AS CALC (10)	AS CALC (10)	AS CALC (10)	AS CALC (10)	
3.3.1(b) 3.3.1.1	15	ROLLING PULL-OUT ACCELERATED ROLL	ALL SPEEDS TO V_L	0-MILITARY RATED POWER	1.0 to .8n	AS CALC (10)	AS CALC (10)	AS CALC (10)	AS CALC (10)	AS CALC (10)	AS CALC (10)	AS CALC (10)	AS CALC (10)	AS CALC (10)	AS CALC (10)	AS CALC (10)	
3.3.3.1	16	UNSYMMETRICAL THRUST ZERO SIDESLIP	V_H ONE FAN OUT	TAKE OFF POWER	1.0	AS CALC	AS CALC	0	0	0	0	0	0	50-50	AS CALC (4)	50-50	
3.3.3.2(a)	17	FAN FAILURE NEUTRAL RUDDER	(13)	(13)	1.0	AS CALC	AS CALC	0	0	AS CALC	0	0	AS CALC	50-50	AS CALC (4)	50-50	
3.3.3.2(b)	18	FAN FAILURE RUDDER DEFL.	(13)	(13)	1.0	AS CALC (10)	AS CALC (10)	0	0	AS CALC (10)	0	0	AS CALC (10)	50-50	AS CALC (4)	50-50	

WING LOAD DISTRIBUTION %	HORIZONTAL TAIL LOAD	HORIZONTAL TAIL LOAD % DISTRIB.	VERTICAL TAIL LOAD	VERTICAL TAIL LOAD % DISTRIB.	REF. PAR.	COND. NO.	CONDITIONS	FWD SPEED (EAS)	POWER SETTINGS	LOAD FACTOR VERT.	LOAD FACTOR LAT.	LOAD FACTOR LONG.	ANGULAR VELOCITY PITCH RAD/SEC	ANGULAR VELOCITY ROLL RAD/SEC	ANGULAR VELOCITY YAW RAD/SEC	ANGULAR ACC. PITCH RAD/SEC^2	ANGULAR ACC. ROLL RAD/SEC^2	ANGULAR ACC. YAW RAD/SEC^2	WING LOAD DISTRIBUTION %	HORIZ LOAD
UNSYMMETRICAL FLIGHT CONDITIONS (BASIC CONFIGURATION)																				
50-50	NOTE (2)	(11) 50-50	0	-	3.3.3.3	19	STEADY SIDESLIP	ALL SPEEDS TO V_L	0-MILITARY RATED POWER	1.0	AS CALC	AS CALC	0	0	0	0	0	0	50-50	AS CALC (4)
50-50	NOTE (2)	(11) 50-50	0	-	3.3.3.4	20	LOW SPEED RUDDER KICK	ALL SPEEDS TO 0.6 V_H	0-MILITARY RATED POWER	1.0	AS CALC (10)	AS CALC (10)	0	0	AS CALC (10)	0	0	AS CALC (10)	50-50	AS CALC (4)
50-50	AS CALC (10)	(11) 50-50	0	-	3.3.3.5	21	HIGH SPEED RUDDER KICK	ALL SPEEDS TO V_H	0-MILITARY RATED POWER	1.0	AS CALC (10)	AS CALC (10)	0	0	AS CALC (10)	0	0	AS CALC (10)	AS CALC (10)	AS CALC (4)
50-50	AS CALC (6)	(11) 50-50	0	-	3.3.3.7	22	ONE-FAN-OUT OPERATION	(14)	NORMAL RATED POWER	2.25	AS CALC	AS CALC	Ω_R/V	0	0	0	0	0	50-50	AS CALC (2)
50-50	AS CALC (6)	(11) 50-50	0	-	3.6	23	HORIZONTAL GUST 66 FT/SEC	V_G	0-MILITARY RATED POWER	1.0	AS CALC (6)	AS CALC	0	0	0	0	0	AS CALC (3)	50-50	AS CALC (4)
50-50	AS CALC (6)	(11) 50-50	0	-	3.6	24	HORIZONTAL GUST 50 FT/SEC	V_H	0-MILITARY RATED POWER	1.0	AS CALC (6)	AS CALC	0	0	0	0	0	AS CALC (3)	50-50	AS CALC (4)
50-50	AS CALC (6)	(11) 50-50	0	-	3.6	25	HORIZONTAL GUST 25 FT/SEC	V_L	0-MILITARY RATED POWER	1.0	AS CALC (6)	AS CALC	0	0	0	0	0	AS CALC (3)	50-50	AS CALC (4)
50-50	AS CALC (6)	(11) 50-50	0	-	3.6	26	HORIZONTAL GUST-66 FT/SEC STEADY SIDESLIP	V_G	0-MILITARY RATED POWER	1.0	AS CALC (5)	AS CALC	0	0	0	0	0	AS CALC (3)	50-50	AS CALC (4)
50-50	AS CALC (6)	(11) 50-50	0	-	3.6	27	HORIZONTAL GUST-50 FT/SEC STEADY SIDESLIP	V_H	0-MILITARY RATED POWER	1.0	AS CALC (5)	AS CALC	0	0	0	0	0	AS CALC (3)	50-50	AS CALC (4)
					3.6	28	HORIZONTAL GUST-25 FT/SEC STEADY SIDESLIP	V_L	0-MILITARY RATED POWER	1.0	AS CALC (5)	AS CALC	0	0	0	0	0	AS CALC (3)	50-50	AS CALC (4)
UNSYMMETRICAL FLIGHT CONDITIONS (TAKE-OFF AND LANDING APPROACH CONFIGURATION)																				
50-50	(2)	(11) 50-50	0	-	3.3.2	29	ROLL IN TAKE-OFF AND LANDING	$V_{L_{JF}}$ (12)	0-MILITARY RATED POWER	1.0	AS CALC (10)	AS CALC (10)	AS CALC (10)	AS CALC (10)	AS CALC (10)	AS CALC (10)	AS CALC (10)	AS CALC (10)	AS CALC (10)	AS CALC (10)	AS CALC (10)
50-50	AS CALC (10)	(11) 50-50	0	-	3.3.3.1	30	UNSYMMETRICAL THRUST ZERO SIDESLIP	$V_{L_{JF}}$ (12)	TAKE OFF POWER	1.0	AS CALC	AS CALC	0	0	0	0	0	0	50-50	AS CALC (4)
50-50	AS CALC (6)	(11) 50-50	0	-	3.3.3.4	31	LOW SPEED RUDDER KICK	ALL SPEEDS TO $V_{L_{JF}}$	0-MILITARY RATED POWER	1.0	AS CALC (10)	AS CALC (10)	0	0	AS CALC (10)	0	0	AS CALC (10)	50-50	AS CALC (4)
50-50	AS CALC (6)	(11) 50-50	0	-	UNSYMMETRICAL FLIGHT CONDITIONS (LANDING APPROACH CONFIGURATION)															
AS CALC (10)	AS CALC (10)	AS CALC (10)	AS CALC (10)	100	3.6	32	HORIZONTAL GUST 50 FT/SEC	ALL SPEEDS TO $V_{L_{JF}}$	0-MILITARY RATED POWER	1.0	AS CALC (6)	AS CALC	0	0	0	0	0	AS CALC (3)	50-50	AS CALC (4)
AS CALC (10)	AS CALC (10)	AS CALC (10)	AS CALC (10)	100	3.6	33	HORIZONTAL GUST-50 FT/SEC STEADY SIDESLIP	ALL SPEEDS TO $V_{L_{JF}}$	0-MILITARY RATED POWER	1.0	AS CALC (5)	AS CALC	0	0	0	0	0	AS CALC (3)	50-50	AS CALC (4)
50-50	AS CALC (4)	50-50	AS CALC	100																
50-50	AS CALC (4)	50-50	AS CALC	100																
50-50	AS CALC (4)	50-50	AS CALC (10)	100																

TABLE XIII

[illegible]

	FWD SPEED (EAS)	POWER SETTINGS	LOAD FACTOR			ANGULAR VELOCITY			ANGULAR ACC.			WING LOAD DISTRIBUTION %	HORIZONTAL TAIL		VERTICAL TAIL	
			VERT.	LAT.	LONG.	PITCH RAD/ SEC	ROLL RAD/ SEC	YAW RAD/ SEC	PITCH RAD/ SEC^2	ROLL RAD/ SEC^2	YAW RAD/ SEC^2		LOAD	LOAD % DISTRIB.	LOAD	LOAD % DISTRIB.
	UNSYMMETRICAL FLIGHT CONDITIONS (BASIC CONFIGURATION)															
	ALL SPEEDS TO V_L	0-MILITARY RATED POWER	1.0	AS CALC	AS CALC	0	0	0	0	0	0	50-50	AS CALC (4)	50-50	AS CALC	100
	ALL SPEEDS TO 0.6 V_H	0-MILITARY RATED POWER	1.0	AS CALC (10)	AS CALC (10)	0	0	AS CALC (10)	0	0	AS CALC (10)	50-50	AS CALC (4)	50-50	AS CALC (10)	100
	ALL SPEEDS TO V_H	0-MILITARY RATED POWER	1.0	AS CALC (10)	AS CALC (10)	0	0	AS CALC (10)	0	0	AS CALC (10)	AS CALC (10)	AS CALC (4)	50-50	AS CALC (10)	100
	(14)	NORMAL RATED POWER	2.25	AS CALC	AS CALC	$g\alpha/V$	0	0	0	0	0	50-50	AS CALC (3)	50-50	AS CALC	100
	V_G	0-MILITARY RATED POWER	1.0	AS CALC (6)	AS CALC	0	0	0	0	0	AS CALC (3)	50-50	AS CALC (4)	50-50	AS CALC (6)	100
	V_H	0-MILITARY RATED POWER	1.0	AS CALC (6)	AS CALC	0	0	0	0	0	AS CALC (3)	50-50	AS CALC (4)	50-50	AS CALC (6)	100
	V_L	0-MILITARY RATED POWER	1.0	AS CALC (6)	AS CALC	0	0	0	0	0	AS CALC (3)	50-50	AS CALC (4)	50-50	AS CALC (6)	100
/SEC	V_G	0-MILITARY RATED POWER	1.0	AS CALC (5)	AS CALC	0	0	0	0	0	AS CALC (3)	50-50	AS CALC (4)	50-50	AS CALC (7)	100
/SEC	V_H	0-MILITARY RATED POWER	1.0	AS CALC (5)	AS CALC	0	0	0	0	0	AS CALC (3)	50-50	AS CALC (4)	50-50	AS CALC (7)	100
/SEC	V_L	0-MILITARY RATED POWER	1.0	AS CALC (5)	AS CALC	0	0	0	0	0	AS CALC (3)	50-50	AS CALC (4)	50-50	AS CALC (7)	100
	UNSYMMETRICAL FLIGHT CONDITIONS (TAKE-OFF AND LANDING APPROACH CONFIGURATION)															
	$V_{L_{JF}}$ (12)	0-MILITARY RATED POWER	1.0	AS CALC (10)	AS CALC (10)	AS CALC (10)	AS CALC (10)	AS CALC (10)	AS CALC (10)	AS CALC (10)	AS CALC (10)	AS CALC (10)	AS CALC (10)	AS CALC (10)	AS CALC (10)	100
T	$V_{L_{JF}}$ (12)	TAKE OFF POWER	1.0	AS CALC	AS CALC	0	0	0	0	0	0	50-50	AS CALC (4)	50-50	AS CALC	100
	ALL SPEEDS TO $V_{L_{JF}}$	0-MILITARY RATED POWER	1.0	AS CALC (10)	AS CALC (10)	0	0	AS CALC (10)	0	0	AS CALC (10)	50-50	AS CALC (4)	50-50	AS CALC (10)	100
	UNSYMMETRICAL FLIGHT CONDITIONS (LANDING APPROACH CONFIGURATION)															
	ALL SPEEDS TO $V_{L_{JF}}$	0-MILITARY RATED POWER	1.0	AS CALC (5)	AS CALC	0	0	0	0	0	AS CALC (3)	50-50	AS CALC (4)	50-50	AS CALC (6)	100
/SEC	ALL SPEEDS TO $V_{L_{JF}}$	0-MILITARY RATED POWER	1.0	AS CALC (5)	AS CALC	0	0	0	0	0	AS CALC (3)	50-50	AS CALC (4)	50-50	AS CALC (7)	100

Notes - Table XIII

1. Investigate all critical points on and within the V-n diagram. The specified load factor is applicable to weights up to the basic flight design gross weight. At higher gross weights, a constant nW product shall be maintained except that the maximum load factor shall not be less than +2.5 and the minimum load factor algebraically greater than -1.0.
2. The horizontal tail load shall be determined as the balancing tail load necessary for equilibrium of flight loads and an incremental horizontal tail load to overcome the damping effect of the airplane to the pitching velocity ($\omega = g\alpha/V$).
3. The angular acceleration of the airplane shall be such that the product is balances the aerodynamic moment about the airplane C.G. attributed to the gust.
4. The horizontal tail load shall be determined as the balancing tail load necessary for 1g level flight.
5. The airplane lateral load factor shall be that produced by a steady sideslip and a horizontal side gust. The airplane shall be in a wings-level steady sideslip with the most critical fin incidence when a horizontal side gust is encountered.
6. Gust factors shall be as specified in MIL-A-8861(ASG), paragraphs 3.5 and 3.6.
7. The vertical tail load shall be that resulting from the steady sideslip plus the horizontal gust.
8. The altitudes for flight loading conditions, other than take-off and landing approach, shall be the altitude at which the limit speed in KAS is a maximum, the altitude at which the Mach number is a maximum, sea level, and any intermediate altitudes that result in critical loads, sea level shall be used for landing approach and takeoff.
9. The design center of gravity position at each gross weight shall be the actual maximum forward and aft position from all possible distribution of loadings plus a tolerance. The tolerance shall be 1.5% mac or 15% of the distance between the actual most forward or aft values from the complete envelope, whichever is greater.
10. As calculated by airplane equations of motion for the control movement and time specified in MIL-A-8861(ASG). The load factors to be attained shall be all values on and within the V-n diagram.
11. The horizontal tail load distribution shall be as shown and also shall be distributed unsymmetrically. The unsymmetrical distribution shall be obtained by multiplying the airloads on the horizontal tail on one side of the plane of symmetry by (1 + X) and on the other side by (1 - X). The value of X shall be:
    X = .5 for (+ HAA) and for all points representing aerodynamic stall or buffet.
    X = .15 for all other points on V-n diagram.
12. $V_{L_{JF}}$ = Limit speed jet flap. As specified in MIL-A-8860(ASG) for conventional flap.
13. The airspeeds shall be all speeds from the approved one-fan-out minimum takeoff speed to V_H. The critical fan shall suddenly fail. The engine shall deliver normal-rated power or thrust, except that takeoff power or thrust is applicable at speeds up to 2 V_{S_1}. Automatic feathering, decoupling, or thrust-controlling devices shall be operating and alternately not operating. With these devices operating, limit strength is required. With automatic devices not operating, ultimate strength is required.
14. For multifan aircraft, sudden stopping of a fan at all speeds above the approved one-fan-out minimum takeoff speed up to V_H shall not result in unacceptable aircraft motions or vibrations within these specified speed ranges. The limit strength of the airplane shall not be exceeded in a symmetrical pull-out to a load factor of 2.25.

TECHNICAL PROGRAM (PHASE III)

TABLE XIV

BASIC FATIGUE LOADING SCHEDULE

CONDITION	% SERVICE LIFE	
GROUND CONDITION		
Taxiing	.5	
Jump Take-Off	.5	
Fan Starting	.5	
HOVERING	20.0	
FORWARD FLIGHT, POWER ON		11.5
Transition (From Vertical to Fwd Flight)	15.0	
Cruise	20.0	
Maximum Level Flight Speed	10.0	
Maximum Power Climb	6.0	
V_L	.5	71.5
Right and Left Turns	10.0	
SIDEWARD FLIGHT, POWER ON	2.0	
REARWARD FLIGHT, POWER ON	2.0	
MANEUVERS, POWER ON		4.0
Pull-Ups	1.5	
Landing Approach	1.5	
Change to Partial Power Descent	.5	
Yawing	.5	
Steady Descent	4.0	13.0
Partial Power Descent	2.0	
CONTROL REVERSALS AT V_{CRUISE}		
Lateral	1.0	
Longitudinal	1.0	
Directional	1.0	

TABLE XV

LANDING GEAR CRITERIA

REFERENCE: ANC-2, CHAPTER 3 (THREE POINT ATTITUDE)

CONDITION NO.		I	II	III	IV	V	VI
CONDITION		BRAKED ROLL	UNSYMMETRICAL BRAKING	REVERSE BRAKING	TURNING	PIVOTING	MINIMUM LOAD FACTOR AT TAKE OFF
MAIN GEAR REACTION (ONE SIDE)	V_M	(3)	(2)	(2)	LOADS IN ACCORDANCE WITH ANC-2 PARA 7.4	LOADS IN ACCORDANCE WITH ANC-2 PARA 3-4	(6)
	D_M	$.8\ V_M$	$.8\ V_M$ & 0	$-.8\ V_M$			0
	S_N	0	(5)	0			0
AUXILIARY GEAR REACTION	V_A	(3)	(2)	(2)			(6)
	D_A	0	0	0			0
	S_A	0	(5)	0			0

Notes - Table XV

1. Vertical Load Factor at C. G. = 1.2. Aircraft Minimum Flying Weight = 6,240 lbs
2. Vertical Load Factor at C. G. = 1.0. Aircraft Take-Off Weight = 8,000 lbs.
3. Maximum Value of (1) and (2).
4. Pitching Moment Balanced by Wheel Reactions.
5. Yawing Moment Balanced by Wheel Reactions.
6. Vertical Load Factor at C. G. = 2.0. Aircraft Maximum Take Off Weight = 8,000 lbs.
7. Drag and Side Loads Act At Ground Level.

HANDLING CRITERIA - TOWING LIMIT LOADS

TOW POINT		LOAD MAGNITUDE	LOAD DIRECTION	BALANCING FORCE
AT EACH MAIN GEAR		$0.75F_{TOW}$	FWD PARALLEL TO DRAG AXIS	SIDE COMPONENT OF TOWING LOAD AT MAIN GEAR IS REACTED BY SIDE FORCE AT STATIC GROUND LINE AT THE WHEEL TO WHICH LOAD IS APPLIED. THE TOWING LOADS AT THE AUXILIARY GEAR AND THE DRAG COMPONENT OF THE TOWING LOADS AT THE MAIN GEAR ARE REACTED BY: A. 1) A FORCE ACTING AT THE AXLE OF THE WHEEL TO WHICH LOAD IS APPLIED, OPPOSITE TO THE APPLIED LOAD AND EQUAL IN MAGNITUDE TO THE APPLIED LOAD OR THE VERTICAL REACTION AT THE GEAR, WHICHEVER IS LESSER. 2) TRANSLATIONAL AND ROTATIONAL INERTIA OF AIRPLANE AS REQUIRED FOR EQUILIBRIUM. B. TRANSLATIONAL AND ROTATIONAL INERTIA OF THE AIRPLANE.
			FWD AT 30° TO DRAG AXIS	
			AFT PARALLEL TO DRAG AXIS	
			AFT PARALLEL TO DRAG AXIS	
			AFT AT 30° TO DRAG AXIS	
AT AUXILIARY GEAR	SWIVELED FORWARD	$1.0F_{TOW}$	FORWARD	
			AFT	
	SWIVELED AFT		FORWARD	
			AFT	
	SWIVELED 45° FROM FORWARD	$0.5F_{TOW}$	FWD IN PLANE OF WHEEL	
			AFT IN PLANE OF WHEEL	
	SWIVELED 45° FROM AFT		FWD IN PLANE OF WHEEL	
			AFT IN PLANE OF WHEEL	

Notes - Table XVI

1. These loads shall be applied at the towing fittings and act parallel to the ground. For all towing conditions, the vertical reaction on each gear is equal to the static reaction. The towing load $F_{TOW} = 0.3W$:

   Where W = Maximum Design Gross Weight

2. D = drag reaction on a wheel (parallel to ground).

3. S = side reaction on a wheel (parallel to ground and normal to plane of symmetry of airplane).

HANDLING CRITERIA - JACKING AND HOISTING LIMIT LOADS

REFERENCE: MIL-A-8862

CONDITION	LANDING GEAR JACKING	PRIMARY FLIGHT JACKING	HOISTING
ATTITUDE	3 POINT	LEVEL	LEVEL
REFERENCE PARAGRAPH	3.4.2	3.4.2	3.4.3
VERTICAL COMPONENT	$1.35F_{oj}$	$2.0F_{oj}$	$2.0F_{oj}$
FORE OR AFT COMPONENT	$0.4F_{oj}$	$0.5F_{oj}$	0
LATERAL COMPONENTS	$0.4F_{oj}$	$0.5F_{oj}$	0
DESIGN GROSS WEIGHT	MAXIMUM DESIGN GROSS WEIGHT	LAND PLANE LANDING DESIGN GROSS WEIGHT	HOISTING DESIGN GROSS WEIGHT

Notes - Table XVII

1. F_{oj} = Maximum static reaction on jacking or hoisting points.
2. The C. G. positions used for design shall be all those that are critical and shall be determined by consideration of all practicable arrangements of variable and removable items for which provision is required.
3. The vertical load shall act singly and in combination with the longitudinal load, the lateral load, and both longitudinal and lateral loads.
4. The horizontal loads at the jacking points shall be reacted by inertia forces so as to cause no change in the vertical loads at the jack points.

HANDLING CRITERIA - SECURING LIMIT LOADS

REFERENCE: MIL-A-8862(ASG) and MIL-A-8863(ASG)

LOADING CONDITION	ATTITUDE	LOADS	BALANCING FORCE
WIND LOADING REFERENCE: MIL-A-8862(ASG) PAR 3.4.4 MIL-A-8863(ASG) PAR 3.5.1.3	AIRPLANE ON LEVEL GROUND OR DECK.	WEIGHT OF AIRPLANE W, AND LOADS RESULTING FROM 100 KNOT WIND FROM ANY HORIZONTAL DIRECTION	REACTIONS AT MAIN AND AUXILIARY GEAR (NORMAL TO DECK) AND TENSION IN SECURING LINES.
LOADS RESULTING FROM MOTION OF SHIP REFERENCE: MIL-A-8863(ASG) PAR 3.5.1.4	AIRPLANE SECURED TO DECK OF SHIP WITH SHIP PITCH AND ROLL TO DEVELOPE SPECIFIED LOADS.	V = 1.0W S = 1.0W and V = 0.4W S = 1.0W (2)	

Notes - Table XVIII

1. W = Maximum design gross weight of airplane.
2. V = Force normal to deck.
   S = Force normal to the plane of symmetry of the airplane.
3. Flaps and high-lift devices shall be in neutral or retracted positions.
4. Control surfaces shall be held in neutral by locks or battens.

TABLE XIX

TAIL TO WIND LOADS (LIMIT LOADS)

REFERENCE: MIL-A-8865(ASG) PAR 3.8

CONDITION	CONTROL SURFACE	DIRECTION OF LOAD	POSITION OF SURFACE	LOCATION OF REACTION
1	LATERAL	DOWN ON EACH AILERON	NEUTRAL AND UNLOCKED	AT CONTROL STICK OR WHEEL GRIP
2		DOWN ON EITHER AILERON AND UP ON THE OTHER	AGAINST STOPS	AT STOPS
3	LONGITUDINAL	DOWN		
4		UP		
5	DIRECTIONAL	RIGHT		
6		LEFT		
7	LATERAL	DOWN ON EITHER AILERON AND UP ON THE OTHER	LOCKED	AT LOCKS
8	LONGITUDINAL	UP		
9		DOWN		
10	DIRECTIONAL	RIGHT		
11		LEFT		

Notes - Table XIX

Loads on ailerons, elevators and rudders shall be those from a 75 knot horizontal tail wind or the resulting moment shall be:

H = 16.5 cS
H = Hinge moment - ft. lbs.
C = Average chord length of control surface aft of hinge line - ft.
S = Area of control surface aft of hinge line - ft^2.

The load at each station shall vary linearly from zero at the hinge line to a maximum value at the trailing edge.

Control System Criteria

TABLE XX

PILOT & POWER BOOST APPLIED LOADS

REFERENCES: MIL-S-8698(ASG) PARA. 3.5
MIL-A-8865(ASG) TABLE II

CONTROL	LIMIT LOAD (LB)	POINT OF APPLICATION	DIRECTION OF LOAD
DIRECTIONAL	300	POINT OF CONTACT OF FOOT WITH PEDAL	PARALLEL TO THE PROJECTION ON THE AIRPLANE PLANE OF SYMMETRY OF A LINE CONNECTING THE POINT OF APPLICATION AND THE PILOTS' HIP JOINT, WITH THE PILOTS' SEAT IN ITS MEAN FLYING POSITION.
BRAKE	300	POINT OF CONTACT OF FOOT WITH PEDAL	PARALLEL TO THE PROJECTION ON THE AIRPLANE PLANE OF SYMMETRY OF A LINE CONNECTING THE POINT OF APPLICATION AND THE PILOTS' HIP JOINT, WITH THE PILOTS' SEAT IN ITS MEAN LANDING POSITION.
LATERAL	100	TOP OF STICK GRIP	A LATERAL FORCE PERPENDICULAR TO A STRAIGHT LINE JOINING THE TOP OF STICK GRIP AND PIVOT POINT.
LONGITUDINAL	200	TOP OF STICK GRIP	A LONGITUDINAL FORCE PERPENDICULAR TO A STRAIGHT LINE JOINING TOP OF STICK GRIP AND PIVOT POINT.
CRANK, WHEEL OR LEVER	$50\ \frac{1+R}{3}$ but ≤ 50 ≥ 150	CIRCUMFERENCE OF WHEEL OR GRIP OF CRANK OR LEVER	ANY ANGLE WITHIN 20° OF PLANE OF CONTROL.
SMALL WHEEL OR KNOB	133 IN. LB. IF OPERATED ONLY BY TWISTING 100 LB. IF OPERATED ONLY BY PUSH OR PULL		

REACTIONS TO LOADS SHALL BE PROVIDED AS FOLLOWS:

1. BY THE CONTROL SYSTEM STOPS ONLY.
2. BY THE CONTROL SYSTEM LOCKS ONLY.
3. BY ANY IRREVERSIBLE MECHANISM ONLY, WITH THE IRREVERSIBLE MECHANISM LOCKED WITH THE CONTROL SURFACE IN ANY POSITION WITHIN ITS LIMIT OF MOTION.
4. BY THE ATTACHMENT OF THE CONTROL SYSTEM TO THE SURFACE CONTROL HORN, WITH THE CONTROL IN ANY POSITION WITHIN ITS LIMIT OF MOTION.

Notes - Table XX

1. Control Loads applied separately unless specified.
2. Where the boost unit is so designed that the pilot effort may become additive to the boost output, then the combined loads must be considered.
3. Where dual control systems are provided such that two pilots may exert forces at the same time, the loads specified in above table shall apply for a single pilot operation.
4. Where dual control systems are provided such that the pilot and co-pilot can operate the dual controls simultaneously, that portion of the system which will be subject to the combined action shall be designed to withstand the sum of the loads resulting when each pilot is exerting simultaneously a limit control load equal to 75 percent of the system normal design load.
5. All components of the primary flight control systems shall be designed for 2500 hour service life under the steady and oscillatory loads resulting from the basic fatigue loading schedule of Table VIII.

REFERENCES - STRUCTURAL DESIGN CRITERIA

1. Specification MIL-S-8698 (ASG) Amendment-1, 28 February 1958, Structural Design Requirements - Helicopters

2. ANC 2, October 1952, Ground Loads.

3. Specification MIL-A-8860 (ASG), 18 May 1960, Airplane Strength and Rigidity - General.

4. Specification MIL-A-8861 (ASG), 18 May 1960, Airplane Strength and Rigidity Flight Loads.

5. Specification MIL-A-8862 (ASG), 18 May 1960, Airplane Strength and Rigidity, Landplane Landing and Ground Handling Loads.

6. Specification MIL-A-8863 (ASG), 18 May 1960, Airplane Strength and Rigidity, Additional Loads For Carrier Based Landplanes.

7. Specification MIL-A-8864 (ASG), 18 May 1960, Airplane Strength and Rigidity, Water Handling Loads For Seaplanes.

8. Specification MIL-A-8865 (ASG), 18 May 1960, Airplane Strength and Rigidity, Miscellaneous Loads.

9. Specification MIL-A-8866 (ASG), 18 May 1960, Airplane Strength and Rigidity, Reliability Requirements, Repeated Loads And Fatigue.

10. Specification MIL-A-8867 (ASG), 18 May 1960, Airplane Strength and Rigidity, Ground Tests.

11. Specification MIL-A-8869 (ASG), 18 May 1960, Airplane Strength and Rigidity, Special Weapons Effects.

12. Specification MIL-A-8870 (ASG), 18 May 1960, Airplane Strength and Rigidity, Vibration, Flutter and Divergence.

13. Specification MIL-F-9490B (USAF) Amendment 1, 18 July 1958, Design, Installation and Test Of Flight Control Systems - General.

Weight and Balance Analysis

The weights of the Flight Research Vehicle (FRV) were determined from a practical combination of statistical trend curve weights for airplanes and preliminary layout analysis (see Table XXI). These airplane data are based upon Vertol Division design and manufacturing experience as well as the Transport Division fixed wing experience. The fan, tail, ground handling gear and drive system weights have been obtained from comparison of statistical trends adjusted for unusual features with the weight analysis of the inboard profile shown in Figure 91.

TABLE XXI

DETAILED WEIGHT SUMMARY

GETOL UTILITY AIRCRAFT

Wing Group		790
Tail Group		167
Body Group		635
Alighting Gear		125
Flight Controls		532
Engine Section		80
Propulsion Group		2,533
Engine(s)	572	
Air Induction	18	
Exhaust System	26	
Lubricating System	10	
Fuel System	228	
Engine Controls	30	
Starting System	38	
Propeller Inst.	536	
Drive System	615	
Prop. Duct	460	
Instr. and Nav.		40
Electrical Group		60
Electronics Group		140
Furn. & Equip. Group		65
Weight Empty		5,167
Fixed Useful Load		433
Crew	400	
Trapped Liquids	18	
Engine Oil	15	
Fuel		2,000
Cargo		400
Gross Weight		8,000

In the layout study it was required to have the Center of Pressure at the Center of Gravity to obtain the required hover control. Through careful slot design and layout studies this compatibility of the Center of Pressure (33.4% mac) and the Center of Gravity (32.3% mac) was obtained.

Boeing-Vertol Recommended GETOL Program

Program Schedule

In the development of the Flight Research Vehicle submitted in this report, certain areas of investigation are required to verify the estimation of performance and control improvement. These improvements are divided into two specific tests that must be accomplished before construction of the aircraft is initiated and are described as follows:

Distribution Tests: It has been shown from the testing at the University of Toronto that the slot flow distribution of the GETOL model is poor. This distribution has significant effect on the performance. It is therefore necessary to determine the effect of slot flow distribution on GETOL performance. To best determine this effect, an additional model having the same planform as the wind tunnel model is required. The basic difference between the models is the thickness of the spanwise flow area and slot entry. This additional model would have internal screens and/or baffles to provide a uniform distribution and slot flow. This type model should result in the best attainable performance of a GETOL configuration. A change in the baffles and screens can effect a change in distribution. The use of an additional model will permit the determination of this variation of performance with distribution and indicate what amount of improvement can be achieved in an actual aircraft.

Center of Pressure Tests: From the results of the tests conducted at NASA, it was evident that the stability was neutral and there were large nose down Pitching Moments. The solution to this problem was indicated by the cruciform tests conducted at Princeton University. To overcome the Pitching Moment problem, it was concluded that a "T" shaped peripheral jet as incorporated in the Flight Research Vehicle (FRV) is required. Test of this peripheral slot configuration is required to determine the amount of trim moment attainable and the effect of this slot shape on the stability.

Development of this Flight Research Vehicle requires the maximum utilization of the state-of-the-art in fixed wing and GETOL aircraft. The development plan proposed by the Vertol Division of The Boeing Co. takes full cognizance of this situation by providing design spans for careful layouts and by allowing adequate aerodynamic, dynamic and structural substantiation through analysis and tests of all advanced features at the earliest possible stage in the program. The flight test program is arranged to investigate the hover and transition regimes early so as to permit the earliest evaluation of these specialized flight conditions. Only by such a program is it possible to avoid serious setbacks and delays in the latter phases of the program resulting from failure to explore fully potential problem areas.

To accomplish the overall program, a period of 27 months is required to fully evaluate this aircraft as shown by Figure 98, GETOL Program Schedule.

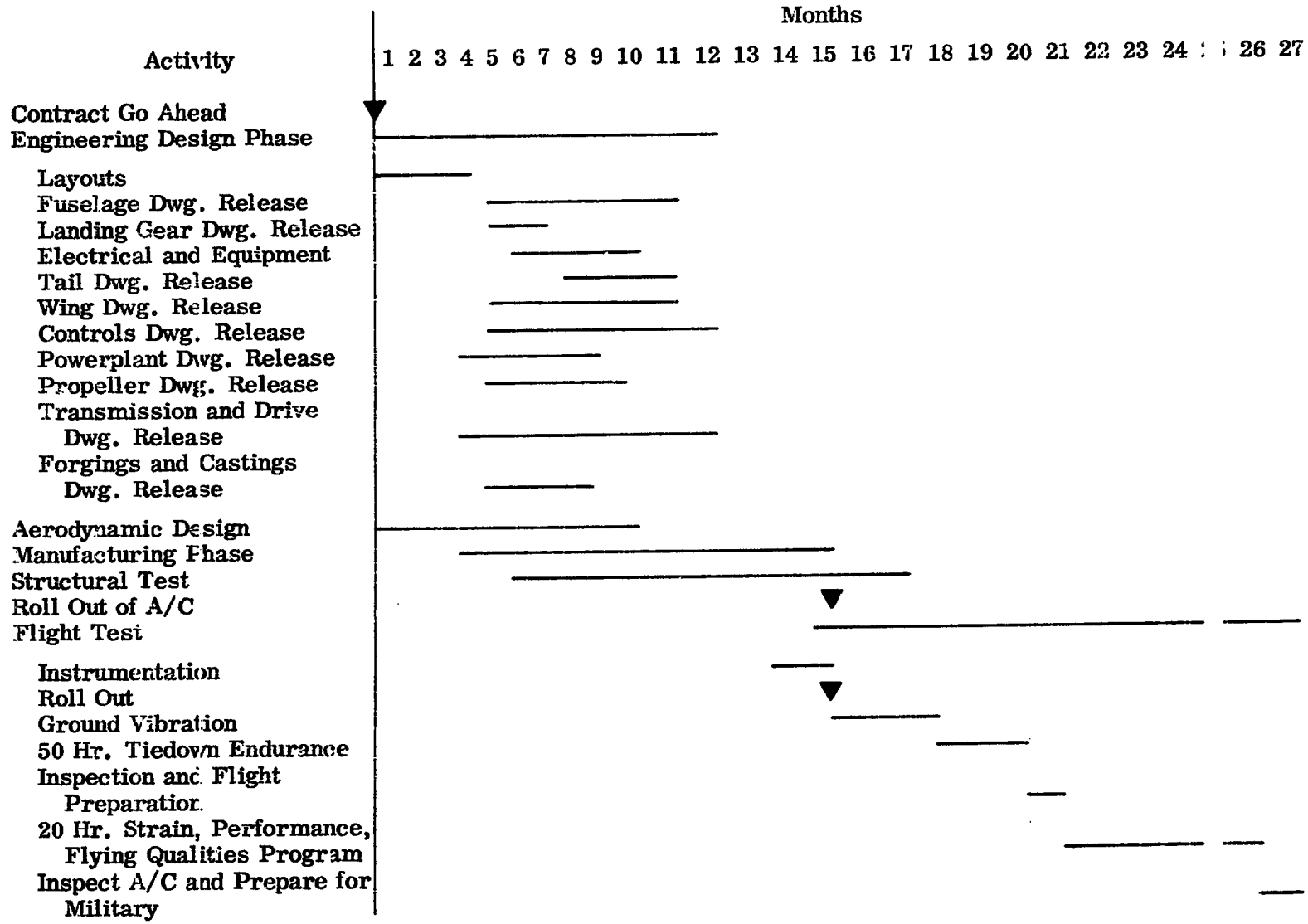

Figure 98. Program Schedule - GETOL Flight Research Vehicle (FRV)

TECHNICAL PROGRAM (PHASE III)

GETOL for a 40,000 Pound Gross Weight Transport

It can be expected that in analogy to the GEM's hovering and the general performance of GETOL, both vehicles should improve with their size and gross weight. Expected size increase in the GETOL configuration should improve the ground clearance and result in an aircraft more competitive with other STOL aircraft of the same gross weight class.

From the requirements of height in hovering and a power match in hover and forward flight, it was indicated that a GETOL in the 40,000 pound gross weight transport class would probably have some interesting possibilities. A preliminary study was conducted by Vertol for different GETOL configurations (60° delta, 3.3 and 5.0 aspect ratio wings) of this category to obtain comparative general trends with existing aircraft of the same class. Figure 99 shows the planview of the configurations studied. The basic data used in hover and transition performance predictions were obtained from the Boeing-Vertol wind tunnel model tests conducted at Langley Field, Virginia.

Since this study is of a general nature, parameters such as lift/drag ratio, relative productivity and ton-miles per pound of fuel consumed were chosen. The drag of the GETOL configurations was determined based upon constant values of

$$\frac{AF}{GW} = \frac{\text{Equivalent Flat Plate Area}}{\text{Gross Weight}}.$$

Expressing the relative productivity in terms of cruise speed, it becomes

$$RP_c = \frac{\text{Payload x Cruise Speed}}{\text{Weight Empty}}.$$

The following ratio is an important factor in determining the overall economy of a transport:

$$\frac{\text{Ton-Miles}}{\text{Fuel Used}} = \frac{\text{Payload Range}}{\text{Weight of Fuel}}.$$

This latter ratio assumes a great importance for military operations because of its logistic implications. The presentation of relative productivity and ton-miles per pound of fuel versus range for various aircraft indicates the economic advantage of one over the other and also the range for which this advantage exists.

From the initial calculations, it became evident that configurations 3, 4 and 7 were most promising (see Figures 100 and 101) on the basis of lift/drag ratio and relative productivity. More detailed studies were then conducted on these configurations and the results were compared with conventional and STOL transport aircraft as well as helicopters. These comparisons, although preliminary

(Figures 102 and 103), indicate that the GETOL transport of the 40,000 pound gross weight class may be competitive at medium ranges in relative productivity with STOL aircraft, helicopters and also conventional aircraft. Furthermore, the GETOL concept assures much greater freedom of transport operation than conventional and STOL aircraft. This comparison leads to the conclusion that the GETOL concept is sufficiently promising performancewise to deserve both further theoretical and experimental analysis as well as flight testing using suitable flight research vehicles.

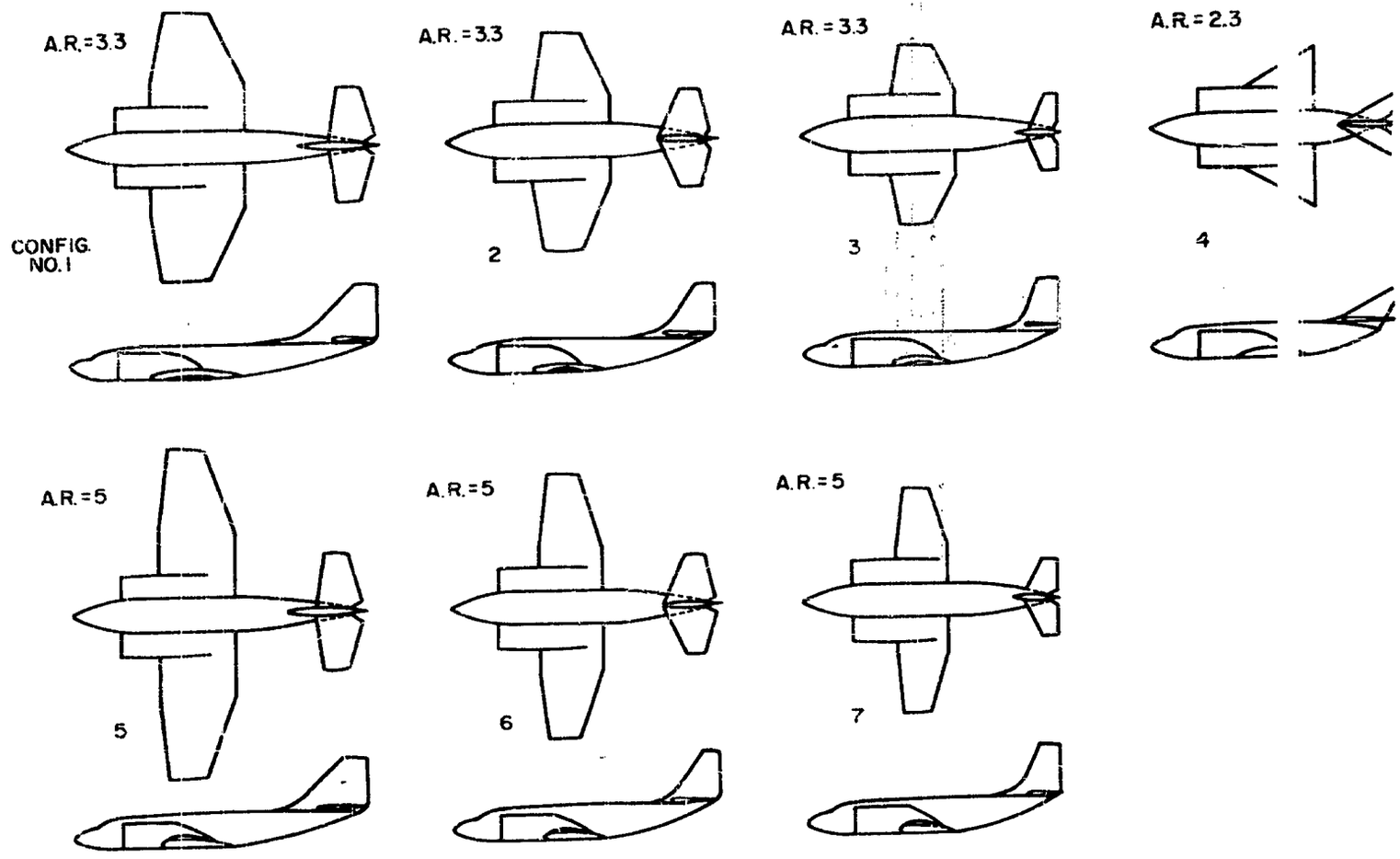

Figure 99. Investigated Configurations of GETOL

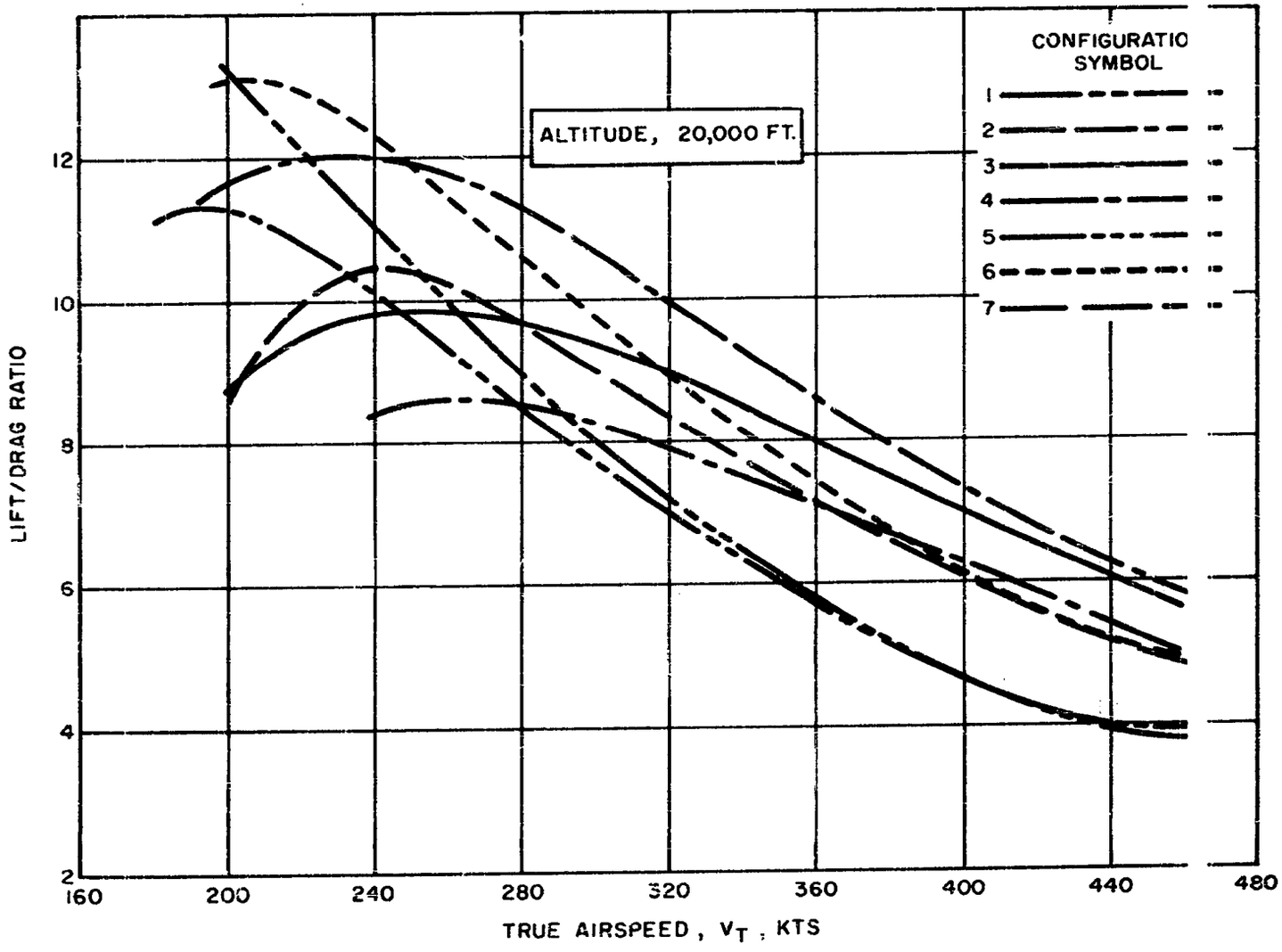

Figure 100. Lift/Drag Ratio vs. True Airspeed

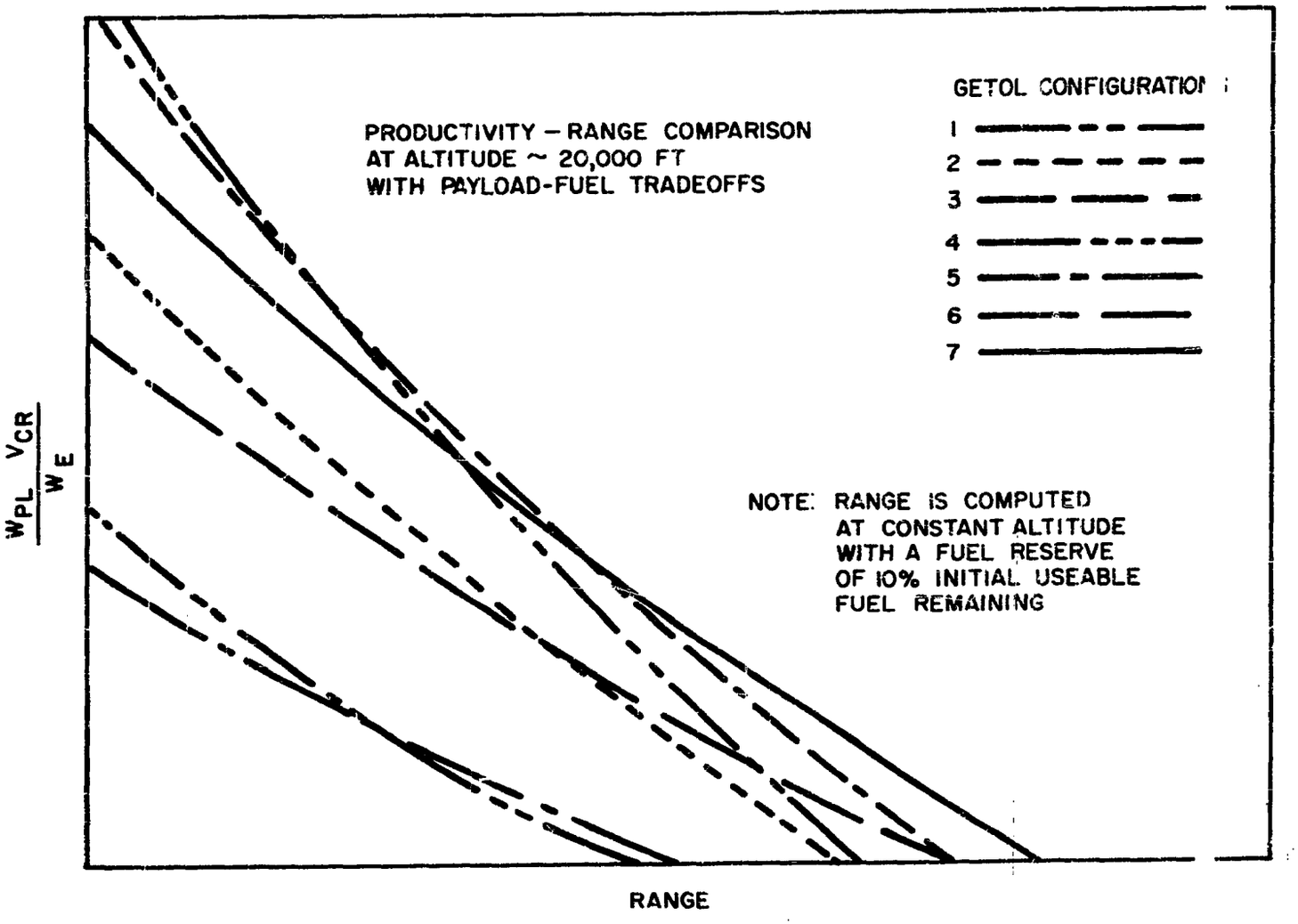

Figure 101. Preliminary Comparison on the Relative Productivity – Range Basis of GETOL Configur ions (From Figure 103)

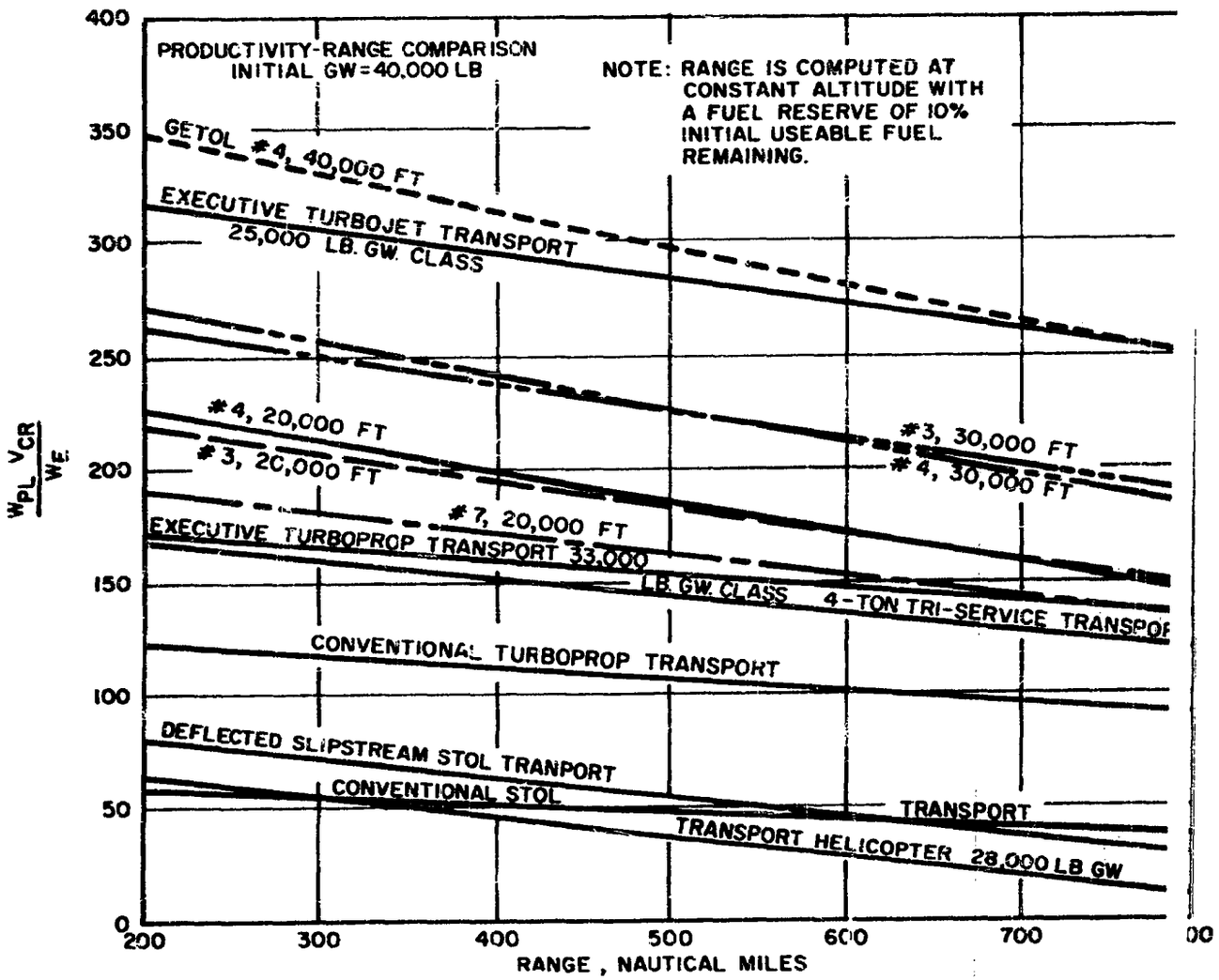

Figure 102. Relative Productivity of the More Promising GETOL Configurations in Comparison with Other Aircraft

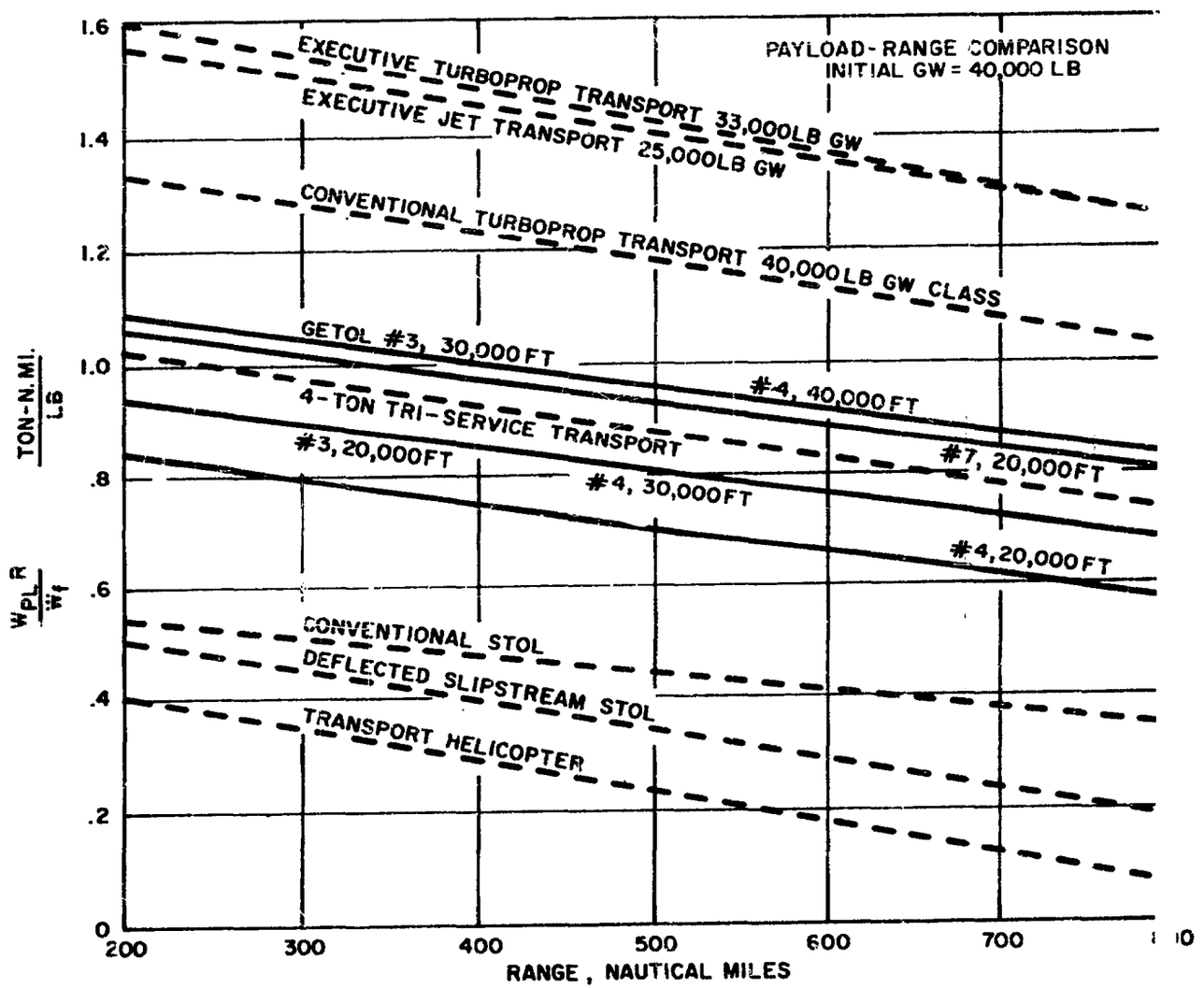

Figure 103. Comparison of Ton Miles Per Pound of Fuel for the More Promising GETOLS a Other Aircraft

BIBLIOGRAPHY

1. McHugh, P.S. [illegible] September 21-30, 1959 (Vertol Aircraft Corp)

2. Martin, L.W., Higgins, H.C. "The Effects of Surface Geometry and Vehicle Motion on the Forces Produced by a Ground Pressure Element", Wichita, Kan., October 9, 1959 (Boeing Airplane Co.)

3. Hoerner, S.F. "Fluid-Dynamic Drag", Midland Park, N.J. 1958

4. Chaplin, H.R. "A Preliminary Design Technique for Annular-Jet Ground-Effect Machines (Gem's)", Wash., September 1959 (David Taylor Model Basin Aero Report 966)

5. Chaplin, H.R. "Ground Effect Machine Research and Development in the United States", Wash., December 1960. (David Taylor Model Basin Aero Report 994)

6. Sweeney, T.E. "The Effect of Planform on the Static Characteristics of Peripheral Jet Wings"(Princeton Report 524)

DISTRIBUTION

USAAVNBD	1
ARO, Durham	2
OCRD, DA	1
ARO, OCRD	1
CofT	2
USATCDA	1
USATMC	1
USATRECOM	26
USATRECOM LO, USARDG (EUR)	1
TCLO, USAAVNS	1
AFSC (SCS-3)	1
AFSC (Aero Sys Div)	1
CNR	2
Dav Tay Mod Bas	1
USASGCA	1
Canadian LO, USATSCH	3
BRAS, DAQMG (Mov & Tn)	4
USASG, UK	1
Langley Rsch Cen, NASA	1
NASA, Wash., D.C.	6
Ames Rsch Cen, NASA	2
USGPO	1
ASTIA	10
BUWEPS, DN	1
Wind Tun Br, NASA	2
Institute of Aerophysics	1
Forrestal Research Center	1
AMC	1
MOCOM	3
USSTRICOM	1
Vertol Division, The Boeing Co.,	10

TRECOM
Vertol Division, Boeing Company, Morton, Pennsylvania
RESEARCH PROGRAM TO DETERMINE THE FEASIBILITY AND POTENTIAL OF THE GROUND EFFECT TAKE-OFF AND LANDING (GETOL) CONFIGURATION. Volume I and II – Research Program to Determine the Feasibility and Potential of the Ground Effect Take-Off and Landing (GETOL) Configuration by W. Stepniewski, H. Wahl, F. McHugh, R. Hooper and J. Gaffney. TCREC 62-63. March 28, 1962 Volume I, 207 pages, Volume II, 198 pages. (Contract DA44-177-TC-663) USATRECOM Task 437-7820.

UNCLASSIFIED REPORT

Boeing-Vertol final report (R276) has been prepared as Volume I and Volume II under Contract DA44-177-TC-663 to describe the effort expended to determine the feasibility and potential of the Ground Effect Take-Off and Landing (GETOL) configuration. The object of such an aircraft is to combine relatively high cruising speeds with the capability of operating from any flat surface (unprepared fields, water, snow, etc.)

The main part of testing was performed by NASA at their Langley Field facilities, namely in the static room, tow track, and wind tunnel. Princeton and Toronto Universities also contributed data as the result of their development testing effort. NASA test results were utilized as the basic information. Analytical methods for data reduction and presentation were developed, thus permitting evaluation of the performance, stability and control characteristics of the GETOL type aircraft. The results of the whole GETOL program provided a basis for a subsequent design analysis and layouts of the Flight Research Vehicle (FRV).

Acquisition of basic GETOL aerodynamic data and development of method of analysis and data presentation should be considered as the most significant technical advance achieved under this program.

1. Final Summary Report GETOL Configuration
2. Contract DA44-177-TC-663

TRECOM
Vertol Division, Boeing Company, Morton, Pennsylvania
RESEARCH PROGRAM TO DETERMINE THE FEASIBILITY AND POTENTIAL OF THE GROUND EFFECT TAKE-OFF AND LANDING (GETOL) CONFIGURATION. Volume I and II – Research Program to Determine the Feasibility and Potential of the Ground Effect Take-Off and Landing (GETOL) Configuration by W. Stepniewski, H. Wahl, F. McHugh, R. Hooper and J. Gaffney. TCREC 62-63. March 28, 1962 Volume I, 207 pages, Volume II, 198 pages. (Contract DA44-177-TC-663) USATRECOM Task 437-7820.

UNCLASSIFIED REPORT

Boeing-Vertol final report (R276) has been prepared as Volume I and Volume II under Contract DA44-177-TC-663 to describe the effort expended to determine the feasibility and potential of the Ground Effect Take-Off and Landing (GETOL) configuration. The object of such an aircraft is to combine relatively high cruising speeds with the capability of operating from any flat surface (unprepared fields, water, snow, etc.)

The main part of testing was performed by NASA at their Langley Field facilities, namely in the static room, tow track, and wind tunnel. Princeton and Toronto Universities also contributed data as the result of their development testing effort. NASA test results were utilized as the basic information. Analytical methods for data reduction and presentation were developed, thus permitting evaluation of the performance, stability and control characteristics of the GETOL type aircraft. The results of the whole GETOL program provided a basis for a subsequent design analysis and layouts of the Flight Research Vehicle (FRV).

Acquisition of basic GETOL aerodynamic data and development of method of analysis and data presentation should be considered as the most significant technical advance achieved under this program.

1. Fina ummary Report GETOL
Conl ration
2. Cont t DA44-177-TC-663

TRECOM
Vertol Division, Boeing Company, Morton, Pennsylvania
RESEARCH PROGRAM TO DETERMINE THE FEASIBILITY AND POTENTIAL OF THE GROUND EFFECT TAKE-OFF AND LANDING (GETOL) CONFIGURATION. Volume I and II – Research Program to Determine the Feasibility and Potential of the Ground Effect Take-Off and Landing (GETOL) Configuration by W. Stepniewski, H. Wahl, F. McHugh, R. Hooper and J. Gaffney. TCREC 62-63. March 28, 1962 Volume I, 207 pages, Volume II, 198 pages. (Contract DA44-177-TC-663) USATRECOM Task 437-7820.

UNCLASSIFIED REPORT

Boeing-Vertol final report (R276) has been prepared as Volume I and Volume II under Contract DA44-177-TC-663 to describe the effort expended to determine the feasibility and potential of the Ground Effect Take-Off and Landing (GETOL) configuration. The object of such an aircraft is to combine relatively high cruising speeds with the capability of operating from any flat surface (unprepared fields, water, snow, etc.)

The main part of testing was performed by NASA at their Langley Field facilities, namely in the static room, tow track, and wind tunnel. Princeton and Toronto Universities also contributed data as the result of their development testing effort. NASA test results were utilized as the basic information. Analytical methods for data reduction and presentation were developed, thus permitting evaluation of the performance, stability and control characteristics of the GETOL type aircraft. The results of the whole GETOL program provided a basis for a subsequent design analysis and layouts of the Flight Research Vehicle (FRV).

Acquisition of basic GETOL aerodynamic data and development of method of analysis and data presentation should be considered as the most significant technical advance achieved under this program.

1. Final Summary Report GETOL Configuration
2. Contract DA44-177-TC-663

TRECOM
Vertol Division, Boeing Company, Morton, Pennsylvania
RESEARCH PROGRAM TO DETERMINE THE FEASIBILITY AND POTENTIAL OF THE GROUND EFFECT TAKE-OFF AND LANDING (GETOL) CONFIGURATION. Volume I and II – Research Program to Determine the Feasibility and Potential of the Ground Effect Take-Off and Landing (GETOL) Configuration by W. Stepniewski, H. Wahl, F. McHugh, R. Hooper and J. Gaffney. TCREC 62-63. March 28, 1962 Volume I, 207 pages, Volume II, 198 pages. (Contract DA44-177-TC-663) USATRECOM Task 437-7820.

UNCLASSIFIED REPORT

Boeing-Vertol final report (R276) has been prepared as Volume I and Volume II under Contract DA44-177-TC-663 to describe the effort expended to determine the feasibility and potential of the Ground Effect Take-Off and Landing (GETOL) configuration. The object of such an aircraft is to combine relatively high cruising speeds with the capability of operating from any flat surface (unprepared fields, water, snow, etc.)

The main part of testing was performed by NASA at their Langley Field facilities, namely in the static room, tow track, and wind tunnel. Princeton and Toronto Universities also contributed data as the result of their development testing effort. NASA test results were utilized as the basic information. Analytical methods for data reduction and presentation were developed, thus permitting evaluation of the performance, stability and control characteristics of the GETOL type aircraft. The results of the whole GETOL program provided a basis for a subsequent design analysis and layouts of the Flight Research Vehicle (FRV).

Acquisition of basic GETOL aerodynamic data and development of method of analysis and data presentation should be considered as the most significant technical advance achieved under this program.

1. Fir Summary Report GETOL
Co uration
2. Co ct DA44-177-TC-663

TRECOM
Vertol Division, Boeing Company, Morton, Pennsylvania
RESEARCH PROGRAM TO DETERMINE THE FEASIBILITY AND POTENTIAL OF THE GROUND EFFECT TAKE-OFF AND LANDING (GETOL) CONFIGURATION. Volume I and II -- Research Program to Determine the Feasibility and Potential of the Ground Effect Take-Off and Landing (GETOL) Configuration by W. Stepniewski, R. Wahl, F. McHugh, R. Hooper and J. Gaffney. TCREC 62-63. March 28, 1962 Volume I, 207 pages, Volume II 198 pages. (Contract DA44-177-TC-663) USATRECOM Task 437-7-20.

UNCLASSIFIED REPORT

Boeing-Vertol final report (R276) has been prepared as Volume I and Volume II under Contract DA44-177-TC-663 to describe the effort expended to determine the feasibility and potential of the Ground Effect Take-Off and Landing (GETOL) configuration. The object of such an aircraft is to combine relatively high cruising speeds with the capability of operating from any flat surface (unprepared fields, water, snow, etc.)

The main part of testing was performed by NASA at their Langley Field facilities, namely in the static room, tow track, and wind tunnel. Princeton and Toronto Universities also contributed data as the result of their development testing effort. NASA test results were utilized as the basic information. Analytical methods for data reduction and presentation were developed, thus permitting evaluation of the performance, stability and control characteristics of the GETOL type aircraft. The results of the whole GETOL program provided a basis for a subsequent design analysis and layouts of the Flight Research Vehicle (FRV).

Acquisition of basic GETOL aerodynamic data and development of method of analysis and data presentation should be considered as the most significant technical advance achieved under this program.

1. Final Summary Report GETOL Configuration
2. Contract DA44-177-TC-663

TRECOM
Vertol Division, Boeing Company, Morton, Pennsylvania
RESEARCH PROGRAM TO DETERMINE THE FEASIBILITY AND POTENTIAL OF THE GROUND EFFECT TAKE-OFF AND LANDING (GETOL) CONFIGURATION. Volume I and II -- Research Program to Determine the Feasibility and Potential of the Ground Effect Take-Off and Landing (GETOL) Configuration by W. Stepniewski, R. Wahl, F. McHugh, R. Hooper and J. Gaffney. TCREC 62-63. March 28, 1962 Volume I, 207 pages, Volume II, 198 pages. (Contract DA44-177-TC-663) USATRECOM Task 437-7-20.

UNCLASSIFIED REPORT

Boeing-Vertol final report (R276) has been prepared as Volume I and Volume II under Contract DA44-177-TC-663 to describe the effort expended to determine the feasibility and potential of the Ground Effect Take-Off and Landing (GETOL) configuration. The object of such an aircraft is to combine relatively high cruising speeds with the capability of operating from any flat surface (unprepared fields, water, snow, etc.)

The main part of testing was performed by NASA at their Langley Field facilities, namely in the static room, tow track, and wind tunnel. Princeton and Toronto Universities also contributed data as the result of their development testing effort. NASA test results were utilized as the basic information. Analytical methods for data reduction and presentation were developed, thus permitting evaluation of the performance, stability and control characteristics of the GETOL type aircraft. The results of the whole GETOL program provided a basis for a subsequent design analysis and layouts of the Flight Research Vehicle (FRV).

Acquisition of basic GETOL aerodynamic data and development of method of analysis and data presentation should be considered as the most significant technical advance achieved under this program.

1. Final Summary Report GETOL Configuration
2. Contract DA44-177-TC-663